

THE PHASE BEHAVIOR OF METHANE  
IN A NATURAL GAS CONDENSATE

By

ALTO NELSON STUCKEY, JR.

Bachelor of Science  
The University of Alabama  
University, Alabama  
1956

Master of Science  
Oklahoma State University  
Stillwater, Oklahoma  
1963

Submitted to the Faculty of the Graduate School of  
the Oklahoma State University  
in partial fulfillment of the requirements  
for the degree of  
DOCTOR OF PHILOSOPHY  
May, 1966

JUN 13 1966

THE PHASE BEHAVIOR OF METHANE  
IN A NATURAL GAS CONDENSATE

Thesis Approved:

*K. C. Chao*

Thesis Adviser

*John B. Whit*

*John H. Eubank*

*W. D. Morrison*

*J. H. Boyce*

Dean of the Graduate School

## PREFACE

Vapor-liquid equilibrium K-values and phase densities were obtained experimentally for a methane-Morrow condensate system at 150 and 250°F and pressures from 100 psia to the dew or critical points of the system at these temperatures. The purpose of this investigation was the development of certain equipment and methods for obtaining K-values and phase densities for the components of complex hydrocarbon systems.

I am deeply indebted to Professor W. C. Edmister for suggesting the problem of this thesis and for the aid and inspiration supplied by him during the period of preparation. I sincerely appreciate the encouragement and help received from the staff of the School of Chemical Engineering and my fellow students.

The financial assistance of the American Petroleum Institute is gratefully acknowledged. Phillips Petroleum Company and the American Petroleum Institute Hydrocarbon Depository donated the pure hydrocarbons used for calibration purposes. Appreciation is expressed to the Esso Research Laboratories for granting educational leave to the author for graduate study. The assistance and cooperation of the Esso Research Laboratories, Pan American Petroleum Corporation and the Continental Oil Company in various phases of this work is appreciated.

The greatest expression of my gratitude goes to my wife, Wysie, whose never ending devotion and encouragement made this study possible.

## TABLE OF CONTENTS

Chapter	Page
I. INTRODUCTION . . . . .	1
II. PRIOR INVESTIGATIONS. . . . .	4
Experimental Investigations. . . . .	4
Experimental Methods . . . . .	14
Constant Volume Apparatus . . . . .	14
Variable Volume Bomb. . . . .	15
Bubble and Dew Point Method . . . . .	16
The Dynamic Flow Method . . . . .	17
Dynamic Distillation Method . . . . .	17
The Liquid Recirculation Method . . . . .	18
The Vapor Recirculation Method. . . . .	19
This Study. . . . .	21
III. THEORY, THERMODYNAMIC CONSISTENCY AND CORRELATION METHODS . . . . .	22
The Criteria of Equilibrium. . . . .	22
Chemical Potential and the Gibbs-Duhem . . . . .	23
Equation	
Fugacity and Vapor-Liquid Equilibrium. . . . .	27
The Evaluation of Fugacity . . . . .	29
The Fugacity of a Component in a Mixture . . . . .	30
Thermodynamic Consistency Tests. . . . .	31
Correlation of Vapor-Liquid Equilibrium Data . . . . .	37
Recent Developments in K-Value Correlation Techniques . . . . .	38
IV. EXPERIMENTAL APPARATUS. . . . .	45
Apparatus. . . . .	45
Feed Section. . . . .	45
Pressure Regulation and Measurement Section . . . . .	47
The Michels Pressure Balance . . . . .	47
Pressure Bench . . . . .	51
The Gas Compressor . . . . .	51
The Equilibrium Cell and Thermostat . . . . .	54
The Equilibrium Cell . . . . .	54
The Thermostat . . . . .	56
Density Measurement . . . . .	59
Vapor Recirculation System. . . . .	61

	Page
Sampling and Analysis Section . . . . .	65
Materials . . . . .	70
V. EXPERIMENTAL PROCEDURE. . . . .	77
Charging of Components . . . . .	77
Equilibration. . . . .	78
Sampling . . . . .	81
Liquid Sample Transfer. . . . .	85
Vapor Sample Transfer . . . . .	88
VI. CHROMATOGRAPHIC ASSAY OF THE EQUILIBRIUM VAPOR-LIQUID PHASES . . . . .	90
Equipment and Operation. . . . .	91
Calibration. . . . .	95
Analysis of the Coexisting Equilibrium Phases. .	98
VII. DISCUSSION OF RESULTS . . . . .	101
Experimental Results . . . . .	101
Experimental Errors. . . . .	103
Thermodynamic Consistency Test . . . . .	111
Data and Correlation Comparisons . . . . .	124
VIII. CONCLUSIONS AND RECOMMENDATIONS . . . . .	133
BIBLIOGRAPHY . . . . .	137
APPENDIX A - CALIBRATION OF THE PRESSURE BALANCE AND MEASURING CYLINDERS. . . . .	142
APPENDIX B - CALIBRATION OF THERMOCOUPLES AND BECKMAN THERMOMETER. . . . .	147
APPENDIX C - CALIBRATION OF VOLUMETRIC APPARATUS. . . . .	152
Analytical Balance Weight Calibrations . . . . .	152
Volumetric Calibrations. . . . .	153
Small Volumetric Bulbs. . . . .	153
U-Tube Manometer. . . . .	155
Capillary Tubing Manifold . . . . .	155
Necks of Volumetric Bulbs . . . . .	158
Four Liter Volumetric Bulb. . . . .	158
Density Traps . . . . .	158
APPENDIX D - CALIBRATION OF GAS COMPRESSOR. . . . .	161
APPENDIX E - SAMPLE CALCULATION OF EXPERIMENTAL DATA. . . . .	165
Temperature. . . . .	165
Pressure . . . . .	166

	Page
Local Acceleration Due to Gravity. . . . .	167
Barometric Pressure. . . . .	167
Buoyancy Correction. . . . .	169
Measuring Cylinder Thermal Expansion Correction . . . . .	170
Correction for Oil Head Above Bottom Guide Pin. . . . .	171
Corrected Balance Pressure . . . . .	171
Correction for Oil and Mercury Heads in Gas Compressor. . . . .	172
Correction for Hydrocarbon Head in Equilibrium Cell . . . . .	172
Vapor Phase Calculations . . . . .	173
Composition . . . . .	174
Chromatographic Assay. . . . .	174
Light Hydrocarbons . . . . .	174
Heavy Hydrocarbons . . . . .	177
Phase Material Balance . . . . .	177
Phase Density. . . . .	178
K-Values . . . . .	178
APPENDIX F - COMPOSITION OF CHROMATOGRAPH STANDARDS. . . . .	179
APPENDIX G - LEAST SQUARES ANALYSIS OF CHROMATOGRAPH CALIBRATION DATA. . . . .	184
APPENDIX H - RAW EXPERIMENTAL DATA . . . . .	206
APPENDIX I - CALCULATED DATA . . . . .	213
APPENDIX J - NOMENCLATURE. . . . .	225
APPENDIX K - PHYSICAL CONSTANTS. . . . .	228

# LIST OF TABLES

Table	Page
I. Experimental Vapor-Liquid Equilibrium Investigations of Complex Hydrocarbon Systems. . . . .	5
II. Analysis of Methane Reagent . . . . .	72
III. Analysis of Condensate Field Samples. . . . .	73
IV. Chromatographic Assay of Condensate . . . . .	75
V. Standard Chromatograph Operating Conditions . . . . .	97
VI. Regression Models of Chromatograph Calibration Data . . . . .	98
VII. Calculated Quantities for Consistency Test. . . . .	115
VIII. Coefficients for Polynomial Fit of Experimental ( $y_1-x_1$ ) Data. . . . .	125
IX. Results of Edmister Isothermal Integral Consistency Test. . . . .	126
X. Comparison of Experimental K-Values for Methane in Complex Systems. . . . .	127
XI. Comparison of Experimental and NGSMA K-Values . . . . .	129
XII. Comparison of Chao-Seader and Experimental K-Values at 150°F. . . . .	131
XIII. Comparison of Chao-Seader and Experimental K-Values at 250°F. . . . .	132
A-I. Pressure Balance Weight Calibrations. . . . .	144
A-II. Measuring Cylinder Calibrations . . . . .	145
B-I. Thermocouple Calibration Equations. . . . .	151
C-I. Calibrations for Weight Set 4775. . . . .	154
C-II. Calibrated Volumes of Volumetric Apparatus. . . . .	156

	Page
D-I. Experimental Data for Calibration of Gas Compressor Level. . . . .	163
F-I. Composition of Chromatograph Calibration Standards - Mixtures NG-1 and NG-2. . . . .	180
F-II. Composition of Chromatograph Calibration Standards - Mixtures 31, 32 and 38. . . . .	180
F-III. Composition of Chromatograph Calibration Standards - Mixtures 90, 103 and 105. . . . .	181
F-IV. Composition of Chromatograph Calibration Standards - Mixtures 55, 73 and 84. . . . .	181
F-V. Composition of Chromatograph Calibration Standards - Mixtures 3, 14 and 65 . . . . .	182
F-VI. Composition of Chromatograph Calibration Standards - Mixtures 19, 20 and 29. . . . .	182
F-VII. Composition of Chromatograph Calibration Standards - Mixtures 2, 5 and 30. . . . .	183
G-I. Chromatograph Calibration Data. . . . .	188
G-II. Analysis of Chromatograph Calibration Data. . . . .	197
H-I. Raw Experimental Data . . . . .	207
H-II. Low Temperature Thermostat Data . . . . .	209
H-III. Liquid Sample Trap Weight Data. . . . .	211
I-I. Vapor Phase Mole Fraction Data. . . . .	214
I-II. Liquid Phase Mole Fraction Data . . . . .	217
I-III. Experimental K-Values . . . . .	220
I-IV. Experimental Liquid Phase Density Data. . . . .	223
I-V. Experimental Vapor Phase Density Data . . . . .	224
K-I. Calculation Constants for Pure Components . . . . .	229



## LIST OF FIGURES

Figure		Page
1.	Schematic Diagram of Apparatus. . . . .	46
2.	Sectional View of Hart Piston-Cylinder. . . . .	48
3.	The Michels Pressure Balance. . . . .	49
4.	The Hart Pressure Bench . . . . .	52
5.	Sectional View of Gas Compressor. . . . .	53
6.	Equilibrium Cell. . . . .	55
7.	Heater and Blower Arrangement - Side View of Thermostat . . . . .	57
8.	Blower Assembly for High Temperature Thermostat . . .	58
9.	Vapor and Liquid Density Traps. . . . .	60
10.	High Pressure Circulating Pump. . . . .	62
11.	Magnet Housing for Circulating Pump . . . . .	64
12.	Circuit Diagram for Magnetic Drive Circulating Pump .	66
13.	Circulating Pump Calibration. . . . .	67
14.	Sampling System . . . . .	68
15.	ASTM Distillation of Condensate . . . . .	76
16.	Typical Chromatogram of Condensate. . . . .	99
17.	Equilibrium Phase Density at 150° F.. . . .	104
18.	Equilibrium Phase Density at 250° F.. . . .	105
19.	Equilibrium Liquid Phase Molar Volumes at 150° F. . .	106
20.	Equilibrium Vapor Phase Molar Volumes at 150° F. and 250° F. . . . .	107
21.	K-Values at 150° F. . . . .	108

	Page
22. K-Values at 250° F. . . . .	109
23. $(y_1 - x_1)$ vs Pressure, 150° F.. . . .	116
24. $(y_1 - x_1)$ vs Pressure, 250° F.. . . .	117
25. $\ln \phi_1 / \phi_2$ vs Pressure at 250° F. . . . .	118
26. $\ln \phi_1 / \phi_2$ vs Pressure at 150° F. . . . .	119
27. $\ln y_1 / y_2$ vs Pressure, 250° F. . . . .	120
28. $\ln y_1 / y_2$ vs Pressure, 150° F. . . . .	121
29. $\underline{V}^V - \underline{V}^L / RT$ vs Pressure, 250° F. . . . .	122
30. $\underline{V}^V - \underline{V}^L / RT$ vs Pressure, 150° F. . . . .	123
B-1. Thermocouple Wiring Diagram . . . . .	149
D-1. Gas Compressor Level Calibration Apparatus. . . . .	162

## CHAPTER I

### INTRODUCTION

The equilibrium phase behavior of complex hydrocarbon systems is of both theoretical and practical interest; theoretical because of the need for the development of better correlations for the thermodynamic properties of coexisting gas-liquid phases, and practical because of the need for vapor-liquid equilibrium ratios and phase densities for design calculations and economic studies.

The vapor-liquid equilibrium ratio for a component in a fluid mixture is defined as the ratio of the mole fraction of the component in the vapor phase,  $y_i$ , to the mole fraction of the component in the liquid phase,  $x_i$ , with which the vapor phase is in equilibrium. Symbolically,

$$K_i = y_i/x_i \quad (I-1)$$

This equilibrium ratio is generally referred to as the 'K-value'.

K-values were first evaluated by using a combination of Raoult's and Dalton's laws which state respectively that the partial pressure of any component in a mixture will equal the vapor pressure of that component in the pure state multiplied by its mole fraction in the liquid mixture and that the total pressure,  $P$ , of a mixture is equal to the sum of partial pressures of the components present.

$$y_i = p_i^{\circ} x_i / P \quad (I-2)$$

where  $P$  = the system pressure

$p_i^o$  = the pure component vapor pressure

Combining Equations I-1 and I-2

$$K_i = p_i^o / P \quad (I-3)$$

There are relatively few systems whose equilibrium relations can be calculated from Raoult's and Dalton's laws; and there are a large number of industrially important systems whose equilibrium relations cannot be predicted from purely theoretical and empirical considerations and which must be obtained by direct experimental investigation.

The experimental determination of a series of vapor-liquid equilibrium ratios can be carried out either along an isotherm or along an isobar. The isobaric data are particularly important in separations calculations while the isothermal data are important in petroleum reservoir studies. The experimental determination of K-values involves obtaining samples of the coexisting liquid and vapor phases which are in true equilibrium and the measurement of the concentration of the components in each phase. If useful equilibrium measurements are to be made, it is necessary not only to have perfect control of temperature and pressure but also an accurate method for the composition assay of the equilibrium phases.

The increasing importance of natural gas has made the accurate prediction of the phase behavior and composition of produced natural gas streams an economic necessity. The work reported here was undertaken to develop certain equipment and methods for obtaining accurate K-values and phase densities for the components of complex hydrocarbon systems.

In the following chapters, the prior work in vapor-liquid equilibria

of complex systems is reviewed. This review covers experimental methods and previous investigations of complex systems. In Chapter III, vapor-liquid equilibria theory is discussed, especially as it pertains to the present work. The experimental apparatus and procedure are described next. Chapter VI reports on the development of a gas chromatography technique which provides a rapid and economical method for obtaining the composition data needed in vapor-liquid equilibrium ratio determinations. Finally, the experimental data are analyzed and the results of correlation work are discussed.

## CHAPTER II

### PRIOR INVESTIGATIONS

During the past three decades much effort has been devoted to the study of the volumetric and phase behavior of pure paraffin hydrocarbons and of binary and ternary mixtures of these compounds. Many of these studies were carried out with the objective of using this binary and ternary data to predict the behavior of more complex hydrocarbon mixtures. The behavior of the simple systems served at one time as a qualitative illustration of the probable characteristics of the more complex systems found in nature, however, it fell far short of requirements for quantitative predictions.

Concurrently with the study of binary and ternary systems, investigations were made of natural hydrocarbon systems. Many of these studies were made in the laboratories of private oil companies. Only a few of these studies have been reported in the literature. These reported studies will be reviewed chronologically in this chapter together with the various experimental methods used in vapor-liquid equilibrium studies. Table I lists the references and conditions at which measurements were made of equilibrium phase compositions for complex systems including natural gas.

### Experimental Investigations

In the early 1900's when the petroleum industry first became

TABLE I

EXPERIMENTAL VAPOR-LIQUID EQUILIBRIUM INVESTIGATIONS  
OF COMPLEX HYDROCARBON MIXTURES

<u>System</u>	<u>Temperature, °F</u>	<u>Pressure, psia</u>	<u>Reference</u>	<u>Year</u>	<u>Investigators</u>
Light Hydrocarbon-Absorber Oil	77		30	1933	Matheson, Cummings
Natural Gas-Crude Oil	100	15-3000	57	1934	Sage, Kircher
Natural Gas-Crude Oil	40-300	15-3000	24	1937	Katz, Hachmuth
Natural Gas-Natural Gasoline	85-212	1300-2600	25	1940	Katz, Vink, David
Natural Gas-Absorber Oil	33-180	100-500	70	1941	Webber
Natural Gas-Distillate	40-200	200-4000	51	1941	Roland, Smith, Kaveler
Gas-Distillate	300-820	50-700	72	1942	White, Brown
Natural Gas-Absorber Oil	85	125-3100	27	1943	Kirkbride, Bertetti
Natural Gas-Crude Oil	35-250	1000-8220	63	1944	Standing, Katz
Natural Gas-Hexane	100	500-1800	19	1945	Hanson, Brown
Natural Gas-Crude Oil	120,200	1000-10,000	52	1945	Roland
CO <sub>2</sub> - Natural Gas-Condensate	100-250	500-2900	41	1946	Poettmann, Katz
Methane - Kensol 16	60-260	10,000-25,000	54	1950	Rzasa
CO <sub>2</sub> - Natural Gas-Crude Oil	38-202	600-8500	43	1951	Poettmann
CO <sub>2</sub> - H <sub>2</sub> S - Natural Gas	100-200	200-5000	21	1952	Jacoby, Rzasa
Crude and Absorber Oils					
Light Gas-Absorber Oil	100-220	500,1000	61	1952	Solomon
Gas Condensate	200	500-3000	23	1953	Hoffman, Crump, Hocutt
CO <sub>2</sub> ,H <sub>2</sub> S - Crude Oil	154	700-2500	69	1954	Vagtborg
Natural Gas-Crude Oil	190	1000-6000	14	1956	Evans, Harris
Natural Gas-Natural Gasoline	214	1130-3192	26	1963	Kehn

interested in natural gasoline and the 'front end' components of crude oil, it became apparent that the design of processing equipment required some quantitative expression for the composition of a vapor in equilibrium with a liquid. Such an expression was available in a combination of Raoult's and Dalton's laws which state respectively that the partial pressure of any component in a mixture will equal the vapor pressure of that component in the pure state multiplied by its mole fraction in the liquid mixture and that the total pressure,  $P$ , of a mixture is equal to the sum of the partial pressures of the components present.

In 1933 Matheson and Cummings (30) determined experimentally the vapor pressures of n-butane, n-pentane, isopentane and n-hexane at various concentrations in absorber oil at 25°C. The experimental vapor pressures were compared to those calculated by Raoult's law. The data showed an appreciable positive deviation from the calculated values.

Sage and Kircher (57) presented values of the solubility of natural gas in several different crude oils at 100°F. and at pressures from atmospheric to 3000 psi. These investigations concluded that the assumption of a simple dissolving process occurring when a gas is brought to equilibrium with a liquid in complex hydrocarbon systems is valid only when the system is far enough below the critical temperature of the solvent and the critical pressure of the mixture that there is no appreciable transfer of the components of the original liquid phase into the gas phase.

In the 1937 work of Katz and Hachmuth (24) experimental K-values for methane through hexane in a natural gas-crude oil mixture were



presented. These data were observed over a pressure range from atmospheric to 3000 psi and temperatures from 40 to 300°F. The rise of the equilibrium constants at high pressures approaching the critical pressure of the mixtures was shown for the first time in complex mixtures of this wide a range of volatility.

By cross-plotting and extrapolation Katz and Hachmuth were able to develop K-charts for methane through hexane in Mid-Continent oil over the range of temperature -30 to 270°F. and pressures 5 to 3000 psi. The outstanding feature of the data is the convergence of the equilibrium constant toward a critical pressure. Sage, Lacey and Schaafsma (58) had noted this convergence previously, but this was the first time that the position of the critical and the behavior of the several constituents was shown.

A phase diagram showing the boundary curve and the quantity of liquid in the two phase region was determined for a mixture of natural gas and natural gasoline in the region of the critical by Katz, Vink and David (25). The temperatures and pressures of the phase measurements were in the range of 85-212°F. and 1300 to 2600 psi with critical conditions at 169°F and 2615 psi. The approximate densities of the single and two phase regions were determined.

A striking color phenomenon accompanying the measurements near the critical temperature has been noted. At pressures considerably above the two phase region the system was colorless. At the pressure was lowered toward the bubble or dew point, the single phase took on a reddish color. At temperatures near the critical this color was a bright mahogany red. The single phase grew in color over a range of about 5-10 psi above the phase boundary and reached its greatest depth

just prior to the formation of two phases. A gradual increase in maximum intensity of color occurred as the isotherms approached the critical temperature.

Webber (70) determined the equilibrium distribution of the hydrocarbons, methane through hexane, between natural gas and a typical absorber oil. The ranges of temperature and pressure chosen were from 33-180°F. from 100-5000 psi. The absorber oil had an initial boiling point of 300°F. and an average molecular weight of 183.

Webber's data are characterized by the fact that he used a fresh charge of absorber oil for each vapor-liquid equilibria determination. Webber noted that when the K-values for the components were plotted that the K-values for all components approached unity at the higher pressures but that there was a significant reduction in the rate of approach to unity at 5000 psi.

The data of Webber check very well with the data of Katz and Hachmuth (24) at pressures up to the minimum K-values. As the pressure was increased above this point, the disagreement became pronounced. This disagreement can be attributed to composition effects.

Roland, Smith and Kaveler (51) present data for a typical Gulf Coast gas-distillate system in the range of 200-4000 psi and 40-200°F. The earlier data of Katz and Hachmuth (24) and Webber (70) on absorber oil-natural gas indicated that the numerical value of K for any component varies not only with pressure but also with the composite composition of the system and with inherent characteristics of the individual components present in the mixture. Roland, Smith and Kaveler felt that the agreement of their data for the 50, 75, 85 and 90 mole per cent methane composites for methane through hexane was sufficiently

good to prove that variations in composite composition have little effect on the equilibrium constants for the natural gas-distillate system studied.

In 1942 White and Brown (72) obtained experimental vapor-liquid equilibria data for petroleum fractions boiling from 95-750°F. at temperatures from 300 to 820°F. at pressures from 50-700 psi. These data were used to extend the estimated ideal K-values to hydrocarbons having boiling points up to 925°F. at temperatures from 0° to 1000°F. at pressures from 1 atm. to 1000 psi. The data were further used to develop a relation for estimating K-values in the critical and retro-grade regions of complex hydrocarbon mixtures.

White and Brown found that the K-values for components of complex mixtures are generally the same for the same components in different mixtures except as they are influenced by the approach to the critical conditions.

Kirkbride and Bertetti (27) reported K-values for methane, ethane, propane, n-butane and n-pentane in three types of absorber oil. The range of pressure was 125 to 3100 psi and the average temperature about 85°F. The three types of absorber oil were paraffinic, aromatic and naphthenic. The K-values at a given temperature and pressure were found to be dependent on the type of lean oil used.

In 1944 Standing and Katz (63) reported on the composition and densities of coexisting vapor and liquid phases as a function of pressure and temperature for four hydrocarbon systems prepared from crude oil and natural gas. The data were observed over a range of pressures from 1000 to 8220 psi and at temperatures ranging from 35 to 250°F.

The compositions of the hydrocarbon systems were such that the

critical temperatures of the mixtures were lower than the range of investigation. Under these conditions it was shown that the composition of the system has a marked effect on both the absolute value of the equilibrium constants and the change of the constants with pressure for the several components comprising the system. At pressures above 1000 psi the effect of the composition of the system on the equilibrium constant-pressure relationship becomes very important. Also it was shown that the heptanes and heavier fraction K-values do not approach unity in the same manner as the lighter components.

Hanson and Brown (19) prepared two five-component mixtures of volatile paraffin hydrocarbons having critical temperatures of approximately 100°F. and critical pressures of about 2000 psi. K-value determinations were made on these mixtures at 100°F. at pressures up to that of the single phase. The results indicated that the K-values of the volatile paraffin hydrocarbons in binary or complex mixtures of paraffins may be defined by specifying the temperature, pressure and convergence pressure corresponding to the equilibrium temperature.

Roland (52) obtained K-values for a natural gas-crude oil mixture at pressures from 1000 to 10,000 psi and temperatures of 120 and 200°F. An analysis of the experimental data showed that variables other than temperature, pressure and the general type of system are important in determining the K-values. These variables are the relative amount of each component present in the mixture. The word 'component' refers to each individual chemical component.

Roland also noticed the appearance of colored hydrocarbons in all the high pressure vapor-phase samples. The degree of color shown was roughly an indication of the pressure of the equilibrium, the higher

the pressure the darker the liquid.

K-values for carbon dioxide in a natural gas-condensate system were determined by Poettman and Katz (41) over the range of 1-10 mole per cent carbon dioxide. The densities and molecular weights were determined for saturated vapor and liquid phases for 24 hydrocarbon mixtures containing carbon dioxide at temperatures from 100 to 250°F. and pressures from 500 to 2900 psi.

The data showed that the lower the molecular weight of the hydrocarbon in the binary carbon dioxide systems, the greater the deviation from ideal behavior. The K-values for carbon dioxide in the carbon dioxide-natural gas-condensate system deviate the most from ideal K-values.

Rzasa (54) used a windowed cell to study a methane-Kensol 16 system at pressures to 25,000 psi and temperatures to 260°F. It was shown that for the temperature range 60 to 260°F. that this particular system exists in two phases to a pressure of approximately 14,000 psi. Data are presented giving the relative amounts of liquid and vapor phases coexisting under these conditions.

Poettmann (43) studied the vaporization characteristics of carbon dioxide in a natural gas-crude oil system at 38, 120 and 202°F. at pressures from 600 to 8500 psi. A variation of carbon dioxide up to 12 mole per cent in the composite showed no effect on the K-values of the hydrocarbon constituents or on the K-value of the carbon dioxide itself. It was shown that carbon dioxide is more soluble in crudes than in distillates which is contrary to the behavior of methane.

Jacoby and Rzasa (21) obtained K-values for nitrogen, methane, ethane, hydrogen sulfide and carbon dioxide in two natural gas-absorber

oil mixtures and in two natural gas-crude oil mixtures.

For each mixture of constant over-all composition, data were obtained at 100, 150 and 200° F. and at various pressures in the range of 200-5000 psi. Some effects of composition on the K-values were obtained to serve as a guide in choosing K-values for engineering calculations on other mixtures. The effects of composition were so mingled with pressure effects that it was impossible to segregate the effects.

Solomon (61) obtained vapor-liquid equilibrium data on mixtures of methane-ethylene-isobutane with the following absorber oils: n-hexadecane, dicyclohexyl, methylnaphthalene, Mid-Continent virgin gas oil and hydroformer still bottoms. The data were taken at 100 and 220° F. and at 500 and 1000 psia.

Solomon was interested in correlating his experimental data with the Kellogg K-value charts (6). In order to do this, he found that it was necessary to characterize the liquid phase by some property indicating paraffinicity or aromaticity. This was in addition to the characterization of both the liquid and vapor phase by molal average boiling points. Solomon introduced the quantity 'a' defined as follows:

$$a = \frac{K_{\text{observed}}}{K_{\text{Kellogg charts}}} \quad (\text{II-1})$$

The values of 'a' were found to be correlatable with the Watson characterization factors (60) for the equilibrium liquid phases. This relationship was shown to be essentially independent of temperature and pressure.

Hoffmann, Crump and Hocutt (23) obtained equilibrium constants

for a gas-condensate system by first obtaining field samples from two different wells, one completed in the oil zone and the other in the gas cap. Portable test equipment, consisting of several high pressure separators, was used in the field to make the equilibrium measurements. There was great scatter in the experimental data, probably due to the field conditions of the measurements.

Vagtborg (69) obtained K-values for nitrogen, carbon dioxide and hydrogen sulfide in a reservoir fluid containing 35 mole percent hydrogen sulfide at 154° F. in the pressure range of 700-2500 psia.

Vagtborg found that when large amounts of hydrogen sulfide are present, the K-values for ethane and the heavier hydrocarbons are greater than the values in systems containing little or no hydrogen sulfide. Large amounts of hydrogen sulfide have the reverse effect on the K-values for methane.

Evans and Harris (14) reported K-values for methane through heptanes-plus in two natural gas-crude oil mixtures from a common source. The experimental data were obtained at 190° F. and 1000-6000 psi.

The primary objective of this work was to show the effect of varying the amount of the heptanes-plus while holding the relative amounts of the other components constant. Most previous investigators varied the composition by changing the gas-oil ratio. If the fluids used to make up the mixtures contained components which were common to both fluids, the relative amounts of these components would not remain constant in the resulting mixtures. In this investigation the mixtures were recombined in such a manner that this effect would be eliminated.

Evans and Harris concluded from the experimental data that for the systems investigated, the equilibrium ratios for methane and the heptanes-plus fraction remain reasonably constant when the concentration of the heptanes-plus is decreased by a factor of two. The effect of a decrease in the heptanes-plus served mainly to extend the pressure region over which these ratios were defined. Decreasing the amount of the heptanes-plus does have a slight effect on the K-values of the intermediate components, ethane through the hexanes; the net effect being a small increase at the higher pressures.

### Experimental Methods

Experimental vapor-liquid equilibrium measurements have occupied many investigators over the last 75 years. Few scientific fields have produced so many devices and modifications of these devices for the measurement of a single property. Yet there is not agreement today on which apparatus and technique is best for making vapor-liquid equilibrium determinations.

The experimental techniques and apparatus used in obtaining vapor-liquid equilibrium data have been reviewed in some detail by Barr-David (5), Robinson and Gilliland (49) and Hipkin (20). A brief word picture of the experimental devices and techniques used will now be presented.

#### Constant Volume Apparatus

The simple bomb appears at first glance to be the simplest apparatus for making vapor-liquid equilibrium measurements. In the bomb method the sample is placed in a closed evacuated vessel. The



vessel is then agitated by rocking or by internal mixing at constant temperature until the two phases are at equilibrium. Theoretically, equilibrium is attained after sufficient time has elapsed.

The main difficulty with the constant volume apparatus is that the mass of material in the gas phase is small at low pressures and withdrawing enough sample for analysis upsets the equilibrium appreciably. For this reason the constant volume bomb is used mostly for measurements where the pressure is high enough that the vapor sample amounts to less than 10% of the gas phase volume.

Other problems associated with the constant volume bomb are chiefly mechanical. These include the problems of the design of the agitator and thermostat. Magnetic agitation is preferable to direct mechanical agitation.

#### Variable Volume Bomb

During sampling from the constant volume bomb there are pressure changes due to the removal of material. These pressure changes can be large in magnitude. In order to avoid these pressure changes, one adds a confining fluid such as mercury to the system while the samples are being taken in order to prevent vaporization or condensation. Connolly (9) and Evans and Harris (14) used the variable volume cell in recent studies.

Sage, Lacey et al.(55) have used the variable volume bomb with great success in their work. These investigators were able to determine the vapor-liquid K-values for binary mixtures without composition analyses of the phases. This was done by charging a known weight of the binary mixture to the bomb and then monitoring the amount of the liquid phase with an internal probe. The procedure of Sage and Lacey has the

advantage of eliminating the dead volume of sample lines and the equilibrium uncertainty caused by the withdrawal of the vapor sample. Furthermore, the problem of component analysis, often the weakest step in a vapor-liquid equilibrium determination, is eliminated in this procedure.

#### Bubble and Dew Point Method

This technique consists of introducing a mixture of known composition into an evacuated equilibrium cell of variable volume. The system temperature is held constant. The mixture is pressured with mercury, and two pressures are measured - the pressure at which the first condensation occurs from the vapor and the pressure at which the first bubble of vapor appears in the liquid.

The dew and bubble point curves of pressure vs. temperature for a number of different mixtures are obtained and, by cross-plotting, the conditions of phase equilibrium are found by locating points at which saturated liquid and saturated vapor exist at the same temperature and pressure.

The pressures at the dew and bubble points are determined in two ways. In one method the dew and bubble points are visually observed. In the other method the pressure isotherm is measured and plotted with the dew and bubble points being observed as discontinuities in the curve. The discontinuities are not always well defined, e.g., wide boiling mixtures and mixtures near the critical. The major limitation to this technique is that it is restricted to binary systems. The phase rule shows that complex systems are not a unique function of temperature and pressure and hence the dew and bubble points can not by

themselves define the composition of two equilibrium phases.

#### The Dynamic Flow Method

In the dynamic flow method the vapor is bubbled slowly through one or more cells containing liquid. The gas should become saturated if the liquid and gas have been intimately contacted. Following the contacting period vapor and liquid samples are removed and analyzed.

The major theoretical problem with the dynamic flow method is that true equilibrium may be impossible, since the static head in the bubbler requires that the entering gas be at higher pressure than the gas leaving the liquid phase.

Entrainment is also possible in the dynamic flow cell. Any liquid phase mechanically carried over with the gas will change the composition of the liquid in subsequent bubblers when more than one bubbler is used. Entrainment is minimized by low gas velocities, but then a corollary problem arises in that the gas may not be adequately mixed with the liquid.

#### Dynamic Distillation Method

The dynamic distillation method was a popular technique for obtaining vapor-liquid equilibrium data during the period 1875 to 1915. The method is no longer used (20) but will be discussed briefly because of its long period of use.

A liquid mixture was boiled batchwise in a still and its vapor condensed into a receiver. Since the composition of both the liquid and the condensate changed as the condensate changed while distillation proceeded, a large still charge was used and relatively small

condensate samples were taken and analyzed. The condensate composition was plotted against the volume of distillate and the curve was extrapolated back to zero volume distilled. This zero volume composition was assumed to be in equilibrium with the original still charge.

The assumption is made that the vapor over a boiling liquid is in equilibrium with it. Since the vapor may well be superheated, this assumption is not correct.

Additional problems must be considered. Heat leak from the vapor through the walls of the still can cause condensation which changes the vapor composition, i.e., the vapor entering the condenser would be of different composition from that leaving the liquid. Entrainment, the non-homogeneity of the liquid and temperature control are difficulties often encountered in this technique.

For these reasons, and because the device never reaches steady state, the dynamic distillation still is no longer used.

#### The Liquid Recirculation Method

The dynamic distillation method can be converted to steady state operation by recycling the condensate back to the still. This recycling of the condensate is the essence of the liquid recirculation method.

One assumes that the vapor and liquid phases are in equilibrium when the steady state has been reached. This assumption presents the most important problem in the liquid recirculation method, that is, that the steady state condition is not necessarily a true equilibrium condition. As in the dynamic distillation method, the question of equilibrium can be traced to the still itself. If the vapor in the

still is not in equilibrium with the boiling liquid, then continued recirculation will not bring the system closer to equilibrium. This follows from the fact that vapor is being continuously generated from the liquid, and the condensate returning to the still merely maintains it at some steady state composition.

The fact that many good data have been obtained by this technique indicates that the vapor composition is not generally far from the true equilibrium composition.

The basic liquid recirculation still is that of Othmer. This is simple to construct and easy to operate. Because of these advantages, more atmospheric pressure systems have been run in Othmer stills than in any other apparatus. There have been many modifications made of the basic Othmer still. Hala et al. (18) list over 49 papers which present modifications, by other authors, of the basic Othmer still.

The Othmer still is not restricted to use at atmospheric pressure. Williams (71) modified an Othmer still for vacuum work. Othmer (36) himself describes an apparatus for superatmospheric determinations.

#### The Vapor Recirculation Method

In the vapor recirculation method, vapor is continuously removed from the top of the equilibrium cell and recirculated to the bottom of the cell where it is contacted with the liquid phase. This method is, in fact, the dynamic flow method with vapor recirculation.

The vapor recirculation apparatus does bring the liquid and vapor phase into equilibrium as circulation is continued if we ignore the static head that causes the gas entering the liquid to be under a

different pressure than the gas leaving and, therefore, at a different equilibrium condition. Ignoring the static head effect, which we can do at high pressures, it can be seen that any differential amount of the vapor phase will be subjected to diffusional forces on each pass through the liquid, and will change in composition until these diffusional forces become infinitesimal.

At this point, the vapor is in equilibrium with the liquid and additional contacting will not change the composition of either phase. It should be pointed out that this is not the case when the vapor is returned to the equilibrium cell as condensate.

In operation, the system must be completely pressure tight, otherwise, steady state will never be reached. The quantities of liquid and vapor must be kept constant during recirculation. The vapor flow rate must be kept constant during recirculation. The vapor flow rate must be kept constant in order to maintain a constant pressure drop through the system. Finally, condensation of the vapor must not occur, since this will change the vapor composition. If the vapor is slightly superheated, then no difficulty will be encountered.

Dodge and Dunbar (10) took the vapor from the equilibrium cell from their low temperature bath, passed it through a mercury pump at room temperature and then bubbled the vapor through the liquid in the equilibrium cell.

The mercury pump varied the enclosed volume of the system causing pressure fluctuations. Aroyan and Katz (4) modified this arrangement to eliminate the pressure fluctuations during gas circulation by using a magnetic pump which maintained a constant volume during the movement of the gas phase. This pump has been described in the literature by

Exline and En Dean (15).

The vapor-liquid equilibrium measurements of Aroyan and Katz were made for the most part at sub-ambient temperatures. In obtaining equilibrium the vapor was removed from the cell and circulated by a pump at room temperature. The vapor then passed through a cooling coil before it was bubbled through the liquid. Vapor circulation was continued for two hours before sampling.

Roberts and McKetta (48) used a magnetic pump for vapor recirculation. Their pump was located inside a constant temperature bath with the equilibrium cell. These investigators found that a one hour circulation time was needed to insure the attainment of equilibrium. However, in most cases the circulation of the vapor was maintained for four hours. The pumping rate used was 20-25 strokes/minute at 10-15 cc/stroke. At the end of the recirculation at least one hour was allowed for the phases to separate.

#### This Study

The vapor recirculation method is used in this study. The apparatus used is, for the most part, identical to that used by Michels (31). The pressure balance, pressure bench, gas compressor and equilibrium cell were manufactured by W. C. t'Hart and Zn, Rotterdam, Holland. Vapor is recirculated by means of a magnetic pump. Calibrated volumetric traps are provided for measuring the densities of the equilibrium phases. A detailed description of the apparatus used in this study is presented in Chapter IV. This experimental procedure is discussed in Chapter V.

## CHAPTER III

### THEORY, THERMODYNAMIC CONSISTENCY AND CORRELATION METHODS

#### The Criteria of Equilibrium

A system is in the equilibrium state if the rates of change in either direction between the phases are equal and if no apparent change in the intensive properties with respect to time can be observed. The intensive properties themselves, such as concentration, partial molal enthalpy, density, etc., however, may, in general be different in the different phases of the system. The only requirement for a system to be in the equilibrium state is that all of the potentials (driving forces) which cause changes be in a well balanced state. A system is not in equilibrium unless the temperature (thermal potential) is the same everywhere. Also the pressure (mechanical potential) must be the same everywhere.

Another driving force, namely, chemical potential, must be balanced in the case of vapor-liquid equilibria. The term 'chemical potential' originated with Gibbs (16). Chemical potential is the driving force which causes the transfer of substances among the coexisting phases.

We can then summarize the necessary and sufficient conditions for equilibrium in an isolated heterogeneous system as

$$T^I = T^{II} = T^{III} = \dots \quad (III-1)$$

$$P^I = P^{II} = P^{III} = \dots \quad (III-2)$$



$$\mu_1^I = \mu_1^{II} = \mu_1^{III} = \dots \quad (\text{for all } i) \quad (\text{III-3})$$

where the primes refer to different phases.

Gibbs also deduced the important phase rule

$$D = N - \Phi + 2 \quad (\text{III-4})$$

where  $D$  = degrees of freedom, or the number of independent intensive thermodynamic variables

$\Phi$  = the number of phases in the  $N$ -component system

#### Chemical Potential and the Gibbs - Duhem Equation

Consider a closed system, i.e., a system in which the mass is constant. The 'First Law of Thermodynamics', a conservation of energy statement, for this closed system is written

$$dU = \delta Q + \delta W \quad (\text{III-5})$$

where  $dU$  = the change in internal energy of the system, energy units

$\delta Q$  = an infinitesimal quantity of heat added to the system, energy units

$\delta W$  = an infinitesimal amount of work performed on the system, energy units

The  $\delta Q$  and  $\delta W$  terms are not properties of the state of the system and are, therefore, not exact differentials. The internal energy term,  $dU$ , is an exact differential, the value of the internal energy being fixed for a given state of the system.

Reversible work is expressed as follows for a system in which pressure is the only force acting on the system

$$\delta W = - PdV \quad (\text{III-6})$$

where  $P$  = the total pressure exerted on the system, force/unit area

$V$  = the system volume

The 'Second Law of Thermodynamics' deals with energy degradation and states the for a reversible process

$$\delta Q = TdS \quad (\text{III-7})$$

where  $T$  = the absolute temperature of the system, degrees

$S$  = the entropy of the system, energy/degree

Combining equations III-5, III-6 and III-3, one obtains a fundamental equation of equilibrium for a one component homogeneous system in which only mechanical forces are acting.

$$dU = TdS - PdV \quad (\text{III-8})$$

Enthalpy is defined as

$$H = U + PV \quad (\text{III-9})$$

Differentiating

$$dH = dU + PdV + VdP \quad (\text{III-10})$$

Combining Equations III-8 and III-10

$$dH = TdS + VdP \quad (\text{III-11})$$

The 'Gibbs free energy' of the system is defined as

$$G = H - TS \quad (\text{III-12})$$

Differentiating

$$dG = dH - TdS - SdT \quad (\text{III-13})$$

Combining Equations III-11 and III-13

$$dG = VdP - SdT \quad (\text{III-14})$$

Equation III-14 is the equivalent form of Equation III-8, using the free-energy function.

Now let us consider an open system, i.e., a system of variable mass. The Gibbs free energy of this system will not only be a function of temperature and pressure, but also of the amount of each component present.

$$G = G(T, P, n_1, \dots, n_N) \quad (\text{III-15})$$

where  $n_1, \dots, n_N$  = the number of moles of components 1,  $\dots$ , N, respectively

N = the total number of components in the system

Differentiating Equation III-15

$$dG = \left( \frac{\partial G}{\partial T} \right)_{P, n_i} dT + \left( \frac{\partial G}{\partial P} \right)_{T, n_i} dP + \sum_{i=1}^N \left( \frac{\partial G}{\partial n_i} \right)_{T, P} dn_i \quad (\text{III-16})$$

where  $\sum_{i=1}^N$  = the summation over all components of the system, i.e., from 1 to N. The symbol  $\sum$  will be used in following equations for simplicity.

One obtains from Equation III-14 the following

$$\left( \frac{\partial G}{\partial P} \right)_{T, n_i} = V \quad (\text{III-17})$$

$$\left( \frac{\partial G}{\partial T} \right)_{P, n_i} = -S \quad (\text{III-18})$$

Combining Equations III-16, III-17, and III-18

$$dG = -SdT + VdP + \sum \left( \frac{\partial G}{\partial n_i} \right)_{T,P} dn_i \quad (\text{III-19})$$

Following the method of Guggenheim (17), let us consider a system at constant temperature and pressure. For this system Equation III-15 becomes

$$dG = \sum \left( \frac{\partial G}{\partial n_i} \right)_{T,P} dn_i \quad (\text{III-20})$$

If we allow the quantity of each component in the system to change by an amount proportional to itself, i.e.,

$$dP = dT = 0 \quad \text{and} \quad dn_i = n_i d\xi_i \quad (\text{III-21})$$

where  $d\xi_i$  = the fractional change in the system mass  
then the Gibbs free energy will also change by

$$dG = G d\xi_i \quad (\text{III-22})$$

Combining Equations III-20, III-21 and III-22

$$G d\xi_i = \sum \left( \frac{\partial G}{\partial n_i} \right)_{T,P} n_i d\xi_i \quad (\text{III-23})$$

Dividing by  $d\xi_i$

$$G = \sum \left( \frac{\partial G}{\partial n_i} \right)_{T,P} n_i \quad (\text{III-24})$$

Chemical potential is defined as

$$\mu_i = \left( \frac{\partial G}{\partial n_i} \right)_{T,P} \quad (\text{III-25})$$

Therefore,

$$G = \sum \mu_i n_i \quad (\text{III-26})$$

Equation III-26 was obtained by a special integration but it is generally valid.

Differentiating Equation III-26

$$dG = \sum \mu_i dn_i + \sum n_i d\mu_i \quad (\text{III-27})$$

Equating the right hand side of Equation III-19 and Equation III-27

$$\sum n_i d\mu_i = -SdT + VdP \quad (\text{III-28})$$

Equation III-28 is the most general form of the Gibbs-Duhem Equation.

It may be recalled that the mole fraction of a component in a system is

$$x_i = n_i / \sum n_i \quad (\text{III-29})$$

If we divide Equation III-28 by  $\sum n_i$ , the total moles in the system, and then make use of Equation III-29, then

$$\sum x_i d\mu_i = -\underline{S}dT + \underline{V}dP \quad (\text{III-30})$$

where the subscript  $\underline{\quad}$  indicates the value of the property per mole.

Equation III-30 is written for the liquid phase. It is made equally applicable to the vapor phase by replacing  $x_i$  with  $y_i$ .

Equation III-28 or III-30 is the basis for thermodynamic consistency tests. Both of these equations involve the use of chemical potential.

### Fugacity and Vapor-Liquid Equilibrium

While fundamental, chemical potential is not readily suitable for

practical applications. For this purpose Lewis (28) invented fugacity which is related to chemical potential and bears resemblance to pressure. Lewis defined the fugacity,  $f$ , as

$$d\bar{G} = RT \, d\ln f \quad (\text{III-31})$$

$$\lim_{P \rightarrow 0} \left( \frac{f}{P} \right) = 1.0 \quad (\text{III-32})$$

The fugacity of a component in a solution may be defined by

$$\left[ d\mu_i = RT \, d\ln \bar{f}_i \right]_{T,n} \quad (\text{III-33})$$

where  $\bar{f}_i$  denotes the fugacity of component 'i'.

At constant temperature

$$\left[ d\mu_i = d\bar{G} = V dP = RT \, d\ln \bar{f}_i \right]_{T,n} \quad (\text{III-34})$$

For an ideal gas  $V = RT/P$ , hence

$$\left[ d\mu = d\bar{G} = V dP = RT \, d\ln P \right]_{T,n} \quad (\text{III-35})$$

Equations III-34 and III-35 illustrate the resemblance in nature between fugacity and pressure.

In the case of a mixture at very low pressure, the fugacity of component 'i' in the mixture equals the partial pressure of component 'i'. Namely,

$$\lim_{P \rightarrow 0} \bar{f}_i = x_i P \quad (\text{III-36})$$

where  $x_i$  is the mole fraction of component 'i' and  $x_i P$  is the partial pressure of component 'i'.

At equilibrium, the fugacities of every one of the components in

one of the co-existing phases in the system must be equal to that of the corresponding component in the other phase of the system.

$$f_i^L = f_i^V \quad i = 1 \text{ to } N \quad (\text{III-37})$$

The superscripts V and L represent the vapor and liquid phases, respectively.

### The Evaluation of Fugacity

If we subtract  $RT \ln P$  from both sides of Equation III-33, we obtain

$$RT \, d \ln \left( \frac{f}{P} \right) = V dP - RT \, d \ln P = \left( V - \frac{RT}{P} \right) dP \quad (\text{III-38})$$

or 
$$d \ln \frac{f}{P} = \left( \frac{V}{RT} - \frac{1}{P} \right) dP \quad (\text{III-39})$$

Integrating at constant temperature from  $P = 0$  to some particular pressure  $P = P^*$ , we obtain

$$\ln \left( \frac{f}{P} \right)_{P=P^*} - \ln \left( \frac{f}{P} \right)_{P=0} = \int_0^{P^*} \left( \frac{V}{RT} - \frac{1}{P} \right) dP \quad (\text{III-40})$$

In view of Equation III-32

$$\ln \left( \frac{f}{P} \right)_{P=P^*} = \int_0^{P^*} \left( \frac{V}{RT} - \frac{1}{P} \right) dP \quad (\text{III-41})$$

Equation III-41 gives the fugacity at  $P$  and  $T$  in terms of an integrand which can be computed either from experimental data or by means of an equation of state.

### The Fugacity of a Component in a Mixture

At constant temperature and constant composition, the following thermodynamic relation exists

$$d\mu_i = \bar{V}_i dP \quad (\text{III-42})$$

where  $\bar{V}_i$  is the partial molal volume of component 'i'

Combining Equations III-31 and III-42

$$RT \, d \ln f_i = \bar{V}_i \, dP \quad (\text{III-43})$$

Subtracting  $RT \, d \ln P$  from both sides of the above equation for the isothermal case

$$RT \, d \ln (f_i/P) = \bar{V}_i \, dP - RT \, d \ln P = \left( \bar{V}_i - \frac{RT}{P} \right) dP \quad (\text{III-44})$$

Rearranging

$$d \ln (f_i/P) = \left( \frac{\bar{V}_i}{RT} - \frac{1}{P} \right) dP \quad (\text{III-45})$$

Integrating at constant temperature from  $P=0$  to  $P=P^*$  one obtains

$$\ln \left( \frac{f_i}{P} \right)_{P=P^*} - \ln \left( \frac{f_i}{P} \right)_{P=0} = \int_0^{P^*} \left( \frac{\bar{V}_i}{RT} - \frac{1}{P} \right) dP \quad (\text{III-46})$$

Now if we introduce Equation III-36 as a limiting condition, we obtain

$$\ln \left( \frac{f_i}{x_i P} \right)_{P=P^*} = \int_0^{P^*} \left( \frac{\bar{V}_i}{RT} - \frac{1}{P} \right) dP \quad (\text{III-47})$$

Both Equations III-41 and III-47 can be used to calculate the fugacity



of vapor (or gas), or liquid provided that PVT data or an equation of state for the gas or the liquid is available. The evaluation of the partial molal volume from experimental data by graphical means is tedious and to a degree inaccurate. If an equation of state applicable to the mixture under consideration is available, then a more accurate evaluation of the mixture fugacity can be made.

### Thermodynamic Consistency Tests

Vapor-liquid equilibrium data are generally used either directly in process design calculations or in the development of new theories and correlations for such data. It is often necessary to know the accuracy of the experimental data before it is used.

There is no procedure available for terming experimental data as unquestionably correct. However, means are available for detection of much of the incorrect data. Certain thermodynamic considerations may be employed to derive relations which the data must obey if the data are correct. The Gibbs-Duhem equation, Equation III-28, is one such relation. It must be pointed out that compliance with the Gibbs-Duhem equation is a necessary, but not sufficient condition for vapor-liquid equilibrium data to be correct. Data which do not obey this relation are definitely incorrect. Various thermodynamic consistency tests have been based on the Gibbs-Duhem equation and are designed specifically for the testing of vapor-liquid equilibrium data. Robinson (50) realizing that there was confusion and often inaccuracies in the literature with regard to applications of the Gibbs-Duhem equation, prepared an excellent review of the subject of thermodynamic consistency. The reader is referred to the work of Robinson for the detailed

discussion of these tests. The following discussion is supplemental to Robinson's work.

Thompson (65) in testing his vapor-liquid equilibrium data for hydrogen-six carbon hydrocarbon systems was interested in a rigorous test for thermodynamic consistency in terms of K-values. The consistency test in the form proposed by Adler and coworkers (1) appeared to be a most useful test since they used experimental and not derived quantities in the test. Robinson (50) presented the derivation of Adler's isothermal test

$$\int_{K_1(0)}^{K_1(x_1)} x_1 d \ln K_1 + \int_{K_2(1)}^{K_2(1-x_1)} x_2 d \ln K_2 = \int_{P(0)}^{P(x_1)} \left[ Z^L + \bar{Z}_1^V y_1 \left( \frac{1}{K_2} - \frac{1}{K_1} \right) - \frac{Z^V}{K_2} \right] d \ln P \quad (\text{III-48})$$

$$\text{where} \quad \bar{Z}_1^V = \frac{P \bar{V}_1^V}{RT} \quad (\text{III-49})$$

The above equation is thermodynamically rigorous for an isothermal system, however, it does involve the assumption of the Lewis and Randall rule.

Thompson tested his hydrogen-benzene data at 250 °F. for the pressure range of 44.67 to 2000 psia using Equation III-48. He found a difference of 12.6% between the left and right hand sides of Equation III-48. This difference indicates a significant lack of agreement between Thompson's equilibrium composition data and volumetric data when the Lewis and Randall rule is assumed in the development of the Adler consistency test.

Thompson and Edmister (12,66,67) derived an isothermal consistency

equation omitting the assumption of the Lewis and Randall rule. The resulting expression which is similar to Equation III-48 follows

$$\begin{aligned} & \int x_1 (1 + y_1 \xi_1) d \ln K_1 + \int x_2 (1 + y_1 \xi_1) d \ln K_2 \\ &= \int \left[ Z^L + y_1 \bar{Z}_1^V \left( \frac{1}{K_2} - \frac{1}{K_1} \right) - \frac{Z^V}{K_2} \right] d \ln P \end{aligned} \quad (\text{III-50})$$

where

$$\xi_1 = \frac{1}{RT} \int_0^P \frac{\partial \bar{V}_1}{\partial y_1} dP \quad (\text{III-51})$$

and

$$\bar{Z}^V = \frac{P \bar{V}^V}{RT} \quad (\text{III-52})$$

The right hand side of Equation III-50 can be split into a liquid term and a vapor term. This, plus rearrangement, gives

$$\begin{aligned} & \int x_1 (1 + y_1 \xi_1) d \ln K_1 + \int x_2 (1 + y_1 \xi_1) d \ln K_2 \\ &= \int (Z^L - 1) d \ln P + \int Z' d \ln P \end{aligned} \quad (\text{III-53})$$

where

$$Z' = 1 + \frac{1}{K_2} (\bar{Z}_1^V - Z^V) - \bar{Z}_1^V \quad (\text{III-54})$$

If the vapor phase is ideal,  $Z'$  and the  $\xi_1$  terms reduce to zero. If the Lewis and Randall rule holds for the vapor phase,  $\xi_1$  is zero and Equation III-52 reduces to Adler's equation.

Thompson (66) derived a formula for  $\xi_1$  using a truncated form of the Berlin form virial equation of state. This derivation has been reproduced in Tully's thesis (68) and will not be repeated here.

Thompson rechecked his 250 °F. experimental data for the hydrogen-

benzene system using Equation III-53. He found a difference of 0.35% between the left and right hand sides of Equation III-53 indicating that his data are indeed consistent whereas the data were shown to be inconsistent when the Adler thermodynamic consistency test was used. This points up the danger of using the Adler test.

Several comments are in order concerning the consistency test as given by Equation III-53. First, the test is difficult to apply in that all of the terms in the equation are not directly obtainable from the experimental data. The values of the mole fractions, pressure and the K-values are obtained directly from the experimental data. Volumetric data, either experimental data or data obtained from equations of state, are required to complete the calculations. The evaluation of the liquid compressibility term can often be based on the extrapolation of existing volumetric data. As mentioned previously, the Berlin form of the virial equation can be used to evaluate  $\xi$ . Finally, the Leiden form of the virial equation of state can be used to evaluate  $Z^V$  and  $\bar{Z}_i^V$ .

Thompson and Edmister (67) found that Equation III-53 is not very sensitive to errors in the x-y data. Furthermore, they showed that the equation of state chosen to evaluate the compressibility factors can have an effect on the results of the test.

Edmister (12) recently derived a thermodynamic consistency test. The derivation of this isothermal test appears below.

The derivation can be started with Equation III-30, a form of the Gibbs-Duhem equation.

$$\sum x_i du_i = -SdT + VdP \quad (\text{III-30})$$

Fugacity was defined in Equation III-31 as

$$\left[ dp_i = RT \, d \ln f_i \right]_{T,n} \quad (\text{III-31})$$

Substituting Equation III-31 into Equation III-30 and dividing through by  $RT$

$$\frac{v^L}{RT} \, dP - S \, dT = x_1 \, d \ln \bar{f}_1^L \quad (\text{III-55})$$

At constant temperature

$$-S \, dT = 0 \quad (\text{III-55a})$$

and Equation III-55 becomes

$$\frac{v^L}{RT} \, dP = x_1 \, d \ln \bar{f}_1^L + x_2 \, d \ln \bar{f}_2^L \quad (\text{III-56})$$

Equation III-56 is written for the liquid phase and is equally applicable to the vapor phase if  $x_i$  is replaced by  $y_i$ . For the vapor phase, Equation III-56 becomes

$$\frac{v^L}{RT} \, dP = y_1 \, d \ln \bar{f}_1^V + y_2 \, d \ln \bar{f}_2^V \quad (\text{III-57})$$

For a binary mixture  $x_2 = 1 - x_1$  and  $y_2 = 1 - y_1$ , then Equation III-56 becomes

$$x_1 (d \ln \bar{f}_1^L - d \ln \bar{f}_2^L) + d \ln \bar{f}_2^L = \frac{v^L}{RT} \, dP \quad (\text{III-58})$$

and Equation III-57 becomes

$$y_1(d\ln \bar{f}_1^V - d\ln \bar{f}_2^V) + d\ln \bar{f}_2^V = \frac{V^V}{RT} dP \quad (\text{III-59})$$

Applying the criterion of equilibrium

$$\bar{f}_i^L = \bar{f}_i^V \quad (\text{III-60})$$

$$\text{Then} \quad \ln \bar{f}_i^L = \ln \bar{f}_i^V \quad (\text{III-61})$$

$$\text{and} \quad d\ln \bar{f}_i^L = d\ln \bar{f}_i^V \quad (\text{III-62})$$

Substituting Equation III-62 into Equation III-58

$$x_1(d\ln \bar{f}_1^V - d\ln \bar{f}_2^V) + d\ln \bar{f}_2^V = \frac{V^L}{RT} dP \quad (\text{III-63})$$

Now subtracting Equation III-63 from Equation III-59

$$(y_1 - x_1) (d\ln \bar{f}_1^V - d\ln \bar{f}_2^V) = \frac{V^V - V^L}{RT} dP \quad (\text{III-64})$$

Rearranging

$$\frac{d\ln (\bar{f}_1^V / \bar{f}_2^V)}{dP} = \frac{V^V - V^L}{(y_1 - x_1)RT} \quad (\text{III-65})$$

The fugacity coefficient of component 1 in the vapor phase mixture of a binary is defined as

$$\phi_1^V = \bar{f}_1^V / P y_1 \quad (\text{III-66})$$

Then 
$$\ln \frac{\bar{f}_1^V}{f_1^V} = \ln \phi_1^V + \ln P + \ln y_1 \quad (\text{III-67})$$

and 
$$\ln \frac{\bar{f}_2^V}{f_2^V} = \ln \phi_2^V + \ln P + \ln y_2 \quad (\text{III-68})$$

Subtracting Equations III-68 from III-67

$$\ln \frac{\frac{\bar{f}_1^V}{f_1^V}}{\frac{\bar{f}_2^V}{f_2^V}} = \ln \frac{\phi_1^V}{\phi_2^V} + \ln \frac{y_1}{y_2} \quad (\text{III-69})$$

Substituting Equation III-69 into Equation III-65

$$\left( \frac{d \ln \frac{\phi_1}{\phi_2}}{dP} \right) = \left( \frac{\underline{v}^V - \underline{v}^L}{(y_1 - x_1)RT} \right) - \left( \frac{d \ln \frac{y_1}{y_2}}{dP} \right) \quad (\text{III-70})$$

Equation III-70 is the differential relationship for thermodynamic consistency testing of isothermal data. The integral form of this test follows

$$\int d \ln \frac{\phi_1}{\phi_2} + \int d \ln \frac{y_1}{y_2} = \int \frac{\underline{v}^V - \underline{v}^L}{RT (y_1 - x_1)} dP \quad (\text{III-71})$$

Due to the nature of the data taken in this work, the above discussion of recent developments in the field of thermodynamic consistency tests has been confined to isothermal tests. The interested reader is referred to a discussion of recent developments in isobaric consistency tests by Tully (68).

#### Correlation of Vapor-Liquid Equilibrium Data

Vapor-liquid equilibrium data are normally correlated by using

the component distribution coefficient, or vapor-liquid equilibrium ratio. By definition

$$K_i = \frac{y_i}{x_i} = \frac{\text{mol fraction of component 'i' in vapor phase}}{\text{mol fraction of component 'i' in liquid phase}} \quad (\text{III-72})$$

Application of the Gibbs phase rule (Equation III-4) to a binary system shows that the composition of the equilibrium phases is invariant if the system temperature and pressure are specified. The K-value is also a function of the identity of the component in question and the identity of the other component present. Application of the phase rule to a N-component system shows that the specification of temperature and pressure leaves N-2 variables, or relations between variables, to be specified in order for the system to be invariant. For any one temperature and pressure, the K-value of a given component is thus a function of the composition of the equilibrium phases.

Equilibrium ratios can be evaluated by five methods:

Raoult's and Dalton's laws

Ideal equilibrium ratio calculations

Equations of State

High pressure activity coefficients

Empirical correlations

Each method has its advantages and predicts K-values that agree with experimental K-values over limited ranges. Each of the above methods has been reviewed previously by this writer in great detail (64).

There is no need to repeat this discussion here.

Recent Developments in K-Value Correlation Techniques



The recent developments in the correlation of vapor-liquid equilibrium data, not included in the writer's review of this subject (64), will now be discussed.

In 1960, Prausnitz, Edmister and Chao (44) suggested using the following relationship for correlating vapor-liquid equilibrium K-ratios

$$K_i = \frac{y_i}{x_i} = \frac{\gamma_i^L \nu_i^L}{\phi_i^V} \quad (\text{III-73})$$

where  $\gamma_i^L = \frac{\bar{f}_i^L}{f_i^L x_i}$  = the liquid phase activity coefficient for component 'i'

$\nu_i^L = \frac{f_i^L}{P}$  = the liquid phase fugacity coefficient for the pure component 'i'

$\phi_i^V = \frac{\bar{f}_i^V}{P y_i}$  = the vapor phase fugacity coefficient for component 'i'

The three coefficients,  $\gamma_i^L$ ,  $\nu_i^L$ , and  $\phi_i^V$  are evaluated at system conditions, i.e., the temperature and pressure of the system. The reference state for the liquid activity coefficient is the same pure component fugacity that appears in the  $\nu_i^L$  term, thus making the numerator terms,  $\gamma_i^L$  and  $\nu_i^L$  compatible.

The Redlich-Kwong (46) equation of state was used in the original paper to evaluate  $\phi_i^V$  and the Scatchard-Hildebrand relationship (59) was used for evaluating  $\gamma_i^L$ . The Scatchard-Hildebrand 'regular solution theory' equation uses molar liquid volumes and solubility parameters in the following equation

$$\ln \gamma_i^L = - \frac{v_i^L (\delta - \bar{\delta})^2}{RT} \quad (\text{III-74})$$

where  $V_i^L$  = the molar liquid volume of component 'i' assumed to be independent of pressure, but a function of temperature

$\delta_i$  = the solubility parameter of component 'i'

$\bar{\delta}$  = the liquid volume average solubility parameter for the entire mixture

$$\bar{\delta} = \frac{\sum x_i V_i \delta_i}{\sum x_i V_i} \quad (\text{III-75})$$

For light gaseous solutes, for which the pure liquid state would be imaginary, the values of  $V_i$  and  $\delta_i$  would be hypothetical and are evaluated from experimental composition data. The work of Prausnitz, Edmister and Chao demonstrated the following:

1. The calculation of light hydrocarbon vapor-liquid equilibria by use of solubility parameters appears to give correctly the liquid phase composition effects. The solubility parameter is a useful tool for the correlation and prediction of hydrocarbon vapor-liquid equilibria.
2. Composition-corrected K-values are not convenient to apply in practical problems and this method is no exception.
3. A simplification can be obtained by taking the solubility parameter to be pressure insensitive.

Chao and Seader (8) developed a general K-value correlation using the equation used by Prausnitz, Edmister and Chao in their work (Equation III-73). Chao and Seader used the Redlich-Kwong (46) equation of state to evaluate  $\phi_i^V$  and the Scatchard-Hildebrand equation (59) to evaluate  $\gamma_i^L$ . Values of  $\gamma_i^L$ , the pure component liquid fugacity coefficient, were back-calculated from over 3000 sets of experimental x-y data using

the following equation

$$\gamma_i^L = \frac{(y_i/x_i)_{\text{experimental}}}{(\gamma_i^L)_{\text{S-H}}} (\phi_i^V)_{\text{R-K}} \quad (\text{III-76})$$

An empirical correlation was then developed for  $\gamma_i^L$  as a function of reduced temperature, reduced pressure and the acentric factor. Separate  $\gamma_i^L$  equations were derived for hydrogen and methane with all other components being covered by the generalized correlation. Recently, Erbar (12) developed separate  $\gamma_i^L$  equations for hydrogen sulfide, carbon dioxide and nitrogen.

The Chao-Seader K-value correlation has been programmed for a number of digital computers by Erbar (12). These programs were developed for the Natural Gas Processors Association. The equations in the Chao-Seader correlation can be solved to get K-values if the compositions of the coexisting vapor and liquid phases are known (given, assumed or from a previous trial). In applying this method, it is necessary to check bubble point, dew point or flash calculations to see if the resulting compositions agree with those used in the K-value predictions.

A second correlation method can be developed by starting again with the Prausnitz, Edmister and Chao (44) expression (Equation III-73). The fugacity coefficient of a pure liquid component  $\gamma_i^L$ , can be written as follows

$$\gamma_i^L = \gamma_i^o \frac{p_i^o}{P} \exp \frac{V_i^L(P - p_i^o)}{RT} \quad (\text{III-77})$$

where  $\gamma_i^o = f_i^V/p_i^o$  = the fugacity coefficient of pure component 'i' at the saturation or vapor pressure.

$\gamma_i^o$  will be the same for saturated liquid and saturated vapor for a pure component

$$\exp \frac{V_i^L (P - p_i^o)}{RT} = \text{the Poynting effect or the ratio of the fugacity of the liquid at the system pressure to the value at the vapor pressure}$$

$\gamma_i^L$  is the liquid phase fugacity coefficient that appears in the Chao-Seader equation. An equation of state which is available for calculating accurate fugacity coefficients of the vapor phase components can be used for the calculation of  $\gamma_i^o$ . The analytical equations of Stuckey (64) can be used to evaluate  $V_i^L$  and  $p_i^o$ .

An expression for predicting K-values can now be obtained by combining Equations III-73 and III-77

$$K_i = \frac{p_i^o}{P} \frac{\gamma_i^L \gamma_i^o}{\phi_i^V} \exp \frac{V_i^L (P - p_i^o)}{RT} \quad (\text{III-78})$$

A third K-value correlation method can be developed by substituting

$$\gamma_i^o = \gamma_i^V \exp \int_{p_i^o}^P \frac{1}{RT} \left( V_i^V - \frac{RT}{P} \right) dP \quad (\text{III-79})$$

into Equation III-78 to obtain

$$K_i = \left( \frac{p_i^o}{P} \right) \frac{\gamma_i^V \gamma_i^L}{\phi_i^V} \exp \frac{V_i^L (P - p_i^o)}{RT} \exp \int_P^{p_i^o} \left( V_i^V - \frac{RT}{P} \right) dP \quad (\text{III-80})$$

where  $\gamma_i^V = (f/P)^V =$  the fugacity coefficient of component 'i' as a pure vapor at the system temperature and pressure

The imperfection pressure correction,  $\Theta$ , was defined to permit the evaluation of correction factors to be applied to Raoult's K-value.

From the definition of fugacity and the criteria for vapor-liquid equilibrium, we can write

$$\begin{aligned}
 K_i &= \frac{y_i}{x_i} = \frac{\frac{f_i^L}{x_i}}{\frac{f_i^V}{y_i}} = \frac{\frac{f_i^L}{f_i^L} \frac{f_i^L}{x_i}}{\frac{f_i^V}{f_i^V} \frac{f_i^V}{y_i}} = \frac{\frac{f_i^L}{p_i^o}}{\frac{f_i^V}{P}} \frac{p_i^o}{P} \\
 &= \frac{\gamma_i^L}{\gamma_i^V} \frac{1}{\Theta} \frac{p_i^o}{P} \quad (\text{III-81})
 \end{aligned}$$

where  $\gamma_i^L$  and  $\gamma_i^V$  are activity coefficients expressing departure from ideal solutions or mixtures in liquid and vapor mixtures

$$\Theta = \frac{f_i^V / P}{f_i^L / p_i^o} = \text{the imperfection pressure correction}$$

$(f_i^L / p_i^o)$  = the fugacity/pressure ratio for pure liquid at the system conditions, i.e., the fugacity at P and T divided by the vapor pressure at T

$$(p_i^o / P) = K_{\text{Raoult's}}$$

$$K_{\text{Ideal}} = (1/\Theta) K_{\text{Raoult's}}$$

$$\text{But } \ln (f_i^V / P)_P = \int_{p_i^o}^P \left( V_i^V - \frac{RT}{P} \right) dP \quad (\text{III-82})$$

$$\text{and } \ln (f_i^L / p_i^o)_P = \ln (f_i^V / P)_{p_i^o} + \frac{1}{RT} \int_{p_i^o}^P V_i^L dP \quad (\text{III-83})$$

We can write the definitions of the imperfection pressure correction in logarithmic form

$$\ln \Theta_i = \ln (f_i^V / P)_P - \ln (f_i^L / p_i^o)_P \quad (\text{III-84})$$

Combining Equations III-82, III-83 and III-84

$$\ln \Theta_i = \frac{1}{RT} \int_{P_i^o}^P \left( V_i^V - \frac{RT}{P} \right) dP - \frac{1}{RT} \int_{P_i^o}^P V_i^L dP \quad (\text{III-85})$$

Now combining Equations III-80 and III-85

$$K_i = \frac{P_i^o}{P} \frac{1}{\Theta} \frac{\gamma_i^L \gamma_i^V}{\phi_i^V} = K_{\text{Ideal}} \frac{\gamma_i^L}{\gamma_i^V} \quad (\text{III-86})$$

The imperfection pressure correction,  $\phi_i^V$  and  $\gamma_i^V$  can be evaluated from an equation of state. The liquid activity coefficient,  $\gamma_i^L$ , can be calculated using the Scatchard-Hildebrand equation. The problem in using this method is that of finding an equation of state which will give satisfactory values for  $\Theta$ ,  $\phi_i^V$  and  $\gamma_i^V$ .

## CHAPTER IV

### EXPERIMENTAL APPARATUS

The vapor recirculation method was used in this work. This method is actually the dynamic flow method in closed-circuit form. In this chapter the flow diagram of the apparatus is presented and described. Details of the equilibrium cell and its supporting apparatus are discussed. Finally, the reagents used in this study are described.

#### Apparatus

For convenience the description of the equipment is divided into six sections: (1) feed, (2) pressure regulation and measurement, (3) equilibrium cell and thermostat, (4) density measurement, (5) vapor recirculation and (6) sampling and analysis. A schematic diagram of the experimental apparatus is shown in Figure 1.

#### Feed Section

Methane was fed from a supply cylinder through a gauge block, drying tube, CO<sub>2</sub> absorption tube and needle valve to the gas compressor. The 1/8" O.D. x 1/16" I.D. tubing, the fittings and valves in this section were 316 stainless steel. Pressure in this section was limited to 10,000 psi by the needle valves used. The drying tube was an Autoclave Engineers 30 cc. MD test tube reactor packed with commercial Drierite (calcium sulfate). The CO<sub>2</sub> absorption tube was likewise an

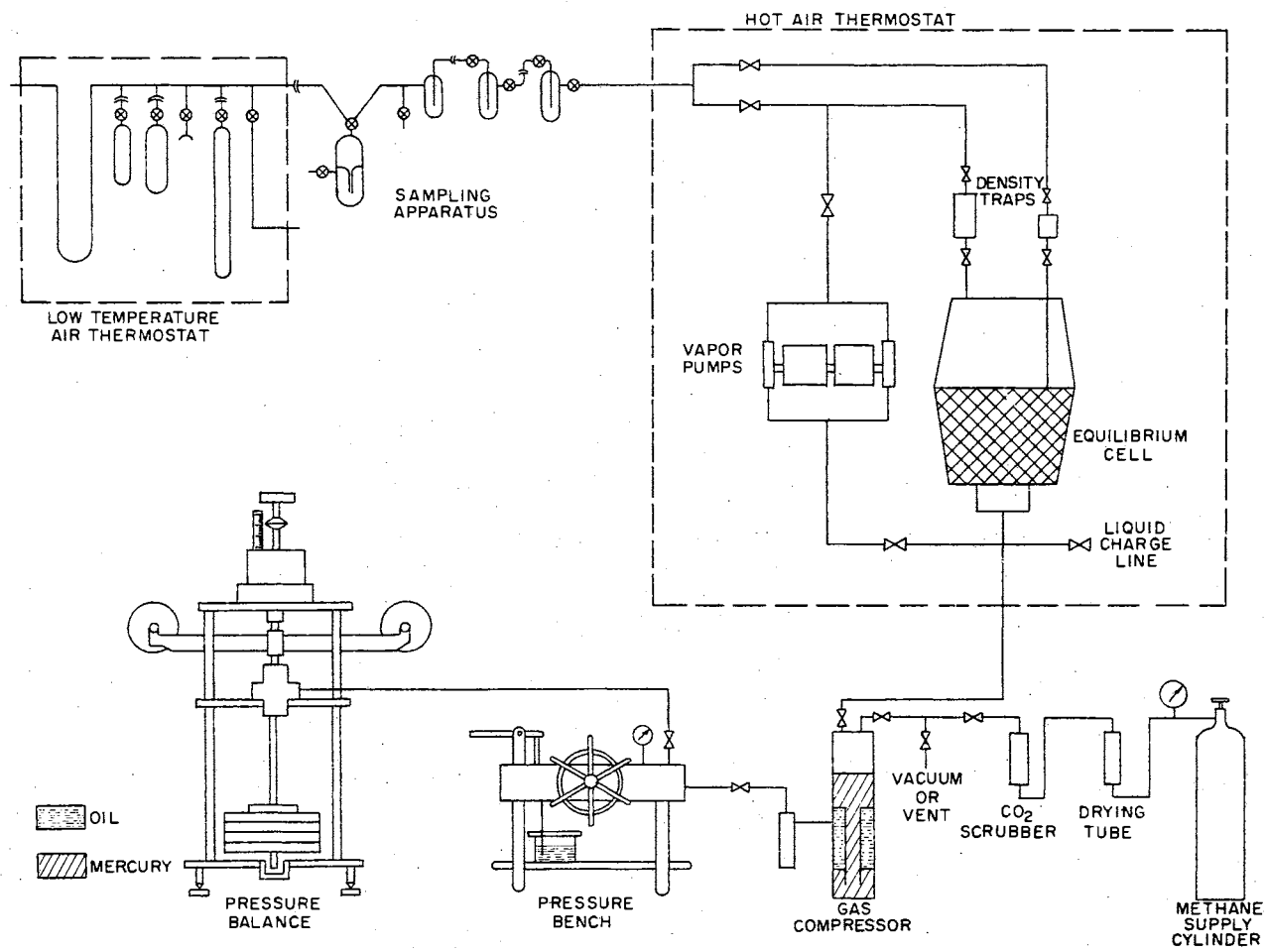


FIGURE 1  
 SCHEMATIC DIAGRAM OF APPARATUS



Autoclave Engineers 30 cc. MD test tube reactor and was packed with Ascarite, a sodium hydrate asbestos material. The maximum working pressure of the drying tube and the CO<sub>2</sub> absorption tube is 10,000 psi.

Liquid hydrocarbons were fed from a glass flask through a short section of 1/8" O.D. tubing to a needle valve at the bottom of the equilibrium cell, then through capillary tubing into the cell.

#### Pressure Regulation and Measurement Section

Pressure regulation and measurement were accomplished by the use of a Michels pressure balance in conjunction with a gas compressor. A pressure bench was used to generate and maintain the system pressure. The pressure balance, pressure bench, gas compressor and the equilibrium cell were manufactured by W. C. t'Hart and Zn, Instrumenten-en Apparatenfabriek N. V., Rotterdam, Holland.

The Michels Pressure Balance. The Michels pressure balance (32) is a dead weight tester distinguished by the use of a differential piston. The dead weight tester is one of the principal instruments used for measuring pressure. The operation of the dead weight tester is based on the use of a piston placed in a cylinder and loaded with a known weight. A sectional view of the piston-cylinder, or measuring cylinder, is shown in Figure 2. A drawing of the entire Michels balance is shown in Figure 3.

The complete pressure balance is mounted on a base-plate, P, which must be adjusted horizontally with levelling screws fitted under the plate. On this base plate are mounted three columns. A middle plate, M, and a top plate, N, are attached to these columns.

The differential piston, A, is connected to the weight axle, B,

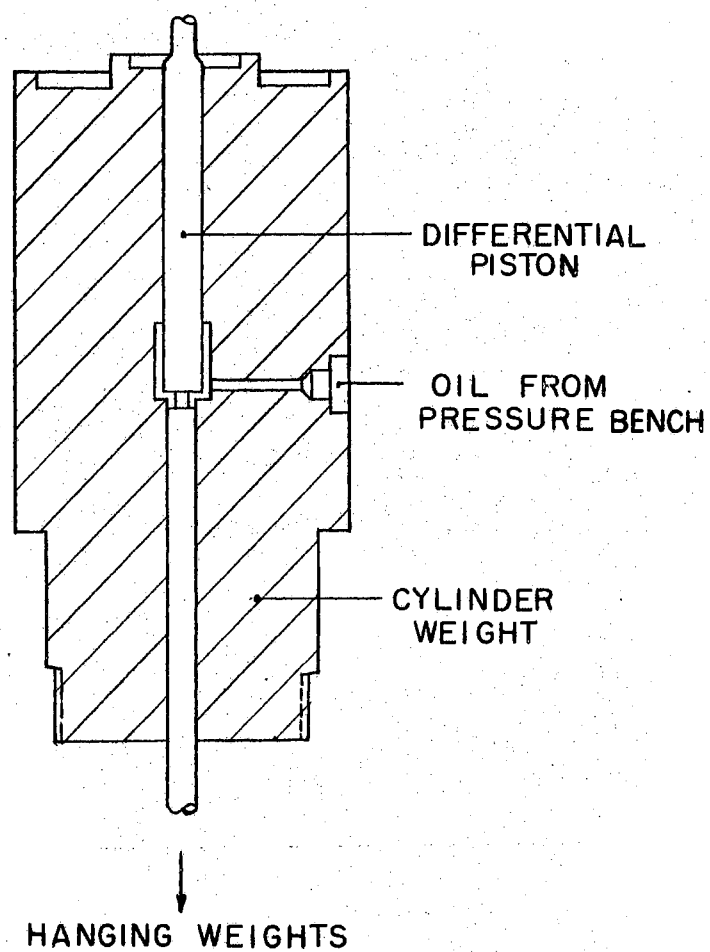


FIGURE 2

SECTIONAL VIEW OF  
HART PISTON-CYLINDER

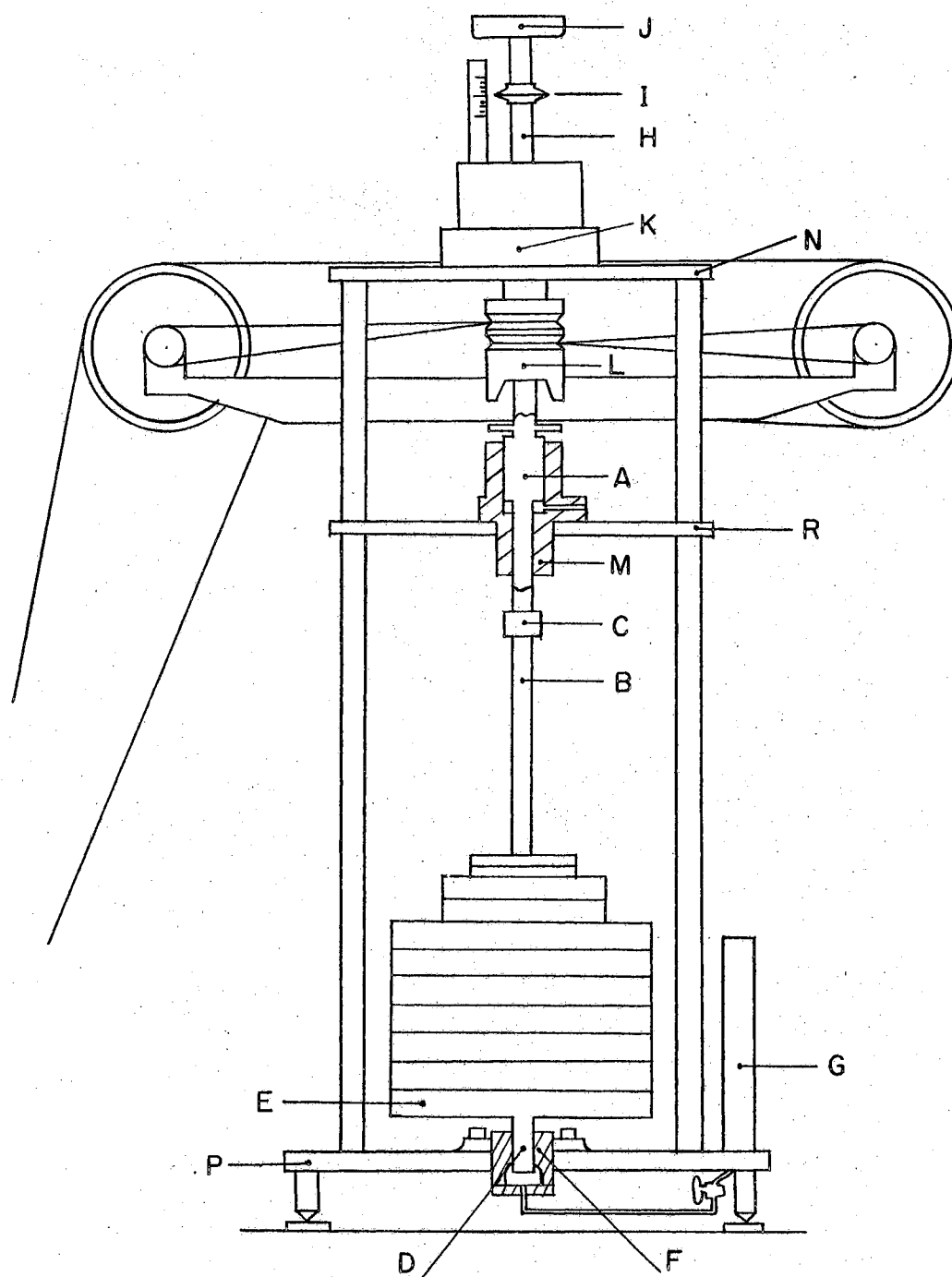


FIGURE 3  
THE MICHELS PRESSURE BALANCE

by a nut and half-ring joint, C. The weight axle has a guide pin, D, under the base weight, E. The guide pin runs in a bronze plain-bearing, F, which is also fitted to the base plate and which can be centered by four adjustment screws. The guide pin is lubricated with oil from the reservoir, G. The oil flows from the oil reservoir to the guide pin bearing via a copper capillary.

The measuring cylinder is placed on the middle plate, R. The top axle, H, is screwed onto the differential piston. The position indicator, I, and a weight pan, J, are mounted on the top axle.

A rotating clutch, K, around the top axle is used to lower the driving mechanism, L, which in turn contacts a claw on the piston. In order to rotate the claw, a round leather belt is put on the pulley of a  $\frac{1}{3}$  HP electric motor. This belt runs on two large pulleys fitted on the frame. From the shafts of the large pulleys two smaller ones are connected by two belts with a two-groove pulley running on ball bearings and a hollow axle. The claw is attached to this two-groove pulley. The claw is moved upward with a handle so that for very accurate measurements each vertical component of the driving forces can be eliminated.

The most essential part of the pressure balance is the measuring cylinder. This contains a pressure chamber which is connected to the pressure bench by a steel capillary. A hardened steel differential piston rotates in this precision cylinder. Pressure is obtained by pumping oil into cylinder M, lifting piston A and all other rotating parts.

The piston is kept rotating in order to minimize the friction between the piston and the wall of the cylinder. The oil supplied by

the pressure bench provides a thin lubricating film between the piston and the cylinder wall. The piston rotates at about 71 rpm.

The pressure range of the measuring cylinders depends on the effective area of the differential piston and the weight attached to the piston. Large weights (1 to 25 Kg) are loaded on the base weight, E. Small weights (less than 1 Kg) are placed in the weight pan, J.

The maximum allowable pressure for the pressure balance is 3,000 atm. In practice, a set of nine piston-cylinders is used to cover the entire pressure range. The balance used in this study was equipped with eight of the piston-cylinders and could be used to measure pressures from 3-2250 atmospheres. The balance is claimed to be accurate to approximately 1 part in 10,000 and to have a precision of 1 part in 100,000. The calibration of the balance and the piston-cylinders is described in Appendix A.

Pressure Bench. A sketch of the pressure bench is presented in Figure 4. A hand pump is provided for pumping oil from the oil reservoir into the system. A screw press provides a fine control of the system volume. A combination of valves and capillary tubing permit the pumping of oil to the pressure balance and/or the gas compressor. Drain lines, each equipped with a filter to remove small particles of foreign matter, are provided for removing oil from the system. A special petroleum oil having good viscosity-pressure properties was used in the system. This oil was filtered before addition to the oil reservoir. The pressure bench is rated at a maximum working pressure of 3000 atmospheres.

The Gas Compressor. A sectional view of the gas compressor is shown in Figure 5. The compressor is composed of an upper and lower

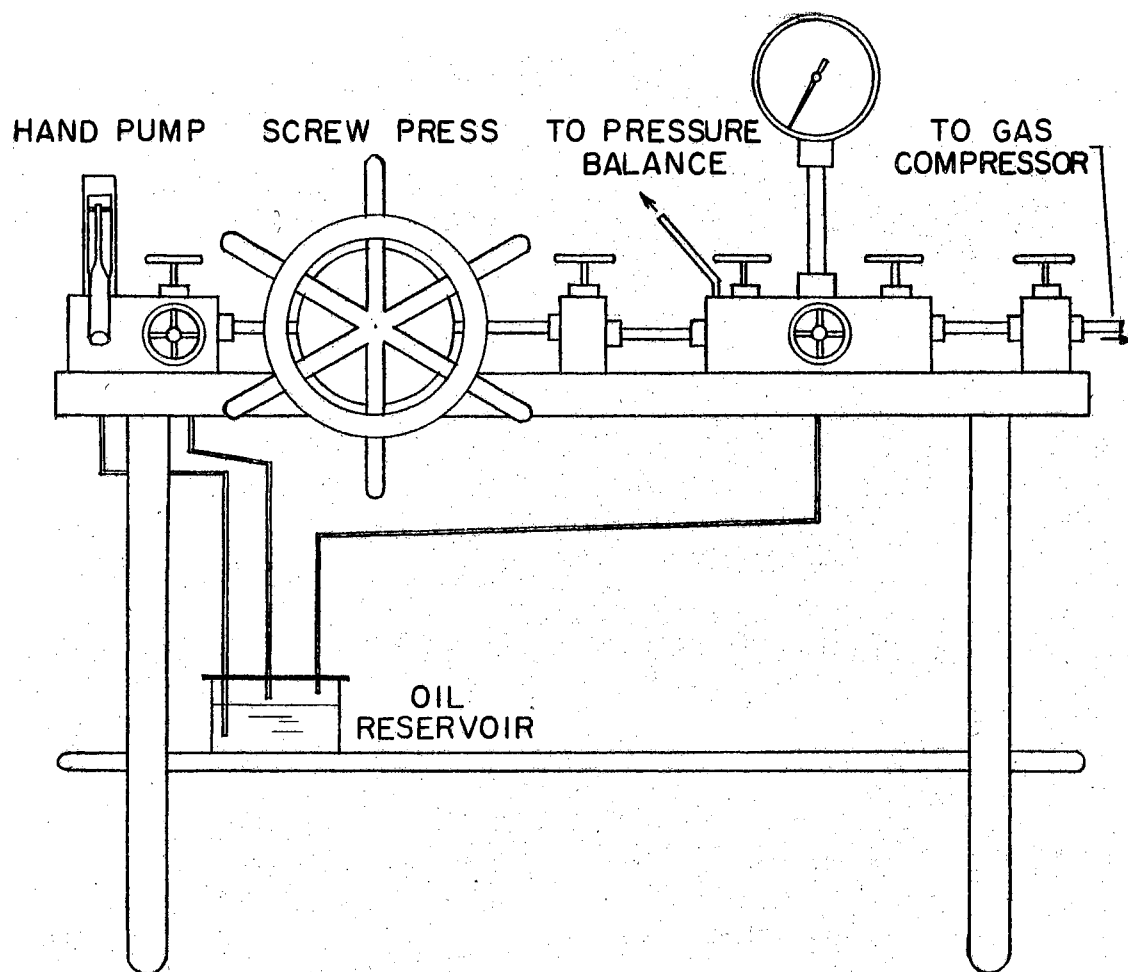


FIGURE 4  
THE HART PRESSURE BENCH

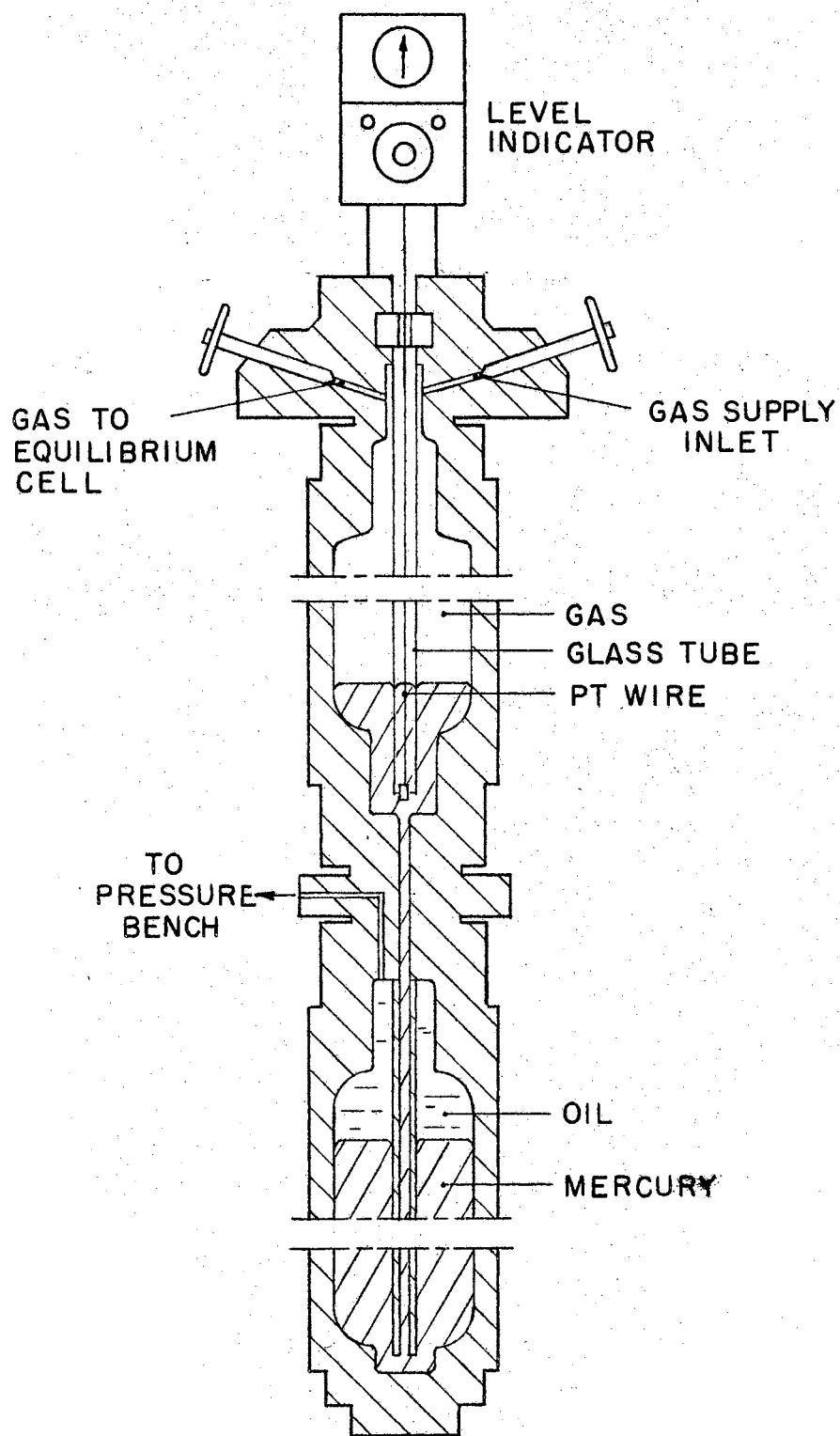


FIGURE 5  
SECTIONAL VIEW OF GAS COMPRESSOR

chamber which are connected by a short tube. Oil from the pressure bench flows into the upper end of the lower chamber on the top of mercury. The mercury, in turn, flows upward through the connecting center tube into the upper compartment. Gas is confined in the upper compartment. A trap (not shown) is provided should the mercury flow back into the incoming oil line. The gas inlet and outlet valves are located at the top of the compressor.

The position of the mercury meniscus in the upper compartment is measured by means of a bridge circuit. One leg of this circuit is a platinum wire which extends the length of the upper compartment. The calibration of the mercury level in the upper compartment as a function of the level indicator reading is described in Appendix D.

The capacity of the gas compressor is 500 cc. The maximum operating pressure is 1500 atmospheres.

#### The Equilibrium Cell and Thermostat

The Equilibrium Cell. The cell used is of the Michels design and is the cell used by Thompson (65) in his investigation of vapor-liquid equilibria for hydrogen-six carbon hydrocarbon binaries. A cross-sectional view of the equilibrium cell is presented in Figure 6.

Gas enters the cell through a capillary tube at the bottom of the cell. The gas stream is broken up into small streams by 0.05 mm. deep grooves in cone E. Further intimate contact of the gas and liquid in the cell is provided in a packed section of coarse woven fiberglass cloth 2-11/16" deep. Metal distributor plates, drilled with many conical-shaped holes, confine the fiberglass cloth top and bottom.

The vapor and liquid samples are removed through lines C and D,



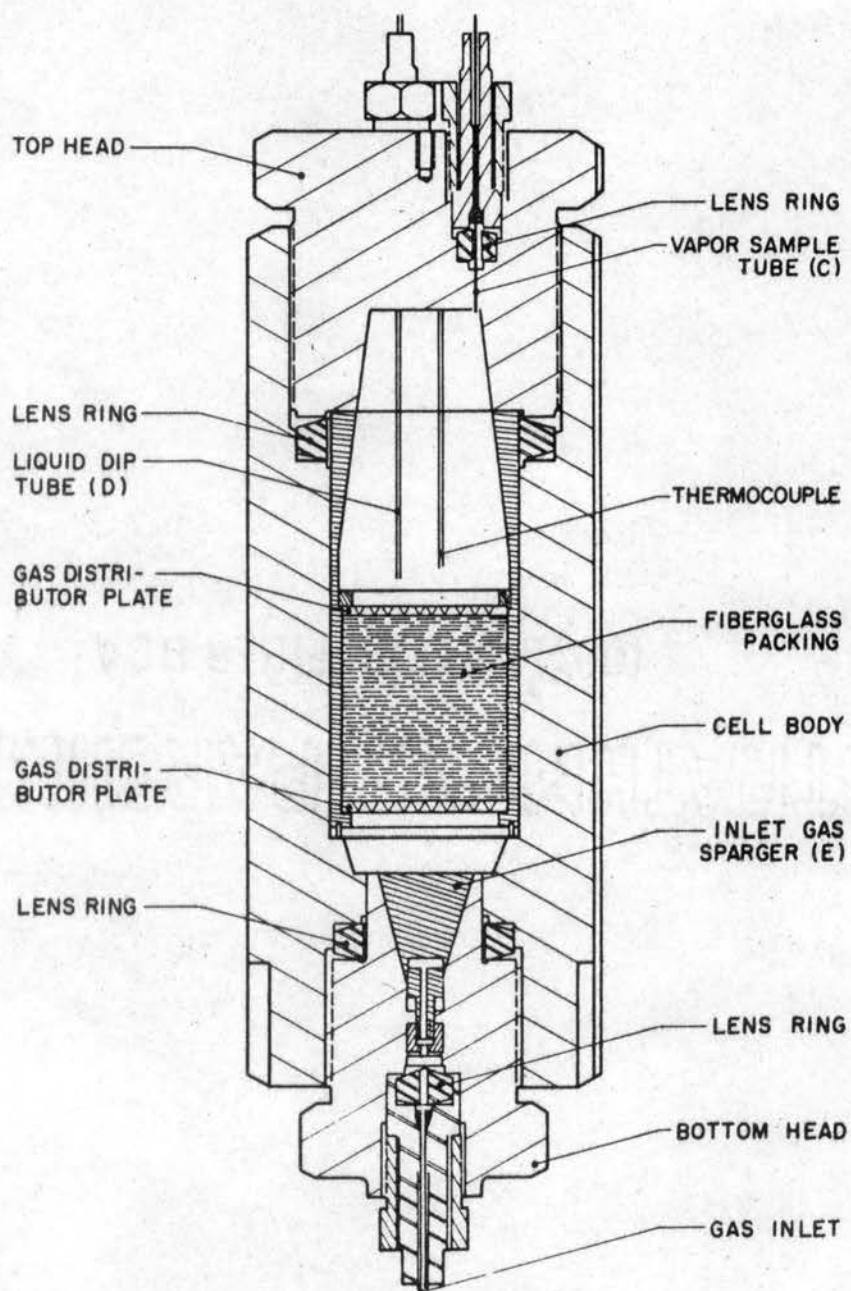


**FIGURE 6**  
**EQUILIBRIUM CELL**

respectively. The liquid dip tube D, extends 1-15/16" into the cell. The vapor outlet extends approximately 3/8" into the cell. All of the capillary tubing lines are 0.6 mm. I.D.

The total internal capacity of the equilibrium cell is approximately 150 cc. The cell and its parts are made for the most part from stainless steel. The maximum working pressure of the cell is 1000 atmospheres.

The Thermostat. A large air thermostat served as a constant temperature bath. The air thermostat has outside dimensions: 48" high, 48" wide and 34" deep. The inside dimensions are: 40 1/2" square and 25 3/4" deep. A large door supported by a piano hinge provided access to the equipment in the thermostat.

The inside walls of Transite were built around a steel frame which provided support for the walls of the air bath and a means of anchoring the equipment. The inner walls were composed of three alternate layers each of 1" Owens Corning PF-615 Fiberglass board and 0.001 guage Alcoa No. 5182 aluminum foil. Alternate layers of Fiberglass board were overlapped at the corners to eliminate convection currents. The outside of the bath was made of 3/4" plywood.

Air was circulated by means of a 6" squirrel cage blower located in one end of the bath. The blower was driven by a 1/2HP electric motor located outside the bath. The intake of the blower was located midway the height of the bath. The exhaust was directed across the electric strip heaters onto the rear wall of the bath. The capacity of the blower was 525 SCFM, providing approximately 21.5 captive air changes per minute in the bath. Sketches showing the blower and heater arrangement are presented in Figures 7 and 8.

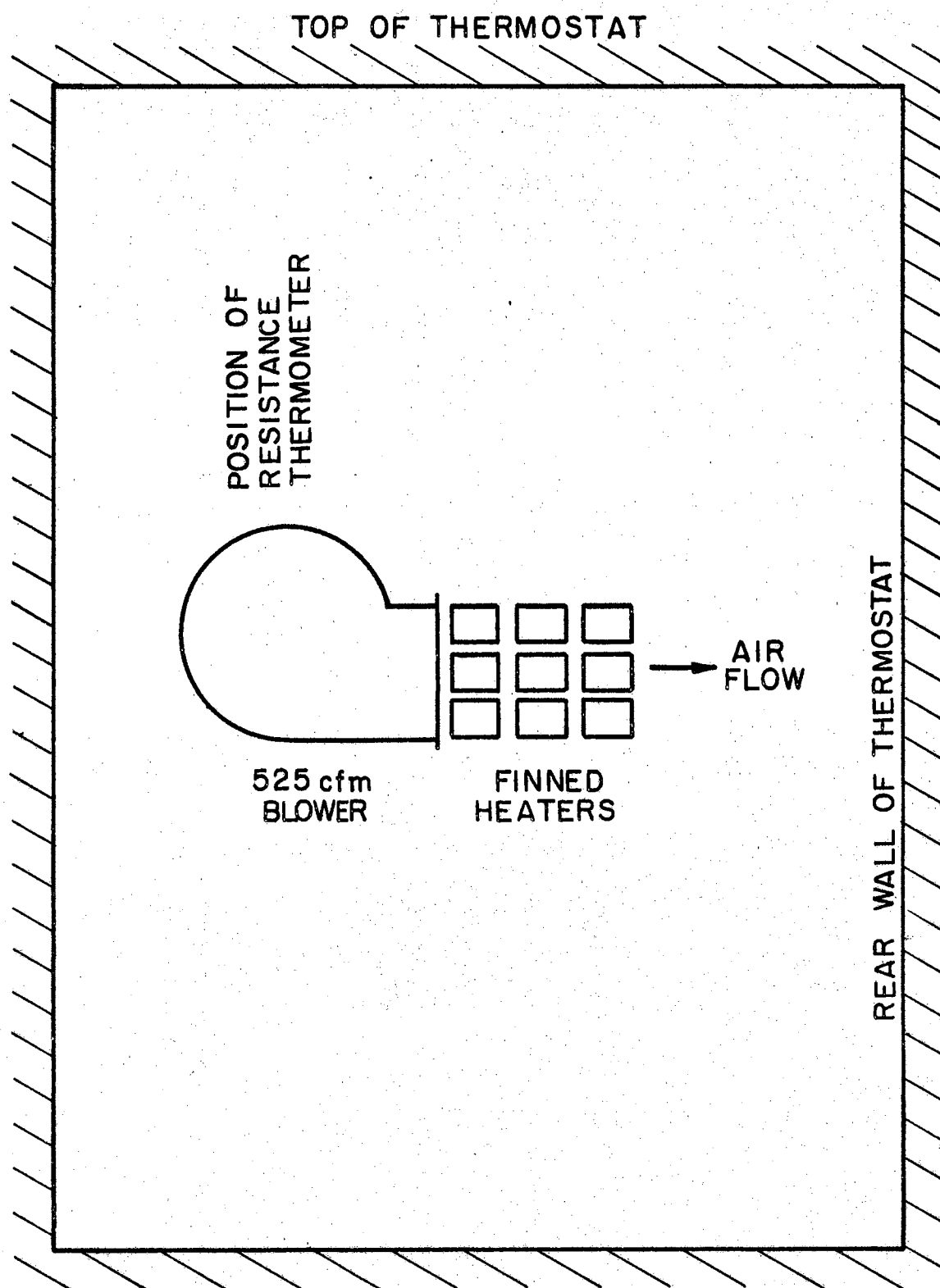


FIGURE 7  
HEATER AND BLOWER ARRANGEMENT  
SIDE VIEW OF THERMOSTAT

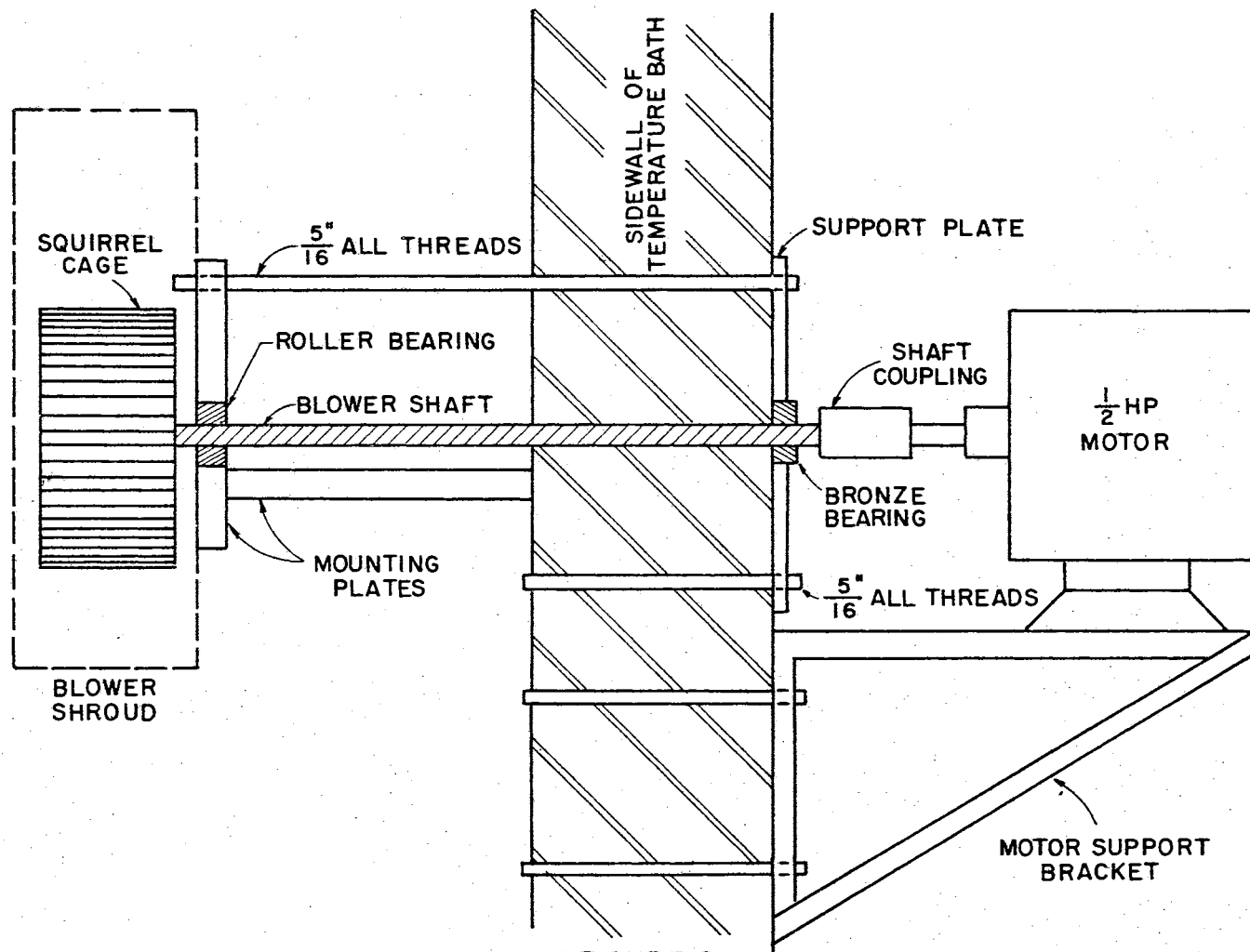


FIGURE 8  
BLOWER ASSEMBLY FOR HIGH  
TEMPERATURE THERMOSTAT

Heat was supplied by nine 250 watt Chromalox PTF-10 finned air heaters. These heaters were mounted in three banks, three high, at the blower discharge. Three heaters were controlled by a Superior Type 116 Powerstat. Three additional heaters were controlled by a similar Powerstat. The remaining three heaters were controlled by a Hallikainen Model 1053A Thermotrol temperature controller. A finned cooling coil 8" x 8" x 1½" deep, placed directly in front of the blower intake, was used to remove heat from the bath. Ethylene glycol from a chilling unit was pumped through this coil at a fixed rate. The use of the cooling coil greatly improved the temperature control of the air bath. A platinum resistance thermometer mounted at the mid-point of the cooling coil served as a sensing element for the Hallikainen controller. The resistance thermometer was a Rosemount No. 104-N, 24" long with a perforated shield especially designed for air temperature sensing.

#### Density Measurement

Samples of the equilibrium vapor and liquid phases were collected in calibrated traps located in the large air thermostat directly above and outside the equilibrium cell. A sketch of the traps is presented in Figure 9. The calibration of these traps is discussed in Appendix C.

The density traps were made from high pressure fittings available from Autoclave Engineers, Inc., Erie, Pennsylvania. Basically, the traps consisted of a high pressure coned and threaded nipple between two Hart valves. The nipple used for the liquid trap was 9/16" O.D. x 3/16" I.D. x 4" long. The nipple used for the vapor trap was 9/16" O.D. x 5/16" I.D. x 6" long. The nipples were connected to the valves

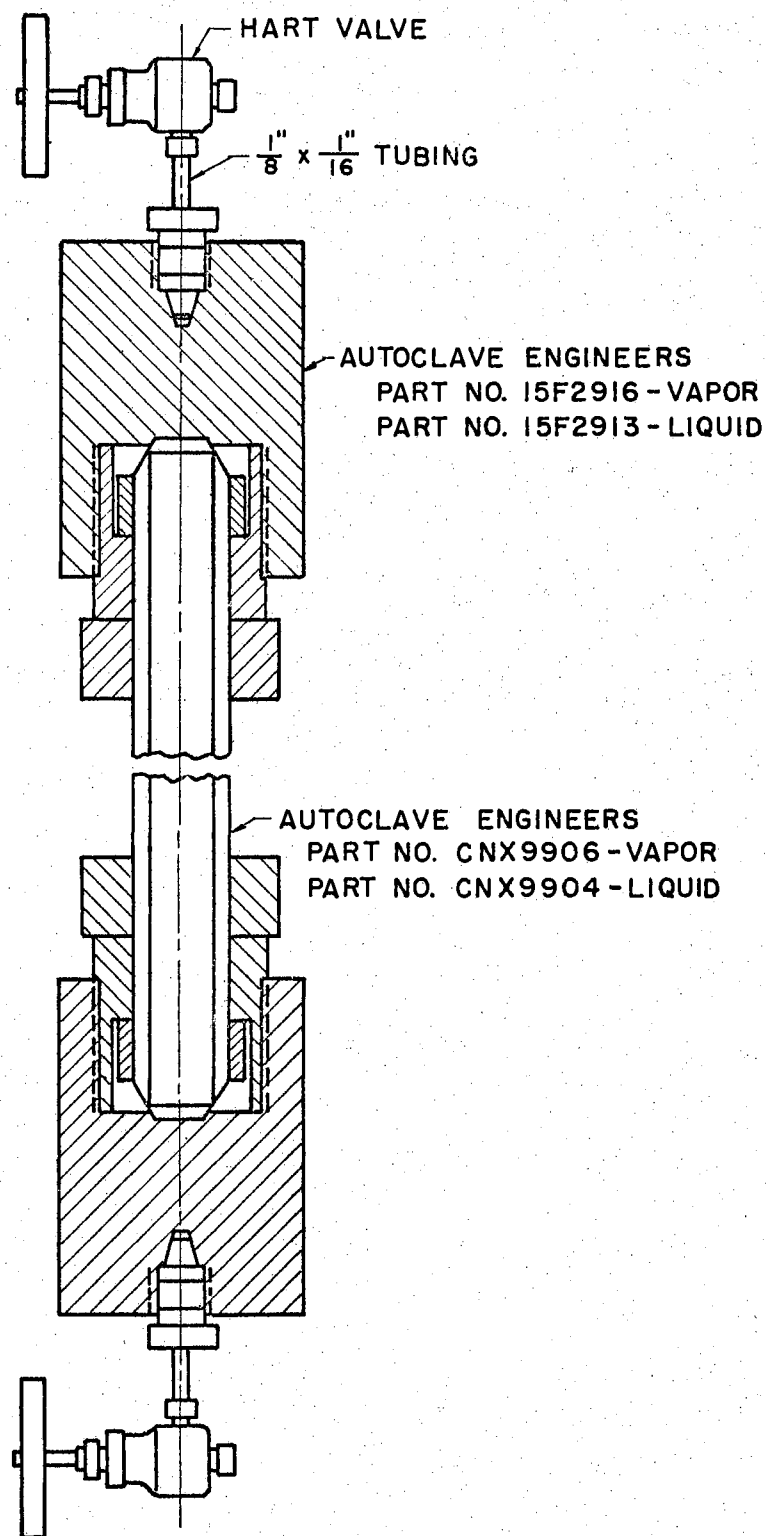


FIGURE 9  
VAPOR AND LIQUID DENSITY TRAPS

by the high pressure adapters noted on Figure 9.

Thermocouples taped to the outside of the traps were used to insure that the temperature of the traps was identical to that in the cell during sampling. The calibration of these thermocouples is presented in Appendix B.

#### Vapor Recirculation System

It will be recalled that in the vapor recirculation method, vapor is continuously removed from the top of the equilibrium cell and recirculated to the bottom of the cell where it is contacted with the liquid phase. A constant volume magnetic pump was built to circulate the vapor in this work. The pump was located in the large hot air thermostat.

Figure 1 shows the relation of the pump to the remainder of the apparatus. Vapor flows from the vapor zone in the equilibrium cell through the vapor density trap to the pump inlet. The flow splits at the pump inlet where a portion of the vapor is made available to each of the inlet check valves. This pump is actually two pumps in one. As one side of the pump is on the intake stroke, the other side is on the exhaust stroke. Vapor from the outlet check valves is combined at a tee and returned to the bottom of the equilibrium cell.

The mechanical details of this pump will be discussed with the aid of Figure 10. The portion of the pump in contact with the vapor is made of parts available from Autoclave Engineers Inc., Erie, Pennsylvania.

Vapor enters the pump through a  $\frac{1}{4}$ " high pressure tee and splits to two double ball angle check valves. The check valves are a

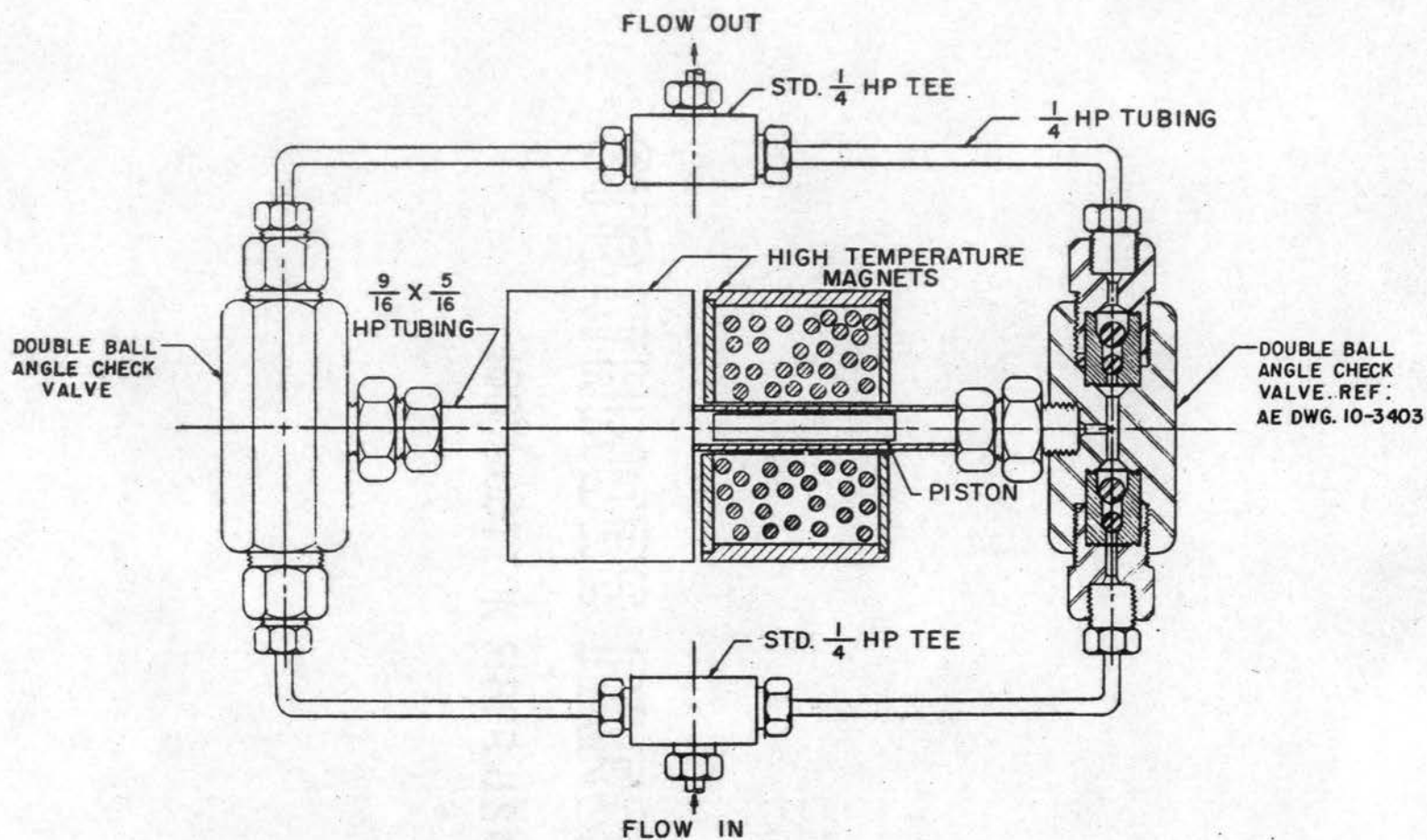


**FIGURE 10**  
**HIGH PRESSURE CIRCULATING PUMP**



special design covered by Autoclave Engineers Drawing No. 10-3403. The two check valves are connected via the pump cylinder. This cylinder is 9/16" O.D. by 5/16" I.D. x 6" long high pressure coned and threaded 316 stainless steel nipple. The inside of the nipple was polished to make a cylinder of uniform diameter. A 2" long piston was machined from a piece of 5/16" O.D. cold drawn 410 stainless steel rod. This material, chosen for its magnetic properties, was obtained from C. A. Roberts, Inc., Tulsa, Oklahoma. Four grooves 1/16" apart were machined on each end of the piston. As the piston moved back and forth in the cylinder, these grooves created areas of turbulence around the piston and, therefore, served as piston rings. A machine tolerance of 0.0005 inch was maintained between the outside diameter of the piston and the inside diameter of the cylinder. Teflon stops 1/4" long were inserted in the ends of the cylinder to keep the piston from sticking in the ports of the check valves. The check valve outlets were combined into a single stream via a second 1/4" high pressure tee. Coned and threaded 1/4" O.D. x 0.083" I.D. tubing was used to connect the various components of the pump.

The pump piston is activated by two magnets. The details of the magnet construction will now be discussed. A sketch of one of the magnet spools is shown on Figure 11. These spools are made of a special silicon steel, Grade M-36, manufactured by the Allegheny Ludlum Steel Corporation. The inside of the spools was coated with fiberglass electrical tape prior to winding the magnets. The outside of the spools was coated with insulating cement.

The magnets were wound on a slow turning lathe with exactly 800 turns of No. 20 Single NL magnet wire. This wire is coated with a

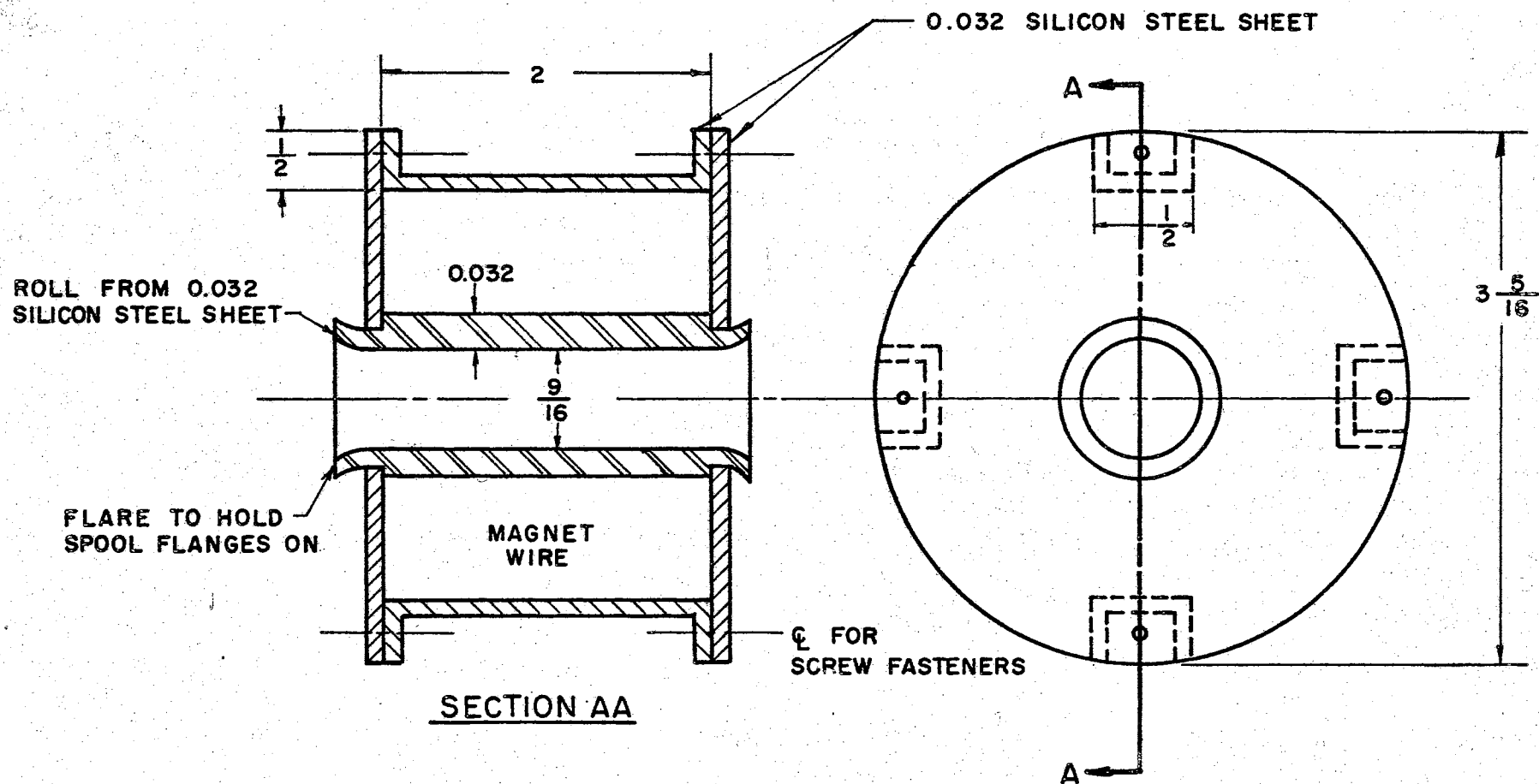


FIGURE II  
MAGNET HOUSING FOR CIRCULATING PUMP

high temperature insulation which permits operation to a maximum wire temperature of 250°C. This wire is available from REA Magnet Wire Co., Fort Wayne, Indiana.

The transistorized electronic control unit for the pump was built from the circuit diagram presented in Figure 12. In building this circuit it is extremely important to heat sink the power transistors and to protect the electronic circuit by fusing the magnets individually.

The number of piston oscillations per minute is controlled by varying a one megohm pot in the circuit. The displacement of this pump was determined with air at 75°F. at various piston cycle rates. The flow rate was found to vary from a low of 407 cc/min to a high of 1200 cc/min. The calibration of the pump is presented in Figure 13.



#### Sampling and Analysis Section

The equilibrium vapor and liquid phase samples were individually analyzed by passing each sample through cold traps, freezing out the heavier hydrocarbons and finally measuring the volume of light hydrocarbon gases remaining. The sample traps were closed, removed and weighed to determine the amount of heavy hydrocarbon present. A diagram of the sampling and analysis section is given in Figure 14.

The metal capillary tubing section of the apparatus was connected to the glass apparatus by a glass metal seal. The seal was coated with Glyptol. The capillary tubing section not in the air thermostat was wrapped with flexible heating tape.

The first and second traps were removable weighing traps. The weighing traps were connected to each other and to the remainder of




 = 
 MR323  
 MR323R IS REVERSED POL

99

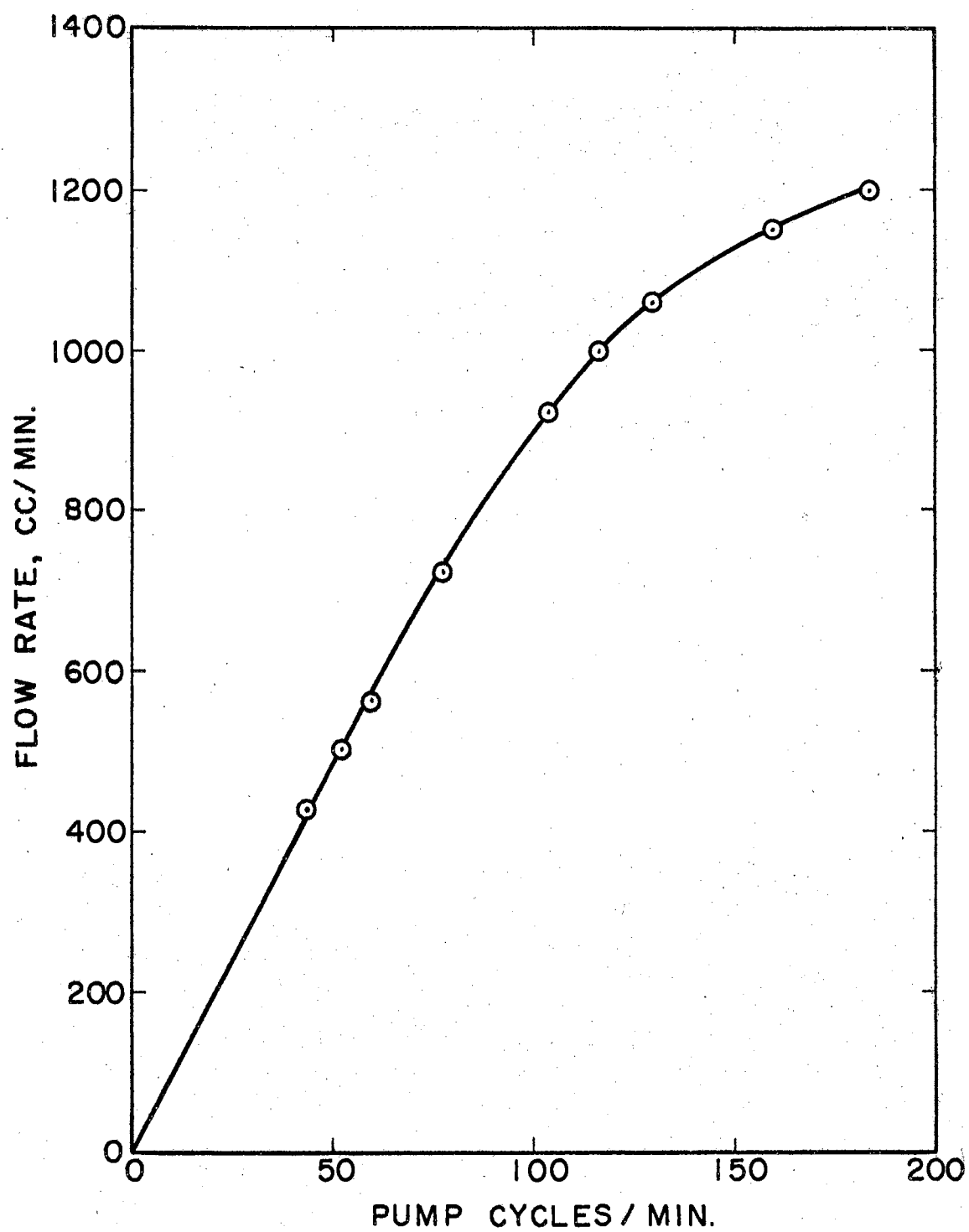


FIGURE 13  
CIRCULATING PUMP CALIBRATION

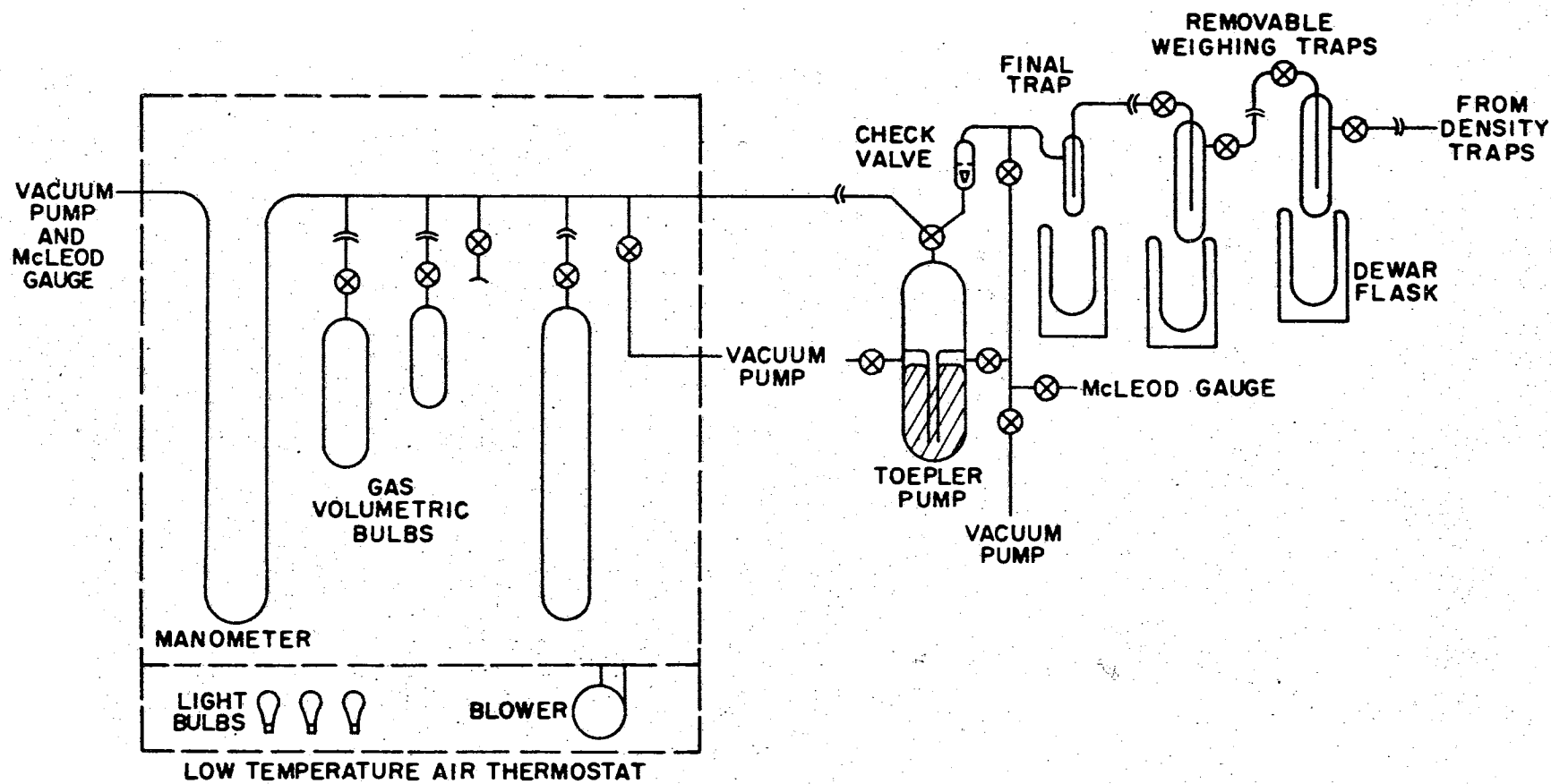


FIGURE 14  
SAMPLING SYSTEM

the sampling apparatus by 12/5 ball-and-socket joints. The final trap, used to freeze out minute traces of hydrocarbon from the vapor stream, was mounted permanently in the apparatus. The weighing and final traps were immersed in dry ice-isooctane baths. A 100 gram Mettler automatic balance was used to weigh the sample traps.

A Toepler pump was used to transfer the uncondensed vapor from the trap side of the apparatus to the volumetric side. The volumetric side of the apparatus consisted of capillary tubing to which was attached a mercury manometer and four side arms with 12/5 ball-and-socket joints. Volumetric bulbs of 25 cc, 500 cc, 1 liter, 2 liter and 4 liter nominal capacity were attached to the side arms. Three of the side arms were used for attaching the volumetric bulbs. The particular bulbs attached depended upon the type of sample, i.e., liquid or vapor, and the temperature and pressure in the equilibrium cell. The fourth side arm could be isolated from the volumetric apparatus by a stopcock. This side arm was used to connect a sample bomb for collection of a vapor sample for analysis by gas chromatography.

The volumetric apparatus was calibrated for volume by the techniques described in Appendix C. The volumetric apparatus was evacuated through side arms conveniently located along the apparatus. Pressure was measured with a Virtis McLeod gauge. Pressure on the vacuum side of the U-tube manometer was measured with a larger McLeod gauge.

The volumetric apparatus was enclosed in a constant temperature air bath. The bath had outside dimensions:  $4\frac{7}{8}$ " high,  $40\frac{1}{2}$ " wide and  $21\frac{1}{4}$ " deep. The outside of the bath was made of  $\frac{1}{2}$ " plywood. The inside of the thermostat was lined with 1" thick styrofoam insulation. The volumetric apparatus was mounted in an upper compartment

measuring  $37\frac{3}{4}$ " high,  $37\frac{1}{2}$ " wide and  $18\frac{1}{4}$ " deep. A lower compartment measuring 8" high,  $39\frac{1}{2}$ " wide and  $20\frac{3}{4}$ " deep housed four light bulbs used to supply heat to the thermostat. Air was circulated from the upper compartment across the light bulbs in the lower compartment and back to the upper compartment by means of a 100 SCFM blower. A Fenwal Model 18021-0 bimetallic temperature controller, mounted in the blower exhaust, controlled the temperature by on-off control. A Beckman differential thermometer was used to measure the temperature of the bath.

A  $21\frac{1}{2}$ " x  $47\frac{3}{4}$ " door on the front of the thermostat permitted access to the interior for changing the volumetric bulbs and taking samples. A fluorescent tube provided interior lighting. An optically flat glass window  $4\frac{1}{4}$ " x 36" was located directly in front of the U-tube manometer.

The height of the mercury in both legs of the U-tube manometer was measured with a Gaertner M-911 cathetometer placed directly in front of the air bath window. The cathetometer scale is made of Type 416 stainless steel and has a temperature coefficient of linear expansion of  $9.9 \times 10^{-6} \text{ }^{\circ}\text{C}^{-1}$ . The scale was standardized at  $20^{\circ}\text{C}$ .

### Materials

The methane used in this study was Phillips Petroleum Company Research-Grade. A sample of the methane was analyzed by Mr. John W. McQuaid of the Esso Research Laboratories, Baton Rouge, Louisiana.

The sample was analyzed by gas chromatography using two different columns. The sample was first analyzed using a five foot long column of 80-100 mesh 5A molecular sieve which had been heat treated at  $400^{\circ}\text{C}$



for 24 hours. During operation the column was temperature programmed to 357°C. A helium rate of 50 cc/min was used. There was some question as to reliability of the carbon dioxide peak, therefore, a second column was prepared to check the results of the first column.

This second column was a 40' long column of 20 parts hexadecane on 100 parts of white 80-100 mesh Chromosorb. The column was operated isothermally at 30°C at a helium rate of 50 cc/min.

The carbon dioxide peak was detected with the second column. The carbon dioxide was scrubbed from the methane and a sample rerun. The carbon dioxide peak was absent in this rerun sample, so it was concluded that carbon dioxide is indeed present in the methane. The analyses obtained on the molecular sieve and the hexadecane columns were in good agreement. The analysis of the methane is presented in Table II.

The natural gas condensate used in this study was obtained through the Pan American Petroleum Corporation, Tulsa, Oklahoma. The source of the condensate was a Morrow sand reservoir in Western Oklahoma producing at a depth of approximately 8500 feet. Table III presents data obtained on the primary separator gas and liquid. The primary separator was operating at 846 psig and 78°F and at a gas/oil ratio of 72,339 SCF primary gas/Bbl. of stock tank oil at the time the samples were taken.

Three condensate liquids were available for vapor-liquid equilibrium determinations:

1. Tagged 'Condensate A' - A heptanes plus cut prepared from the raw stock tank liquid by distillation at Pan American's Tulsa research facility.

TABLE II

## ANALYSIS OF METHANE REAGENT

<u>Component</u>	<u>Volume %</u>
Nitrogen	0.84
Methane	98.9
Oxygen	0.009
Ethane	0.14
CO <sub>2</sub>	0.16

Note: If propane is present, it is present in quantities less than 150 ppm.

TABLE III  
ANALYSIS OF CONDENSATE FIELD SAMPLES

<u>Component</u>	<u>Primary Separator Gas, Mole %</u>	<u>Primary Separator Oil, Mole %</u>
Nitrogen	0.57	0.09
Methane	91.30	27.80
Carbon Dioxide	- - -	0.46
Ethane	4.77	5.04
Propane	2.00	5.69
Isobutane	0.27	1.53
n-Butane	0.56	3.91
i-Pentane	0.15	1.67
n-Pentane	0.15	3.20
Hexanes (118-167°F)	0.12	7.28
Heptanes plus	0.11	43.33
MW C <sub>7+</sub>	- - -	120
Sp. Gr. C <sub>7+</sub>		0.7674

2. Tagged 'Condensate B' - Raw stock tank oil
3. Tagged 'Condensate C' - Raw stock tank oil obtained simultaneously with 'Condensate B' but in a separate container.

Condensate 'B' was used in this study. The composition of this sample as determined by chromatography is presented in Table IV.

ASTM D-86 distillations (2) were run on the condensate sample. The result of this distillation is presented in Figure 15.

TABLE IV  
CHROMATOGRAPHIC ASSAY OF CONDENSATE

COMPONENT	WEIGHT PERCENT	MOLE PERCENT
METHANE	0.00000	0.00000
ETHANE	0.00000	0.00000
PROPANE	0.13605	0.34617
ISOBUTANE	0.17388	0.33564
N-BUTANE	1.03993	2.00735
2,2-DIMETHYLPROPANE	0.05393	0.08386
ISOPENTANE	2.07303	3.22356
N-PENTANE	2.39054	3.71729
2,2-DIMETHYLBUTANE	0.23283	0.30312
CYCLOPENTANE	0.37677	0.60272
2-METHYLPENTANE	3.12204	4.06458
3-METHYLPENTANE	1.92279	2.50327
N-HEXANE	3.42069	4.45339
METHYLCYCLOPENTANE	2.33765	3.11624
2,3-DIMETHYLPENTANE	0.12919	0.14464
CYCLOHEXANE	4.07085	5.42671
3-METHYLHEXANE	0.64660	0.72396
ISOHEPTANE	2.06118	2.30778
2,2,4-TRIMETHYLPENTANE	1.83410	1.80153
N-HEPTANE	4.64846	5.20461
METHYLCYCLOHEXANE	8.82003	10.07801
TOLUENE	2.09397	2.54968
2,3,4-TRIMETHYLPENTANE	2.65922	2.61200
OCTANE ISOMERS	5.52783	5.42967
N-OCTANE	4.34595	4.26878
ETHYLBENZENE	0.99878	1.05547
MIXED XYLENES	3.41485	3.60866
258-303F FRACTION	7.09889	6.20971
N-NONANE	3.33795	2.91985
304-345F FRACTION	7.12954	5.62171
N-DECANE	2.62766	2.07194
346-384F FRACTION	4.30123	3.08721
N-UNDECANE	2.09989	1.50720
385-421F FRACTION	2.53585	1.67023
N-DODECANE	1.56478	1.03063
422-455F FRACTION	2.69268	1.63859
N-TRIDECANE	1.26042	0.76701
456-488F FRACTION	1.57685	0.89173
N-TETRADECANE	0.76936	0.43508
489-519F FRACTION	1.09323	0.57741
N-PENTADECANE	0.47227	0.24944
520-548F FRACTION	0.89773	0.44478
N-HEXADECANE	0.37492	0.18575
549-575F FRACTION	0.48685	0.22714
N-HEPTADECANE	0.16908	0.07888
576-602F FRACTION	0.39648	0.17478
N-OCTADECANE	0.11661	0.05140
603-627F FRACTION	0.16908	0.07064
N-NONADECANE	0.11661	0.04872
628-650F FRACTION	0.11661	0.04630
N-EICOSANE	0.04081	0.01620
651F+ FRACTION	0.02332	0.00882
TOTAL	100.00000	100.00000

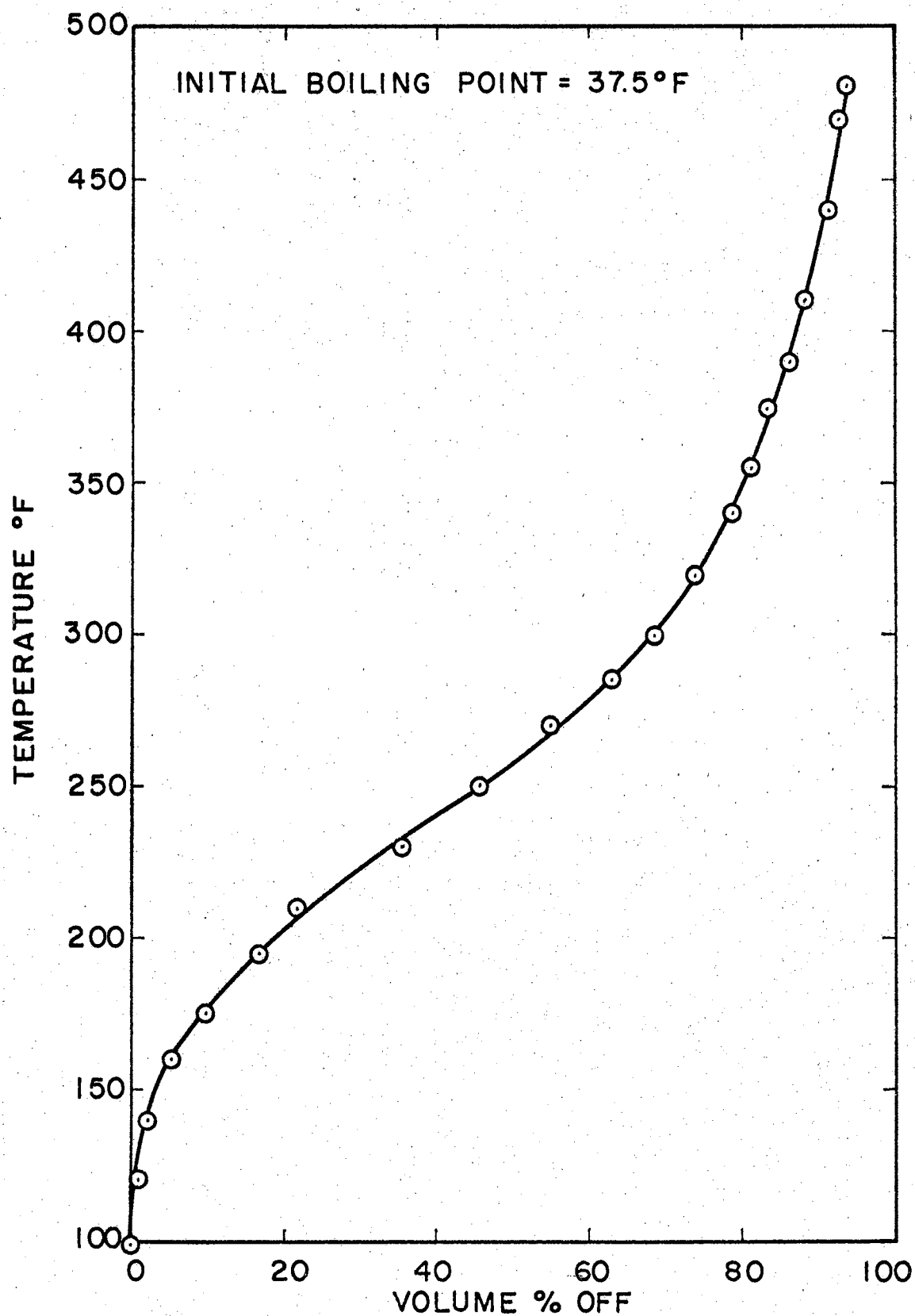


FIGURE 15  
ASTM DISTILLATION OF CONDENSATE

## CHAPTER V

### EXPERIMENTAL PROCEDURE

The discussion of the experimental procedure will be divided into the following sections: (1) charging of the components, (2) equilibration, (3) sampling, and (4) analysis.

#### Charging of Components

The experimental procedure used consisted of making a series of runs at the same temperature, beginning at a pressure of about 100 psia and increasing the pressure in logarithmic increments to the dew point or critical point at this temperature.

Prior to the first run, the equilibrium cell, the gas compressor and the density traps were evacuated to three microns pressure for approximately one hour. The apparatus was pressured to 100 psia with methane and reevacuated. The pressuring with methane and evacuation were repeated two additional times.

The equilibrium cell and density traps were then evacuated via the sample outlet line. The cell and traps were 'blocked off' and approximately 100 cc of methane-saturated natural gas condensate were charged to the equilibrium cell from a glass burette through a connection at the bottom of the cell. Care was taken not to break the liquid seal between the equilibrium cell and the charging burette before the valve in the charge line was closed. This prevented

leakage of air into the cell. The equilibrium cell was pressured with methane immediately following the charging of the condensate in order to pressure the cell and further prevent leakage of air into the cell prior to the equilibrium measurements.

### Equilibration

Following the charging of the methane and condensate to the equilibrium cell, the thermostat was heated to the desired operating temperature and the temperature was allowed to stabilize. The Powerstats and the glycol coolant rate were adjusted to bring the temperature to within 5°F of the desired value. The Hallikainen Thermotrol coarse and fine controls were adjusted to obtain the proper temperature. The temperature was checked periodically with the thermocouple-potentiometer arrangement described in Appendix B.

The pressure regulation and measuring system was prepared for operation during the temperature equilibration period. The proper measuring cylinder was installed in the pressure balance. Six measuring cylinders were needed to cover the 100-15,000 psia pressure range studied. Cylinders not in use were stored in special cannisters. The cylinders were completely immersed in pressure balance oil in these cannisters.

Weights necessary to obtain the desired operating pressure were then placed on the balance. The weights and measuring cylinders were handled with gloves and Kimwipe towels to prevent corrosion to these parts. The valve isolating the pressure balance from the pressure bench was then opened. The hand pump was then used to inject oil into the system and lift the piston and the rotating parts to their



operating height. The weights were set in rotation. Following this procedure the pressure regulation and measuring system was concluded to be in order. The pressure balance then shut down and isolated from the pressure bench.

The gas compressor level was checked to be sure that it contained an adequate supply of methane for the run. If not, methane was added to the compressor from the feed cylinder through the CO<sub>2</sub> and water removal system.

The gas compressor was isolated from the system. The valve separating the pressure bench and the gas compressor was carefully opened. With the pressure balance isolated from the system, oil was added at the pressure bench until the pressure gauge reading indicated that the gas compressor was near the desired operating pressure. The valve separating the gas compressor and the equilibrium cell was slowly opened and as methane began to flow into the cell, oil was added to the system to maintain the pressure on the gauge. After approximately 10-15 minutes the addition of methane to the equilibrium cell was essentially complete and the valve separating the cell and the gas compressor was opened completely.

At the higher operating pressures, it sometimes became necessary to recharge the gas compressor during a run. Recharging was necessary because the methane feed cylinder pressure of 1500-1800 psig prevented the addition of sufficient methane to the gas compressor to fill the equilibrium cell in one loading. In this case, the gas compressor was isolated from the pressure bench and the equilibrium cell was 'blocked off'. The pressure balance and bench were relieved of pressure. The pressure balance was isolated from the system. Then the pressure

in the gas compressor was relieved and the gas compressor was recharged by the procedure described above. Oil was added through the pressure bench to bring the system pressure to the desired value.

A flow path was opened up from the equilibrium cell through the vapor density trap and the vapor circulating pump back to the bottom of the equilibrium cell. Power to the circulating pump was turned on. Simultaneously, the continuous power input through the the Powerstats was reduced by approximately 100 watts to compensate for the heat given off by the pump magnets.

The system pressure decreased as the circulating vapor went into liquid solution. Oil was added to the system at the pressure bench to hold the system pressure constant.

The system pressure became constant after approximately 15 minutes of vapor recirculation. The level of the pressure balance piston was maintained at the desired level by adding oil to the system or by withdrawing oil with the screw press.

The vapor was recirculated at the desired operating temperature and pressure for a minimum of four hours. Frequently, vapor recirculation was maintained overnight. In the latter case, the pressure regulation and maintenance section was isolated from the system and shut down, isolating the compressor, the equilibrium cell and the vapor recirculation system. Reconnecting the pressure regulation and maintenance system showed little or no change in pressure, as indicated by the fact that the pressure balance piston level did not change appreciably when the valve to the gas compressor was reopened.

Following the vapor recirculation period, the vapor pump was shut down and isolated from the system. The constant heat input through the

Powerstats was increased by approximately 100 watts to compensate for the heat previously given off by the magnets. The outlet valves to the equilibrium cell were closed and the contents of the cell were allowed to settle for one hour. If not already connected, the pressure balance was connected to the system and the weights set in rotation. During this settling period the equilibrium cell temperature and the height of the pressure balance piston were frequently checked. The necessary adjustments were made to keep both temperature and pressure at their desired values.

### Sampling

Preparations for sampling were made next. The liquid sample traps were carefully cleaned with ethyl ether. Particular attention was paid to the ball-joint connections. The trap stopcocks were cleaned and regreased with Apiezon N stopcock grease. The traps were evacuated and then weighed immediately on the Mettler balance. The weighing procedure consisted of repeating the weighings until consecutive weighings agreed. A difference in consecutive weighings usually indicated a leak in one of the stopcocks. In this case, the stopcocks were cleaned and regreased and the evacuation and weighing procedure was repeated.

The appropriate gas volumetric bulbs were connected to the volumetric side of the apparatus. The three-way stopcock on the Toepler pump was removed, cleaned with ether, regreased, and replaced. The volumetric side of the apparatus, including the Toepler pump, was evacuated and checked for leaks. The low temperature in the air bath thermostat was established during this period.

Both the liquid and vapor sample lines were purged after the one hour equilibrium cell settling time and about one-half hour before the actual samples were withdrawn. The sample line was opened to the atmosphere. The vapor sample valve and the vapor density trap outlet valve were opened. The vapor density trap inlet valve was opened slightly to purge the vapor sample line. During purging the screw press and/or the hand pump were used to maintain the pressure balance piston at its operating height.

The liquid sample valve and the liquid density trap outlet valve were then opened. The liquid density trap inlet valve was opened slightly to purge the liquid sample line. During purging the pressure balance piston was maintained at its operating height with the screw press and/or the hand pump.

After the purging procedure the sample trap ball-joint connections were greased and two traps were put in place. The two traps which had been previously cleaned, evacuated and weighed were not used at this point since the system was being evacuated prior to taking the actual vapor and liquid phase samples.

The vapor and liquid density traps were next evacuated, leak-tested, and then blocked off. The portable Virtis McLeod gauge was used in the evacuation and leak-testing procedure.

Several preliminary measurements were made before the liquid and vapor samples were taken. The barometric pressure was read. The U-tube manometer located in the low temperature air thermostat was used to make this measurement for the 150°F runs. A calibrated barometer was not available for these runs. The use of the U-tube manometer was considered to be more accurate than the use of an uncalibrated

barometer because no corrections for capillarity, scale expansion, or residual vacuum were necessary for the manometer (18). The temperature of the manometer was assumed to be that of the air bath. The pressure on the vacuum side of the manometer was measured with a large McLeod gauge to insure that it was negligible.

A Texas Instruments Model 141A servo-driven fused quartz precision pressure gauge, Serial No. 346, with a 0-100 cm Hg bourdon tube, Serial No. 599, was used to measure the barometric pressure for the 250°F runs. In the Texas Instruments gauge, the bourdon tube deflection is measured optically. An optical transducer is mounted on a gear that travels concentrically around the bourdon tube. A small mirror is mounted on the quartz bourdon tube. In operation the deflection of the pressured bourdon tube is found by rotating the gear until the light reflected from the tube mirror falls equally on a pair of matched photocells. The deflection of the gauge is converted to a digital reading which is then multiplied by a scale factor to determine the pressure.

The pressure balance measuring cylinder data and weights were next recorded. The room temperature and temperature of the pressure balance were noted. Also recorded were the height of the oil above the bottom of the guide pin on the pressure balance and the level of the mercury in the gas compressor.

A final check was made of the equilibrium cell temperature and pressure to be sure that these had not deviated from the desired values. If either had changed, the run was aborted. If the temperature and pressure were at the desired values, sampling of the equilibrium phases was begun.

With the liquid sample valve closed and the liquid density trap outlet valve open, the liquid density trap inlet valve was opened slightly. The screw press was used to maintain the pressure balance piston at the desired operating level during sampling. The gas compressor mercury level was checked throughout the sampling period. Weights were added to the weight pan on the pressure balance to compensate for the level change in the gas compressor.

The liquid density trap inlet valve was opened gradually until this valve was completely open. The liquid density trap inlet and outlet valves were closed when the pressure balance indicated that the system pressure had completely stabilized. The gas compressor level and the weights added during the liquid phase sampling were recorded.

Sampling of the vapor phase was begun immediately after completion of the liquid phase sampling. With the vapor sample valve closed and the vapor density trap outlet valve open, the vapor density trap inlet was opened slightly. The screw press and hand pump were used to maintain the pressure balance at the desired operating level. Weights were again added to compensate for the level change in the gas compressor. The vapor density trap inlet valve was opened gradually until this valve was completely open. The vapor density trap inlet and outlet valves were closed when the system pressure had completely stabilized. The gas compressor level and the weights added during sampling were recorded. The barometric pressure and the temperature of the equilibrium cell were measured and recorded. The sampling of the equilibrium phases was now considered to be complete.

### Liquid Sample Transfer

The density trap outlet valves were checked to be sure that they were tightly closed. The liquid and vapor sample valves were opened and the material trapped between these valves and the density trap outlet valves was vented. This section of the apparatus was then evacuated.

The two liquid traps which had been previously cleaned, evacuated and weighed were put in place. The liquid sample valve was opened. The trap side of the apparatus was evacuated to less than 25 microns with a leak rate not to exceed 0.1 mm Hg per hour. The portable McLeod gauge was used in the leak testing procedure.

Dry ice-isooctane baths in small Dewar flasks were applied to the two sample traps and the final catch trap. It will be recalled that the appropriate gas volumetric bulbs had been earlier connected to the volumetric side of the apparatus and evacuated. The volumetric apparatus was next opened to the liquid trap section. The entire sampling apparatus was checked for a vacuum to be less than 25 microns with leak rate not to exceed 0.1 mm Hg per hour.

The three-way cock on the Toepler pump was turned so as to connect the liquid trap side of the sampling apparatus with the volumetric side. The U-tube manometer was checked with the cathetometer to be sure that there was no difference in height between the two legs.

The liquid sample valve and the vapor sample valve were closed. The outlet valve on the liquid density trap was opened. The sampling apparatus was isolated from the vacuum system. The liquid sample valve was opened slowly to allow the trapped sample to pass into the

sampling apparatus. The heavier hydrocarbons were condensed and/or frozen out in the liquid traps. The lighter hydrocarbons passed on into the volumetric apparatus. The heating tape on the small metal sample line was used to prevent condensation of light hydrocarbons in this section of line and to facilitate evaporation into the liquid traps.

The three-way cock on the Toepler was turned to isolate the pump. The dry ice-isooctane bath was removed from the final trap and the latter trap was warmed quickly to distill any residual hydrocarbon back into the second trap. There was seldom any observable hydrocarbon in the final trap. This trap was used as a precaution against passage of condensed hydrocarbons into the volumetric side.

The outlet stopcock on the second liquid trap was closed and the dry ice-isooctane bath removed from this trap. This trap was then warmed to distill hydrocarbons in this trap back into the first trap. This procedure eliminated the necessity of sampling liquid from the second trap. The Dewar flasks were filled with warm water and placed under the second and final liquid traps.

The light hydrocarbons in the sample were transferred to the volumetric side by means of the Toepler pump. Vacuum was applied to the lower compartment of the pump to pull down the mercury level in the upper compartment. The three-way cock on the pump was turned to allow the light hydrocarbons to expand from the trap side into the upper compartment. Vacuum was again applied to the lower compartment to allow the upper compartment to be filled with hydrocarbon. The three-way cock was turned to allow the hydrocarbon to pass into the volumetric side. The upper compartment and three-way cock passage



were filled with mercury to displace the hydrocarbon.

The Toepler pump transfer was repeated until the level of the mercury in the U-tube manometer in the volumetric side did not change on three successive pumpings.

The liquid trap stopcocks were closed, the traps were removed, and the ball-joint connections were cleaned carefully. The traps were allowed to reach the temperature of the balance and were then weighed. The liquid in the first trap was chilled in the dry ice-isooctane bath. Then the liquid in the first trap was transferred to a pre-cooled serum vial and stored in the freezing compartment of the refrigerator awaiting analysis on the chromatograph.

The hydrocarbons in the volumetric side of the sampling apparatus were allowed to attain the temperature of the low temperature thermostat as indicated by constancy of the mercury levels in the U-tube manometer. One-half hour was sufficient for this temperature equilibrium. The vacuum side of the U-tube manometer was evacuated to less than 20 microns. The U-tube mercury levels and the height of a reference mark on the manometer were recorded, along with the size of the attached volumetric bulbs and the position (open or closed) of their stopcocks.

A sample bomb was next prepared for taking of a sample from the volumetric apparatus for chromatograph assay. The bomb was first cleaned with dichromate cleaning solution. Following a distilled water rinse, the bomb was flushed with acetone and ethyl ether. The bomb stopcocks were removed, cleaned with ether, regreased and replaced. The bomb was next evacuated.

The evacuated bomb was attached to the volumetric apparatus at a

ball-joint provided for this purpose. The stopcock on the bomb was opened and a corresponding stopcock on the volumetric apparatus was opened to permit entry of the hydrocarbon sample into the sample bomb. The stopcocks were closed and the bomb was removed from the apparatus. The long leg of the sample bomb was inserted into a flask of clean mercury and the mercury allowed to enter the sample bomb to bring the pressure in the bomb to near atmospheric pressure. Pressuring with mercury facilitated later removal of samples for the chromatographic assay.

A sample was immediately injected into the chromatograph to be sure that a sample had been recovered in the sample bomb. This completed the transfer of the liquid phase sample.

#### Vapor Sample Transfer

The procedure used for transferring the vapor phase density trap sample to the volumetric apparatus was essentially that used for the liquid phase sample. The only difference occurred in the use of the dry ice-isooctane baths for the liquid traps. The difference in procedure will be amplified in the discussion below.

Prior to the transfer of the sample, the dry ice-isooctane baths were applied to the liquid sample traps and to the final trap. The transfer of the vapor phase sample was begun in the same manner as the transfer of the liquid sample.

The three-way cock on the Toepler pump was turned to isolate the pump. The dry ice-isooctane trap was removed from the final trap and the latter trap was warmed quickly to distill any residual hydrocarbon back into the second trap. The outlet stopcock on the second liquid

trap was closed and the dry ice-isooctane bath removed from this trap. The trap was warmed to distill hydrocarbons in this trap back into the first trap.

The outlet stopcock on the first liquid trap was closed and the dry ice-isooctane bath removed from this trap. The trap was examined for condensed hydrocarbons. If enough condensed hydrocarbon was present to warrant sampling for the chromatograph, the dry ice-isooctane bath was replaced and the procedure described for the liquid phase transfer was continued.

If there was not enough liquid sample for analysis by chromatography, the dry ice-isooctane bath was replaced with a warm water bath and the liquid phase sampling procedure was continued. When this procedure was followed, there was no hydrocarbon left in the trap side of the sampling apparatus, i.e., all of the hydrocarbon was transferred to the volumetric side of the sampling apparatus.

## CHAPTER VI

### CHROMATOGRAPHIC ASSAY OF THE EQUILIBRIUM VAPOR-LIQUID PHASES

The direct experimental determination of vapor-liquid equilibrium ratios requires not only the measurement of temperature and pressure, but also the determination of the concentrations of the individual components in both phases.

The following methods are available for the separation and identification of components of petroleum mixtures:

Methods based on distillation and extraction,

Spectroscopic methods, notably ultraviolet,  
infrared and mass spectroscopy

Chromatographic methods

These methods supplement rather than replace each other. Distillation methods have the disadvantages of requiring large samples and long analysis times. Spectroscopic procedures offer an improvement over those based on distillation and extraction in ease of identification and speed. However, the use of spectroscopic methods is necessarily restricted to larger laboratories because of the high initial equipment and maintenance costs. Gas chromatography, the analytical tool chosen for this work, provides a rapid and economical method for obtaining the composition data needed in vapor-liquid ratio determinations.

Gas chromatography was first worked out by A. T. James and A. J. P. Martin (22), the 1952 Nobel Prize winner for chemistry. They used the method to effect a biochemical separation. The great

versatility of gas chromatography was soon confirmed by Ray (45), who applied the technique to the separation of hydrocarbons. In the decade following this pioneering work, gas chromatography has developed into a major analytical tool in the petroleum industry, even to the point that the American Society for Testing and Materials has accepted gas chromatography for certain routine analyses of petroleum fractions (3).

Kehn (26) recently used two chromatographs to analyze the vapor and liquid phases of a condensate system containing components from methane to  $C_{20}$ . A chromatograph equipped with a thermal conductivity detector was used for analysis of the methane-through-pentane fraction. A chromatograph consisting of a capillary column and a hydrogen flame ionization detector was used to analyze the pentane-plus fraction. Kehn chose to use two chromatographs because experience gained in his laboratory and reported by other workers in the field of chromatography indicated that the use of a single chromatograph to analyze all the components from methane to  $C_{20}$  was impractical.

There are certain advantages to using a single chromatograph to analyze a  $C_1$  to  $C_{20}$  mixture. The need for elaborate sampling and sample preparation equipment is eliminated. Less attention of the analyst is required to operate the single instrument. These advantages offered enough incentive to develop an analytical technique using a single chromatograph.

#### Equipment and Operation

It was originally planned in this work to obtain the multicomponent analyses of the equilibrium phases on an F & M Scientific

Corporation (hereafter called F & M) Model 609 single column, flame ionization chromatograph equipped for temperature programming. Two problems arose in use of this chromatograph: (a) the unstable baseline which became acute with the use of temperature programming and (b) the non-reproducibility of the temperature programming system of this particular chromatograph. It was possible, however, to use this chromatograph to screen column sizes, column supports and operating conditions to obtain the best analysis of the field condensate sample. The three most promising substrates found were Carbowax 20, Apiezon L and SE 30 methyl silicone polymer. One-eighth inch columns were found to be far superior in performance to  $\frac{1}{4}$ " columns.

The field condensate sample was assayed on a Micro-Tek 2500R dual column, temperature programmed chromatograph equipped with thermal conductivity detectors. One-eighth inch columns packed with Carbowax 20, Apiezon L and SE 30 coated supports were evaluated at the same operating conditions as those used on the F & M Model 609 chromatograph. The degree of component separation obtained with the thermal conductivity unit was not as good as that obtained with the flame ionization unit.

The problems associated with the F & M Model 609 chromatograph coupled with the better analyses obtained with flame ionization led to the purchase of an F & M Model 810 research chromatograph. This chromatograph has dual column flame ionization and thermal conductivity detectors. This chromatograph is equipped not only for programmed temperature operation but also for an automatic analysis cycle that completely eliminates the need for manual resetting during duplicate runs. This automatic feature coupled with a gear driven

temperature programmer ensures almost perfect reproducibility of duplicate runs. While it is possible to evaluate a sample simultaneously using both flame and thermal conductivity detectors, tests indicated that flame ionization would provide an optimum analysis of the mixtures encountered in this work.

The hydrogen flame ionization detector has the sensitivity, linearity of response and rapidity of response for complete analysis of the  $C_1$  to  $C_{20}$  system. Operation of this detector is based on the measurement of electrical conductivity between two electrodes placed in a hydrogen flame. With pure hydrogen, the conductivity is very low. Addition of small amounts of organic material produces a large increase in the conductivity of the flame. According to McNair, et al. (20) the linearity of response for varying concentrations is valid for a sample-size range of several orders of magnitude. This linearity of response was verified in the calibrations described below.

The columns used in the Model 810 chromatograph are twenty feet long and are made of  $\frac{1}{8}$ " copper tubing. The packing is 10% SE 30 silicone rubber on 60-80 mesh non-acid-washed Johns-Manville Chromosorb P. The silicone rubber was dissolved in chloroform and then mixed thoroughly with the Chromosorb P. The chloroform was evaporated by heating the support in a beaker over a steam heater. A forty foot section of  $\frac{1}{8}$ " copper tubing was filled by gravity with the prepared support. Previous experience in preparing  $\frac{1}{8}$ " columns indicated that vibration of the column during filling produced a column with excessive pressure drop. Two twenty foot columns were prepared by simply cutting the forty foot column in half.

A drifting recorder base line becomes a problem when an integrator

is used to measure the areas under the individual component peaks. The drifting of the base line increases with increasing temperature as the substrate vaporizes and increases the conductivity of the hydrogen flame. The tendency of the base line to drift can be compensated for by adding a second flame detector. The bias potential supplied to each detector is equal in value but opposite in polarity. While the substrate bleeding off one column is causing a voltage drop in one direction, the bleeding substrate of the second column is causing an equal voltage drop in the opposite direction. The net result of the opposing voltages is cancellation. In order for the second column to cancel the bleed effect of the first, the columns must be balanced. This is done by heating the columns to the desired upper limit temperature value with the desired helium flow rate through the analytical column and regulating the reference column helium flow rate to return the recorder pen to the zero baseline level. When a sample component passes through the flame and the columns are balanced, the current through the analytical flame (helium + sample + substrate bleed) will be greater than the current through the reference flame (helium + substrate bleed). The difference in currents will be the net change caused by the presence of the sample. The end result is a peak representing the sample on a flat baseline.

The helium rate through the analytical column was 9 cc/min and 11 cc/min through the reference column. Additional helium was added after each column to bring the total helium flow rate to 50 cc/min. This additional helium resulted in a cooler hydrogen flame and better detector performance.

The Model 810 chromatograph can normally be temperature programmed



from room temperature to 500°C. The lower temperature limit of room temperature was too high for adequate separation of the components, methane through normal butane. Consequently, the chromatograph was modified to operate from a lower temperature of 0°C. This temperature was obtained by charging dry ice to the oven five minutes before sample injection. The syringes used for vapor sample injection and the vapor sample bomb were heated prior to sample injection. Following sample injection, the chromatograph was programmed at a rate of 2°C/min. to an upper limit of 260°C. The conditions chosen as standard for the vapor and liquid sample analyses are presented in Table V.

#### Calibration

The chromatograph must be calibrated for each of the equilibrium phase mixture components. In order to obtain meaningful results, these calibrations must be made at the same chromatograph operating conditions as those used in the composition analyses of the equilibrium phases. Calibration of the chromatograph is necessary in order to convert the area percent obtained from the chromatogram to weight or mole percent.

A number of calibration standards containing four or more liquid components were prepared from research grade hydrocarbons obtained from the Phillips Petroleum Company and the American Petroleum Institute Hydrocarbon Depository. The desired hydrocarbon mixture components were injected one at a time into stoppered serum vials with the net weight of each component being determined from weighings on the Mettler B-6 balance. The compositions of these standards were

calculated from this weight data. Where possible, three different standards, containing the same components, were prepared with a given component present in a different concentration in each of the mixtures.

The calibration standards for the light gases were obtained directly from the Phillips Petroleum Company. Laboratory analyses accompanied these samples. The compositions of the various standards are presented in Appendix F.

The calibration of the chromatograph for a large number of compounds is necessarily a long and tedious process. Samples of the calibration standards were analyzed a minimum of eight times at the predetermined standard conditions (Table V). The resulting chromatograms were then evaluated as follows.

The chromatograph strip chart recorder was equipped with a Disc integrator. This integrator provides a trace readout which is continuously recorded on the side of the chromatogram. The integrator trace is directly proportional to the peak areas on the chromatogram and can be converted to a numerical value. The area percent under a given peak is calculated simply as the trace value for that peak divided by the total trace area value.

The pure component calibration data for the Model 810 chromatograph were evaluated using multiple regression techniques. The reader is referred to the text of Natrella (33) for the calculation procedures used. This data analysis was done on the IBM 1410 digital computer using a program developed by the writer and R. C. Lee. This computer program permitted the estimation of the coefficients of, and the answering of various questions about, an  $m^{\text{th}}$  degree polynomial relationship.

TABLE V

## STANDARD CHROMATOGRAPH OPERATING CONDITIONS

Column: 1/8" copper tubing x 20' long

Substrate: 10% SE 30 silicone rubber

Support: 60-80 mesh Chromosorb P

Helium Rate-Analytical Column: 9 cc/min

Helium Rate-Reference Column: 15 cc/min

Auxillary Helium Rate: 41 cc/min

Hydrogen Cylinder Pressure: 20 psig

Helium Cylinder Pressure: 80 psig

Air Cylinder Pressure: 33 psig

Initial Temperature: 0°C

Final Temperature: 260°C

Detector Temperature: 350°C

Temperature Programming Rate: 2°C/min

Detector: Flame

Injection Port Temperature: 255°C

Vapor Sample Size: 3 cc

Liquid Sample Size: 1.6 µl

$$Y = B_0 + B_1 X + B_2 X^2 + \dots + B_m X^m \quad (V-1)$$

between a dependent variable Y and single independent variable X. Four models representing the calibration data were studied. These are summarized in Table VI.

Model 2 was chosen as the one which best represented the data. The coefficients for this model were determined for each of the calibration hydrocarbons. The standard deviations of these coefficients were determined and an analysis of variance was made. Finally, the standard deviations of the points regressed were determined. It is possible to estimate the accuracy of the chromatograph calibrations from this statistical analysis. The results of the statistical treatment of the chromatograph calibration data are presented and discussed in Appendix G.

TABLE VI

## REGRESSION MODELS OF CHROMATOGRAPH CALIBRATION DATA

<u>Model</u>	<u>Y, Dependent Variable</u>	<u>X - Independent Variable</u>
1	Component Weight Percent	Component Area Percent
2	Component Area Percent	Component Weight Percent
3	Component Mole Percent	Component Area Percent
4	Component Area Percent	Component Mole Percent

## Analysis of the Coexisting Equilibrium Phases

Figure 16 shows a typical chromatogram obtained from the analysis of a naturally occurring condensate system. Methane was added to this condensate in order to show the point on the

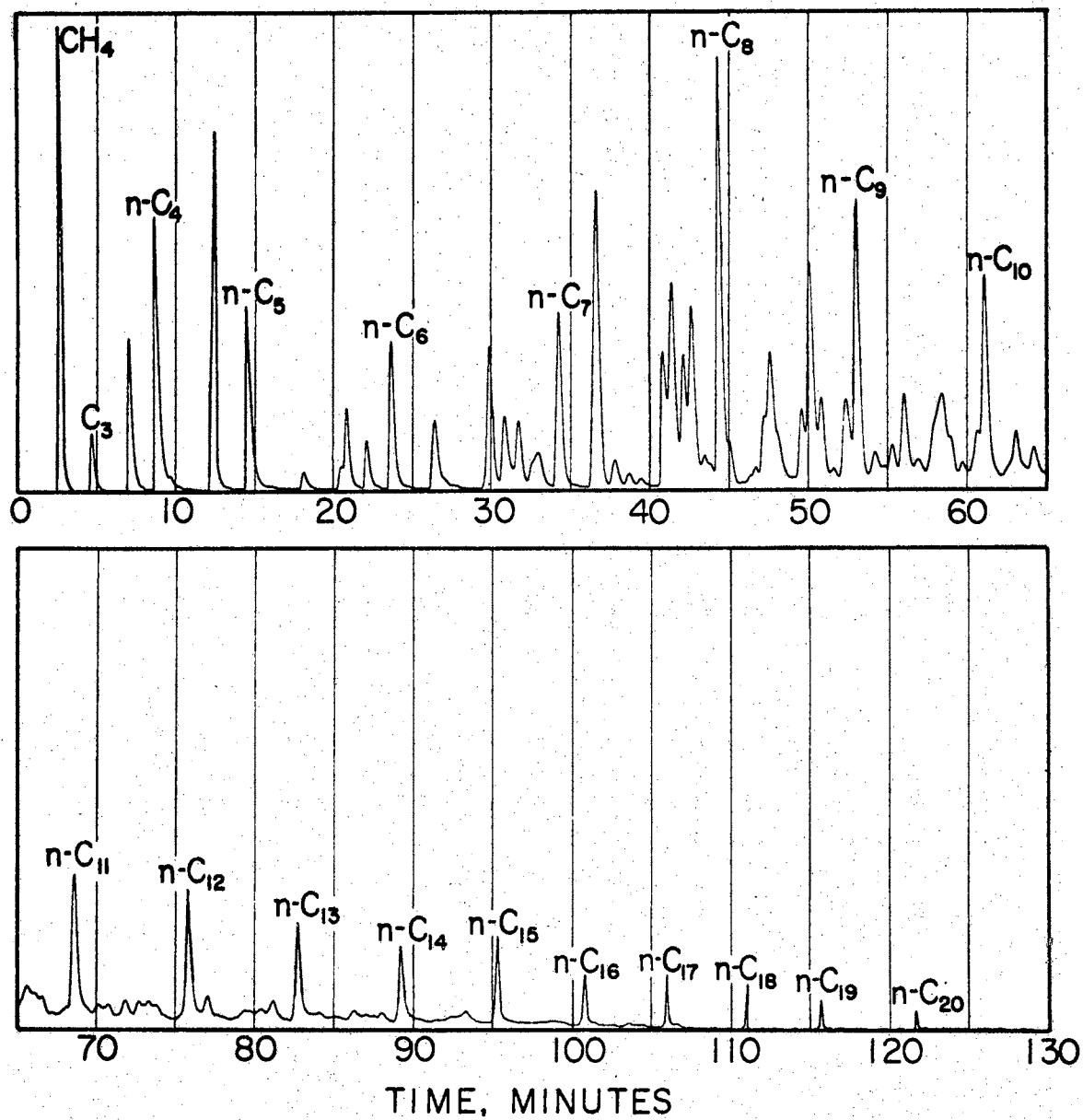


FIGURE 16  
TYPICAL CHROMATOGRAM OF CONDENSATE

chromatogram where methane is eluted. The elution time for the individual pure hydrocarbons was noted during each of the chromatograph calibration runs. These elution times permitted rapid identification of the components in the equilibrium phase samples. The elution time for methane was 2.8 minutes and the elution time for  $C_{20}$  was 134 minutes. It was not possible to identify each individual hydrocarbon in the heavy fraction of the condensate. The identified normal paraffins in this region served as convenient markers for dividing this heavy material into fractions. The individual fractions were then designated by boiling point range and for calculation purposes the fractions were assumed to behave as isoparaffins.

A chromatographic assay of the condensate used in this study was presented in Chapter IV, Table IV. The procedure for sampling the equilibrium phases was discussed in Chapter V while the procedure used in operating the chromatograph was discussed earlier in this chapter.

## CHAPTER VII

### DISCUSSION OF RESULTS

#### Experimental Results

Composition and density data were taken for the equilibrium coexisting phases of a methane-Morrow condensate system at 150°F and 250°F and pressures from 100 psia to the dew or critical points of the system at these temperatures. The temperatures were selected on the basis of the temperature range encountered in producing natural gas condensate reservoirs and the limitations of the experimental apparatus. The experimental apparatus can be operated at temperatures up to and including 250°F. Attempts were made to operate the apparatus at temperatures greater than 250°F. These attempts failed due to difficulties experienced with high pressure valves exposed to these higher temperatures.

Pressure limitations involved operating characteristics rather than the physical limitations of the apparatus. The operating range of the apparatus is 45 - 15,000 psia and is limited by the equilibrium cell. At pressures below 100 psia insufficient methane is dissolved in the liquid phase for accurate composition analysis with the sampling techniques and apparatus used here. The upper pressure limit was dictated by the dew or critical point of the system at the temperatures studied. The particular values of pressure selected were based on approximately equal logarithmic

increments of pressure.

The experimental data were converted to P-T-x-y data in the following manner. Pressures in the equilibrium phases were calculated from the weights and piston area used on the pressure balance. Corrections were applied for the buoyancy of air, and the hydrostatic heads of hydraulic oil, mercury and hydrocarbon. Barometric pressure was added to obtain absolute pressure.

Two samples were taken for chromatographic assay for each of the equilibrium phases: (1) a sample of the heavy hydrocarbon fraction frozen out in the cold traps and (2) a sample of the light hydrocarbons transferred to the volumetric apparatus. The moles of each component in the heavy fraction were obtained from the chromatographic assay and the cold trap weight data. The moles of the light hydrocarbon components were calculated from the gas law, using compressibility factors evaluated from the virial equation of state terminated after the second virial coefficient. The generalized second virial coefficients of Pitzer (40) were used in this calculation. The moles of each component in the equilibrium phase were then calculated by material balance. The K-values were calculated directly from the mole fraction data and the phase densities were calculated from the knowledge of the number of moles of each component present in each phase and the volumetric calibration data for the density traps.

The calculation of P-T-x-y data from the raw experimental data is illustrated by sample calculations in Appendix E. The raw experimental data are tabulated in Appendix H. The experimental results in the form of P-T-x-y data are tabulated in Appendix I. The equilibrium phase densities are also tabulated in Appendix I. The



equilibrium phase densities are presented graphically in Figures 17 and 18 in units gm/cc and in Figures 19 and 20 as molar volumes in cc/g mole. A portion of the experimental K-data is presented graphically in Figures 21 and 22. The experimental data points are designated on these figures.

### Experimental Errors

In discussing experimental errors it is important to differentiate between precision and accuracy. Accuracy refers to the magnitude of the error between the observed and the true behavior, irrespective of precision. Accuracy is determined by the agreement of measurements made by different methods. Thermodynamic consistency tests could be used to establish the accuracy of vapor-liquid equilibrium data. Precision, on the other hand, refers to the magnitude of the variations of observations in direct measurements. The precision, or variability of the data can be studied by the method of propagation of errors, as was done by Thompson (65) and/or by comparing a few repetitions in measurements.

Duplicate runs were made at a given temperature and pressure in this work in order to determine the precision of the experimental measurements. These duplicate runs will be discussed and, in addition, certain known sources of error in the experimental measurements will be reported.

It will be recalled that the number of moles of light hydrocarbons in each equilibrium phase sample was determined from measurements of the pressure, volume and temperature of the hydrocarbon sample and the gas law.

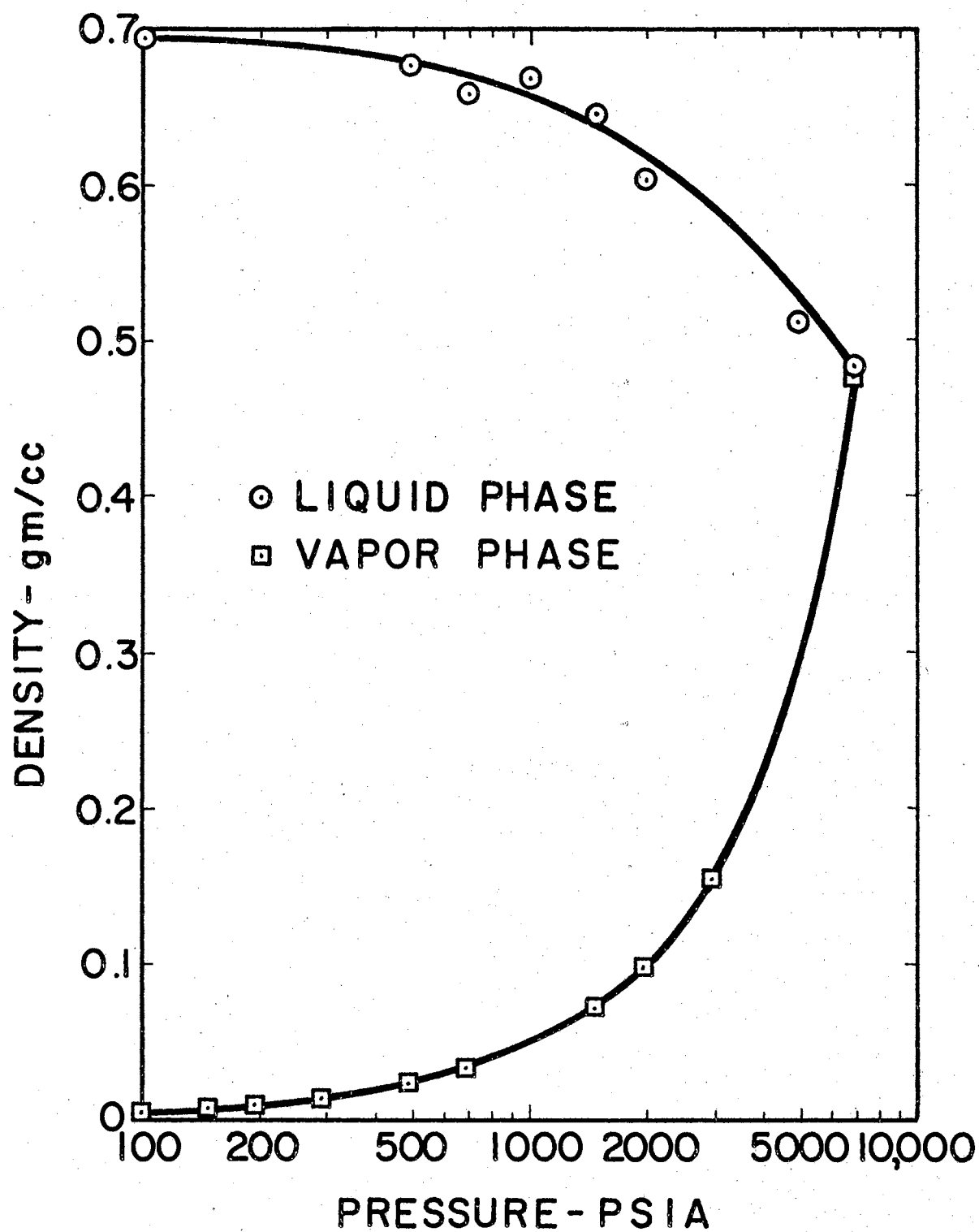


FIGURE 17  
EQUILIBRIUM PHASE DENSITY  
AT 150° F.

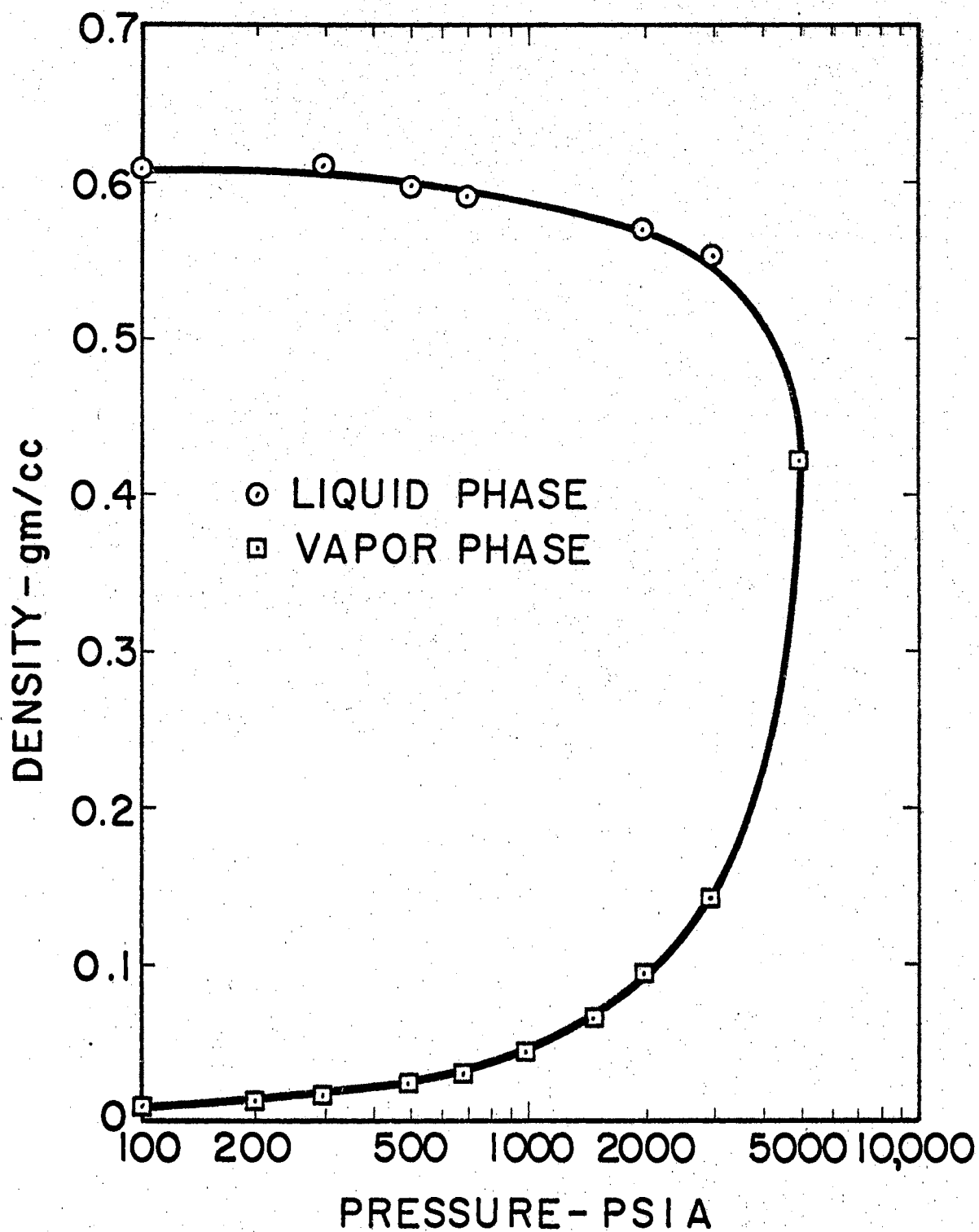


FIGURE 18  
EQUILIBRIUM PHASE DENSITY  
AT 250° F.

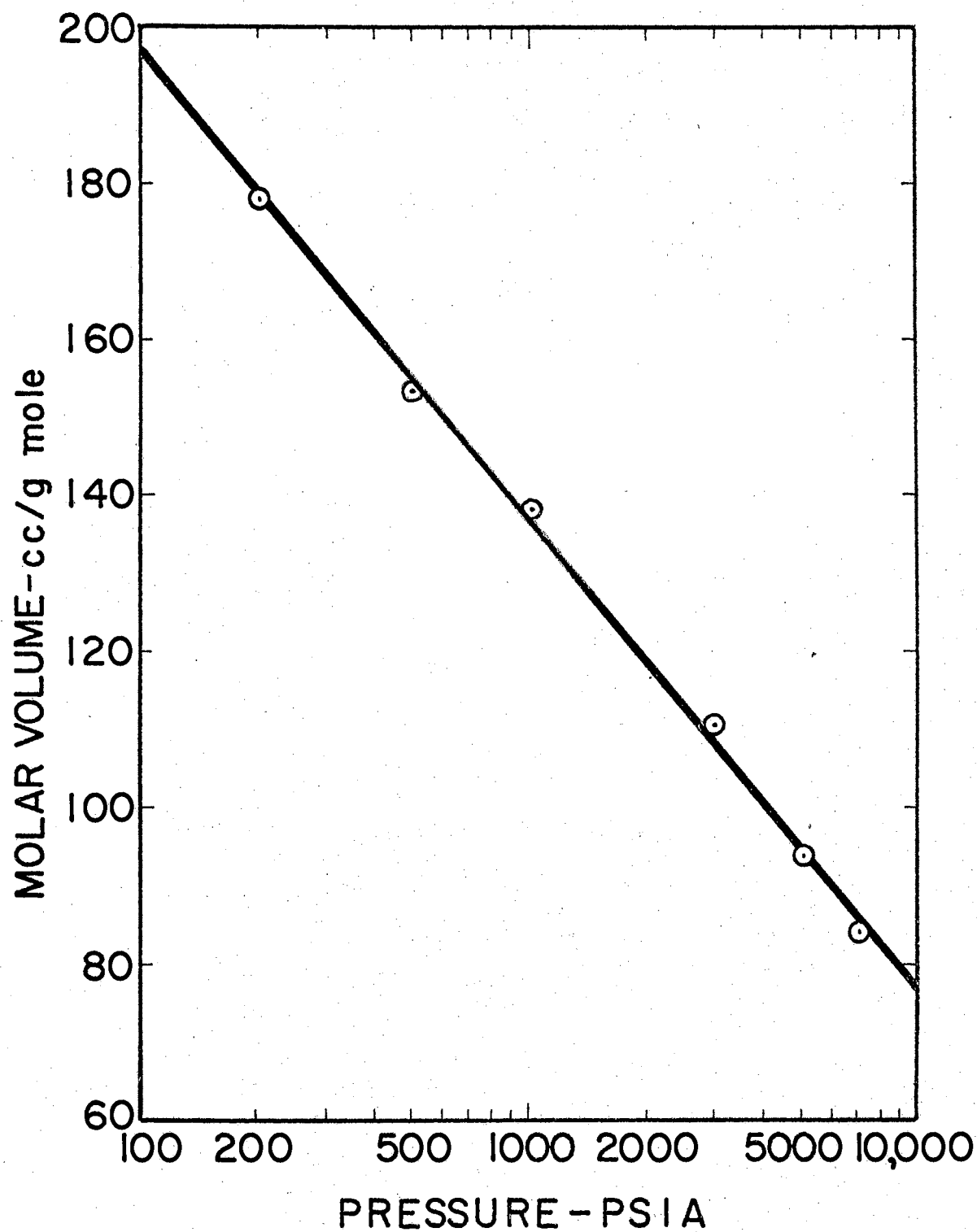


FIGURE 19  
EQUILIBRIUM LIQUID PHASE MOLAR  
VOLUMES AT 150° F.

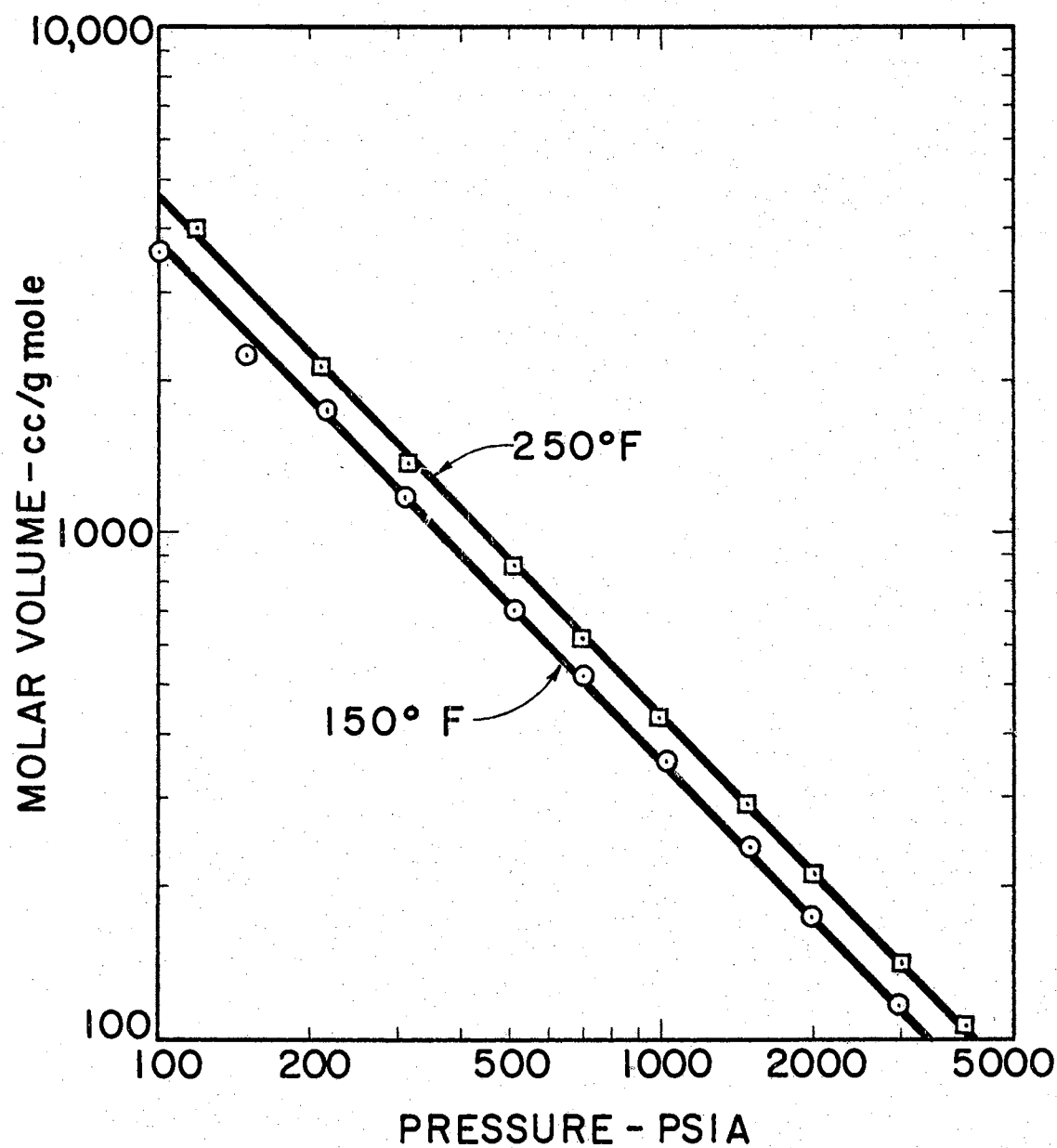


FIGURE 20  
EQUILIBRIUM VAPOR PHASE MOLAR  
VOLUMES AT 150°F AND 250°F.

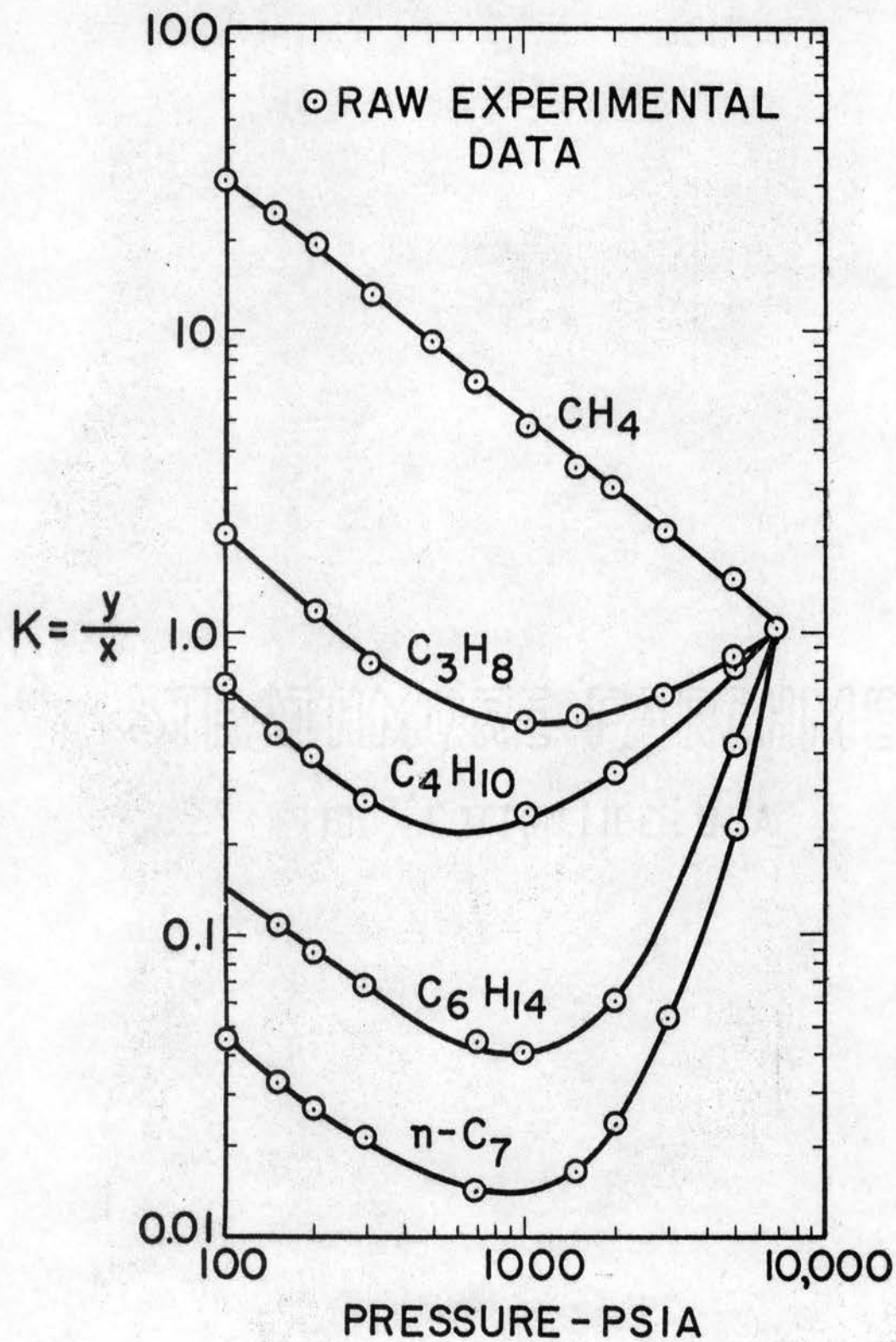


FIGURE 21  
K-VALUES AT 150°F.

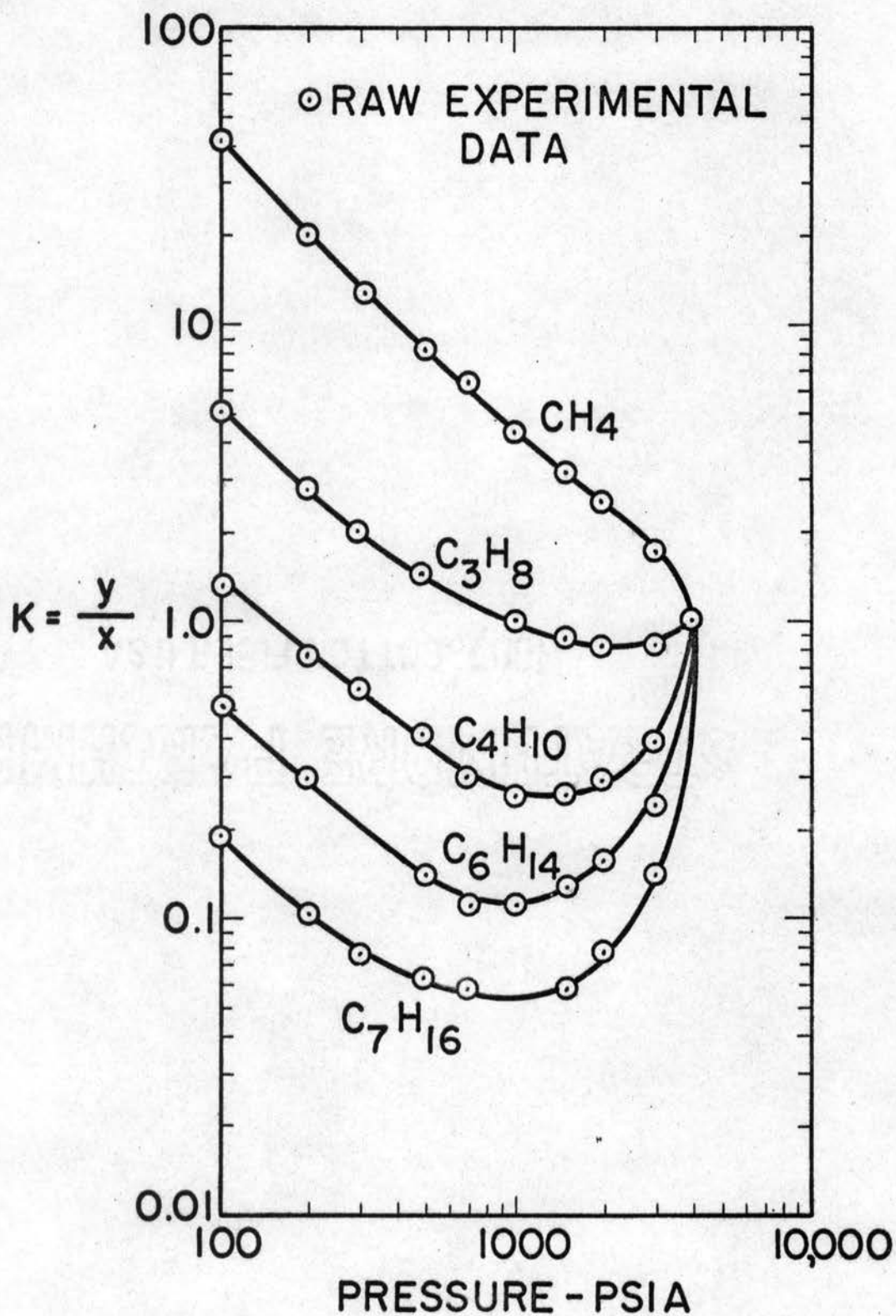


FIGURE 22  
K-VALUES AT 250° F.

The temperature in the air bath housing the volumetric sampling apparatus was measured with a Beckman differential thermometer which was calibrated against a platinum resistance thermometer. The air bath temperature was controlled to  $\pm 0.1^{\circ}\text{F}$ . The temperature of the gas sample was taken to be that of the bath. Readings taken during a run indicated that the temperature varied a maximum of  $0.2^{\circ}\text{F}$  during the run.

The U-tube manometer mercury levels were measured with a cathetometer that could be read to 0.05 mm. Repetitions of measurements indicated that observational errors rarely exceeded 0.05 mm Hg. The maximum error in pressure measurement was estimated to be 0.2 mm Hg. Volumetric errors are discussed in Appendix C.

The thermocouple in the equilibrium cell was calibrated against a N.B.S. calibrated platinum resistance thermometer. The error in this calibration is approximately  $0.05^{\circ}\text{F}$ . Temperature in the equilibrium cell was controlled to  $\pm 0.1^{\circ}\text{F}$  from the start of the vapor recirculation to the end of sampling.

The pressure in the cell was measured to within  $\pm 0.2\%$  of the pressure measured. Errors in pressure and temperature of the magnitude reported should have little or no effect on the compositions of the equilibrium phases.

The errors in the composition assay of the equilibrium phases by chromatography are considered to be the largest experimental errors. The manufacturer of the chromatograph states that an accuracy of 1.5% of the true composition value is the best that the analyst can expect for non-routine analyses. The statistical analysis of the chromatographic calibration data indicated that the accuracy of the



the composition data is on the order of 1.5-2.5% of the true value.

Runs 127 and 128 were made at 250°F and 713 psia for duplicate run comparison. The methane K-values were 6.77 and 6.52 respectively, a difference of 4%. The equilibrium vapor and liquid densities differed by 2 and 5% respectively.

#### Thermodynamic Consistency Test

Tully (68) applied three different thermodynamic consistency tests to his experimental vapor-liquid equilibria data for the methane-ethylene system. The tests used were (1) the Thompson-Edmister (67) test, (2) the Edmister (12) test, and (3) a modified form of the Thompson-Edmister test. These tests were discussed in Chapter III of this thesis.

Of the consistency tests evaluated, Tully (68) found that the Edmister (12) test is the best. The Edmister integral form consistency test was chosen for use in this work on the basis of Tully's recommendations.

The Edmister test circumvents the two principal difficulties encountered in the Thompson-Edmister test. These difficulties are the determinations of  $\xi_i$  and the different forms of data required for the integral test.

Thompson (67) used a truncated Berlin form virial equation of state to evaluate  $\xi_i$ . This truncated form does not adequately describe the complex behavior of gas mixtures. Any errors in  $\xi_i$  are directly reflected in the consistency test, due to the important role which  $\xi_i$  plays in the test.

The derivation of the Edmister isothermal thermodynamic consistency

test was presented in Chapter III. The integral form of this test follows

$$\int_{P_1}^{P_2} d \ln \phi_1 / \phi_2 + \int_{P_1}^{P_2} d \ln y_1 / y_2 = \int_{P_1}^{P_2} \frac{\underline{V}^V - \underline{V}^L}{RT(y_1 - x_1)} dP \quad (\text{III-71})$$

This consistency test was derived for a binary system. In order to apply the test to the methane-condensate data of this work, it was necessary to consider the system as a binary, one component being methane and the other component being the condensate. The evaluation of the various terms in Equation III-71 will now be discussed.

The fugacity coefficients of vapor mixture components,  $\phi_i$ , and the mean fugacity coefficient for the total vapor mixture,  $\phi_m$ , can be calculated from the critical constants of the components and combinations of them by means of the Redlich-Kwong equation of state (46). The logarithm of the fugacity coefficient for a mixture component is calculated from the following equation (46).

$$\ln \phi_i = (Z - 1) \frac{B_i}{B} - \ln (Z - BP) - \frac{A^2}{B} \left[ 2 \frac{A_i}{A} - \frac{B_i}{B} \right] \ln(1 + BP) \quad (\text{VII-1})$$

where      subscripts denote component values; no subscripts denote mixture values

$$A_i = 0.6541/T_r^{1.25} P_c^{0.5} \quad (\text{VII-2})$$

$$B_i = 0.0867/T_r P_c \quad (\text{VII-3})$$

$$A^2/B = 4.933/T_r^{1.5} \quad (\text{VII-4})$$

$$A = \sum y_i A_i \quad (\text{VII-5})$$

$$B = \sum y_i B_i \quad (\text{VII-6})$$

The value of  $Z$  must be determined by successive approximations of the original Redlich-Kwong (46) equation in  $Z$  form. Equation VII-1 reduces to the following equation for the logarithm of the fugacity coefficient for the total vapor mixture

$$\ln \phi_m = (Z - 1) - \ln (Z - BP) - \frac{A^2}{B} \ln (1 + BP) \quad (\text{VII-7})$$

The mean fugacity coefficient for a mixture,  $\phi_m$ , is defined by (47)

$$\ln \phi_m = \sum y_i \ln \phi_i \quad (\text{VII-8})$$

If the fugacity coefficient for one component of a binary mixture is known and the mean fugacity coefficient is also known, then the fugacity coefficient for the second component can be calculated from Equation VII-3 as follows

$$\ln \phi_2 = \frac{\ln \phi_m - y_1 \ln \phi_1}{y_2} \quad (\text{VII-9})$$

Equation VII-9 was used to evaluate the fugacity coefficient for the condensate.

The critical constants for methane used in Equation VII-1 were obtained from the API 44 tabulation (53). The critical constants for the condensate were evaluated as follows

$$T_c = \sum y_i T_{c_i} \quad (\text{VII-10})$$

$$P_c = \sum y_i P_{c_i} \quad (\text{VII-11})$$

The compositions used in Equations VII-10 and VII-11 were obtained from the chromatographic assay of the condensate reported in Table IV.

The critical constants used were also from the API 44 tabulation (53) and are presented in Appendix K.

The quantities, A and B, used in Equation VII-7 to evaluate the mixture fugacity coefficient were evaluated via Equations VII-5 and VII-6. The compositions used were obtained from the chromatographic assay of the vapor mixture for which the mean fugacity coefficient was being evaluated. The critical constants used were those tabulated in Appendix K.

The quantity  $\underline{V}^V - \underline{V}^L$  in Equation III-71 was evaluated from the experimental molar vapor and liquid volumes. The values of  $\ln(\phi_1/\phi_2)$ ,  $\ln(y_1/y_2)$  and  $\underline{V}^V - \underline{V}^L/RT$  calculated from experimental data are tabulated in Table VII. These quantities are plotted as a function of pressure in Figures 23 through 30.

The integration of Equation III-71 is facilitated by rearranging the equation as follows

$$\int_{P_1}^{P_2} (y_1 - x_1) d \ln \frac{\phi_1}{\phi_2} + \int_{P_1}^{P_2} (y_1 - x_1) d \ln \frac{y_1}{y_2} = \int_{P_1}^{P_2} \frac{\underline{V}^V - \underline{V}^L}{RT} dP \quad (\text{VII-12})$$

The two left hand terms are now in a form which can be readily integrated according to the following relationship.

$$\int u dv = uv - \int v du \quad (\text{VII-13})$$

The first term of Equation VII-12 would then be integrated as follows:

$$\int_{P_1}^{P_2} (y_1 - x_1) d \ln \frac{\phi_1}{\phi_2} = (y_1 - x_1) \ln \frac{\phi_1}{\phi_2} - \int_{P_1}^{P_2} \ln \frac{\phi_1}{\phi_2} \frac{d(y_1 - x_1)}{dP} dP \quad (\text{VII-14})$$

TABLE VII

## CALCULATED QUANTITIES FOR CONSISTENCY TEST

<u>Pressure, psia</u>	<u><math>\ln \phi_1/\phi_2</math></u>	<u><math>\ln y_1/y_2</math></u>	<u><math>\frac{v^V - v^L}{RT}</math></u>
<u>Temperature - 150°F</u>			
152.56	0.93925	2.45162	0.00472
214.46	0.96171	2.71885	0.00378
313.76	0.98817	3.13716	0.00244
513.51	1.01124	3.50193	0.00133
711.00	1.03329	3.71398	0.00091
1034.45	1.05831	3.99695	0.00052
1510.73	1.08914	3.91035	0.00024
2012.43	1.11756	3.89358	0.00010
3010.10	1.17006	3.35291	0.00000
5009.31	1.16964	2.36140	0.00019
<u>Temperature - 250°F</u>			
218.56	0.86825	1.65399	0.00390
314.74	0.90553	2.13311	0.00247
513.39	0.9573	2.41907	0.00143
712.98	0.98718	2.70113	0.00113
1013.31	1.00450	2.93271	0.00064
1512.99	1.03046	2.97042	0.00034
2012.38	1.05136	2.95799	0.00014
3011.43	1.09075	2.70890	0.00007

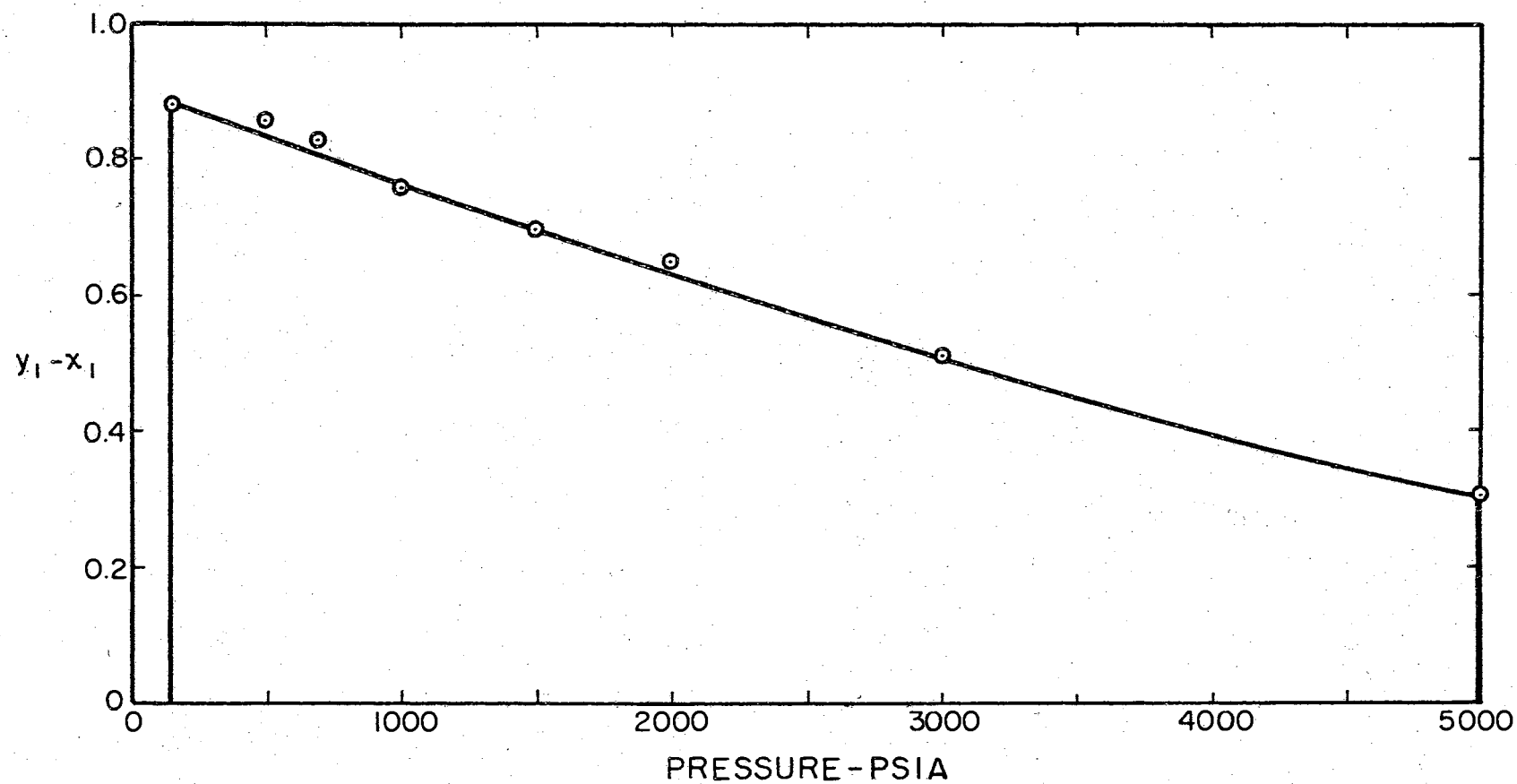


FIGURE 23  
( $y_1 - x_1$ ) VS. PRESSURE, 150°F

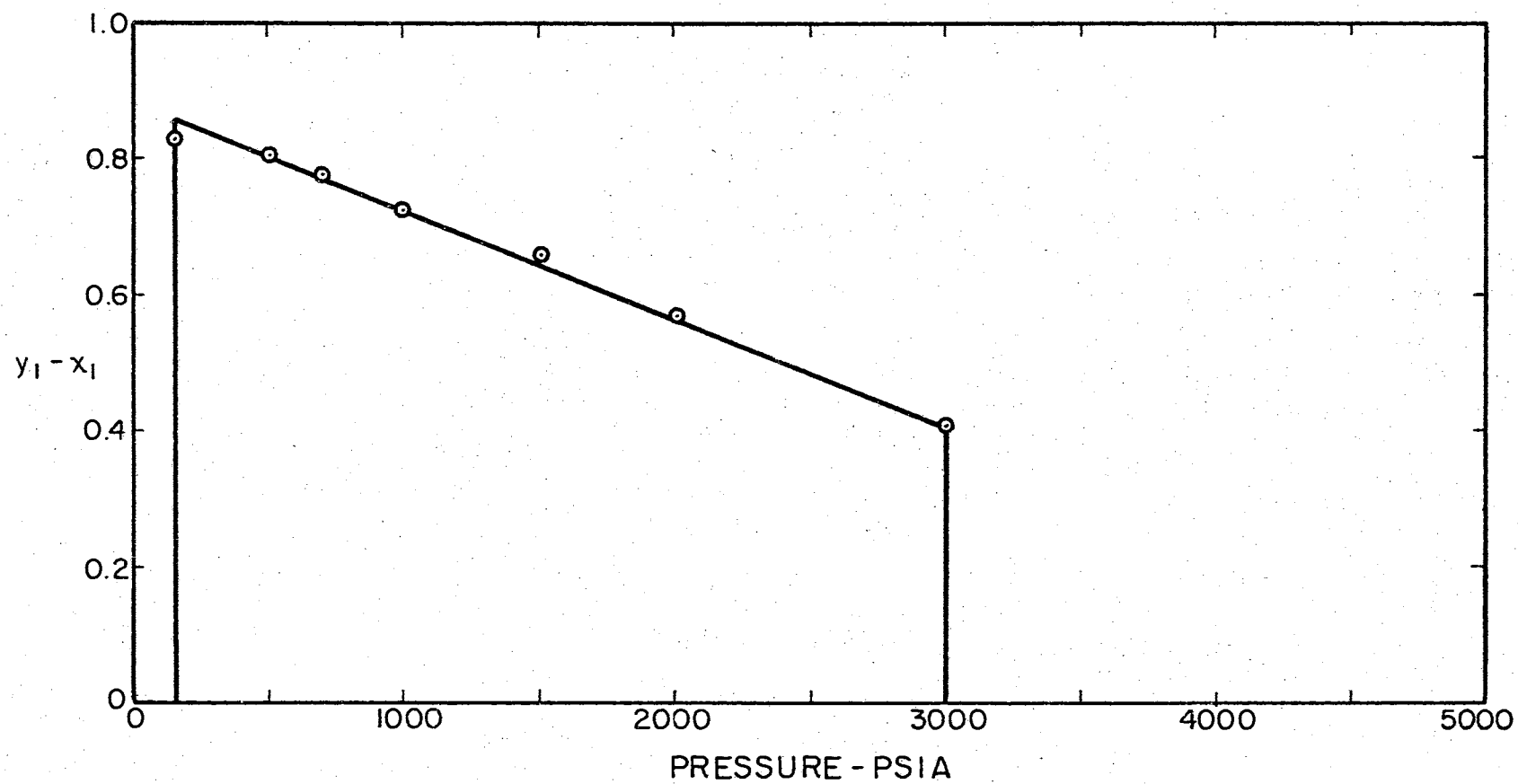


FIGURE 24  
( $y_1 - x_1$ ) VS. PRESSURE, 250°F

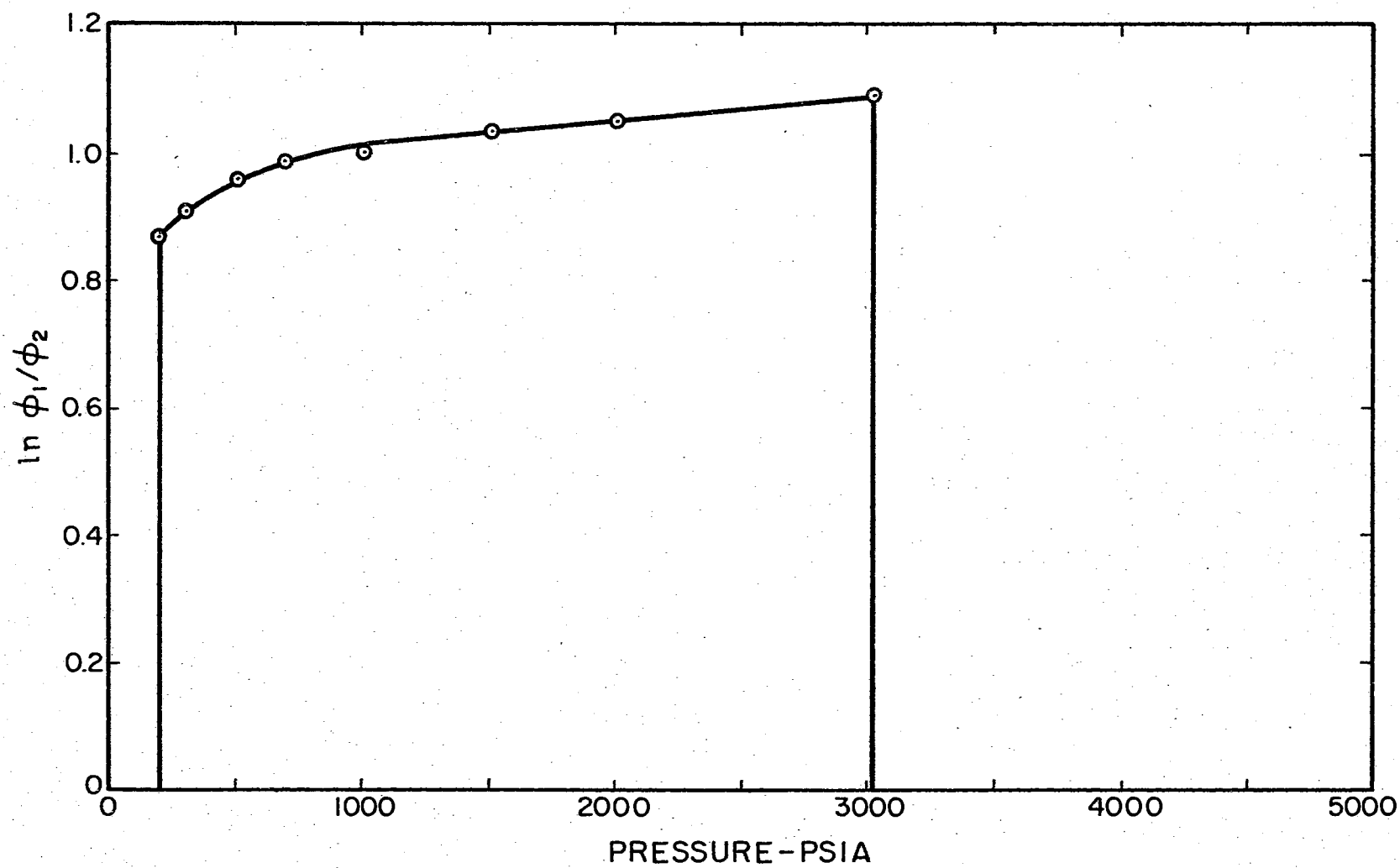


FIGURE 25  
 $\ln \phi_1/\phi_2$  VS. PRESSURE, 250°F



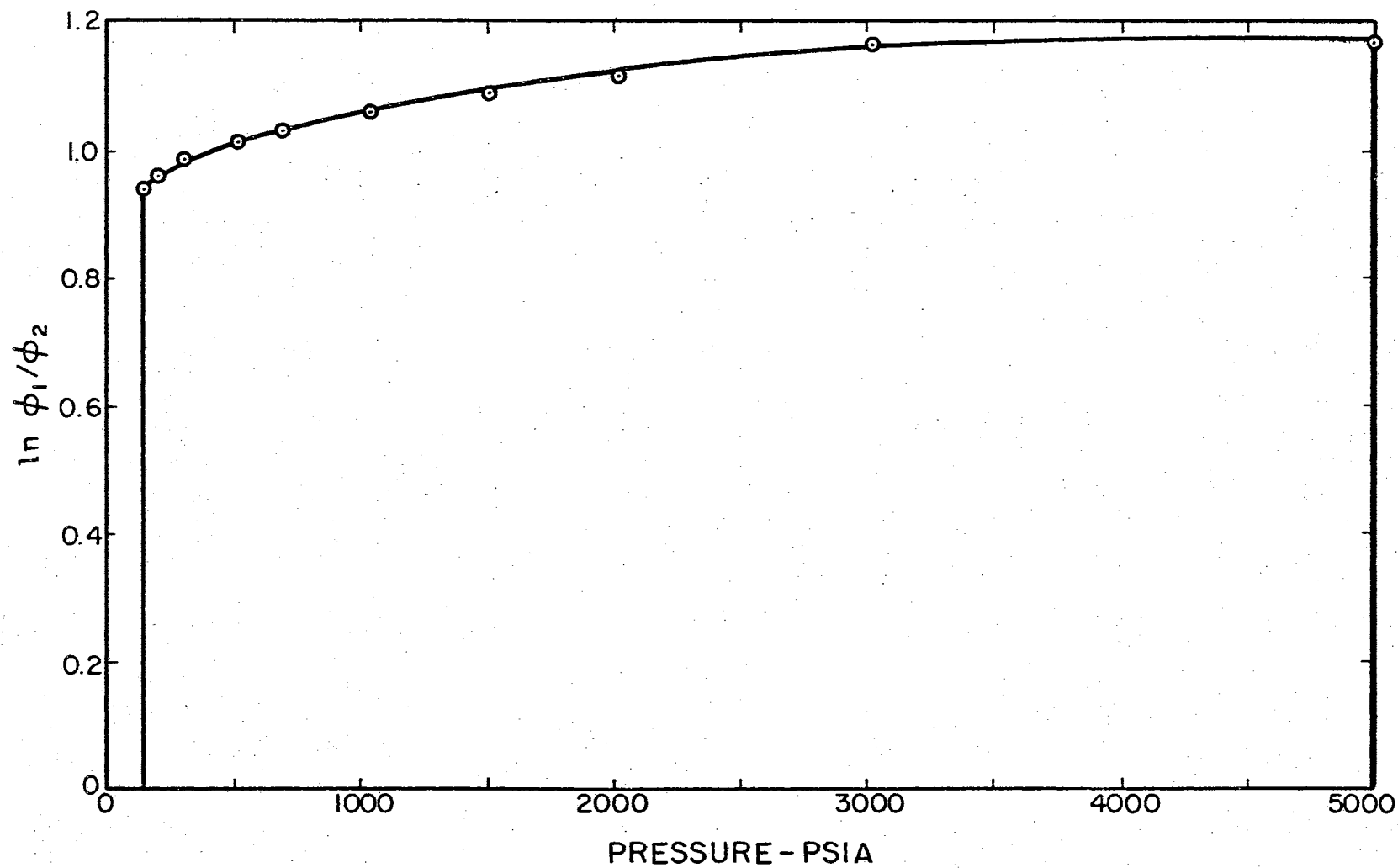


FIGURE 26  
 $\ln \phi_1/\phi_2$  VS. PRESSURE, 150°F

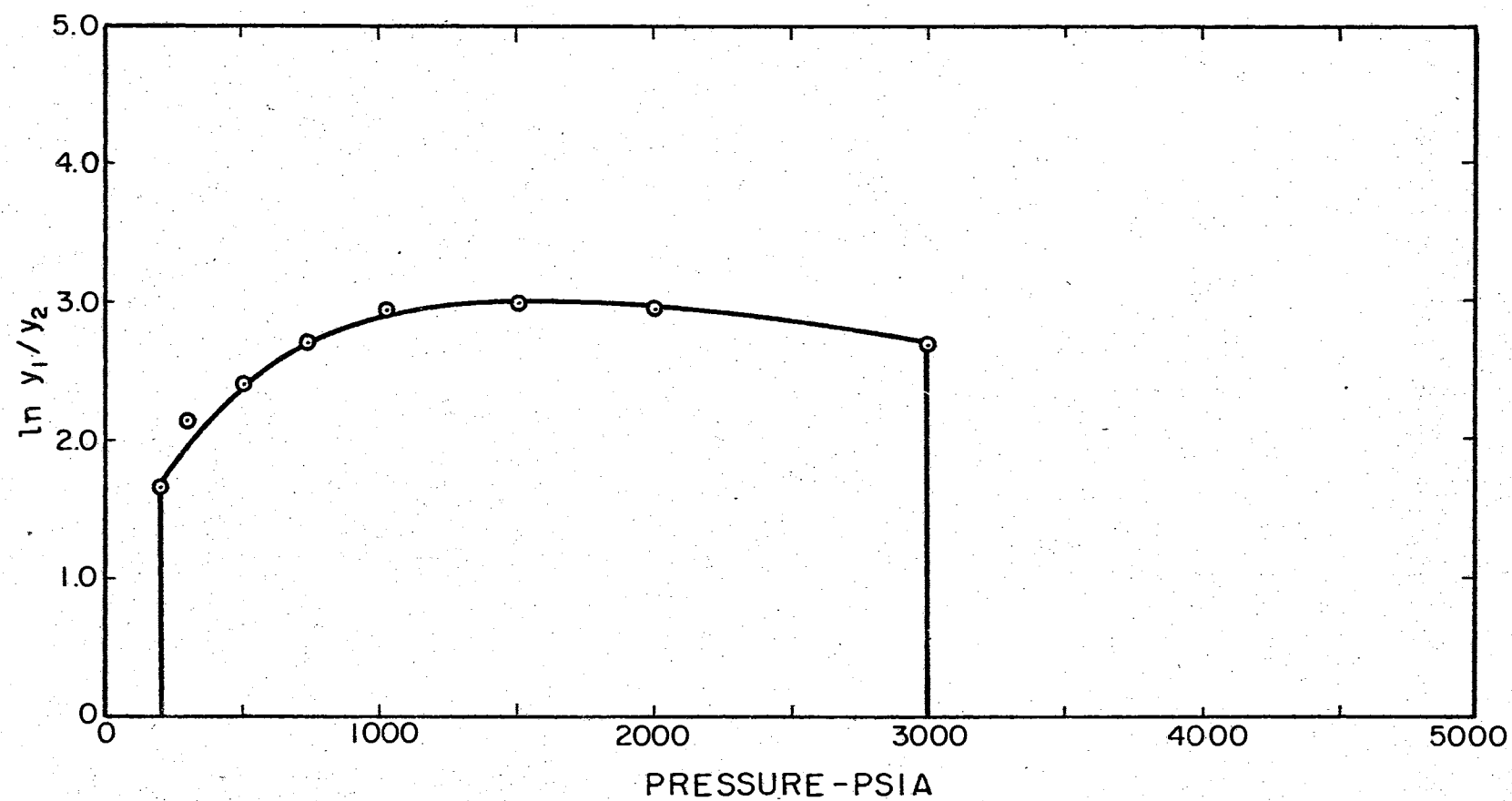


FIGURE 27  
 $\ln y_1/y_2$  VS. PRESSURE, 250°F

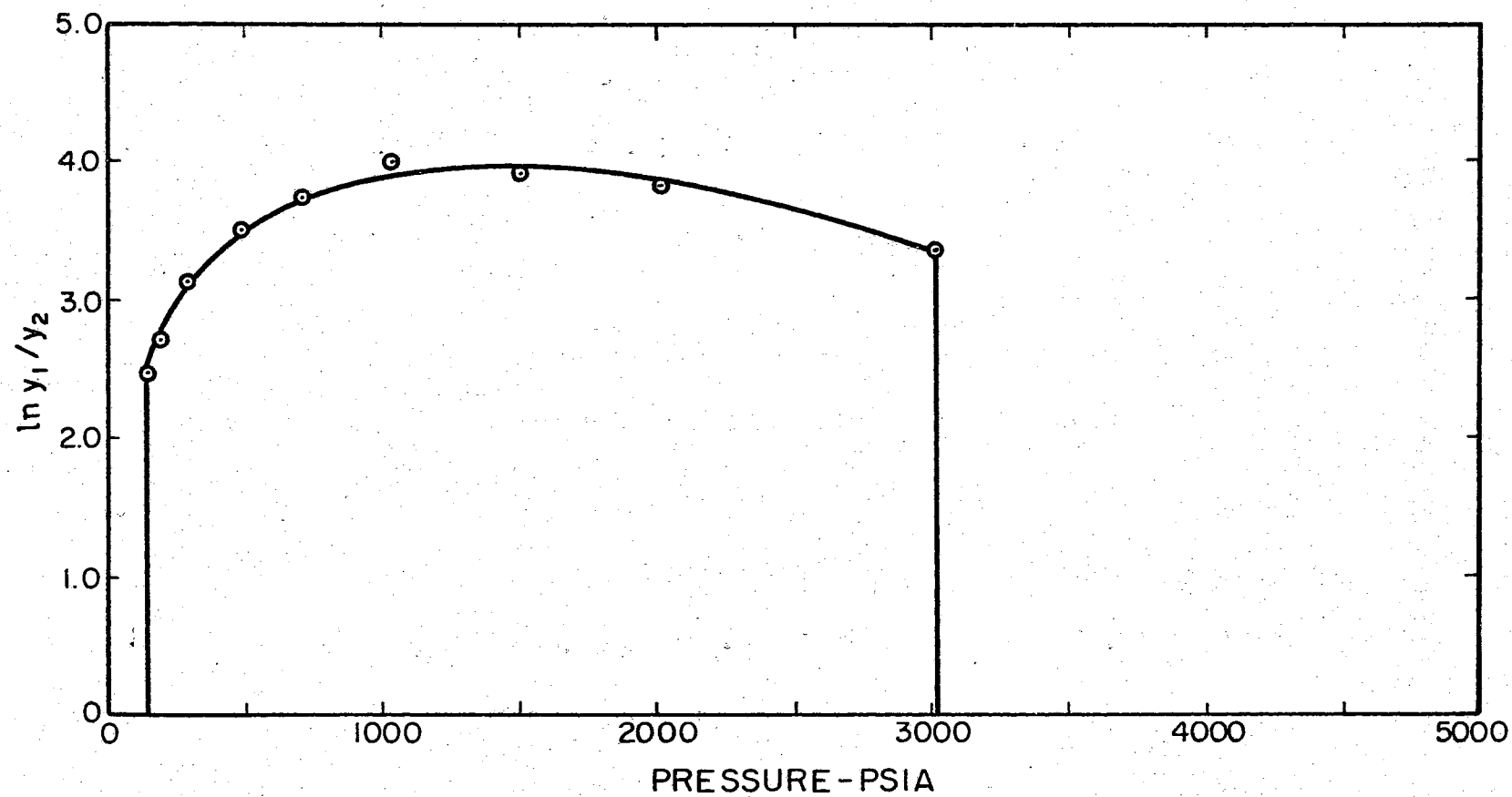


FIGURE 28  
 $\ln y_1/y_2$  VS. PRESSURE, 150 °F

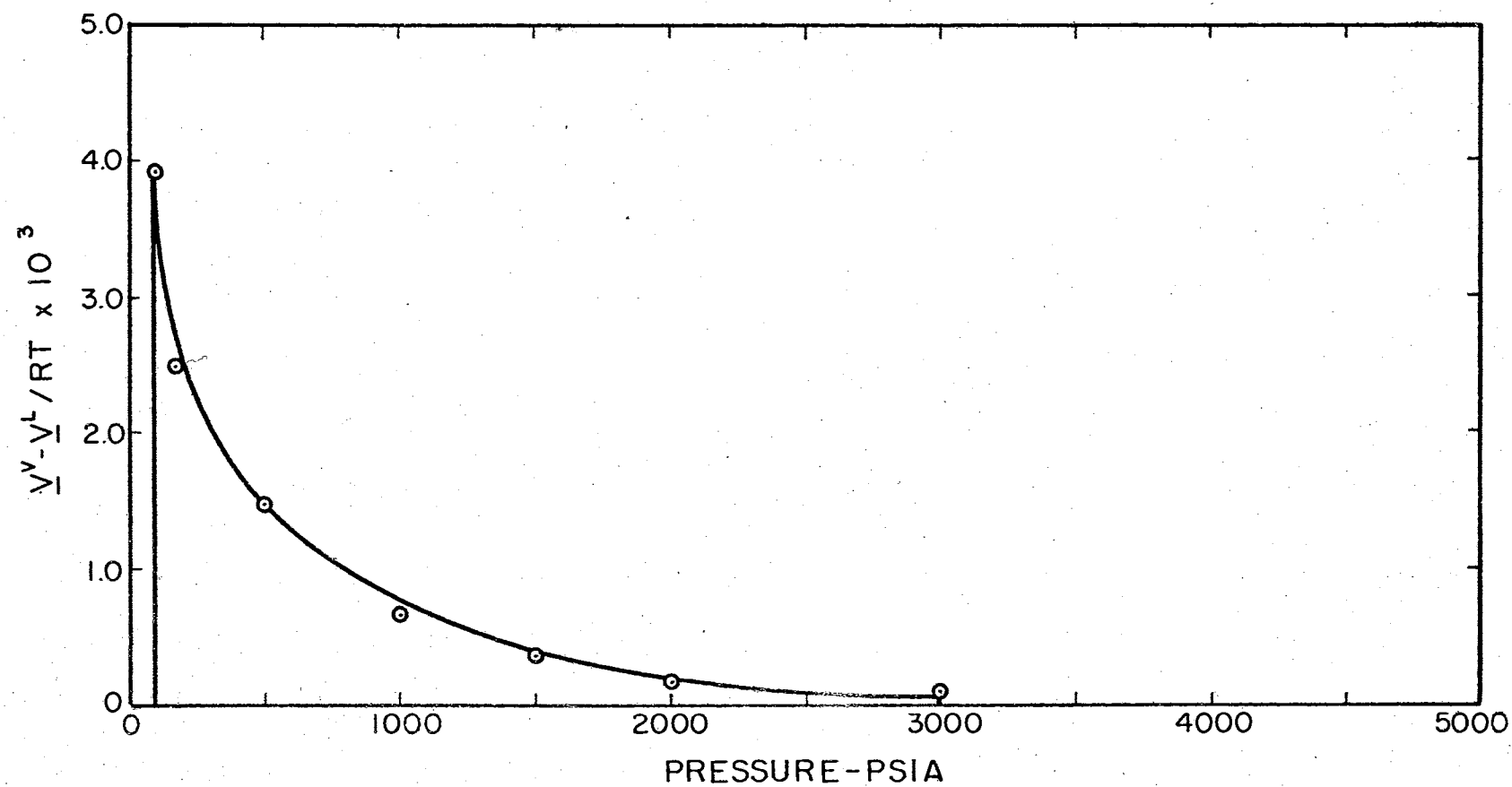


FIGURE 29  
 $\underline{V}^v - \underline{V}^l / RT$  VS. PRESSURE, 250°F

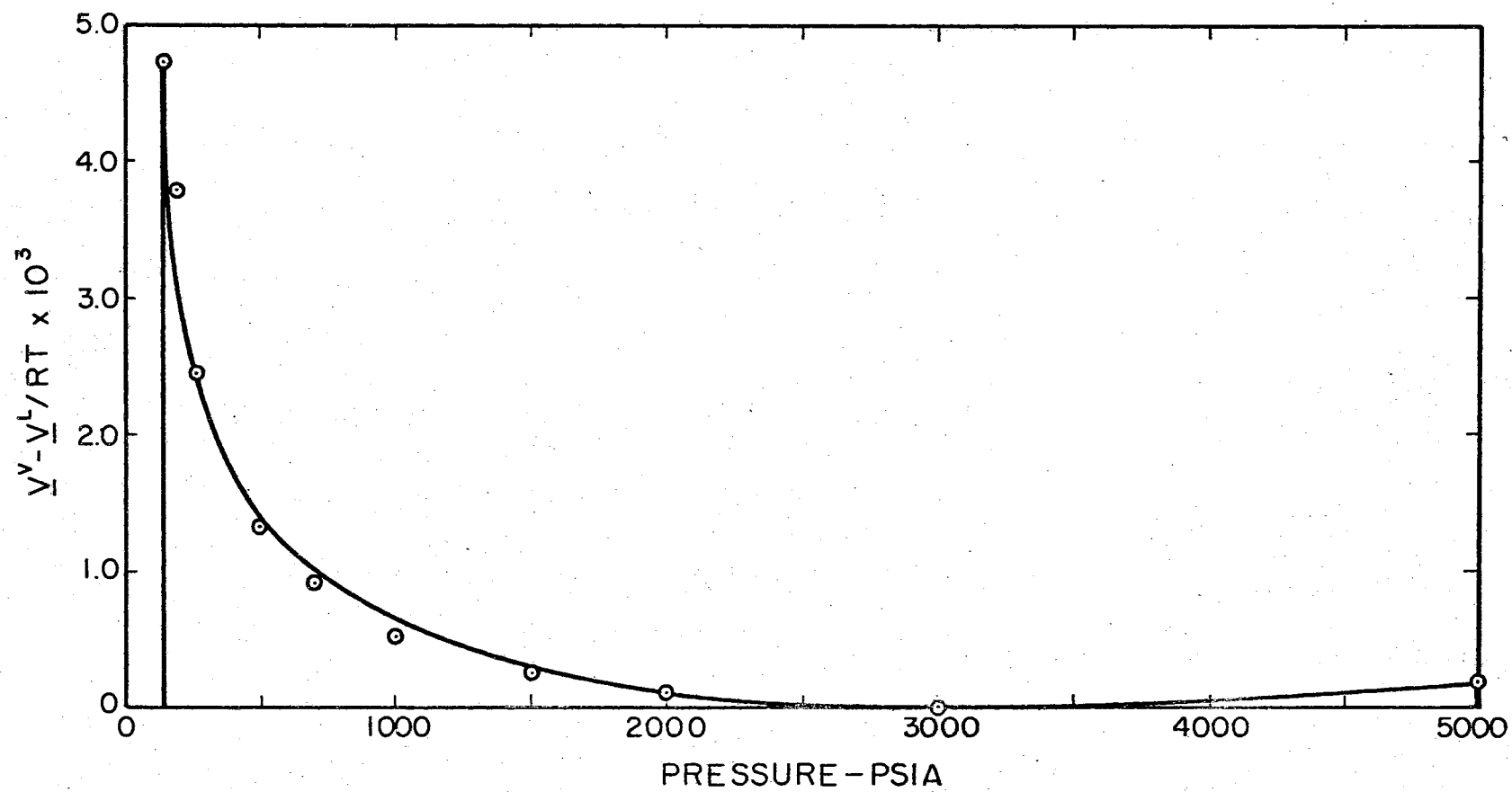


FIGURE 30  
 $\underline{V}^v - \underline{V}^l / RT$  VS. PRESSURE, 150°F

The integration of the second term would be handled in a similar manner. An analytical expression for  $(y_1 - x_1)$  vs. pressure was required to perform the integral test of Equation VII-12. This expression was obtained by fitting a fourth degree polynomial to the experimental  $(y_1 - x_1)$  values. The coefficients for this polynomial are presented in Table VIII.

The results of the Edmister consistency test are summarized in Table IX. The results of the test of the methane-condensate data of this work indicate that the 150°F data are consistent in the range 150-1500 psia while the 250°F data are consistent in the range 218-2000 psia. It is not safe to conclude that the high pressure data are not consistent. The vapor fugacity coefficients were calculated via the Redlich-Kwong equation of state. The reduced pressure for the condensate at 3000 psia was 7.25 increasing to 16.8 at 7000 psia. The accuracy of the Redlich equation is questionable in this high reduced pressure range.

#### Data and Correlation Comparisons

The comparison of experimental vapor-liquid equilibrium data for complex hydrocarbon systems is difficult unless the data compared are at the same temperature and pressure and for identical systems. Data have not been published for a methane-condensate system at temperatures and pressures corresponding to those investigated in this work.

Katz and Hachmuth (24) did study a natural gas-crude oil system at 150 and 250°F. The techniques used in their work were discussed in Chapter II. The methane K-values obtained in this work are compared in Table X with those obtained by Katz and Hachmuth. There is

TABLE VIII

COEFFICIENTS FOR POLYNOMIAL FIT OF

EXPERIMENTAL  $(y_1 - x_1)$  DATA

$$\text{Model: } (y_1 - x_1) = B_1 + B_2 P + B_3 P^2 + B_4 P^3 + B_5 P^5$$

Temperature - 150°F

$$B_1 = 0.91256117$$

$$B_2 = 0.21167821 \times 10^{-3}$$

$$B_3 = 0.84530336 \times 10^{-7}$$

$$B_4 = -.28757997 \times 10^{-10}$$

$$B_5 = 0.30905587 \times 10^{-14}$$

Temperature - 250°F

$$B_1 = 0.85955146$$

$$B_2 = 0.95785730 \times 10^{-4}$$

$$B_3 = 0.35206084 \times 10^{-7}$$

$$B_4 = 0.5609912 \times 10^{-11}$$

$$B_5 = 0.0$$

TABLE IX

## RESULTS OF EDMISTER ISOTHERMAL INTEGRAL

## THERMODYNAMIC CONSISTENCY TEST

<u>Upper</u> <u>Limits of</u> <u>Integration, psia</u>	<u>Lower</u> <u>Limits of</u> <u>Integration, psia</u>	Area 1 (1) First Term Left Side <u>Equation VII-12</u>	Area 2 Second Term Left Side <u>Equation VII-12</u>	Area 1 Plus Area 2	Area 3 Third Term Right Side <u>Equation VII-12</u>	% Diff. (2)
<u>Temperature = 150°F</u>						
313.7	152.6	0.62409	-0.05329	0.57079	0.57189	0.19
513.5	152.6	1.00923	-0.10024	0.90899	0.94842	4.15
1034.5	152.6	1.58577	-0.19733	1.38844	1.43029	3.20
1510.7	152.6	1.96155	-0.34954	1.61128	1.61200	0.04
2012.4	152.6	2.60085	-0.55597	2.04487	1.69657	-20.70
3010.1	152.6	3.15524	-0.83600	2.31923	1.74645	-32.74
<u>Temperature = 250°F</u>						
712.9	218.5	0.95055	0.13863	0.81191	0.94917	14.46
2012.4	218.5	2.04787	-0.52139	1.52647	1.57966	3.36
3011.4	218.5	2.66284	-0.80474	1.85805	1.68456	-10.29

(1) See Equation VII-12

(2) % Diff. =  $\left( \frac{\text{Right side} - \text{left side}}{\text{Right side}} \right) 100$



TABLE X  
COMPARISON OF EXPERIMENTAL K-VALUES  
FOR METHANE IN COMPLEX SYSTEMS

<u>Temperature, °F</u>	<u>Pressure, psia</u>	<u>Values of <math>K = y/x</math></u>	
		<u>Katz-Hachmuth (25)</u>	<u>This Work</u>
150	200	21.0	18.9
	500	8.3	8.5
	700	6.2	6.6
	1000	4.6	4.6
	2000	2.8	2.9
	3000	2.2	2.1
250	200	20.5	17.2
	500	8.7	8.3
	1000	4.5	4.3
	2000	2.8	2.5
	3000	2.1	1.7

favorable agreement between these two sets of data. The differences in the K-values compared can be attributed to the composition effects of the different solvents.

The data obtained in this work were next compared with the NGSMA Correlation (34). This graphical correlation published in 1955 was constructed by the Fluor Corporation from data compiled by Dr. G. G. Brown and Fluor. The interested reader is referred elsewhere (64) for a discussion of this widely used correlation.

The 150°F experimental methane K-values were compared with the 10,000 psi convergence pressure NGSMA K-values. The 250°F experimental data were compared with the 5000 psi convergence pressure K-values. These comparisons are presented in Table XI. The experimental values are 13% higher than the NGSMA values at 150°F and 16% higher at 250°F.

The regular solution correlation method of Chao and Seader (8) was applied to a 16 component system made up from components in the experimental system. The first 15 components corresponded to the 15 components in the experimental system lighter than normal heptane. The 16<sup>th</sup> component was a heptanes-plus fraction.

The Chao-Seader method is a composition dependent correlation. The equations in the Chao-Seader correlation can be solved to get K-values if the compositions of the coexisting vapor and liquid phases are known (given or assumed from a previous trial). If the compositions are assumed, then it is necessary to check bubble point, dew point or flash calculations to see if the resulting compositions agree with those used in the K-value predictions.

The experimental vapor and liquid compositions obtained in this work were used directly in the Chao-Seader equations to predict

TABLE XI  
COMPARISON OF EXPERIMENTAL AND NGSMA  
K-VALUES FOR METHANE

<u>Temperature, °F</u>	<u>Pressure</u>	<u>NGSMA (34)</u>	<u>This Work</u>
150	100	32.0	31.9
	150	21.2	23.8
	200	16.2	18.9
	300	11.5	12.8
	500	7.4	9.0
	700	5.5	6.6
	1000	4.15	5.1
	2000	2.5	2.95
	3000	1.95	2.11
	5000	1.45	1.45
250	200	15.5	17.2
	500	6.7	8.3
	1000	3.8	4.3
	2000	2.3	2.5
	3000	1.65	1.7

K-values. Comparisons of the calculated and experimental K-values for the 16-component system described above are presented in Tables XII and XIII. Data was tested up to the 2000 psia limit of the Chao-Seader correlation. The average difference between the experimental and calculated methane K-values was 12.7% at 150°F and 3.3% at 250°F. The difference between the experimental and calculated methane K-values can be reduced by using a solubility parameter of 5.5 for methane rather than the value of 5.68 recommended in Chao-Seader publication.

TABLE XII

COMPARISON OF CHAO-SEADER AND EXPERIMENTAL K-VALUES AT 150 F.

TEMPERATURE, F.	150.05	150.06	150.07	150.09
PRESSURE, PSIA	152.56	214.47	313.77	513.50
	K-VALUE = Y/X			
	C-S	EXP.	C-S	EXP.
METHANE	22.839	23.765	16.450	18.860
ETHANE	6.327	- - -	4.579	- - -
PROPANE	2.174	2.091	1.615	1.124
ISOBUTANE	.994	.718	.750	.532
N-BUTANE	.774	.463	.586	.392
2,2-DIMETHYLPROPANE	.610	.555	.466	.406
ISOPENTANE	.352	.202	.270	.190
N-PENTANE	.289	.162	.223	.162
2,2-DIMETHYLBUTANE	.214	.064	.166	.116
CYCLOPENTANE	.181	.111	.138	.156
2-METHYLPENTANE	.146	.095	.114	.168
3-METHYLPENTANE	.130	.089	.101	.170
N-HEXANE	.108	.078	.084	.085
METHYLCYCLOPENTANE	.095	.064	.074	.068
CYCLOHEXANE	.076	.049	.059	.057
HEPTANE PLUS FRACTION	.001	.007	.001	.008

TEMPERATURE, F.	150.06	150.04	150.04	150.06
PRESSURE, PSIA	711.00	1034.45	1510.73	2012.43
	K-VALUE = Y/X			
	C-S	EXP.	C-S	EXP.
METHANE	5.490	5.700	3.920	4.377
ETHANE	1.585	- - -	1.157	- - -
PROPANE	.677	.552	.553	.493
ISOBUTANE	.354	.313	.310	.293
N-BUTANE	.283	.231	.251	.268
2,2-DIMETHYLPROPANE	.241	.261	.220	.222
ISOPENTANE	.145	.175	.137	.143
N-PENTANE	.120	.159	.114	.135
2,2-DIMETHYLBUTANE	.096	.066	.092	.072
CYCLOPENTANE	.073	.067	.070	.070
2-METHYLPENTANE	.067	.058	.066	.046
3-METHYLPENTANE	.059	.049	.059	.043
N-HEXANE	.050	.045	.050	.040
METHYLCYCLOPENTANE	.042	.034	.043	.026
CYCLOHEXANE	.035	.024	.036	.018
HEPTANE PLUS FRACTION	.000	.005	.000	.003

TABLE XIII

COMPARISON OF CHAO-SEADER AND EXPERIMENTAL K-VALUES AT 250 F.

TEMPERATURE, F.	249.98		250.00		250.00		250.00	
PRESSURE, PSIA	113.86		213.41		314.74		513.39	
			K-VALUE = Y/X					
	C-S	EXP.	C-S	EXP.	C-S	EXP.	C-S	EXP.
METHANE	33.979	31.476	18.518	20.183	12.748	12.719	7.944	8.178
ETHANE	14.920	- - -	7.931	- - -	5.316	- - -	3.184	- - -
PROPANE	5.845	4.408	3.244	2.784	2.267	2.034	1.483	1.491
ISOBUTANE	3.090	3.305	1.756	1.982	1.254	1.386	.862	1.139
N-BUTANE	2.586	2.899	1.478	1.707	1.062	1.400	.739	1.080
2,2-DIMETHYLPROPANE	2.103	1.731	1.214	.730	.880	.475	.625	.489
ISOPENTANE	1.360	1.394	.794	.857	.582	.532	.423	.467
N-PENTANE	1.199	1.231	.702	.787	.515	.602	.376	.417
2,2-DIMETHYLBUTANE	.936	.628	.553	.415	.410	.377	.305	.239
CYCLOPENTANE	.820	.894	.481	.468	.354	.349	.260	.213
2-METHYLPENTANE	.711	.624	.422	.359	.314	.291	.237	.207
3-METHYLPENTANE	.646	.579	.384	.340	.286	.267	.216	.178
N-HEXANE	.565	.515	.337	.314	.252	.112	.192	.140
METHYLCYCLOPENTANE	.490	.391	.291	.245	.217	.182	.164	.135
CYCLOHEXANE	.395	.313	.236	.190	.177	.135	.136	.104
HEPTANE PLUS FRACTION	.017	.067	.010	.037	.004	.026	.000	.024

TEMPERATURE, F.	250.00		250.00		250.00		250.00	
PRESSURE, PSIA	712.98		1013.31		1512.99		2012.38	
				K-VALUE = Y/X				
	C-S	EXP.	C-S	EXP.	C-S	EXP.	C-S	EXP.
METHANE	5.042	6.775	4.181	4.271	2.929	3.228	2.289	2.490
ETHANE	1.911	- - -	1.508	- - -	.985	- - -	.722	- - -
PROPANE	.971	1.374	.854	1.163	.675	.890	.583	.822
ISOBUTANE	.600	1.015	.550	.735	.481	.641	.451	.513
N-BUTANE	.521	.861	.484	.601	.432	.570	.411	.460
2,2-DIMETHYLPROPANE	.430	.600	.424	.619	.395	.085	.386	.105
ISOPENTANE	.320	.366	.302	.294	.293	.306	.295	.317
N-PENTANE	.286	.293	.271	.263	.265	.266	.268	.293
2,2-DIMETHYLBUTANE	.219	.139	.227	.148	.229	.121	.235	.189
CYCLOPENTANE	.241	.155	.193	.142	.191	.192	.198	.191
2-METHYLPENTANE	.181	.136	.180	.128	.185	.147	.193	.188
3-METHYLPENTANE	.170	.120	.165	.126	.171	.138	.179	.164
N-HEXANE	.156	.108	.149	.113	.156	.127	.164	.157
METHYLCYCLOPENTANE	.151	.079	.128	.087	.134	.098	.143	.256
CYCLOHEXANE	.134	.061	.109	.060	.117	.080	.128	.102
HEPTANE PLUS FRACTION	.000	.008	.000	.015	.000	.006	.000	.025

## CHAPTER VIII

### CONCLUSIONS AND RECOMMENDATIONS

The purpose of this study was to develop certain techniques and equipment for obtaining vapor-liquid equilibrium ratios and phase densities for components of complex hydrocarbon systems. Experimental P-T-x-y and density data were obtained for a methane-natural gas condensate system at 150°F and 250°F at pressures from 100 psia to the dew or critical point of the system at these temperatures.

The theoretical aspects of this work were primarily concerned with the evaluation and correlation testing of the experimental vapor-liquid equilibrium data.

The major conclusions for the experimental part of the work are as follows:

1. The variability of the experimental composition data is approximately  $\pm 2.5$  percent.
2. The dynamic type equilibrium cell used in this work is satisfactory for obtaining vapor-liquid equilibria data for complex systems. Sampling from this cell is blind, however, and one cannot tell whether or not two phases are present until the samples have been collected and analyzed.
3. Vapor recirculation is considered a must in experimental vapor-liquid equilibrium determinations. The circulation time of four hours is more than adequate. This time can be safely reduced to two hours.

4. Hydrocarbon samples containing components from methane ( $C_1$ ) through eicosane ( $C_{20}$ ) can be analyzed quantitatively using a single column, temperature programmed chromatograph.
5. The chromatographic assay technique for composition determination of the equilibrium phases can be coupled with conventional experimental techniques to give vapor-liquid K-values for components of complex hydrocarbon systems which agree with those obtained by more complicated procedures.
6. Valuable by-products of the chromatographic assay technique are densities of the equilibrium phases and K-values for individual components and fractions in the heptanes-plus fraction.

Major conclusions based on the theoretical part of the work are:

1. The Edmister isothermal integral consistency test indicates that the experimental data obtained in this work are consistent in the pressure range 100-2000 psia.
2. The Edmister isothermal integral consistency test can be applied to multicomponent vapor-liquid equilibrium data if the multicomponent system is treated as a binary.
3. The Edmister consistency test indicated that the experimental data obtained at pressures greater than 2000 psia are not consistent. However, an equation of state was used to calculate fugacity coefficients at these pressures. The data inconsistency at the higher pressures may be attributed, in part, to a break down of this equation of state at the higher pressure saturated vapor states.
4. The Chao-Seader regular solution theory K-value correlation



provides a convenient semi-empirical method for the correlation of experimental multicomponent vapor-liquid equilibrium data.

The following recommendations are made:

1. The Michels-type equilibrium cell should be replaced with a windowed cell to permit observation of the dew and bubble points of the mixtures studied. Consideration should be given to the design of a variable volume cell with internal vapor and liquid recirculation.
2. The accuracy of the K-values obtained is limited by the resolution of the chromatograph used in the sample analysis. A natural gas condensate has a large number of components which makes complete resolution of each of the higher boiling components difficult, if not impossible. This incomplete resolution results in K-values of limited accuracy, particularly if the components are present in concentrations less than 0.5 mole percent. The accuracy of these K-values can be improved by either the use of an automatic integrator for the chromatograph or the use of a simulated natural gas condensate.
3. If a simulated natural gas condensate is used, it should be composed of 7-10 components whose identity and magnitude are determined from analyses of producing condensate reservoirs.
4. In this work, the equilibrium vapor and liquid phase samples are removed from the density traps and split into two phases by freezing out the heavy components. This necessitates

making separate analyses of these fractions as well as a material balance to obtain K-values and equilibrium phase densities. The largest portion of the experimental error arises from this technique. The development of a system for the direct sampling of the equilibrium phases into the chromatograph is urged as a means of reducing this error.

## BIBLIOGRAPHY

1. Adler, S. E. et al. "Thermodynamic Consistency of Binary Liquid-Vapor Equilibrium Data When One Component Is Above Its Critical Temperature". AICHE Journal 6, 104 (1960).
2. American Society for Testing and Materials. 1958 Book of ASTM Standards, Part 7, p. 8. American Society of Testing Materials, Philadelphia, Pa. (1959).
3. American Society for Testing and Materials. 1965 Book of ASTM Standards - Parts 17 and 18. American Society for Testing and Materials, Philadelphia, Pa. (1965).
4. Aroyan H. J. and D. L. Katz "Low Temperature Vapor Liquid Equilibrium in  $H_2$ - $nC_4$  System". Ind. Eng. Chem. 43, 185 (1931).
5. Barr-David, F. H. "Vapor-Liquid Equilibrium at High Pressures. Systems: Ethanol-Water and 2-Propanol-Water", unpub. PhD Thesis Yale University (1956).
6. Benedict, M. et al. "Vapor-Liquid Equilibrium in Mixtures of Light Hydrocarbons". Chem. Eng. Prog. 46, No. 3, 20 (1950).
7. Condon, E. U. and H. Odishaw. Handbook of Physics, McGraw-Hill Book Co., New York (1958).
8. Chao, K. C. and J. D. Seader. "A General Correlation of Vapor-Liquid Equilibria in Hydrocarbon Mixtures". AICHE Journal 7, 598 (1961).
9. Conolly, J. F. "Hydrogen-Hydrocarbon Interaction Virial Coefficients" Notes for Applied Thermodynamics Conference, Oklahoma State University, Stillwater, Oklahoma (1961).
10. Dodge, B. F. and A. K. Dunbar. "Investigation of Coexisting Phases of Oxygen and Nitrogen". JACS 49, 591-610 (1927).
11. Dodge, B. F. Chemical Engineering Thermodynamics - McGraw Hill Book Co., New York (1944).
12. Edmister, W. C. "Tools for Mixtures". Paper presented at Thermodynamics Conference, Oklahoma State University (1965).
13. Edmister, W. C., H. G. McMath and R. C. Lee, "Pressure Comparisons for Dead Weight Pressure Gages and the Vapor Pressure of  $CO_2$ ". Interoffice Memorandum of the School of Chemical Engineering,

Oklahoma State University, Stillwater (1964).

14. Evans, R. B. and D. Harris. "Hydrocarbon Mixture Containing Two Concentrations of Heptanes and Heavier Fraction". J. Chem. Engr. Data 1, 45 (1956).
15. Exline, P. G. and H. J. EnDean. "Apparatus for Analyzing Reservoir Fluids". Trans. ASME 70, 279 (1948).
16. Gibbs, J. W. Collected Works. Vol I. Longmans, Green and Co., New York (1928).
17. Guggenheim, E. A. Thermodynamics. North Holland Publishing Co., Amsterdam (1957).
18. Hala, E., J. Pick, V. Fried, and O. Vilim. Vapor-Liquid Equilibrium, Pergamon Press, New York (1958).
19. Hanson, G. H. and G. G. Brown. "Vapor-Liquid Equilibria in Mixtures of Volatile Paraffins". Ind. Eng. Chem. 37, 821 (1943).
20. Hipkin, H. "Experimental Measurement of Vapor-Liquid Equilibria". Notes for Conference on Vapor-Liquid Phase Equilibria, Oklahoma State University, Stillwater, Oklahoma (1959).
21. Jacoby, R. H. and M. J. Rzasas. "Equilibrium Vaporization Ratios for Nitrogen, Methane, CO<sub>2</sub>, Ethane and H<sub>2</sub>S in Absorber Oil-Natural Gas and Crude-Oil-Natural Gas Systems". Trans. AIME 195, 99 (1952).
22. James, A. T. and A.J.P. Martin. "Gas-Liquid Partition Chromatography: the Separation and Micro-estimation of Volatile Fatty Acids from Formic Acid to Decanoic Acid". Biochem. Journal 50, 679 (1952).
23. Hoffman, A. E., J. S. Crump and C. R. Hocutt, "Equilibrium Constants for a Gas-Condensate System". Trans. AIME 198, 1 (1953).
24. Katz, D. L. and K. H. Hachmuth. "Vaporization Equilibrium Constants in a Crude Oil-Natural Gas System". Ind. Eng. Chem. 29, 1072 (1937).
25. Katz, D. L., D. J. Vink and R. A. David. "Phase Diagram of a Mixture of Natural Gas and Natural Gasoline Near the Critical Conditions". AIME 136, 106 (1940).
26. Kehn, D. M. "Rapid Analysis of Condensate Systems by Chromatography". Paper presented at Oct. 6, 1963, Meeting of the Society of Petroleum Engineers, New Orleans, La.
27. Kirkbride, C. G. and J. W. Bertetti. "High Pressure Absorption of Low Boiling Hydrocarbons". Ind. Eng. Chem. 35, 1242 (1943).

28. Lewis, G. N. Proc. Amer. Acad. Arts Sci. 37, 49 (1901).
29. McNair, H. M., K.A.M.G. Cramer and A.I.M. Keulemans. Paper presented at the Symposium on Gas Chromatography, American Chemical Society (March 22-25, 1961).
30. Matheson, G. L. and L.W.T. Cummings. "Vapor Pressure of Low Boiling Paraffin Hydrocarbons in Absorber Oil". Ind. Eng. Chem. 25, 723 (1933).
31. Michels A., G. F. Skelton and E. M.L. Dumoulin, "Gas-Liquid Phase Equilibrium for the System Ammonia-Hydrogen-Nitrogen". Physica 25, 840 (1959).
32. Michels, A. "Accuracy and Sensitivity of a Pressure Balance with a So-called Amagat Cylinder". Ann. Physik (Series 4) 73, 557 (1924).
33. Natrella, M. G. Experimental Statistics - National Bureau of Standards Handbook 91. U. S. Government Printing Office, Washington (1963).
34. Natural Gasoline Supply Men's Association, Engineering Data Book, Seventh Edition, Natural Gasoline Association of America, Tulsa, Oklahoma (1957).
35. Organick, E. A Fortran Primer - Addison-Wesley Publishing Co., Reading, Mass. (1963).
36. Othmer D. F. and F. R. Morley. "Composition of Vapors from Boiling Binary Solutions". Ind. Eng. Chem. 38, 751, (1946).
37. Patten, F. V. L. and D. C. Ivey. "Phase Equilibria in High Pressure Condensate Wells". Oil Weekly p. 20 (December 12, 1938).
38. Paauwe, J., Private Communication to R. E. Thompson (1962).
39. Perry, J. H. Chemical Engineers Handbook, 2nd Ed. McGraw-Hill Book Co., Inc., New York (1940).
40. Pitzer, K. S. "The Volumetric and Thermodynamic Properties of Fluids I. Theoretical Basis and Virial Coefficients". JACS 77, 3427 (1955).
41. Poettmann, F. H. and D. L. Katz. "Carbon Dioxide in a Natural Gas-Condensate System". Ind. Eng. Chem. 38, 530 (1946).
42. Poettmann, F. H. and B. J. Mayland. "Equilibrium Constants for High Boiling Fractions of Varying Characterization Factor". Pet. Ref. 28, No. 7, 101 (1949).
43. Poettmann, F.H. "Vaporization Characteristics of CO<sub>2</sub> in a Natural Gas-Crude Oil System". Trans. AIME 192, 141 (1951).<sup>2</sup>

44. Prausnitz, J. M., W. C. Edmister and K. C. Chao. "Hydrocarbon Vapor-Liquid Equilibria and Solubility Parameter". AICHE Journal 6, 214 (1960).
45. Ray, N. J. "Gas Chromatography. I. The Separation and Estimation of Volatile Organic Compounds by Gas-Liquid Partition Chromatography". J. Applied Chem. 4, 21 (1954).
46. Redlich, O. and J.N.S. Kwong. "On the Thermodynamics of Solutions. V. An Equation of State". Chem. Reviews 44, 233-244 (1949).
47. Redlich, O. "Old and New Problems in the Field of Vapor-Liquid Equilibria". Lawrence Radiation Laboratory Publication UCRL-11354 University of California, Berkeley (1964).
48. Roberts, L. R. and J. J. McKetta. "Vapor Liquid Equilibrium in the  $nC_4-N_2$  System". AICHE Journal 7, 173 (1961).
49. Robinson, C. S. and E. R. Gilliland. Elements of Fractional Distillation, 4th Ed., McGraw-Hill Book Co., Inc., New York (1950).
50. Robinson, R. L., Jr. "A Theoretical and Experimental Investigation of Vapor-Liquid Equilibria in the Binary Systems Formed Among the Constituents Normal Hexane, Methylcyclohexane and Toluene". M.S. Thesis, Oklahoma State University (1962).
51. Roland, C. H., D. E. Smith and H. H. Kaveler. "Equilibrium Constants for a Gas-Distillate System". Oil & Gas J. 39, No. 46, 128 (1941).
52. Roland, C. H. "Vapor-Liquid Equilibria for Natural Gas-Crude Oil Mixtures". Ind. Eng. Chem. 37, 930 (1945).
53. Rossini, F. D., et al. Selected Values of Physical and Thermodynamic Properties of Hydrocarbons and Related Compounds. Carnegie Institute of Technology, Pittsburgh (1953).
54. Rzsá, M. J. "The Coexistence of Liquid and Vapor Phases at Pressure Above 10,000 psi". Trans. AIME 189, 119 (1950).
55. Sage, B. H. and W. N. Lacey. "Apparatus for Study of Pressure-Volume-Temperature Relations of Liquids and Gases". Trans. AIME 136, 136 (1940).
56. Sage, B. H. and W. N. Lacey. "Behavior of Binary, Ternary and Multicomponent Systems at States Similar to Those Encountered in Condensate Fields". Trans. AIME 186, 143 (1949).
57. Sage, B. H. and C. E. Kircher, Jr. "Phase Equilibria in Hydrocarbon Systems-Solubility of Dry Natural Gas in Crude Oil". Ind. Eng. Chem. 26, 652 (1934).
58. Sage, B. H., W. N. Lacey and J. G. Schaafsma. "Phase Equilibria

- in Hydrocarbon Systems". Ind. Eng. Chem. 26, 214 (1934).
59. Scatchard, G. "Equilibria in Non-Electrolyte Solutions in Relation to the Vapor Pressures and Densities of the Components". Chem. Reviews 8, 321 (1931).
60. Smith, R. L. and K. M. Watson. "Boiling Points and Critical Properties of Hydrocarbon Mixtures". Ind. Eng. Chem. 29, 1408 (1937).
61. Solomon, E. "Liquid-Vapor Equilibrium in Light Hydrocarbon-Absorber Oil Systems". Chem. Eng. Prog. Symp. Series 48, No. 3, 93 (1952).
62. Souders, M., G. W. Selheimer and G. G. Brown. "Equilibria Between Liquid and Vapor Solutions of Paraffin Hydrocarbons". Ind. Eng. Chem. 24, 517 (1932).
63. Standing, M. B. and D. L. Katz. "Vapor-Liquid Equilibria of Natural Gas-Crude Oil Systems". Trans. AIME 155, 230 (1944).
64. Stuckey, A.N., Jr. "On the Development of an Ideal K-Value Correlation for Hydrocarbons and Associated Gases". M. S. Thesis, Oklahoma State University (1963).
65. Thompson, R. E. "Investigation of Vapor-Liquid Equilibria for Hydrogen-Six Carbon Hydrocarbons". PhD Thesis, Oklahoma State University (1963).
66. Thompson, R. E. Private communication to W. C. Edmister (1964).
67. Thompson, R. E. and W. C. Edmister. "Vapor-Liquid Equilibria in Hydrogen-Benzene and Hydrogen-Cyclohexane Mixtures". AIChE Journal 11, 457 (1965).
68. Tully, P. C. "The Simultaneous Investigation of the Isobaric Integral Heat of Vaporization and Vapor-Liquid Equilibrium Data of Methane-Ethylene Mixtures at High Pressure". PhD Thesis, Oklahoma State University (1965).
69. Vagtborg, H. "Equilibrium Vaporization Ratios for a Reservoir Fluid Containing a High Concentration of  $H_2S$ ". Trans. AIME 201, 31 (1954).
70. Webber, G. E. "Equilibrium Constants for Hydrocarbons in a Absorption Oil". Trans. AIME 142, 192 (1941).
71. Williams, F. E. "A Binary Mixture for Evaluating Low Pressure Distillation Columns". Ind. Eng. Chem. 39, 779 (1947).
72. White, R. R. and G. G. Brown. "Phase Equilibria High Temperature". Ind. Eng. Chem. 34, 1162 (1942).

## APPENDIX A

### CALIBRATION OF THE PRESSURE BALANCE AND MEASURING CYLINDERS

The Michels pressure balance and measuring cylinders used in this investigation were calibrated by the Meetinstituut Bemetel - T.N.O. (the Dutch equivalent of the Pressure Standards Section of the U.S. National Bureau of Standards), located at the van der Waals Laboratory in Amsterdam, Holland. The technique used in this calibration is reviewed briefly below (38).

In practice, a master balance is calibrated and periodically checked by a careful calibration procedure. At all pressures the effective area of a piston is determined by back-calculation using the following equation.

$$\text{where } A = \frac{F}{P} \quad (A-1)$$

A = the effective piston area

F = the force acting on the effective piston area

P = the pressure acting against the piston

The force acting on the effective piston area is determined from the calibrated weights used on the balance. The pressure is determined at low pressures by measuring the height of mercury in an open column that is connected to the pressure balance through a pressure bench.

At the higher pressures a 22 meter mercury column is used in



conjunction with a piezometer. The piezometer is filled with nitrogen to a pressure at which the effective area has been determined previously. The weights on the balance are adjusted until the mercury in the piezometer just touches an electrical contact. The mercury column is then interposed between the balance and the piezometer. Weights are added until the mercury in the piezometer again touches the electrical contact. The new pressure is calculated and the effective areas are obtained. In all the above measurements the mercury column and piezometer temperatures are carefully measured and regulated, and corrections are made for the oil heights.

The effective area of each standard Hart piston-cylinder was determined at several pressures and was found to be accurate to  $\pm 1$  part in 12,500 for the low pressure piston-cylinders to  $\pm 1$  part in 25,000 for the higher pressure piston-cylinders.

The effective areas of the piston-cylinders used in this investigation were determined by calibration against the 'master piston-cylinders' discussed above.

Table A-I lists the calibrated masses of the various rotating parts of the pressure balance. Table A-II lists the effective area and masses for each of the measuring cylinders. In addition to these data, Bemtel-T.N.O. determined that the area of the guide pin is 1.76 sq. cm. and that the height of oil above the bottom of the guide pin is equal to the oil reservoir height plus 1.6 cm. All measurements refer to operation at 20°C. with the piston height indicator at 10 on the scale. The pressures are referred to the center line of the oil outlet on the measuring cylinder.

Comparison tests have been made between the Hart differential

TABLE A-I

## PRESSURE BALANCE WEIGHT CALIBRATIONS

<u>Item</u>	<u>Mass</u>
Indicator axis plus indicator	0.9957 Kg <sub>m</sub>
Cone	0.2468
Oil Shield	1.6542
Weight Pan	0.6090
Lowest Weight with the axis of suspension	29.7729
Weight No. 1	25.0131
2	25.0120
3	25.0151
4	25.0138
5	25.0139
6	25.0166
7	25.0141
8	25.0161
9	10.0053
10	5.0005
11	5.0061
12	0.9974
13	1.0036
14	1.0042
15	1.0046
16	1.0044

TABLE A-II

## MEASURING CYLINDER CALIBRATIONS

<u>Range of Cylinder</u>	<u>Effective Area</u>	<u>Mass of piston, claw, nut and half-rings</u>
3-20 Kg <sub>m</sub> /cm <sup>2</sup>	12.512 ± 0.001 cm <sup>2</sup>	1.4095 Kg <sub>m</sub>
20-50	5.0058 ± 0.004	0.8817
50-125	2.0004 ± 0.0001	0.6719
125-300	0.83393 ± 0.00004	0.5913
300-600	0.41938 ± 0.00002	0.5598
600-1000	0.24461 ± 0.00001	0.5173
1000-1600	0.15930*	0.5075

\* The effective area of this piston changes with the load. A distortion correction is applied according to the following equation:

$$\text{Area (cm}^2\text{)} = 0.15932 - (.11900 \times 10^{-6}) (\text{load, kg})$$

piston pressure balance and two Ruska dead-weight piston gauges (13). The results of these tests showed the Hart to be 2 to 3 parts in 10,000 higher at 500 psi than the Ruska and 5 parts higher in 10,000 at 12,000 psi. Using the Ruska dead weight piston guage, the vapor pressure of  $\text{CO}_2$  at  $0^\circ\text{C}$  was found to be 26,139.6 mm Hg, which value agrees well with the mean of four observations by Meyers and Van Dusen, (13) i.e. 26,139.5. From the comparison test data, it is estimated that the Hart balance would have given a  $\text{CO}_2$  vapor pressure at  $0^\circ\text{C}$  of about 26,145 mm Hg. This is in good agreement with the mean of four observations by Bridgeman, (13) i.e., 26,144.7 mm Hg. The difference between the Hart and Ruska have not been completely resolved. Further comparison tests are planned in the future.

The interested reader is directed to the paper of Edmister, McMath and Lee (13) for the details of these comparison tests.

## APPENDIX B

### CALIBRATION OF THERMOCOUPLES AND BECKMAN THERMOMETER

Three chromel-constantan and one iron constantan thermocouples were used in this investigation. The chromel-constantan thermocouples were used to measure the outside metal temperatures of the vapor density trap, the liquid density trap and the circulating pump cylinder, respectively. The iron-constantan thermocouple was a 0.062" O.D. mineral insulated thermocouple with the hot junction welded to the tip of its stainless steel sheath. This thermocouple was placed inside the equilibrium cell at a distance of  $3\frac{1}{4}$ " from the top of the cell. As a point of reference, the liquid dip tube extends 3" into the cell from the cell top. This thermocouple extends approximately  $2\frac{3}{16}$ " into the cell. The thermocouple is in the center of the cell radially about  $\frac{1}{8}$ " to  $\frac{1}{4}$ " above the top liquid distributor plate.

The four thermocouples used in this work were calibrated against a Leeds and Northrup platinum resistance thermometer, Model 8163, Serial No. 1576919. The thermometer was calibrated by the National Bureau of Standards on May 7, 1964. The NBS calibration data were furnished in both tabular and equation form with temperature being presented as a function of a resistance ratio  $R/R_0$ .  $R_0$  is the resistance of the thermometer at the ice point while  $R$  is the thermometer resistance at the unknown temperature. The approximate value of  $R_0$  was given as 25.5168 ohms at a thermometer current of 2.0 milliamps.

The thermometer resistance was determined on a calibrated Leeds and Northrup Model 8069-B Mueller bridge, Serial No. 1550042. Leeds and Northrup calibrated this Mueller bridge and furnished calibration tables for use in the laboratory. A Leeds and Northrup Model 2284-D ballistic type galvanometer with a sensitivity of 0.2 microvolt/mm was used in conjunction with the Mueller bridge. A Leeds and Northrup Model 2170 reading scale was used with the galvanometer. The galvanometer was placed on a pedestal that was sunk approximately four feet into the earth to isolate the galvanometer from the building to minimize vibrations.

The thermocouples and platinum resistance thermometer were placed in a silicone oil reservoir in the large air thermostat. Each day the calibrations were performed, the resistance of the platinum thermometer was checked at the ice point to determine  $R_0$ .

The thermocouple emf was measured with a Leeds and Northrup Type K-3 potentiometer, Serial No. 1553853. The null-detecting device was a Leeds and Northrup Model 2430 galvanometer. The reference junctions were inserted in an ice bath in a Dewar flask. Figure B-1 shows the thermocouple measuring circuit. The emf of the thermocouples could be measured to  $\pm 0.0002$  mv.

The calibrations were carried out at approximately 150 and 250°F. The thermocouples were calibrated separately. One man read the resistance of the thermometer on the Mueller bridge while another determined the thermocouple emf simultaneously on the K-3 potentiometer. A minimum of twenty points were taken at each temperature for each thermocouple.

A plot was made for each thermocouple of emf vs. the temperature

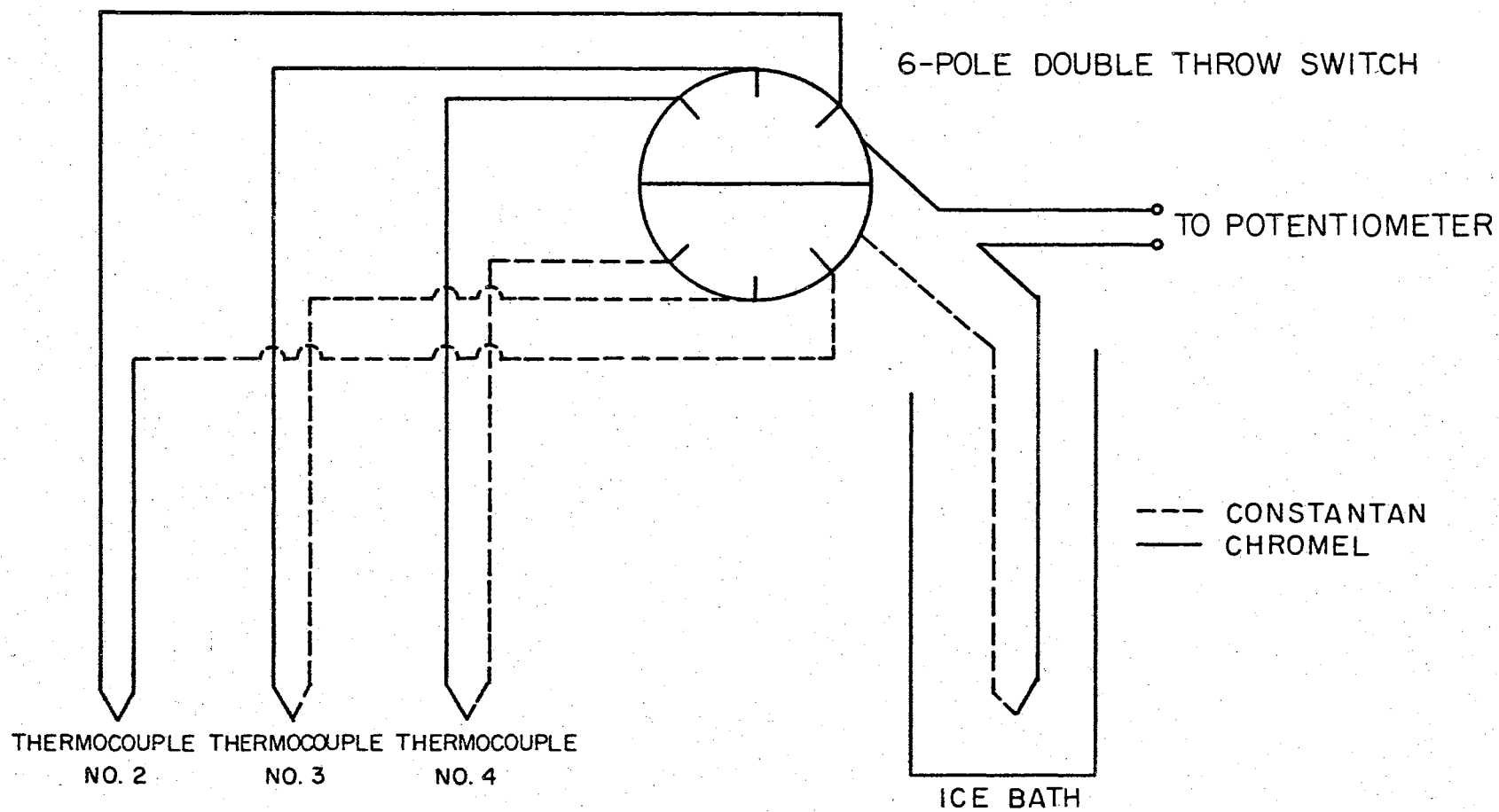


FIGURE B-1  
THERMOCOUPLE WIRING DIAGRAM

obtained from the resistance thermometer calibration equation. A straight line, having the same slope as a theoretically ideal thermocouple, was fitted to the emf-temperature data. The result was an equation for temperature as a function of emf for each thermocouple at 150, 250 and 350°F. The coefficients for these equations are presented in Table B-I.

The Beckman differential thermometer was calibrated at 85°F. in a manner similar to that of the thermocouples. The thermometer was placed in the low temperature air thermostat adjacent to the platinum resistance thermometer. One man read the Beckman thermometer scale while another read the resistance of the platinum thermometer simultaneously on the Mueller bridge. The twenty data points taken were fitted in equation form with temperature being expressed as a function of the Beckman thermometer scale reading. The coefficients for this equation are presented below.

$$T, ^\circ\text{C} = 30.422 - 0.71976R - 0.24944 R^2 \quad (\text{B-1})$$

$$T, ^\circ\text{F} = 86.744 - 1.2168R - 0.54448 R^2 \quad (\text{B-2})$$

where  $R$  = the Beckman thermometer reading



TABLE B-I

## THERMOCOUPLE CALIBRATION EQUATIONS

Thermocouple Equation Form:  $T = A + B$  (potentiometer reading, mv)

<u>Thermocouple</u>	<u>Temperature Range, °F</u>	<u>A</u>	<u>B</u>
1	150	36.14255	33.333
	250	35.60839	33.333
	350	31.74235	33.333
2	150	36.53416	28.000
	250	32.50143	28.000
	350	21.66691	28.000
3	150	36.51006	28.000
	250	32.46713	28.000
	350	21.99185	28.000
4	150	36.53950	28.000
	250	32.26328	28.000
	350	21.57831	28.000

## APPENDIX C

### CALIBRATION OF VOLUMETRIC APPARATUS

The quantity of light hydrocarbon gases collected in the sampling apparatus (Figure 14) was calculated from the pressure, volume, temperature and composition of the gases collected. The pressure was read on a U-tube manometer by observing the height in each leg with a cathetometer. The temperature was read on a calibrated Beckman differential thermometer (Appendix B). The volume was computed by summing the individual volumes of the component parts of the volumetric apparatus. The calibration of the volumetric apparatus will now be discussed.

#### Analytical Balance Weight Calibrations

Two analytical balances were used in the volumetric calibrations. A Mettler Type B6 balance (Serial No. 63592 with 100 gm. capacity) was used for the small weights. A Volland and Sons Balance No. B-125 with a capacity of 6 kg. was used for the large weights.

The Mettler balance was operated on a standard reinforced concrete balance table. This balance was serviced by a Mettler representative in this position. The Mettler has a stated accuracy of 0.02 mg and a sensitivity of 0.02 mg.

The calibration of weights up to the 100 gm weights were carried out on the Mettler which had class S weights. Weights heavier than 100 gm were calibrated on the Volland balance.

Two sets of weights were used in the laboratory in conjunction with the pressure balance. These weights are identified as Set No. 5 and Set No. 4775. For the small set of weights (No. 5) the nominal weights and the listed weights were identical to the nearest milligram. The calibration of the larger weights (No. 4475) is given in Table C-I.

### Volumetric Calibrations

#### Small Volumetric Bulbs

The 25 cc volumetric bulb was calibrated by filling with water and again by filling with mercury. In each case, the bulb was evacuated and weighed and then filled with water. Care was exercised to remove all bubbles of air from the bulb. The bulb was then placed in the air bath. After a few hours at constant temperature, the stopcock on the bulb was closed. The excess water in the neck of the bulb was removed and the water-filled bomb was reweighed.

At 76°F. Evacuated weight = 48.16957 gm.

Filled weight = 73.57268 gm.

Weight of water = 25.40311 gm.

Density of water = 0.997171 gm/cc  
at 76°

Volume of Bulb =  $\frac{25.40311}{0.997171} = 25.475179$  cc

A similar calibration was carried out using mercury instead of water. The volume of the 25 cc bulb was determined to be 25.48 cc.

From these two calibrations, the volume of the 25 cc bulb is determined to be 25.48 cc including the stopcock passage. The volumes of the 500 cc, 1 liter and 2 liter bulbs were determined in a similar manner except that water was used as the calibration fluid. The results

TABLE C-I

## CALIBRATIONS FOR WEIGHT SET 4775

<u>Nominal Weight, gm</u>	<u>Calibrated Weight, gm</u>
1	0.9971
2A	2.0069
2B	2.0062
5	4.9914
10A	10.0010
10B	10.0035
20	19.9923
50	49.9806
100A	99.9755
100B	99.9728
200	200.0333
500	500.0406
1000	999.8841
2000	2000.1353

of the calibrations are presented in Table C-II.

### U-tube Manometer

The right leg of the U-tube manometer was calibrated for volume, since it was an integral part of the volumetric apparatus. The calibration data were obtained prior to fabrication of the U-tube.

A reference mark was first baked onto a four foot section of precision bore glass tubing. A stopcock was attached to one end of the glass tubing and the tube was filled with triple-distilled mercury. Care was exercised during filling of the tube to avoid entrapped air bubbles.

A series of measurements were made in which the heights of the mercury and the reference mark were measured before and after draining a small amount of mercury into a weighing bottle. The heights were measured with the Gaertner cathetometer and the weighings were made on the Mettler balance. The weight and density of the mercury gave the volume of the height increment measured. Data indicated the tube diameter to be constant. The data were fitted by least squares to obtain

$$V = 0.2718 (h_r - h) \quad (C-1)$$

where  $V$  = volume below the reference mark, cc

$h_r$  = height of the reference mark, cm

$h$  = height of the mercury, cm

Following the calibration, the right leg was joined with the left leg of the manometer and the U-joint was formed.

### Capillary Tubing Manifold

TABLE C-II

## CALIBRATED VOLUMES OF VOLUMETRIC APPARATUS

Item	Volume, cc	Maximum Estimated Error, cc ( $\pm$ )
25 cc bulb	25.48	0.02
neck	0.25	- -
500 cc bulb No. 1	445.23	0.06
neck	0.52	- -
500 cc bulb No. 2	458.63	0.09
neck	.63	- -
1 liter bulb	946.63	0.12
neck	0.38	- -
2 liter bulb	2048.36	0.24
neck	.98	- -
4 liter bulb	4555.98	0.64
neck	1.86	- -
U-tube manometer below reference mark	Eqn. C-1	0.04
Manifold above reference mark	22.25	0.05

The capillary tubing manifold in the low temperature thermostat includes the manometer leg above the bottom reference mark and the manifold to the Toepler pump stopcock. The 25 cc, 500 cc and 1 liter volumetric bulbs were attached to the side arm ball-joints. The stopcocks were closed on the two larger bulbs. The low temperature air bath was equilibrated at 85°F. The barometric pressure was determined on the U-tube manometer and the 25 cc gas bulb stopcock was closed. The remainder of the volumetric side of the apparatus was then evacuated. The air in the 25 cc bulb was allowed to expand into the evacuated manifold. The final pressure was observed on the U-tube manometer. A sample calculation follows:

Initial Barometric Pressure,  $P_1 = 746.50$  mm Hg

Initial Volume of Air,  $V_1 = 25.48$  cc

Pressure After Expansion  $P_2 = 350.78$  cc

Assuming ideal behavior,

$$V_2 = \frac{V_1 P_1}{P_2} = 25.48 \frac{746.50}{350.78} = 54.22 \text{ cc}$$

Mercury Level in Right Leg of Manometer = 42.53 cm

Height of Reference Mark = 62.015 cm

Volume in manometer leg below =  $0.2718 (62.015) - 42.5315 =$   
reference mark  $= 5.29$  cc

Volume of Necks of Attached Bulbs = 1.15 cc

Volume of sampling apparatus to side =  $54.22 - 25.48 - 5.29 - 1.15 =$   
arms and reference mark  $= 22.30$  cc

Eight runs were made. The average of these runs is taken as the volume of the manifold. The average is 22.25 cc.

### Necks of Volumetric Bulbs

The volume of the necks of the volumetric bulbs was determined by mercury calibration. The necks of the bulbs were filled with mercury. The mercury was then removed carefully into a weighing bottle, weighed on the Mettler balance, and the volume calculated from the mercury mass and density. The neck volumes are tabulated in Table C-2.

### Four Liter Volumetric Bulb

The volume of the 4-liter bulb was determined by expansion of air in much the same manner as for the manifold. Four expansions were made with the 2-liter bulb being used as the air reservoir. The average volume from the four trials was 4555.98 cc with an absolute average deviation of 0.64 cc.

### Density Traps

The vapor and liquid density traps were calibrated with mercury at room temperature and with nitrogen at 150 and 250°F. The procedure for calibrating both traps was identical. A sample calculation for the vapor density trap will be presented.

The density trap was first evacuated and weighed on the 6 kg balance. Two trials were made on separate days and were in exact agreement. The tare weight for the vapor trap was 1137.8112 grams.

One end of the vapor density trap was connected to a vacuum trap and then to a vacuum pump. The other end was immersed in triple distilled mercury. The vacuum pump was started and mercury was admitted to the bottom of the trap until mercury flowed into the vacuum trap. The density trap was vibrated with a hand vibrator during filling to



remove entrapped air bubbles. The valves on each end of the vapor density trap were closed and the mercury in the valve ports was removed. The temperature of the mercury was recorded and the trap weighed. A sample calculation follows:

$$\begin{aligned}
 \text{Weight filled with mercury} &= 1270.4703 \text{ gm} \\
 \text{Evacuated weight} &= 1137.8112 \text{ gm} \\
 \text{Net weight of mercury} &= 132.6591 \text{ grams} \\
 \text{Mercury temperature} &= 76.0^\circ\text{F} \\
 \text{Density of mercury} &= 13.53524 \text{ gm/cc} \\
 \text{Volume of trap} &= \frac{132.6591}{13.53524} = 9.801 \text{ cc}
 \end{aligned}$$

Six determinations of the volume of the vapor density trap were made. The average of these determinations was 9.7993 cc and will be taken as the volume of the trap. The absolute average deviation of the six determinations was 0.051%.

Six determinations of the volume of the liquid density trap were made. The average of these determinations was 2.3261 cc and will be taken as the volume of the trap. The absolute average deviation of the six determinations was 0.032%.

The vapor and liquid density traps were calibrated at 150 and 250°F as follows. The traps were filled with nitrogen through the equilibrium cell and held at the desired temperature and pressure for one hour. During this hour the traps floated on the gas compressor and pressure balance. The individual traps were isolated and their contents were transferred to the volumetric apparatus using the procedure in Chapter V. The pressure in the traps was calculated using the procedure outlined in Appendix E. For the 150°F determination, this pressure was found to be 677.06 psia. The amount of gas in the traps was found by

the procedure outlined in Appendix E.

The volume of the vapor density trap at 150°F via the nitrogen calibration was 9.7892 cc, a difference of -0.16% from the mercury calibration. The volume of the liquid density trap at 150°F was 2.3327 cc, a difference of 0.28%. The volumes of the vapor and liquid traps at 250°F were 9.7937 cc and 2.3254 cc, respectively, differences of -0.06% and -0.12% from the mercury calibration.

## APPENDIX D

### CALIBRATION OF GAS COMPRESSOR

The pressure in the gas compressor is different from that at the centerline of the measuring cylinder oil outlet due to differences in the oil and mercury head. The gas compressor level indicator was calibrated as a function of the mercury height in the compressor. This work was done by Thompson (65) and is reported in his thesis. Since the gas compressor, pressure bench and pressure balance had not been moved since the completion of Thompson's work, there was no need to recalibrate the compressor. The gas compressor calibration procedure and data will be repeated for the convenience of the reader.

The apparatus shown in Figure D-1 was used for the calibration. A manometer was connected to the pressure bench to indicate the mercury position inside the gas compressor. The upper compartment of the gas compressor and one leg of the manometer were left open to the atmosphere. Oil was pumped from the pressure bench into the lower compartment of the gas compressor. Then the levels in the manometer were read with a cathetometer. The data obtained by Thompson (65) are presented in Table D-I.

The pressure at the surface of the mercury in the gas compressor is seen from Figure D-1 to be

$$P_3 = P_1 + (H_1 - H_2) \rho' \text{ oil} - (H_3 - H_2) \rho' \text{ Hg} \quad (\text{D-1})$$

$$\text{or} \quad P_3 = P_1 - \Delta P \quad (\text{D-2})$$

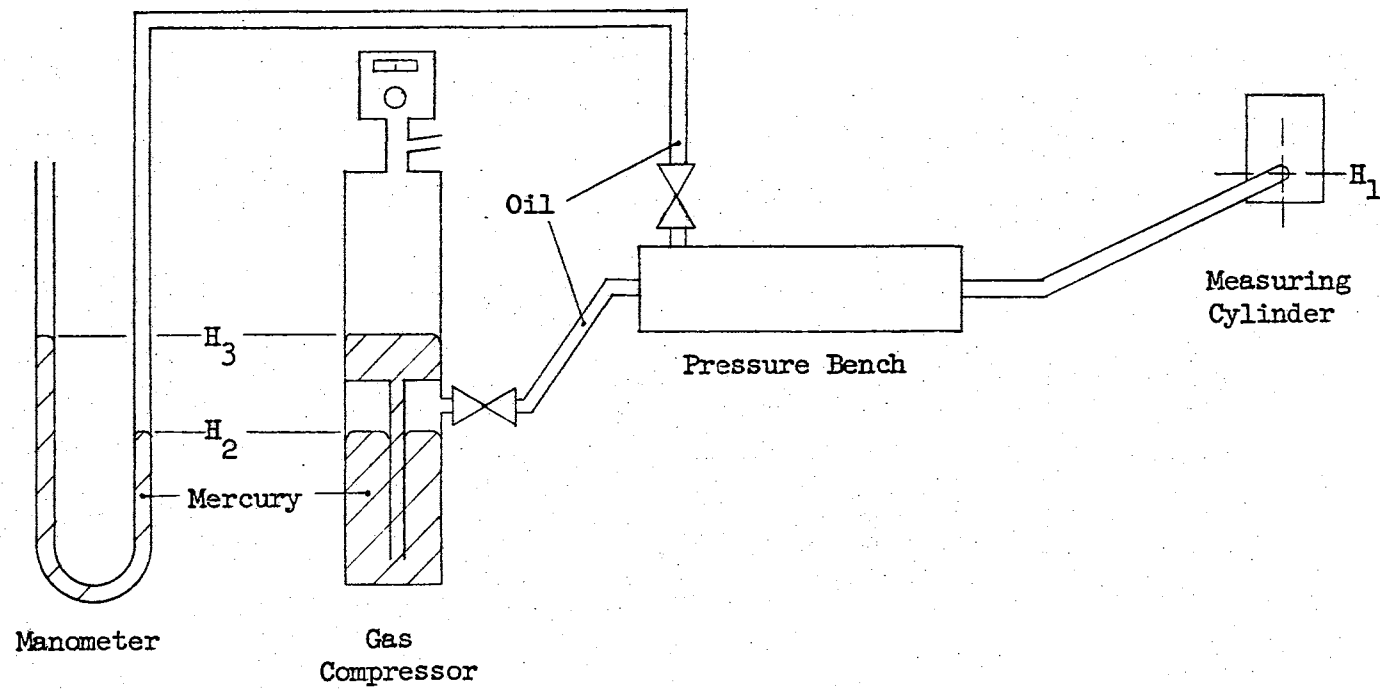


FIGURE D-1  
GAS COMPRESSOR LEVEL CALIBRATION APPARATUS

TABLE D-I  
EXPERIMENTAL DATA FOR CALIBRATION  
OF GAS COMPRESSOR LEVEL

Room Temp. 22.5°C

Gas Compressor Level Indicator Reading	Manometer Heights in cm	
	Low Side	High Side
17.4	28.08	52.73
25.8	25.92	54.99
33.1	23.98	57.02
40.8	21.95	59.12
49.4	19.81	61.37
57.6	17.79	63.48
66.2	15.60	65.70
72.4	14.10	67.30
79.0	12.39	69.01
83.0	11.31	70.10
89.8	9.67	71.78
95.2	8.30	73.17
100.2	7.08	74.38
19.9	27.53	53.40
18.2	28.07	52.87
23.3	26.58	54.38
37.7	22.90	58.19
61.9	16.80	64.50

Centerline of measuring cylinder oil outlet, 82.40 cm.

where  $H$  = height of interface

$\rho'$  = specific weight of fluid

A plot of the data showed a linear relation between the mercury levels and the level indicator reading. The data were fitted by least squares to obtain

$$H_2 = 32.47 - 0.2536 h, \text{cm} \quad (\text{D-3})$$

$$H_3 = 48.31 - 0.2611 h, \text{cm} \quad (\text{D-4})$$

where  $h$  = gas compressor level indicator reading

The density of the pressure balance oil is  $0.876 \text{ gm/cm}^3$ . The mercury density is  $13.54 \text{ gm/cm}^3$  at  $22.5^\circ\text{C}$ .

$$\text{then } \rho' \text{ oil} = 0.876 \frac{\text{gm}}{\text{cm}^3} \times 0.9991 \frac{\text{gm}_f}{\text{gm}_m} = 0.875 \text{ g}_f/\text{cm}^3$$

$$\rho' \text{ Hg} = 13.54 \times 0.9991 = 13.53 \text{ g}_f/\text{cm}^3$$

The  $\Delta P$  term must be multiplied by 0.01422 to convert from  $\text{g}_f/\text{cm}^2$  to psia.

Thus combining Equation D-1, 2, 3 and 4

$$P = \left( \left[ (32.47 - 0.2536 h) - 82.40 \right] \left[ 0.875 \right] + \left[ (48.31 + 0.2611 h) - 32.47 - 0.2536 h \right] \left[ 13.53 (0.01422) \right] \right) = 2.427 + 0.09587 h \text{ psia} \quad (\text{D-5})$$

Equation D-5 is used to calculate the pressure correction from the gas compressor level.

## APPENDIX E

### SAMPLE CALCULATION OF EXPERIMENTAL DATA

A sample calculation of P-T-x-y data from the experimental measurements is presented in this appendix. The actual calculations were made with the use of the IBM 1620 and 1410 digital computers. The data used in the sample calculations below are those from Run 111. All constants and conversion factors were taken from the API Project 44 compilations (53).

#### Temperature

The temperature in the equilibrium cell was determined from the potentiometer reading for the iron-constantan thermocouple located in the liquid phase inside the equilibrium cell. The calibration for the thermocouple appears in Appendix B. In the 150°F range the calibration equation for this thermocouple is as follows:

$$T \text{ } ^\circ\text{F} = 36.14255 + 33.3333 R$$

where  $R$  is the potentiometer reading in millivolts

The emf reading at the start of sampling in Run 111 was 3.4175. The temperature corresponding to this reading is

$$T_s = 36.14255 + (33.333)(3.4175) = 150.06^\circ\text{F}$$

The emf reading at the end of sampling was 3.4185. This reading corresponds to a temperature of 150.09°F.

The temperature for the run is taken as the average of these two

readings

$$\begin{aligned} T &= (150.06 + 150.09)/2 \\ &= 150.07^{\circ}\text{F} \end{aligned}$$

### Pressure

The pressure in the equilibrium cell was determined from the pressure balance pressure, corrected for differences in the hydrostatic head of oil, mercury and hydrocarbon. The pressure at the balance was corrected for the buoyancy of air, the thermal expansion of the measuring cylinder, and the hydrostatic head of oil acting against the pressure balance guide pin. The barometric pressure was added to this corrected pressure to obtain the absolute pressure.

The pressure at the pressure balance outlet is represented by the following equation

$$P_{\text{bal}} = (Mg/Ag_c) + P_{\text{bar}} - P_{\text{oil}} \quad (\text{E-1})$$

where  $P_{\text{bal}}$  = pressure at pressure balance outlet

$g$  = local acceleration due to gravity

$g_c$  = conversion factor,  $980.665 \text{ (kg}_m\text{)(cm)/Kg}_f\text{)(sec)}^2$

$M$  = mass of all rotating parts, corrected for buoyancy

$A$  = effective area of piston, corrected for thermal expansion

$P_{\text{bar}}$  = barometric pressure

$P_{\text{oil}}$  = pressure correction due to head of oil on guide pin



### Local Acceleration Due to Gravity

The local acceleration due to gravity was calculated from the following equation (7)

$$g = 978.0524 \left[ 1 + 0.005297 \sin^2 x - 0.0000059 \sin^2 2x + 0.0000276 \cos^2 x \cos 2(\lambda + 25^\circ) \right] - 0.000060 h \quad (\text{E-2})$$

where  $x$  = latitude

$\lambda$  = longitude (positive east of Greenwich)

$h$  = feet above sea level

At Stillwater,  $x = 36^\circ 7' \text{ N.}$ ,  $\lambda = 97^\circ 4' \text{ W.}$ ,  $h = 930 \text{ ft.}$

Substituting the Stillwater data in Equation E-2,

$$g = 979.777 \text{ cm/sec}^2$$

$$g/g_c = 979.777/980.665 = 0.999094 \text{ Kg}_f/\text{Kg}_m$$

### Barometric Pressure

The U-tube manometer was used in Run 111 to obtain the barometric pressure. One side of the manometer was evacuated to a negligible pressure while the other side was open to the atmosphere. In Run 111 the barometric pressure readings were 733.55 mm Hg at a Beckman thermometer reading of 1.00 before the run and 733.58 mm Hg at a Beckman reading of 1.02 after the run.

The Beckman thermometer readings are converted to  $^\circ\text{F}$  by Equation B-2.

$$T, ^\circ\text{F} = 86.744 - 1.2168R - 0.54448 R^2 \quad (\text{B-2})$$

$R$  = the Beckman thermometer reading

$$T(\text{before run}) = 84.98^\circ\text{F}$$

$$T(\text{after run}) = 84.95^\circ\text{F}$$

The density of the mercury in the manometer must be determined

at the above temperatures. The mercury density is a linear function of temperature between 68 and 86°F. The data in Perry (39) were put in the following equation form by Thompson (65)

$$\rho = 13.6383 - 0.001361 t \quad (E-3)$$

where  $t$  = temperature, °F

Before the run

$$\begin{aligned} \rho &= 13.6383 - 0.001361 (84.98) \\ &= 13.5227 \text{ gm/cm}^3 \\ P_{\text{barometric}} &= h \rho \text{ g/g}_c \end{aligned} \quad (E-4)$$

where  $\rho$  = density of mercury at the temperature of reading, gm/cm<sup>3</sup>

$h$  = observed barometric pressure, mm Hg

$$\begin{aligned} P_{\text{bar}} &= 733.55 \text{ mm} \times \frac{\text{cm}}{10 \text{ mm}} \times 13.5237 \frac{\text{gm}}{\text{cm}^3} \\ &\quad \times \frac{\text{Kg}_m}{1000 \text{ gm}} \times 0.99909 \frac{\text{Kg}_f}{\text{Kg}_m} \end{aligned}$$

$$P_{\text{bar}} = 0.9910 \text{ Kg}_f/\text{cm}^2$$

Similarly, after the run

$$P_{\text{bar}} = 0.9911 \text{ Kg}_f/\text{cm}^2$$

The average barometric pressure for Run 111 was

$$\begin{aligned} P_{\text{bar}} &= (0.9910 + 0.9911)/2 \\ &= 0.9911 \text{ Kg}_f/\text{cm}^2 \\ P_{\text{bar}} &= 0.9911 \text{ Kg}_f/\text{cm}^2 \times 0.9675 \frac{\text{atm}}{\text{Kg}_f/\text{cm}^2} \\ &= 0.959 \text{ atm} \end{aligned}$$

Buoyancy Correction

The experimental procedure was to take the liquid sample first. The balance weights to be used in the calculation for the liquid phase pressure are the weights on the balance at the start of the liquid sampling. The 125-300 Kg/cm<sup>2</sup> piston was used in Run 111 with weights No. 1,2,3,4,5,9,10,12, and 13 plus 535 grams in the weight pan. Using the weight calibration data from Table A-I, the total weight, uncorrected for buoyancy is summed below.

Base Weight	33.2816 Kg <sub>m</sub>
Piston, etc.	0.5913
Weight No. 1	25.0131
2	25.0120
3	25.0151
4	25.0138
5	25.0139
9	10.0053
10	5.0005
12	0.9974
13	1.0036
Extra weights	0.5350
Total weight	<hr/> 176.4826 Kg <sub>m</sub>

Let  $V$  = the volume of a steel weight of in vacuo mass  $M_o$ .

$d$  = the density of steel = 7.8 gm/cm<sup>2</sup>

$\rho_1$  = density of air at temperature  $T_1$  and pressure  $P_1$

$\rho_2$  = density of air at 20°C and 1 atm

$M$  = effective mass of  $M_o$  in air at  $T_1$  and  $P_1$

$M'$  = effective mass of  $M_o$  in air at 20°C and 1 atm

Then  $M = V (d - \rho_1) = M_o (1 - (\rho_1/d))$  (E-5)

$M' = V (d - \rho_2) = M_o (1 - \rho_2/d)$

$$M = M' \left( \frac{1 - \frac{\rho_1}{d}}{1 - \frac{\rho_2}{d}} \right) = M' \left( \frac{d - \rho_1}{d - \rho_2} \right) \approx M' \left( 1 + \frac{\rho_2 - \rho_1}{d} \right) \quad (E-6)$$

where  $1 + \frac{\rho_2 - \rho_1}{d}$  = the buoyancy correction to  $M'$

$M'$  = the total weight calculated above

If one uses the ideal gas law to evaluate the air density, then Equation E-4 becomes

$$M = M' \left[ 1 + 0.000155 (1 - (293 P_1/T_1)) \right] \quad (E-7)$$

In Run 111,  $T_1 = 301.05^\circ\text{K}$  and  $P_1 = \text{barometric pressure} = 0.9589 \text{ atm.}$

Substituting in Equation E-6

$$\begin{aligned} M &= 176.4826 (1.0000104) \\ &= 176.4844 \text{ Kg} \end{aligned}$$

#### Measuring Cylinder Thermal Expansion Correction

The linear expansion coefficient of the steel in the measuring cylinder is  $11 \times 10^{-6} \text{ } ^\circ\text{C}^{-1}$ . The area expansion coefficient is twice the linear coefficient.

$$A = A' \left[ 1 + 0.000022 (T_1 - 293) \right] \quad (E-8)$$

where  $A'$  = the effective piston area at  $20^\circ\text{C}$

$A$  = the effective piston area at  $T_1$

The area of the 125-300  $\text{Kg/cm}^2$  piston from Table A-2 is  $0.83393 \text{ cm}^2$ .

The balance temperature for Run 111 was  $28.54^\circ\text{C}$ .

$$\text{Then } A = 0.83393 \left[ 1 + 0.000022 (301.7 - 293) \right] = 0.83409 \text{ cm}^2$$

### Correction for Oil Head Above Bottom Guide Pin

The height of the oil above the bottom of the guide pin on the pressure balance is equal to the height of the oil in the guide pin reservoir plus 1.6 cm. (Appendix A). The force transmitted to the rotating shaft is

$$F_{oil} = h_o \rho_o A_{gp} (g/g_c) \quad (E-9)$$

where  $h_o$  = reservoir oil level reading + 1.6 cm

$\rho_o$  = the density of the balance oil, 0.876 gm/cm<sup>3</sup>

$A_{gp}$  = cross sectional area of the guide pin, 1.76 cm<sup>2</sup>

The pressure correction due to the oil level is, then,

$$P_{oil} = F_{oil}/A = h_o \rho_o \frac{A_{gp}}{A} \frac{g}{g_c} \quad (E-10)$$

where  $A$  = the corrected piston area

The oil level reading for Run 111 was 24.5.  $h_o$  then is 24.5 + 1.6 = 26.1

$$P_{oil} = 26.1 \text{ cm} \times 0.876 \frac{\text{gm}}{\text{cm}^3} \times \frac{\text{Kg}_m}{1000 \text{ gm}_m} \times \frac{1.76 \text{ cm}^2}{0.83409 \text{ cm}^2} \times 0.99909 \frac{\text{Kg}_f}{\text{Kg}_m} = .04820 \frac{\text{Kg}_f}{\text{cm}^2}$$

### Corrected Balance Pressure

$$P_{bal} = \frac{Mg}{Ag_c} + P_{bar} - P_{oil} = \frac{176.4844 \text{ Kg}_m}{0.83409 \text{ cm}^2} \times 0.999094 \frac{\text{Kg}_f}{\text{Kg}_m} + 0.9911 \frac{\text{Kg}_f}{\text{cm}^2} - 0.04820 \frac{\text{Kg}_f}{\text{cm}^2} = 211.3975 + 0.9911 - 0.048203 = 212.3404 \text{ Kg}_f/\text{cm}^2 \text{ at the centerline of the cylinder outlet}$$

$$P_{bal} = 212.3404 \text{ Kg}_f/\text{cm}^2 \times 14.2234 \frac{\text{lb}_f/\text{in}^2}{\text{Kg}_f/\text{cm}^2}$$

$$= 3020.2024 \text{ psia} \quad (\text{E-11})$$

#### Correction for Oil and Mercury Heads in Gas Compressor

The gas compressor mercury height for the liquid phase sample is the height at the start of sampling. In Run 111 the gas compressor level indicator read 79.4 at the start of liquid sampling.

The correction for the oil and mercury heads in the gas compressor was presented in Appendix D. The equation for this correction is

$$\Delta P_{gc} = 0.09587 h_{gc} + 2.427 \text{ psia} \quad (\text{D-1})$$

where

$h_{gc}$  = the gas compressor level indicator reading

In Run 111 the gas compressor level indicator read 79.4.

$$P_{gc} = (0.09587)(79.4) + 2.427 = 10.039 \text{ psia}$$

then

$$P_{gc} = P_{bal} - \Delta P_{gc}$$

$$P_{gc} = 3020.20 - 10.04$$

= 3010.163 psia in the gas compressor over the mercury surface

#### Correction for Hydrocarbon Head in Equilibrium Cell

In Run 111 the experimental liquid phase density was 0.5725 gm/cc. The height of the liquid in the equilibrium cell is known only approximately. An assumed value of 3 inches should be correct to  $\pm$  0.5 in.

$$P_h = h \rho \text{ g/g}_c \quad (\text{E-12})$$

where  $h$  = liquid height in cell, in.

$\rho$  = density of liquid phase, gm/cc

$$P_h = 3 \text{ in} \times \frac{\text{ft}}{12 \text{ in}} \times 0.5725 \times 62.48 \frac{\text{lb}_m}{\text{ft}^3} \times 0.999094 \frac{\text{lb}_f}{\text{lb}_m} \times \frac{1 \text{ ft}^2}{144 \text{ in}^2} = 0.06155 \text{ psia} \quad (\text{E-13})$$

then  $P_L = P_{gc} - P_h = 3010.163 - 0.06155 = 3010.10 \text{ psia}$ , the liquid phase pressure

This correction is the final one necessary for the calculation of the liquid phase pressure.

#### Vapor Phase Calculations

The above calculations were carried out for the liquid phase. Calculations for the vapor phase are identical to those for the liquid phase with the exceptions noted below.

In the calculation of the total weights on the pressure balance an average of the weights at the start and end of the vapor phase sampling was used. Similarly, the average of the gas compressor level indicator readings at the start and end of sampling was used in the calculation of the pressure correction due to the oil and mercury heads in the gas compressor.

A correction was made to the equilibrium cell pressure for the head of hydrocarbon vapor in the cell. This correction was made using Equation E-12 with  $1\frac{3}{4}$ " being used as the height of the vapor zone.

## Composition

The liquid and vapor phase calculations were made in the same manner. Only the liquid phase calculations for Run 111 will be shown.

### Chromatographic Assay

The chromatographic assay of the equilibrium phases was discussed in Chapter VI while the procedures for sampling the equilibrium phases was discussed in Chapter V.

Duplicate chromatographic analyses were made for the light and heavy hydrocarbon fraction samples taken from the sampling apparatus. The amount of each hydrocarbon present in a sample was obtained in terms of area % from the chromatogram. The area %'s from the duplicate analyses were then simply averaged. Next, these area % values were converted to weight % using the calibration equations presented in Appendix G. These weight % values were then converted to mole %. The result of these calculations, which will not be illustrated here, was a tabulation of mole % for a given hydrocarbon in the light hydrocarbon fraction and in the heavy hydrocarbon fraction.

### Light Hydrocarbons

The light hydrocarbons were collected in the volumetric part of the apparatus. The following volumes were filled with light hydrocarbons in the Run 111 liquid phase transfer. From the volumetric calibrations in Appendix C

500 cc bulb

458.63 cc

neck

0.63



1 l. neck 0.38

2 l. neck 0.98

Sampling lines to reference mark 22.25

$$\sum (\text{volume in lines and bulbs}) = 482.87 \text{ cc}$$

To this must be added the volume above the right-hand mercury level, up to the reference mark. From Appendix C

$$\Delta = 0.02718 (\text{Ref. mark ht., mm} - \text{Right side manometer level, mm})$$

The reference mark and manometer heights were 619.75 and 413.85 mm, respectively.

$$\Delta = 0.02718 (619.75 - 413.85) = 5.59 \text{ cc}$$

$$V = \sum V + \Delta = 482.87 + 5.59 = 488.46 \text{ cc}$$

The pressure is given by the difference in levels of the manometer legs which were 758.25 and 413.85 mm Hg. The Beckman thermometer reading was 0.59. The temperature in the air bath thermostat is obtained by substituting this thermometer reading into Equation B-2.

$$T = 86.744 - (1.2168)(0.59) - (0.5448)(0.59)^2 = 85.84^\circ\text{F}$$

$$\text{and } P = \frac{h \rho g}{g_c} \quad (\text{E-13})$$

$$\text{where } h = 758.25 - 413.85 = 344.4 \text{ mm Hg} = 34.44 \text{ cm Hg}$$

The density of mercury at 85.84°F is found by substituting temperature into Equation E-3

$$\rho = 13.6383 - 0.001361 (85.84) = 13.5215 \text{ gm/cm}^3$$

$$\text{then } P = (34.44 \text{ cm}) (13.5215 \frac{\text{gm}}{\text{cm}^3}) (0.99909 \frac{g_f}{g_m}) (\frac{0.73556 \text{ mm Hg}}{g_f/\text{cm}^3})$$

$$= 342.22 \text{ mm Hg at } 0^\circ\text{C}$$

The gram moles of light hydrocarbons are calculated from the gas law

$$n = \frac{PV}{ZRT} \quad (\text{E-14})$$

where  $R$  = gas constant

$Z$  = mixture compressibility factor

$$= \sum y_i Z_i, \text{ the molar average compressibility factor}$$

The compressibility factor for the individual components was calculated from a truncated virial equation of state

$$Z_i = 1 + \frac{BP_c}{RT_c} \frac{P_r}{ZT_r} \quad (\text{E-15})$$

where  $B$  = the second virial coefficient

$P_r$  = reduced pressure

$T_r$  = reduced temperature

Equation E-15 must be solved by successive approximations since the equation is not explicit in  $Z$ . The second virial coefficients used in these calculations were those of Pitzer (40)

$$\begin{aligned} \text{where } \frac{BP_c}{RT_c} = & (0.1445 + 0.073 \omega) - (0.330 - 0.46 \omega) T_r^{-1} \\ & -(0.1385 + 0.50 \omega) T_r^{-2} - (0.0121 + 0.097 \omega) T_r^{-3} \\ & -(0.0073 \omega) T_r^{-8} \end{aligned} \quad (\text{E-16})$$

The compositions used in calculating the molar average compressibility factor were the mole fractions obtained via the chromatographic assay of the light hydrocarbon fraction collected in the volumetric apparatus. The molar average compressibility factor for the light hydrocarbon fraction of the equilibrium liquid phase in Run 111 was 0.99806. The

moles of light hydrocarbons can now be evaluated from Equation E-14.

$$\text{Gram-moles light hydrocarbon} = \frac{(344.22)(488.46)}{(.99806)(62,363)(303.0)} = 0.00956$$

$$\begin{aligned} \text{The weight of this sample} &= (0.00956)(\text{Molecular weight}) \\ &= (0.00956)(17.98) = 0.17083\text{g} \end{aligned}$$

### Heavy Hydrocarbons

The heavy hydrocarbons were frozen out into two traps. The light hydrocarbons were removed from these traps by means of the Toepler pump. The amount of heavy hydrocarbon was determined by the difference in the weights of the traps, before and after sampling. The trap weights were determined by weighing on the Mettler balance. The trap weights for the liquid phase transfer in Run 111 follow.

	<u>Tare</u>	<u>Gross</u>	<u>Net</u>
Trap No. 1	87.28655 g.	88.58664 g.	1.30009 g.
Trap No. 2	85.58300	85.58000	<u>.00300</u>
		Total	1.30309

The weight % of each component in the heavy hydrocarbon fraction was obtained from the chromatogram for this sample and the chromatograph calibration equations. These weight % values were readily converted to mole %. The moles of each component were determined and summed to determine the total moles in the heavy hydrocarbon fraction. The total moles in this fraction in Run 111 = 0.1066.

### Phase Material Balance

The moles and mole fraction for a particular component in the equilibrium liquid phase sample were obtained by a material balance of

the light and heavy hydrocarbon fractions. The total weight of the sample was similarly determined. For Run 111,

$$\text{Total moles} = \text{Moles light hydrocarbons} + \text{moles heavy hydrocarbons}$$

$$= 0.00956 + 0.01066$$

$$= 0.02022$$

$$\text{Total weight} = 0.17083 + 1.30309$$

$$= 1.47392 \text{ grams}$$

### Phase Density

The equilibrium phase density was determined by dividing the weight or number of moles by the density trap volume. At 150°F the liquid density trap volume (Appendix C) was 2.3327 cc.

$$= \frac{0.02022}{2.3327} = 0.0866 \text{ moles/cc}$$

$$= \frac{1.47392}{2.3327} = 0.63185 \text{ g/cc}$$

### K-Values

The individual component K-values were calculated from the mole fraction data for the vapor and liquid phases. In Run 111 the methane vapor mole fraction = 0.96620 and the liquid mole fraction = 0.45590. Therefore,

$$K = y/x = \frac{0.96620}{0.45590} = 2.12$$

## APPENDIX F

### COMPOSITION OF CHROMATOGRAPH CALIBRATION STANDARDS

TABLE F-I

COMPOSITION OF CHROMATOGRAPH CALIBRATION STANDARDS  
MIXTURES NG-1 AND NG-2

<u>Component</u>	<u>Composition - Weight Percent</u>	
	<u>Mixture NG-1</u>	<u>Mixture NG-2</u>
Methane	79.81	52.57
Ethane	6.87	12.58
Propane	4.08	12.29
Butenes	.92	7.82
Butanes	2.53	8.11
Pentenenes	3.82	3.26
Pentanes	1.96	3.36

TABLE F-II

COMPOSITION OF CHROMATOGRAPH STANDARDS  
MIXTURES 31, 32 AND 38

<u>Component</u>	<u>Composition - Weight Percent</u>		
	<u>Mixture 31</u>	<u>Mixture 32</u>	<u>Mixture 38</u>
Propane	30.63	2.30	8.46
Isobutane	17.74	24.40	14.17
n-Butane	48.94	73.30	29.47
Isopentane	2.69	- - -	14.12
n-Pentane	- - -	- - -	33.78

TABLE F-III

## COMPOSITION OF CHROMATOGRAPH STANDARDS

MIXTURES 90, 103 AND 105

<u>Component</u>	<u>Composition - Weight Percent</u>		
	<u>Mixture 90</u>	<u>Mixture 103</u>	<u>Mixture 105</u>
2,2 - Dimethylbutane	17.39	11.94	24.97
2 - Methylpentane	17.30	12.65	24.80
Methylcyclopentane	19.84	37.88	11.26
2,3,4 - Trimethylpentane	28.29	25.53	11.52
n-Decane	19.18	12.00	27.44

TABLE F-IV

## COMPOSITION OF CHROMATOGRAPH STANDARDS

MIXTURES 55, 73 AND 84

<u>Component</u>	<u>Composition - Weight Percent</u>		
	<u>Mixture 55</u>	<u>Mixture 73</u>	<u>Mixture 84</u>
3-Methylpentane	10.05	12.50	9.69
2,4 - Dimethylpentane	29.66	20.16	8.22
Cyclohexane	13.19	22.23	44.77
Methylcyclohexane	32.84	22.86	8.62
Ethylbenzene	14.26	22.24	28.70

TABLE F-V

## COMPOSITION OF CALIBRATION STANDARDS

MIXTURES 3, 14, AND 65

<u>Component</u>	<u>Composition - Weight Percent</u>		
	<u>Mixture 3</u>	<u>Mixture 14</u>	<u>Mixture 65</u>
n-Hexane	15.22	22.47	7.99
n-Octane	16.43	8.79	23.38
n-Decane	16.39	24.31	8.63
n-Dodecane	17.06	7.94	25.01
n-Tetradecane	17.52	26.62	9.50
n-Hexadecane	17.37	9.86	25.49

TABLE F-VI

## COMPOSITION OF CALIBRATION STANDARDS

MIXTURES 19, 20 AND 29

<u>Component</u>	<u>Composition - Weight Percent</u>		
	<u>Mixture 19</u>	<u>Mixture 20</u>	<u>Mixture 29</u>
n-Heptane	23.42	35.56	11.85
n-Nonane	25.39	13.35	36.70
n-Undecane	25.75	37.25	13.26
n-Tridecane	25.44	13.84	13.19



TABLE F-VII

## COMPOSITION OF CALIBRATION STANDARDS

MIXTURES 2, 5 AND 30

<u>Component</u>	<u>Composition - Weight Percent</u>		
	<u>Mixture 2</u>	<u>Mixture 5</u>	<u>Mixture 30</u>
Cyclopentane	14.869	8.009	23.832
Benzene	18.511	27.124	10.300
Isooctane	14.817	7.591	21.599
Toulene	17.846	26.783	9.866
m-Xylene	17.966	8.469	25.949
n-Decane	15.988	22.022	8.450

## APPENDIX G

### LEAST SQUARES ANALYSIS OF CHROMATOGRAPH

#### CALIBRATION DATA

A least squares analysis of the chromatograph calibration data was made because

A series of equations expressing weight percent for a specific hydrocarbon as a function of chromatogram area percent was needed, and

Information on the accuracy of the chromatograph calibrations was desired

For this data the relationship between the dependent variable Y and the independent variable X was approximated by

$$Y_i = B_1 + B_1 X_i + B_3 X_i^2 + \dots + B_k X_i^{k-1} + \epsilon_i \quad (G-1)$$

where the  $\epsilon_i$  represent deviations from the model. The dependent variable Y corresponds to the chromatogram area percent and the independent variable X corresponds to the weight percent of a specific hydrocarbon in the calibration standard.

In using a polynomial as an approximation to some unknown function, the correct degree for the polynomial usually is not known. One usually fits a high degree polynomial and then deletes those coefficients which are not judged significant. This might lead, for instance, to

$$Y = B_1 + B_2 X + B_4 X^3 + B_5 X^4 + B_9 X^8 \quad (G-2)$$

Such was the procedure applied in the analysis of the chromatograph calibration data presented in Table G-I. The correlation coefficients,  $B_i$ , for use in Equation G-1 are presented in Table G-II for each of the hydrocarbons encountered in this work.

The values of these coefficients are tabulated for convenience in IBM E-format (35). A number expressed in E-format is of the form

$$\pm .XXXXXXXX E \pm n n \quad (G-3)$$

where XXXXXXXX are the integers in the numerical field

n n is the power of 10 to which the number is raised

For example  $+ .123456789E + 04$  is interpreted as  $0.123456789 \times 10^4$ .

Note in Table G-I that multiple measurements were made at different values of the independent variable, weight percent. When more than one measurement is made at a given composition value, then the error,  $\epsilon_i$ , of equation G-1 can be divided into two components - one component associated with the deviation of the assumed model from the true model and the other component associated with the variation of repeat determinations. The  $j^{\text{th}}$  measurement at the  $i^{\text{th}}$  point can be represented as

$$Y_{ij} = B_1 + B_2 X_i + B_3 X_i^2 + \dots + B_k X_i^{k-1} + \epsilon_i^0 + \eta_{ij} \quad (G-4)$$

It is possible to calculate the quantity,  $\eta_{ij}$ . It must be realized that such a quantity is not a truly meaningful statistical concept since "the lack of fit" is not a random error. The  $\eta_{ij}$  value when compared with  $\epsilon_i^0$  can be used, however, as a guide in making decisions about future work.

In this study the "standard deviation due to the lack of fit"

was on the average one-tenth that of the standard deviation associated with the repeat determinations. From this one concludes that the polynomial provides an excellent model for the chromatograph calibration data. If improvement is desired in the chromatograph calibration equations, then effort should be expended in the area of experimental technique rather than in seeking a new mathematical model for the calibration data.

Corresponding to any assigned value of the independent variable  $X$  in Equation G-1, there is a predicted value of  $Y$ . This value of  $Y$  is subject to an uncertainty, since it is obtained by using coefficients which are themselves subject to uncertainty.

In reporting a certain composition analysis, we would like to know the magnitude of the uncertainty associated with this composition. We find the uncertainty by setting a confidence interval on a predicted point. This confidence interval is calculated as follows:

$$\hat{Y} = Y \pm t_{.05, df} s \quad (G-5)$$

where  $Y$  = true value

$\hat{Y}$  = value estimated via Equation G-1

$t_{.05}$  = student's distribution value at the 95% confidence level

$df$  = degrees of freedom used in evaluating  $t$

$s$  = the estimated standard deviation of  $Y$

$$= s_Y \cdot X \sqrt{\frac{1}{n} + \frac{(X - \bar{X})^2}{\sum (X - \bar{X})^2}}$$

The uncertainty in a given composition is

$$\pm t_{.05, df} s_{\hat{Y}} \quad (G-6)$$

The uncertainties in the reported composition analyses for the

condensate components were evaluated at four different composition levels for each component via Equation G-6. These values are tabulated in Table G-II.

TABLE G-I

## CHROMATOGRAPH CALIBRATION DATA

Methane

<u>Weight %</u>	<u>Area %</u>	<u>Wt %</u>	<u>Area %</u>
79.81	79.71	52.57	52.56
	79.76		52.63
	79.85		52.41
	79.79		52.60
	79.91		52.72
	79.79		52.49
	79.90		52.68

Propane

<u>Weight %</u>	<u>Area %</u>	<u>Weight %</u>	<u>Area %</u>	<u>Weight %</u>	<u>Area %</u>
2.301	2.067	8.457	7.893	30.625	29.301
	2.321		7.624		29.747
	2.173		7.768		29.323
	2.148		7.579		29.290
	2.149		7.903		29.345
	2.149		7.840		29.752
	2.120		7.677		29.910
	2.076		7.667		29.414
	2.139		7.814		29.701
	2.097		7.850		29.456

Isobutane

14.172	14.113	17.738	17.114	24.397	24.043
	13.898		17.139		24.067
	13.889		17.015		24.438
	13.958		16.984		23.797
	14.262		17.228		24.727
	13.847		17.304		24.727

TABLE G-1 (cont'd)

## CHROMATOGRAPH CALIBRATION DATA

Isobutane (cont'd)

<u>Weight %</u>	<u>Area %</u>	<u>Weight %</u>	<u>Area %</u>	<u>Weight %</u>	<u>Area %</u>
14.172	14.116	17.738	17.138	24.397	24.552
	14.189		17.414		24.813
	13.818		17.450		24.526
			17.281		24.328

n-Butane

29.466	30.468	48.944	51.381	73.301	73.890
	30.032		50.979		73.613
	30.030		51.559		73.389
	30.074		51.650		74.055
	30.130		51.435		73.298
	30.388		50.503		73.038
	30.708		50.478		73.355
	29.815		51.218		73.938
	30.664		50.718		73.132
			50.904		73.575

Isopentane

<u>Weight %</u>	<u>Area %</u>	<u>Weight %</u>	<u>Area %</u>
2.691	2.204	14.122	14.113
	2.135		14.211
	2.103		14.199
	2.074		14.295
	2.082		14.101
	2.331		14.089
	2.161		13.937
	2.139		13.865
	2.277		14.095
	2.359		14.144

2,2-Dimethylbutane

<u>Weight %</u>	<u>Area %</u>	<u>Weight %</u>	<u>Area %</u>	<u>Weight %</u>	<u>Area %</u>
11.940	10.962	17.392	16.176	24.974	23.773

TABLE G-I (cont'd)

## CHROMATOGRAPH CALIBRATION DATA

2,2-Dimethylbutane (cont'd)

<u>Weight %</u>	<u>Area %</u>	<u>Weight %</u>	<u>Area %</u>	<u>Weight %</u>	<u>Area %</u>
	10.764		16.600		23.998
	10.489		16.296		24.263
	10.683		16.259		24.609
	10.761		16.334		24.110
	10.773		16.064		24.445
	10.689		15.773		23.868
	11.186		16.211		23.868

Cyclopentane

8.009	7.750	14.869	13.290	23.832	23.758
	8.289		14.404		23.652
	7.934		14.189		23.632
	7.770		14.248		23.076
	7.230		14.104		22.869
	7.388		13.806		24.095
	7.340		14.532		

2-Methylpentane

12.649	12.622	17.303	17.711	24.795	24.793
	12.000		17.514		23.568
	12.299		17.889		24.912
	12.415		17.548		25.509
	12.322		17.672		24.950
	12.315		17.854		25.430
	12.453		17.598		25.489
	12.349		17.624		25.285
			17.824		

Normal Hexane

7.991	8.301	15.220	15.955	22.468	22.839
	8.841		15.291		23.310
	8.118		15.552		23.552
	8.919		16.645		22.938
	7.915		15.478		22.432
	8.602		14.465		23.346
	8.830		14.508		22.432
	7.975		16.486		22.344



TABLE G-I (cont'd)

## CHROMATOGRAPH CALIBRATION DATA

Methylcyclopentane

<u>Weight %</u>	<u>Area %</u>	<u>Weight %</u>	<u>Area %</u>	<u>Weight %</u>	<u>Area %</u>
11.266	10.753	19.840	20.542	37.881	38.867
	11.544		20.538		38.588
	11.080		20.635		38.685
	11.152		20.460		38.700
	10.969		20.800		38.785
	10.950		20.342		38.560
	11.497		20.211		38.991
	11.487		20.112		38.721
	11.022		20.678		38.721

2,4-Dimethylpentane

8.215	7.907	20.163	19.982	29.658	30.138
	7.904		20.074		30.636
	7.757		19.984		30.545
	8.016		20.176		30.169
	7.707		20.162		29.952
	8.016		20.359		29.998
	7.875		20.069		30.092
	7.788		19.985		30.302
			20.215		30.157

Cyclohexane

13.190	13.225	22.227	22.488	44.771	45.824
	12.697		22.521		45.830
	12.575		22.976		46.300
	13.074		22.341		45.495
	13.044		23.087		46.665
	13.411		22.188		45.961
	12.923		22.521		45.372
	13.067		22.531		46.102
	13.909		22.706		
	13.016				

3-Methylhexane

9.637	8.720	10.051	9.230	12.503	11.364
-------	-------	--------	-------	--------	--------

TABLE G-I (cont'd)

## CHROMATOGRAPH CALIBRATION DATA

3-Methylhexane(cont'd)

<u>Weight %</u>	<u>Area %</u>	<u>Weight %</u>	<u>Area %</u>	<u>Weight %</u>	<u>Area %</u>
	8.867		9.217		11.585
	8.777		9.048		11.606
	8.786		9.119		11.625
	8.674		9.127		11.862
	8.806		9.029		11.805
			9.182		11.650
			9.025		11.700

Isooctane

7.591	7.666	14.817	14.321	21.599	20.856
	8.011		14.430		20.888
	7.934		14.057		20.935
	7.249		14.193		21.250
	7.078		14.442		20.502
	6.899		14.308		21.196
	7.094		14.377		20.685
	7.298				

Normal Heptane

11.845	12.130	23.422	23.237	35.562	37.743
	11.414		22.466		37.890
	11.689		23.169		36.181
	11.187		22.628		34.671
	11.753		22.562		35.015
	11.098		22.600		
			22.669		

Methylcyclohexane

8.618	8.251	22.864	23.247	32.843	33.604
	8.071		23.085		33.703
	8.307		23.213		33.603
	8.277		23.235		33.077
	8.299		23.187		33.629

TABLE G-I (cont'd)

## CHROMATOGRAPH CALIBRATION DATA

Methylcyclohexane (cont'd)

<u>Weight %</u>	<u>Area %</u>	<u>Weight %</u>	<u>Area %</u>	<u>Weight %</u>	<u>Area %</u>
	8.183		22.965		33.143
			23.289		33.120
			23.066		33.775

Toluene

9.866	9.896	17.846	18.954	26.783	27.328
	9.799		18.727		27.168
	9.944		18.742		27.586
	9.768		18.705		28.024
	9.894		19.048		28.346
			18.521		28.255
			18.204		28.200
					28.036

2,3,4-Trimethylpentane

11.521	11.603	25.528	25.122	28.285	28.528
	11.732		25.305		28.807
	11.707		25.998		27.971
	11.068		25.843		28.528
	12.342		26.161		28.460
	11.252		25.681		28.364
	11.206		25.883		28.688
	11.632		25.373		28.170
	11.287		26.142		

Normal Octane

8.793	8.737	16.427	17.140	23.379	24.765
	8.916		16.828		25.000
	9.016		17.481		24.775
	9.649		16.726		25.111
	9.139		16.699		24.012
	8.934		16.471		24.215
	8.915		16.271		24.699
	9.052		17.380		24.279

TABLE G-I (cont'd)

## CHROMATOGRAPH CALIBRATION DATA

Ethylbenzene

<u>Weight%</u>	<u>Area %</u>	<u>Weight %</u>	<u>Area %</u>	<u>Weight %</u>	<u>Area %</u>
14.255	14.261	22.240	22.917	28.706	29.316
	13.907		22.734		29.105
	13.862		21.745		29.104
	13.911		22.639		29.031
	14.246		21.937		28.981
	14.206		22.460		28.921
	14.082		22.637		
	14.020		22.543		
	13.821		22.310		

m-Xylene

8.469	8.130	17.966	18.769	25.949	27.375
	8.246		18.291		27.551
	8.109		18.643		27.597
	8.258		18.623		26.858
	8.124		18.222		26.492
	8.316		18.802		27.623
			18.671		27.217

Normal Nonane

13.347	13.214	25.389	25.529	36.696	35.940
	13.222		25.806		37.656
	13.126		25.270		36.851
	13.274		25.436		36.597
	13.224		25.537		37.564
	13.363		25.458		37.145
			25.822		

Normal Decane-Mixtures 3,14 and 65

8.627	8.701	16.392	16.632	24.308	24.684
	8.347		16.708		25.309
	8.771		16.726		24.741
	8.740		16.610		24.377
	8.934		17.154		25.297

TABLE G-I (cont'd)

## CHROMATOGRAPH CALIBRATION DATA

Normal Decane-Mixtures 3, 14 and 65 (cont'd)

<u>Weight %</u>	<u>Area %</u>	<u>Weight %</u>	<u>Area %</u>	<u>Weight %</u>	<u>Area %</u>
	8.868		16.761		24.770
	8.715		16.749		24.797

Normal Decane-Mixtures 90, 103 and 105

12.000	12.457	17.178	17.374	27.442	28.958
	12.121		17.721		28.059
	11.897		17.138		29.039
	12.329		17.117		28.912
	11.992		17.041		28.361
	12.427		17.208		27.786
	12.392		17.203		27.520
	12.351				27.682
	12.567				27.393
	12.234				

Normal Undecane

13.264	13.351	25.747	26.165	37.248	36.493
	13.140		26.257		36.833
	13.310		26.292		37.593
	13.359		26.198		38.412
	13.054		26.201		38.219
	13.571		26.094		

Normal Dodecane

7.943	7.876	17.064	16.837	25.012	25.110
	7.337		16.947		24.506
	7.640		16.464		25.276
	8.109		16.935		24.520
	8.054		17.215		25.297
	7.836		16.854		24.767
	7.814		17.319		24.716
	7.836		17.410		25.430
	7.928		17.206		

TABLE G-I (cont'd)

## CHROMATOGRAPH CALIBRATION DATA

Normal Tridecane

<u>Weight %</u>	<u>Area %</u>	<u>Weight %</u>	<u>Area %</u>	<u>Weight %</u>	<u>Area %</u>
13.841	12.547	25.442	25.068	38.193	38.577
	12.003		25.468		37.787
	13.098		26.098		38.148
	13.641		25.642		38.855
	13.540		25.702		37.627
			25.739		38.184
			25.414		

Normal Tetradecane

9.497	9.390	17.524	17.345	26.624	26.783
	9.313		17.768		26.469
	9.295		16.792		26.232
	9.331		17.668		25.867
	9.655		17.686		26.297
	9.601		17.595		26.566
	9.497		18.059		26.181
	9.422		18.218		26.865
			16.772		27.208

Normal Hexadecane

9.860	9.077	17.370	16.088	25.492	23.731
	8.656		16.455		23.991
	8.815		15.414		23.762
	9.057		16.505		23.374
	8.783		16.303		24.184
	9.321		16.621		23.884
	8.971		16.922		23.364
	9.104		16.841		24.176
	8.348				

TABLE G-II

## ANALYSIS OF CHROMATOGRAPH CALIBRATION DATA

## Methane

<u>B Coefficient</u>	<u>B Value</u>	<u>Weight %</u>	<u>95% Confidence Interval, + %</u>
1	-.50000000E-05	0.00	0.027
2	.10006594E+01	52.57	0.056
3	-.73659812E-05	79.81	0.058
4	.00000000E+00	- - -	0.058

Propane

1	-.13160000E-03	80.00	0.071
2	.94011553E+00	2.30	0.051
3	-.39478088E-02	8.46	0.080
4	.15442743E-03	30.63	0.083

Isobutane

1	.50000000E-04	0.00	0.064
2	.12893287E+01	14.20	0.134
3	-.34043318E-01	17.73	0.128
4	.90452975E-03	24.39	0.128

Normal Butane

1	-.60000000E-04	0.00	0.098
2	.91809120E+00	29.46	0.206
3	.53920850E-02	48.94	0.197
4	-.57738922E-04	73.30	0.197

2,2-Dimethylpropane

1	.00000000E+00	- -	- -
2	.10000000E+01	- -	- -
3	.00000000E+00	- -	- -
4	.00000000E+00	- -	- -

TABLE G-II (cont'd)

## ANALYSIS OF CHROMATOGRAPH CALIBRATION DATA (cont'd)

<u>Normal Pentane</u>			
<u>B Coefficient</u>	<u>B Value</u>	<u>Weight %</u>	<u>95% Confidence Interval, ±%</u>
1	.00000000E+00	- -	- -
2	.10000000E+01	- -	- -
3	.00000000E+00	- -	- -
4	.00000000E+00	- -	- -
<u>2,2-Dimethylbutane</u>			
1	-.18000000E-04	0.00	0.067
2	.83909938E+00	11.94	0.135
3	.55363843E-02	17.39	0.135
4	-.15483413E-04	24.97	0.143
<u>Cyclopentane</u>			
1	-.32000000E-04	0.00	0.026
2	.99919549E+00	8.01	0.188
3	-.84495490E-02	14.87	0.198
4	.33244857E-03	23.83	0.286
<u>2-Methylpentane</u>			
1	-.20000000E-05	0.00	0.023
2	.63518160E+00	12.64	0.212
3	.39365751E-01	17.30	0.181
4	-.98132516E-03	24.79	0.230
<u>3-Methylpentane</u>			
1	-.20000000E-05	0.00	0.023
2	.63518160E+00	12.64	0.212
3	.39365751E-01	17.30	0.181
4	-.98132516E-03	24.79	0.230
<u>Normal Hexane</u>			
1	-.31000000E-04	0.00	0.058
2	.11296016E+01	7.99	0.173
3	-.11564393E-01	15.22	0.127
4	.29319650E-03	22.47	0.221



TABLE G-II (cont'd)

## ANALYSIS OF CHROMATOGRAPH CALIBRATION DATA (cont'd)

<u>Methylcyclopentane</u>			
<u>B Coefficient</u>	<u>B Value</u>	<u>Weight %</u>	<u>95% Confidence Interval, ± %</u>
1	.33000000E-04	0.00	0.068
2	.90501670E+00	11.27	0.150
3	.95135445E-02	19.84	0.160
4	-.16920217E-03	37.88	0.159
<u>2,3 and 2,4-Dimethylpentanes</u>			
1	.45000000E-04	0.00	0.071
2	.92317810E+00	8.21	0.087
3	.46480711E-02	20.16	0.75
4	-.47805922E-04	29.65	0.093
<u>Cyclohexane</u>			
1	-.20000000E-05	0.00	0.067
2	.93571520E+00	15.33	0.156
3	.52321863E-02	22.57	0.220
4	-.71727496E-04	49.77	0.216
<u>3-Methylhexane</u>			
1	-.35800000E-04	0.00	0.073
2	.31186404E+01	9.69	0.087
3	-.40710184E+00	10.00	0.087
4	.18572574E-01	12.50	0.220
<u>Isoheptanes</u>			
1	.92000000E-04	0.00	0.051
2	.10276519E+01	11.84	0.057
3	-.66104360E-02	23.42	0.061
4	.18042664E-03	35.56	0.118
<u>Isooctane</u>			
1	.17000000E-04	0.00	0.091
2	.99952338E+00	7.59	0.147
3	-.41210045E-02	14.81	0.102
4	.12261294E-03	21.60	0.152

TABLE G-II (cont'd)

## ANALYSIS OF CHROMATOGRAPH CALIBRATION DATA (cont'd)

Normal Heptane

<u>B Coefficient</u>	<u>B Value</u>	<u>Weight %</u>	<u>95% Confidence Interval, + %</u>
1	.92000000E-04	0.00	0.051
2	.10276519E+01	11.84	0.057
3	-.66104360E-02	23.42	0.061
4	.18042664E-03	35.56	0.118

Methylcyclohexane

1	-.16000000E-04	0.00	0.061
2	.89420850E+00	8.61	0.112
3	.83349778E-02	22.86	0.116
4	-.13762256E-03	32.84	0.137

Toluene

1	-.50000000E-04	0.00	0.046
2	.86785260E+00	9.86	0.098
3	.17355546E-01	17.84	0.111
4	-.40731272E-03	26.78	0.121

2,3,4-Trimethylpentane

1	-.46000000E-04	0.00	0.063
2	.98706570E+00	11.52	0.097
3	.16465151E-02	25.52	0.094
4	-.35210996E-04	28.28	0.081

231-258°F Fraction

1	.41000000E-04	0.00	0.076
2	.10582207E+01	8.79	0.106
3	-.57652380E-02	16.43	0.111
4	.23617381E-03	23.38	0.168

Normal Octane

1	.41000000E-04	0.00	0.076
2	.10582207E+01	8.79	0.106
3	-.57652380E-02	16.43	0.111
4	.23617381E-03	23.38	0.168

TABLE G-II (cont'd)

## ANALYSIS OF CHROMATOGRAPH CALIBRATION DATA (cont'd)

<u>Ethylbenzene</u>			
<u>B Coefficient</u>	<u>B Value</u>	<u>Weight %</u>	<u>95% Confidence Interval, ± %</u>
1	-.18000000E-04	0.00	0.051
2	.88870370E+00	14.25	0.105
3	.90923977E-02	22.24	0.135
4	-.16602160E-03	28.70	0.167
<u>Mixed Xylenes</u>			
1	.23000000E-04	0.00	0.077
2	.86611070E+00	8.47	0.080
3	.14409042E-01	17.96	0.098
4	-.28228892E-03	25.94	0.119
<u>259-303°F Fraction</u>			
1	.44300000E-03	0.00	0.094
2	.95057030E+00	13.35	0.134
3	.40366794E-02	25.39	0.101
4	-.72207295E-04	36.95	0.132
<u>Normal Nonane</u>			
1	.44300000E-03	0.00	0.094
2	.95057030E+00	13.35	0.134
3	.40366794E-02	25.39	0.101
4	-.72207295E-04	36.95	0.132
<u>304-345°F Fraction</u>			
1	.13000000E-04	0.00	0.053
2	.98174660E+00	8.92	0.071
3	.48831020E-02	16.39	0.115
4	-.12985997E-03	24.31	0.146
<u>Normal Decane</u>			
1	.13000000E-04	0.00	0.053
2	.98174660E+00	8.92	0.071
3	.48831020E-02	16.39	0.115
4	-.12985997E-03	24.31	0.146

TABLE G-II (cont'd)

## ANALYSIS OF CHROMATOGRAPH CALIBRATION DATA (cont'd)

346-384°F Fraction

<u>B Coefficient</u>	<u>B Value</u>	<u>Weight %</u>	<u>95% Confidence Interval, ± %</u>
1	.27000000E-04	0.00	0.071
2	.95607740E+00	13.26	0.139
3	.46812524E-02	25.74	0.151
4	-.8895078E-04	47.24	0.165

Normal Undecane

1	.27000000E-04	0.00	0.071
2	.95607740E+00	13.26	0.139
3	.46812524E-02	25.74	0.151
4	-.88950784E-04	37.24	0.165

385-421°F Fraction

1	-.41000000E-04	0.00	0.061
2	.96429268E+00	7.94	0.080
3	.32387040E-02	17.06	0.146
4	-.75872131E-04	25.01	0.170

Normal Dodecane

1	-.41000000E-04	0.00	0.061
2	.96429268E+00	7.94	0.080
3	.32387040E-02	17.06	0.146
4	-.75872131E-04	25.01	0.170

422-455°F Fraction

1	.13000000E-04	0.00	0.076
2	.76178540E+00	13.84	0.153
3	.16281150E-01	25.44	0.209
4	-.26292112E-03	38.19	0.163

Normal Tridecane

1	.13000000E-04	0.00	0.076
2	.76178540E+00	13.84	0.153
3	.16281150E-01	25.44	0.209
4	-.26292112E-03	38.19	0.163

TABLE G-II (cont'd)

## ANALYSIS OF CHROMATOGRAPH CALIBRATION DATA (cont'd)

456-488°F Fraction

<u>B Coefficient</u>	<u>B Value</u>	<u>Weight %</u>	<u>95% Confidence Interval, ± %</u>
1	-.22000000E-04	0.00	0.080
2	.96972093E+00	9.49	0.108
3	.34093199E-02	17.62	0.114
4	-.92094988E-04	26.62	0.106

Normal Tetradecane

1	-.22000000E-04	0.00	0.080
2	.96972093E+00	9.49	0.108
3	.34093199E-02	17.52	0.114
4	-.92094988E-04	26.62	0.106

489-519°F Fraction

1	.00000000E+00	-- --	-- --
2	.10000000E+01	-- --	-- --
3	.00000000E+00	-- --	-- --
4	.00000000E+00	-- --	-- --

Normal Pentadecane

1	-.15000000E-04	0.00	0.084
2	.77667881E+00	9.86	0.118
3	.17001274E-01	17.37	0.090
4	-.42491224E-03	25.49	0.103

Normal Hexadecane

1	-.15000000E-04	0.00	0.084
2	.77667991E+00	9.86	0.118
3	.17001274E-01	17.37	0.090
4	-.42491224E-03	25.49	0.103

549-575°F Fraction

1	.00000000E+00	-- --	-- --
2	.10000000E+01	-- --	-- --
3	.00000000E+00	-- --	-- --
4	.00000000E+00	-- --	-- --

TABLE G-II (cont'd)

## ANALYSIS OF CHROMATOGRAPH CALIBRATION DATA (cont'd)

Normal Heptadecane

<u>B Coefficient</u>	<u>B Value</u>	<u>Weight %</u>	<u>95% Confidence Interval, ± %</u>
1	.00000000E+00	--	--
2	.10000000E+01	--	--
3	.00000000E+00	--	--
4	.00000000E+00	--	--

576-602°F Fraction

1	.00000000E+00	--	--
2	.10000000E+01	--	--
3	.00000000E+00	--	--
4	.00000000E+00	--	--

Normal Octadecane

1	.00000000E+00	--	--
2	.10000000E+01	--	--
3	.00000000E+00	--	--
4	.00000000E+00	--	--

603-627°F Fraction

1	.00000000E+00	--	--
2	.10000000E+01	--	--
3	.00000000E+00	--	--
4	.00000000E+00	--	--

Normal Nonadecane

1	.00000000E+00	--	--
2	.10000000E+01	--	--
3	.00000000E+00	--	--
4	.00000000E+00	--	--

628-650°F Fraction

1	.00000000E+00	--	--
2	.10000000E+01	--	--
3	.00000000E+00	--	--
4	.00000000E+00	--	--

TABLE G-II (cont'd)

## ANALYSIS OF CHROMATOGRAPH CALIBRATION DATA (cont'd)

<u>Normal Eicosane</u>			
<u>B Coefficient</u>	<u>B Value</u>	<u>Weight %</u>	<u>95% Confidence Interval <math>\pm</math> %</u>
1	.00000000E+00	- -	- -
2	.10000000E+01	- -	- -
3	.00000000E+00	- -	- -
4	.00000000E+00	- -	- -
<u>Isopentane</u>			
1	.33000000E-05	0.00	0.058
2	.76867000E+00	2.69	0.058
3	.16295079E-01	14.12	0.058
4	.00000000E+00	- - -	- - -

## APPENDIX H

### RAW EXPERIMENTAL DATA



TABLE H-I  
RAW EXPERIMENTAL DATA

RUN NO.	CELL TEMP.	PHASE	MEAS. CYL. RANGE-ATM.	TOTAL WT. ON BALANCE, KG.		OIL LEVEL CM	GAS COMPR. LEVEL		BAL. TEMP.	ROOM TEMP.
	F			INIT	FINAL		INIT	FINAL	F	F
101	150.05	LIQUID	20-50	60.1806	60.2206	20.3	59.8	60.5	75.7	73.3
101	150.05	VAPOR	20-50	60.2006	60.2556	20.3	60.5	62.0	75.7	73.3
102	150.05	LIQUID	20-50	52.8243	52.8444	21.1	92.2	93.0	78.4	76.5
102	150.05	VAPOR	20-50	52.8444	52.9194	21.1	93.0	95.0	78.4	76.5
103	150.06	LIQUID	20-50	75.4596	75.5896	20.3	120.5	124.4	75.8	74.0
103	150.06	VAPOR	20-50	75.5896	75.8546	20.3	124.4	132.2	75.8	74.0
104	150.07	LIQUID	20-50	107.4355	107.4655	29.5	28.2	29.2	80.6	83.5
104	150.07	VAPOR	20-50	107.4655	107.5355	29.5	29.2	31.3	80.6	83.5
105	150.05	LIQUID	20-50	178.0622	178.0772	26.4	40.2	40.6	74.1	71.0
105	150.05	VAPOR	20-50	178.0772	178.1422	26.4	40.6	42.4	74.1	71.0
106	150.06	LIQUID	20-50	248.4430	248.4580	25.9	61.5	62.0	77.4	77.0
106	150.06	VAPOR	20-50	248.4580	248.5180	25.9	62.0	63.8	77.4	77.0
107	150.04	LIQUID	50-125	144.4628	144.4728	22.8	29.2	29.9	80.8	79.5
107	150.04	VAPOR	50-125	144.4728	144.4878	22.8	29.9	31.1	80.8	79.5
109	150.04	LIQUID	50-125	211.5531	211.5631	25.9	33.2	34.0	83.7	81.2
109	150.04	VAPOR	50-125	211.5631	211.5831	25.9	34.0	35.5	83.7	81.2
110	150.06	LIQUID	125-300	117.6538	117.6538	23.5	32.8	33.1	80.7	79.5
110	150.06	VAPOR	125-300	117.6538	117.6638	23.5	33.1	35.0	80.7	79.5
111	150.07	LIQUID	125-300	176.4826	176.4876	24.5	79.4	80.0	83.4	82.2
111	150.07	VAPOR	125-300	176.4876	176.4926	24.5	80.0	81.2	83.4	82.2
112	150.04	LIQUID	300-600	147.8409	147.8409	20.9	106.0	106.7	79.0	77.5
112	150.04	VAPOR	300-600	147.8409	147.8459	20.9	106.7	108.1	79.0	77.5
113	150.05	LIQUID	300-600	206.7688	206.7688	27.1	87.1	87.4	82.6	81.0
113	150.05	VAPOR	300-600	206.7688	206.7738	27.1	87.4	88.2	82.6	81.0
114	150.04	LIQUID	600-1000	172.2523	172.2523	28.0	106.0	106.3	79.1	79.4
114	150.04	VAPOR	600-1000	172.2523	172.2573	28.0	106.3	107.6	79.1	79.4
115	150.05	LIQUID	1000-1600	170.2097	170.2097	25.6	92.2	92.9	82.2	79.5
115	150.05	VAPOR	1000-1600	170.2097	170.2097	25.6	92.9	94.5	82.2	79.5

TABLE H-I (CONTINUED)

## RAW EXPERIMENTAL DATA

RUN NO.	CELL TEMP. F	PHASE	MEAS. CYL. RANGE-ATM.	TOTAL WT. ON BALANCE, KG.		OIL LEVEL CM	GAS COMPR. BAL LEVEL TEMP.		ROOM TEMP. F
				INIT	FINAL		INIT	FINAL	
118	249.98	LIQUID	20-50	38.0185	38.0385	23.6	59.4	60.0	79.2
118	249.98	VAPOR	20-50	38.0385	38.0885	23.6	60.0	61.5	79.2
120	249.99	LIQUID	20-50	37.3684	37.3884	23.5	41.0	41.7	70.1
120	249.99	VAPOR	20-50	37.3884	37.4384	23.5	41.7	43.1	70.1
121	250.00	LIQUID	20-50	72.7369	72.7669	21.2	54.5	55.2	77.0
121	250.00	VAPOR	20-50	72.7669	72.8069	21.2	55.2	55.6	77.0
122	250.00	LIQUID	20-50	37.3684	37.3934	20.7	26.5	27.2	81.8
122	250.00	VAPOR	20-50	37.3934	37.4284	20.7	27.2	28.3	81.8
123	250.00	LIQUID	20-50	72.4768	72.4968	20.2	40.6	41.2	81.9
123	250.00	VAPOR	20-50	72.4968	72.5818	20.2	41.2	43.7	81.9
124	250.00	LIQUID	20-50	73.0119	73.0369	27.0	50.7	51.4	81.8
124	250.00	VAPOR	20-50	73.0369	73.0819	27.0	51.4	52.9	81.8
125	250.00	LIQUID	20-50	107.6705	107.6855	23.5	26.8	27.3	76.2
125	250.00	VAPOR	20-50	107.6885	107.7555	23.5	27.3	29.4	76.2
126	250.00	LIQUID	20-50	177.8922	177.9172	21.3	33.0	33.7	78.6
126	250.00	VAPOR	20-50	177.9172	177.9662	21.3	33.7	35.0	78.6
127	250.00	LIQUID	20-50	248.5231	248.5481	25.9	37.0	37.7	83.4
127	250.00	VAPOR	20-50	248.5481	248.5931	25.9	37.7	39.1	83.4
128	250.00	LIQUID	50-125	99.2444	99.2544	26.6	36.0	36.6	73.5
128	250.00	VAPOR	50-125	99.2544	99.2694	26.6	36.6	37.9	73.5
129	250.00	LIQUID	50-125	99.4944	99.5044	22.8	48.2	48.8	78.5
129	250.00	VAPOR	50-125	99.5044	99.5194	22.8	48.8	49.9	78.5
130	250.00	LIQUID	50-125	141.6440	141.6540	21.3	44.2	44.8	79.8
130	250.00	VAPOR	50-125	141.6540	141.6690	21.3	44.8	46.0	79.8
132	250.00	LIQUID	50-125	212.0723	212.0823	28.4	50.8	51.4	74.4
132	250.00	VAPOR	50-125	212.0823	212.0973	28.4	51.4	52.6	74.4
133	250.00	LIQUID	125-300	117.9234	117.9284	27.4	80.2	80.9	74.7
133	250.00	VAPOR	125-300	117.9284	117.9334	27.4	80.9	82.4	74.7
134	250.00	LIQUID	125-300	117.6439	117.6489	26.4	47.0	47.7	80.3
134	250.00	VAPOR	125-300	117.6489	117.6539	26.4	47.7	49.1	80.3
135	250.00	LIQUID	125-300	176.5476	176.5526	25.9	80.4	81.1	76.5
135	250.00	VAPOR	125-300	176.5526	176.5576	25.9	81.1	82.5	76.5
136	250.00	LIQUID	300-600	147.6559	147.6559	24.9	92.1	92.8	76.7
136	250.00	VAPOR	300-600	147.6559	147.6659	24.9	92.8	95.3	76.7

TABLE H-II  
LOW TEMPERATURE THERMOSTAT DATA

RUN NO.	BAR. PRESS.		MM HG		AIR BATH U-TUBE MANOMETER READINGS							BECK READ	VOL. BULBS ATTACHED
	INIT. MM.	F.	FINAL MM.	F.	FIRST COLLECTION		SECOND COLLECT.						
					LEFT	RIGHT	RF.MK.	LEFT	RIGHT	RF.MK.			
101L	745.8	80.1	746.3	85.8	691.9	456.5	620.3	-----	-----	-----	0.00	25,500X,1X	
101V	745.8	80.1	746.3	85.8	628.5	522.1	620.3	-----	-----	-----	1.13	25X,500,1X	
102L	732.4	85.7	732.3	85.6	800.0	342.2	620.2	650.7	498.9	620.2	1.61	25,500X,1X	
102V	732.4	85.7	732.3	85.6	660.1	498.2	620.2	-----	-----	-----	1.58	25X,500,1X	
103L	750.7	83.4	750.6	83.3	648.0	501.1	620.2	-----	-----	-----	4.07	25X,500,1X	
103V	750.7	83.4	750.6	83.3	694.8	480.8	620.2	-----	-----	-----	1.01	25X,500,1X	
104L	737.6	86.3	737.6	86.6	672.7	503.8	620.2	-----	-----	-----	1.08	25X,500,1X	
104V	737.6	86.3	737.6	86.6	744.7	434.1	620.2	-----	-----	-----	1.60	25X,500,1X	
105L	756.1	83.4	756.1	83.5	622.9	554.7	619.9	-----	-----	-----	1.50	25X,500,1X	
105V	756.1	83.4	756.1	83.5	813.5	357.7	619.9	-----	-----	-----	1.77	25X,500,1X	
106L	745.3	84.1	745.3	84.1	632.0	545.5	620.0	-----	-----	-----	0.14	25X,500,1X	
106V	745.3	84.1	745.3	84.1	763.2	409.6	620.0	-----	-----	-----	1.10	25X,500X,1	
107L	725.0	85.7	725.0	85.7	666.3	509.3	619.5	-----	-----	-----	1.62	25X,500,1X	
107V	725.0	85.7	725.0	85.7	818.5	352.5	620.1	645.7	531.5	620.1	1.39	25X,500X,1	
109L	737.3	86.7	737.3	86.6	681.3	494.0	619.6	-----	-----	-----	0.34	500,1X,2X	
109V	737.3	86.7	737.3	86.6	769.8	402.5	619.7	-----	-----	-----	0.93	500X,1X,2	
110L	739.1	84.0	739.1	84.0	700.4	474.3	619.8	-----	-----	-----	1.53	500,1X,2X	
110V	739.1	84.0	739.1	84.0	790.4	381.3	619.8	-----	-----	-----	1.54	500,1X,2	
111L	733.6	85.0	733.6	84.9	758.3	413.9	619.8	-----	-----	-----	4.59	500,1X,2X	
111V	733.6	85.0	733.6	84.0	808.8	362.0	619.8	-----	-----	-----	1.29	500,1,2	
112L	741.9	80.8	741.9	80.7	698.4	476.1	619.8	-----	-----	-----	0.79	500,1,2X	
112V	741.9	80.8	741.9	80.7	706.6	474.3	619.7	-----	-----	-----	1.39	1X,2X,4	
113L	740.2	82.6	740.2	82.5	786.2	392.1	619.8	-----	-----	-----	2.56	500X,1,2X	
113V	740.2	82.6	740.2	82.6	662.9	520.1	619.8	-----	-----	-----	1.79	1X,2,4	
114L	745.6	84.3	745.6	84.2	672.5	509.9	619.8	-----	-----	-----	1.94	1,2,4X	
114V	745.6	84.3	745.6	84.2	789.4	389.0	619.7	-----	-----	-----	1.20	1,2X,4	
115L	738.9	86.3	738.9	86.2	685.6	508.5	619.9	-----	-----	-----	1.46	1,2,4X	
115V	738.9	86.3	738.9	86.2	742.2	436.9	619.4	-----	-----	-----	0.34	1,2,4	

TABLE H-11 (CONTINUED)  
LOW TEMPERATURE THERMOSTAT DATA

RUN NO.	BAR. PRESS., MM HG				AIR BATH U-TUBE MANOMETER READINGS						BECK READ	VOL. BULBS ATTACHED
	INIT.		FINAL		FIRST COLLECTION			SECOND COLLECT.				
	MM.	F.	MM.	F.	LEFT	RIGHT	RF.MK.	LEFT	RIGHT	RF.MK.		
118L	747.6	79.0	747.6	79.0	705.9	492.6	619.8	-----	-----	-----	0.00	25,500X,1
118V	747.6	79.0	747.6	79.0	649.1	556.2	619.8	-----	-----	-----	1.14	
120L	749.5	70.2	749.7	70.2	705.7	492.6	619.9	-----	-----	-----	0.00	25,500X,1X
120V	749.5	70.2	749.7	70.2	654.7	564.1	619.8	-----	-----	-----	1.80	25X,500,1X
121L	753.5	78.0	753.4	77.8	799.9	412.1	620.0	-----	-----	-----	-.50	25,500X,1
121V	753.5	78.0	753.4	77.8	-----	-----	-----	-----	-----	-----	-----	25X,500,1X
122L	745.6	82.0	745.5	82.0	660.5	543.2	619.7	-----	-----	-----	0.10	25,500X,1X
122V	745.6	82.0	745.5	82.0	640.1	564.7	620.0	-----	-----	-----	1.07	25X,500,1X
123L	743.4	83.2	743.5	83.2	703.1	521.1	619.8	-----	-----	-----	2.88	25,500X,1X
123V	743.4	83.2	743.5	83.2	-----	-----	-----	-----	-----	-----	-----	25X,500,1X
124L	740.0	86.1	739.5	85.0	709.3	514.5	619.7	-----	-----	-----	4.67	25,500X,1X
124V	740.0	86.1	739.5	80.0	702.4	521.8	619.6	-----	-----	-----	2.94	25X,500,1X
125L	750.4	76.2	750.4	76.2	755.2	468.2	619.6	-----	-----	-----	3.76	25,500X,1X
125V	750.4	76.2	750.4	76.2	744.3	478.2	619.7	-----	-----	-----	4.46	25X,500,1X
126L	745.7	78.8	745.7	78.8	813.3	408.7	619.6	-----	-----	-----	5.17	25,500X,1X
126V	745.7	78.8	745.7	78.8	717.9	506.5	619.6	-----	-----	-----	4.95	25X,500X,1
127L	747.0	82.5	747.0	82.5	-----	-----	-----	-----	-----	-----	-----	25X,500,1X
127V	747.0	82.5	747.0	82.5	761.8	461.9	619.6	-----	-----	-----	1.01	25X,500X,1
128L	748.5	74.0	748.5	74.0	640.2	569.1	619.6	-----	-----	-----	4.72	25X,500,1X
128V	748.5	74.0	748.5	74.0	703.2	504.2	619.6	-----	-----	-----	3.98	25X,500X,1
129L	752.3	80.0	752.3	80.0	645.6	573.2	619.6	-----	-----	-----	1.51	25X,500,1X
129V	752.3	80.0	752.3	80.0	751.9	453.5	619.6	-----	-----	-----	3.00	25X,500X,1
130L	745.3	82.5	745.3	82.5	665.9	508.8	619.6	-----	-----	-----	0.20	25X,500,1X
130V	745.3	82.5	745.3	82.5	754.3	461.1	619.6	-----	-----	-----	0.94	25X,500,1
132L	749.0	76.1	748.6	75.0	663.2	555.2	619.8	-----	-----	-----	4.82	500X,1,2X
132V	749.0	76.1	748.6	75.0	760.6	454.8	619.7	-----	-----	-----	1.76	500X,1X,2
133L	739.0	77.2	739.0	77.5	-----	-----	-----	-----	-----	-----	-----	25X,500,1X
133V	739.0	77.2	739.0	77.5	784.5	430.5	619.8	-----	-----	-----	2.21	500,1X,2
134L	749.4	78.1	749.4	78.1	666.6	536.9	619.8	-----	-----	-----	4.43	500X,1,2X
134V	749.4	78.1	749.4	78.1	767.7	432.3	619.8	-----	-----	-----	4.47	500,1X,2
135L	745.1	82.0	745.1	82.0	712.0	489.6	619.8	-----	-----	-----	4.29	500X,1,2X
135V	745.1	82.0	745.1	82.0	779.7	419.9	619.8	-----	-----	-----	4.50	500,1,2
136L	748.2	80.8	748.2	80.8	803.6	421.5	619.5	-----	-----	-----	0.24	1,2X,4X
136V	748.2	80.8	748.2	80.8	741.6	484.9	619.5	-----	-----	-----	3.21	1X,2X,4

TABLE H-III

## LIQUID SAMPLE TRAP WEIGHT DATA

Run No.	Trap No. 1		Trap No. 2	
	Tare Wt., g	Gross Wt., g	Tare Wt., g	Gross Wt., g
101-V	87.43744	87.434216	95.01215	95.01210
101-L	95.19085	96.77249	94.96019	95.09570
102-V	95.17501	95.17589	94.97224	94.97217
102-L	95.17861	96.09140	94.98715	94.98736
103-V	87.31162	87.30812	85.63832	85.64143
103-L	87.23819	88.36016	85.62322	85.62886
104-V	87.26675	87.26804	85.61436	85.61552
104-L	87.30129	88.38526	85.60857	85.60862
105-V	95.19518	95.19836	94.93720	94.93380
105-L	95.17200	96.70888	94.94943	94.95286
106-V	95.17854	95.18429	94.95124	94.95612
106-L	95.18104	96.68146	94.92138	94.91954
107-V	95.18629	95.19145	94.97538	94.97638
107-L	95.11035	96.57936	94.93516	94.93638
109-V	87.33347	87.33319	94.91662	94.91600
109-L	87.31311	88.72298	94.90029	94.90086
110-V	87.24963	87.25122	94.98492	94.98260
110-L	87.37115	88.66504	94.89116	94.89990
111-V	87.25556	87.25563	85.59652	85.59743
111-L	87.28655	88.58664	85.58300	85.58000
112-L	87.30957	87.31590	85.53086	85.53290
112-L	87.31261	88.20822	85.55259	85.55418
113-V	87.34572	91.05060	85.51961	85.52506
113-L	87.27719	88.02465	85.60552	85.60507
114-V	87.27176	88.14492	85.60995	85.61304
114-L	87.32950	87.83371	85.53682	85.53617
115-V	87.24094	88.57574	85.62266	85.65781
116-V	87.21662	87.23077	85.56331	85.56293
118-V	87.21472	87.21452	85.57504	85.57546
118-L	87.26180	87.27168	85.61608	85.61565
119-V	87.33298	87.33308	85.59648	85.59641
120-V	95.11909	95.11913	94.94326	94.94338
120-L	87.36337	87.36917	85.55957	85.55904
121-V	95.14689	95.14679	94.94818	94.94812
121-L	87.31961	87.31968	85.60900	85.60835
122-V	87.22973	87.23384	85.60233	85.60049
122-L	95.09380	96.49296	94.94405	94.94204
123-V	87.23889	87.23896	85.55953	85.55946
123-L	87.23889	88.63992	85.55953	85.56291
124-V	95.08572	95.08854	94.93326	94.93714
124-L	87.23012	88.53686	85.56761	85.56080
125-V	87.22823	87.22684	85.57510	85.57282
125-L	95.06865	96.46285	94.90689	94.90770
126-V	95.07581	95.07576	94.90917	94.90824
126-L	95.07576	96.42711	94.90828	94.90959
127-V	95.13507	95.13811	94.89366	94.89509

TABLE H-III (cont'd)

## LIQUID SAMPLE TRAP WEIGHT DATA

Run No.	Trap No. 1		Trap No. 2	
	<u>Tare Wt., g</u>	<u>Gross Wt., g</u>	<u>Tare Wt., g</u>	<u>Gross Wt., g</u>
128-V	95.11484	95.11476	94.90629	94.90638
128-L	87.31773	88.65767	85.46740	85.46871
129-V	87.28489	87.28489	85.46651	85.46659
129-L	87.28532	88.67188	85.48142	85.48312
130-V	95.19680	95.19685	94.85743	94.85857
130-L	87.29777	88.75941	85.47413	85.47773
131-V	95.08973	95.08970	94.85477	94.85483
132-V	95.11089	95.11470	85.46287	85.46294
132-L	87.25671	88.68661	85.45229	85.45426
133-V	95.09308	95.09466	94.54653	94.54803
133-L	95.07873	96.26488	94.84559	94.84959
134-V	87.25911	87.26134	85.44946	85.45048
134-L	95.06864	96.25479	94.85286	94.85629
135-V	87.24888	87.26869	94.83029	94.83363
135-L	87.24056	88.28587	94.83057	94.84464
136-V	87.26796	90.21144	85.46541	85.50094
136-L	95.07936	95.99386	94.86213	94.91040

APPENDIX I

CALCULATED DATA

TABLE I-1  
VAPOR PHASE MOLE FRACTION DATA

RUN NO.	101	102	103	104	106	107	109	110	111
TEMPERATURE, F.	150.05	150.05	150.06	150.07	150.06	150.04	150.04	150.06	150.07
PRESSURE, PSIA	114.56	152.56	214.46	313.77	711.00	1034.45	1510.73	2012.44	3010.11
METHANE	.87766	.92068	.93813	.95840	.97620	.98196	.98036	.97895	.96620
PROPANE	.01742	.01138	.00759	.00468	.00223	.00153	.00129	.00087	.00110
ISOBUTANE	.00632	.00418	.00277	.00183	.00092	.00069	.00061	.00048	.00067
N-BUTANE	.02549	.01731	.01187	.00781	.00404	.00320	.00280	.00250	.00339
2,2-DIMETHYLPROPANE	.00075	.00045	.00026	.00017	.00012	.00010	.00008	.00007	.00009
ISOPENTANE	.01690	.01146	.00809	.00561	.00322	.00275	.00254	.00258	.00374
N-PENTANE	.01590	.01043	.00741	.00537	.00305	.00261	.00247	.00261	.00385
2,2-DIMETHYLBUTANE	.00075	.00056	.00036	.00028	.00016	.00015	.00013	.00015	.00025
CYCLOPENTANE	.00179	.00118	.00105	.00064	.00032	.00025	.00029	.00032	.00052
2-METHYLPENTANE	.00715	.00480	.00629	.00284	.00180	.00134	.00155	.00188	.00304
3-METHYLPENTANE	.00405	.00271	.00369	.00160	.00097	.00076	.00084	.00104	.00169
N-HEXANE	.00621	.00390	.00303	.00244	.00145	.00113	.00132	.00164	.00279
METHYLCYCLOPENTANE	.00353	.00214	.00169	.00148	.00085	.00059	.00076	.00100	.00160
2,3-DIMETHYLPENTANE	.00011	.00003	.00002	.00004	.00006	.00003	.00005	.00007	.00005
CYCLOHEXANE	.00429	.00258	.00227	.00172	.00107	.00071	.00100	.00126	.00216
3-METHYLHEXANE	.00043	.00025	.00023	.00017	.00028	.00008	.00012	.00015	.00027
ISOHEPTANE	.00162	.00092	.00070	.00067	.00046	.00037	.00043	.00051	.00095
2,2,4-TRIMETHYLPENTANE	.00101	.00053	.00046	.00039	.00029	.00019	.00027	.00033	.00059
N-HEPTANE	.00207	.00119	.00106	.00092	.00059	.00040	.00069	.00086	.00163
METHYLCYCLOHEXANE	.00352	.00190	.00178	.00154	.00096	.00059	.00106	.00132	.00246
TOLUENE	.00039	.00051	.00001	.00002	.00002	.00000	.00002	.00002	.00016
2,3,4-TRIMETHYLPENTANE	.00033	.00002	.00039	.00031	.00007	.00008	.00028	.00034	.00064
OCTANE ISOMERS	.00111	.00051	.00041	.00051	.00048	.00026	.00043	.00048	.00091
N-CTANE	.00042	.00017	.00018	.00020	.00011	.00006	.00019	.00022	.00023
ETHYLBENZENE	.00002	.00000	.00000	.00001	.00000	.00000	.00001	.00001	.00005
MIXED XYLENES	.00003	.00000	.00002	.00002	.00001	.00000	.00003	.00002	.00009
258-303F FRACTION	.00035	.00005	.00010	.00015	.00010	.00003	.00020	.00017	.00064
N-NONANE	.00005	.00001	.00001	.00001	.00002	.00000	.00002	.00001	.00006
304-345F FRACTION	.00013	.00000	.00000	.00000	.00003	.00000	.00002	.00000	.00003
N-DECANE	.00005	.00000	.00000	.00000	.00000	.00000	.00000	.00000	.00000
346-384F FRACTION	.00000	.00000	.00000	.00000	.00000	.00000	.00000	.00000	.00000
N-UNDECANE	.00000	.00000	.00000	.00000	.00000	.00000	.00000	.00000	.00000
385-421F FRACTION	.00000	.00000	.00000	.00000	.00000	.00000	.00000	.00000	.00000
N-DODECANE	.00000	.00000	.00000	.00000	.00000	.00000	.00000	.00000	.00000
422-455F FRACTION	.00000	.00000	.00000	.00000	.00000	.00000	.00000	.00000	.00000
N-TRIDECANE	.00000	.00000	.00000	.00000	.00000	.00000	.00000	.00000	.00000
456-488F FRACTION	.00000	.00000	.00000	.00000	.00000	.00000	.00000	.00000	.00000
N-TETRADECANE	.00000	.00000	.00000	.00000	.00000	.00000	.00000	.00000	.00000
489-519F FRACTION	.00000	.00000	.00000	.00000	.00000	.00000	.00000	.00000	.00000
N-PENTADECANE	.00000	.00000	.00000	.00000	.00000	.00000	.00000	.00000	.00000
520-548F FRACTION	.00000	.00000	.00000	.00000	.00000	.00000	.00000	.00000	.00000
N-HEXADECANE	.00000	.00000	.00000	.00000	.00000	.00000	.00000	.00000	.00000
549-575F FRACTION	.00000	.00000	.00000	.00000	.00000	.00000	.00000	.00000	.00000
N-HEPTADECANE	.00000	.00000	.00000	.00000	.00000	.00000	.00000	.00000	.00000
576-602F FRACTION	.00000	.00000	.00000	.00000	.00000	.00000	.00000	.00000	.00000
N-OCTADECANE	.00000	.00000	.00000	.00000	.00000	.00000	.00000	.00000	.00000
603-627F FRACTION	.00000	.00000	.00000	.00000	.00000	.00000	.00000	.00000	.00000
N-NOADECANE	.00000	.00000	.00000	.00000	.00000	.00000	.00000	.00000	.00000
628-650F FRACTION	.00000	.00000	.00000	.00000	.00000	.00000	.00000	.00000	.00000
N-EICOSANE	.00000	.00000	.00000	.00000	.00000	.00000	.00000	.00000	.00000
651F+ FRACTION	.00000	.00000	.00000	.00000	.00000	.00000	.00000	.00000	.00000



TABLE I-1 (CONTINUED)  
VAPOR PHASE MOLE FRACTION DATA

RUN NO.	112	113	118	124	125	126	127	128
TEMPERATURE, F.	150.04	150.05	249.98	250.00	250.00	250.00	250.00	250.00
PRESSURE, PSIA	5009.34	7006.94	113.86	218.56	314.74	513.40	713.46	712.98
METHANE	.97699	.57734	.73214	.83943	.91000	.91827	.95312	.91696
PROPANE	.00126	.00013	.01812	.01150	.00000	.00516	.00408	.00387
ISOBUTANE	.00066	.00042	.00366	.00567	.00000	.00269	.00212	.00222
N-BUTANE	.00315	.00257	.03949	.02546	.01000	.01246	.01010	.01023
2,2-DIMETHYLPROPANE	.00009	.00019	.00116	.00038	.00000	.00023	.00018	.00020
ISOPENTANE	.00285	.00753	.03325	.02077	.00000	.01028	.00633	.00809
N-PENTANE	.00278	.00876	.03324	.02093	.01000	.01061	.00637	.01207
2,2-DIMETHYLBUTANE	.00015	.00099	.00188	.00108	.00000	.00056	.00033	.00064
CYCLOPENTANE	.00034	.00212	.00465	.00244	.00000	.00114	.00070	.00139
2-METHYLPENTANE	.00178	.01248	.02115	.01202	.00000	.00602	.00411	.00706
3-METHYLPENTANE	.00098	.00817	.01209	.00695	.00000	.00330	.00225	.00403
N-HEXANE	.00158	.01507	.01905	.01108	.00000	.00499	.00361	.00416
METHYLCYCLOPENTANE	.00088	.01151	.01065	.00633	.00000	.00339	.00198	.00347
2,3-DIMETHYLPENTANE	.00005	.00046	.00111	.00014	.00000	.00012	.00013	.00011
CYCLOHEXANE	.00123	.02053	.01484	.00873	.00000	.00466	.00265	.00455
3-METHYLHEXANE	.00014	.00306	.00163	.00093	.00000	.00054	.00031	.00048
ISOHEPTANE	.00053	.00994	.00629	.00302	.00000	.00192	.00118	.00186
2,2,4-TRIMETHYLPENTANE	.00035	.00754	.00373	.00201	.00000	.00117	.00073	.00108
N-HEPTANE	.00091	.02123	.00945	.00504	.00000	.00302	.00179	.00265
METHYLCYCLOHEXANE	.00156	.04125	.01448	.00798	.00000	.00480	.00266	.00419
TOLUENE	.00002	.00868	.00087	.00105	.00000	.00003	.00002	.00016
2,3,4-TRIMETHYLPENTANE	.00027	.01164	.00295	.00160	.00000	.00130	.00043	.00090
OCTANE ISOMERS	.00065	.02518	.00482	.00267	.00000	.00160	.00097	.00117
N-OCTANE	.00029	.01897	.00206	.00109	.00000	.00082	.00026	.00051
ETHYLBENZENE	.00002	.00431	.00008	.00005	.00000	.00003	.00000	.00001
MIXED XYLENES	.00004	.01396	.00023	.00017	.00000	.00011	.00000	.00004
258-303F FRACTION	.00026	.02617	.00157	.00104	.00000	.00059	.00018	.00029
N-NONANE	.00003	.01191	.00015	.00008	.00000	.00006	.00000	.00001
304-345F FRACTION	.00002	.02180	.00008	.00011	.00000	.00002	.00000	.00002
N-DECANE	.00000	.00817	.00001	.00010	.00000	.00000	.00000	.00000
346-384F FRACTION	.00000	.01153	.00000	.00000	.00000	.00000	.00000	.00000
N-UNDECANE	.00000	.00530	.00000	.00000	.00000	.00000	.00000	.00000
385-421F FRACTION	.00000	.00645	.00000	.00000	.00000	.00000	.00000	.00000
N-DODECANE	.00000	.00348	.00000	.00000	.00000	.00000	.00000	.00000
422-455F FRACTION	.00000	.00593	.00000	.00000	.00000	.00000	.00000	.00000
N-TRIDECANE	.00000	.00284	.00000	.00000	.00000	.00000	.00000	.00000
456-488F FRACTION	.00000	.00324	.00000	.00000	.00000	.00000	.00000	.00000
N-TETRADECANE	.00000	.00147	.00000	.00000	.00000	.00000	.00000	.00000
489-519F FRACTION	.00000	.00214	.00000	.00000	.00000	.00000	.00000	.00000
N-PENTADECANE	.00000	.00093	.00000	.00000	.00000	.00000	.00000	.00000
520-548F FRACTION	.00000	.00150	.00000	.00000	.00000	.00000	.00000	.00000
N-HEXADECANE	.00000	.00071	.00000	.00000	.00000	.00000	.00000	.00000
549-575F FRACTION	.00000	.00041	.00000	.00000	.00000	.00000	.00000	.00000
N-HEPTADECANE	.00000	.00029	.00000	.00000	.00000	.00000	.00000	.00000
576-602F FRACTION	.00000	.00051	.00000	.00000	.00000	.00000	.00000	.00000
N-OCTADECANE	.00000	.00019	.00000	.00000	.00000	.00000	.00000	.00000
603-627F FRACTION	.00000	.00026	.00000	.00000	.00000	.00000	.00000	.00000
N-NONADECANE	.00000	.00008	.00000	.00000	.00000	.00000	.00000	.00000
628-650F FRACTION	.00000	.00008	.00000	.00000	.00000	.00000	.00000	.00000
N-EICOSANE	.00000	.00005	.00000	.00000	.00000	.00000	.00000	.00000
651F+ FRACTION	.00000	.00005	.00000	.00000	.00000	.00000	.00000	.00000

TABLE I-I (CONTINUED)  
VAPOR PHASE MOLE FRACTION DATA

RUN NO.	130	132	133	134	135	136
TEMPERATURE, F.	250.00	250.00	250.00	250.00	250.00	250.00
PRESSURE, PSIA	1013.31	1512.99	2012.38	2010.93	3011.41	5004.27
METHANE	.94944	.95122	.95064	.94303	.93755	.67800
PROPANE	.00285	.00138	.00102	.00148	.00107	.00100
ISOBUTANE	.00156	.00095	.00058	.00095	.00077	.00089
N-BUTANE	.00728	.00516	.00323	.00493	.00408	.00539
2,2-DIMETHYLPROPANE	.00044	.00004	.00004	.00012	.00023	.00026
ISOPENTANE	.00666	.00539	.00487	.00542	.00517	.00943
N-PENTANE	.00677	.00571	.00528	.00581	.00570	.01117
2,2-DIMETHYLBUTANE	.00034	.00029	.00033	.00039	.00045	.00131
CYCLOPENTANE	.00069	.00076	.00066	.00085	.00081	.00208
2-METHYLPENTANE	.00409	.00421	.00441	.00477	.00511	.01323
3-METHYLPENTANE	.00256	.00241	.00245	.00276	.00304	.00895
N-HEXANE	.00406	.00407	.00407	.00460	.00506	.01511
METHYLCYCLOPENTANE	.00217	.00219	.00473	.00250	.00317	.01061
2,3-DIMETHYLPENTANE	.00020	.00022	.00024	.00042	.00018	.00070
CYCLOHEXANE	.00272	.00326	.00335	.00393	.00456	.01886
3-METHYLHEXANE	.00031	.00039	.00041	.00047	.00058	.00243
ISOHEPTANE	.00114	.00149	.00156	.00183	.00216	.00828
2,2,4-TRIMETHYLPENTANE	.00074	.00091	.00095	.00119	.00145	.00622
N-HEPTANE	.00168	.00241	.00259	.00297	.00386	.01798
METHYLCYCLOHEXANE	.00243	.00372	.00409	.00482	.00637	.03514
TOLUENE	.00005	.00004	.00006	.00008	.00010	.00856
2,3,4-TRIMETHYLPENTANE	.00020	.00093	.00104	.00128	.00191	.00932
OCTANE ISOMERS	.00108	.00141	.00157	.00258	.00288	.01937
N-OCTANE	.00018	.00068	.00078	.00094	.00140	.01517
ETHYLBENZENE	.00000	.00000	.00005	.00009	.00011	.00331
MIXED XYLENES	.00300	.00002	.00009	.00015	.00025	.01278
258-303F FRACTION	.00026	.00053	.00065	.00109	.00155	.02160
N-NONANE	.00000	.00004	.00006	.00014	.00020	.00999
304-345F FRACTION	.00000	.00002	.00007	.00022	.00006	.01835
N-DECANE	.00000	.00000	.00000	.00001	.00000	.00638
346-384F FRACTION	.00000	.00000	.00000	.00000	.00000	.00873
N-UNDECANE	.00000	.00000	.00000	.00000	.00000	.00380
385-421F FRACTION	.00000	.00000	.00000	.00000	.00000	.00388
N-DODECANE	.00000	.00000	.00000	.00000	.00000	.00186
422-455F FRACTION	.00000	.00000	.00000	.00000	.00000	.00326
N-TRIDECANE	.00000	.00000	.00000	.00000	.00000	.00121
456-488F FRACTION	.00000	.00000	.00000	.00000	.00000	.00164
N-TETRADECANE	.00000	.00000	.00000	.00000	.00000	.00060
489-519F FRACTION	.00000	.00000	.00000	.00000	.00000	.00105
N-PENTADECANE	.00000	.00000	.00000	.00000	.00000	.00037
520-548F FRACTION	.00000	.00000	.00000	.00000	.00000	.00075
N-HEXADECANE	.00000	.00000	.00000	.00000	.00000	.00026
549-575F FRACTION	.00000	.00000	.00000	.00000	.00000	.00024
N-HEPTADECANE	.00000	.00000	.00000	.00000	.00000	.00008
576-602F FRACTION	.00000	.00000	.00000	.00000	.00000	.00009
N-OCTADECANE	.00000	.00000	.00000	.00000	.00000	.00001
603-627F FRACTION	.00000	.00000	.00000	.00000	.00000	.00002
N-NONADECANE	.00000	.00000	.00000	.00000	.00000	.00000
628-650F FRACTION	.00000	.00000	.00000	.00000	.00000	.00001
N-EICOSANE	.00000	.00000	.00000	.00000	.00000	.00000
651F+ FRACTION	.00000	.00000	.00000	.00000	.00000	.00000

TABLE I-II

## LIQUID PHASE MOLE FRACTION DATA

RUN NO.	101	102	103	104	106	107	109	110
TEMPERATURE, F.	150.05	150.05	150.06	150.07	150.06	150.04	150.04	150.06
PRESSURE, PSIA	114.56	152.56	214.46	313.77	711.00	1034.45	1510.73	2012.44
METHANE	.02753	.03874	.04974	.07483	.17112	.22430	.28138	.33142
PROPANE	.00788	.00544	.00675	.00619	.00402	.00310	.00247	.00191
ISOBUTANE	.00452	.00582	.00520	.00490	.00294	.00235	.00139	.00163
N-BUTANE	.01825	.03738	.03022	.02794	.01750	.01192	.00598	.00727
2,2-DIMETHYLPROPANE	.00075	.00081	.00064	.00116	.00046	.00045	.00019	.00044
ISOPENTANE	.02480	.05651	.04240	.03485	.01831	.01922	.00305	.01664
N-PENTANE	.02255	.06426	.04555	.04473	.01907	.01929	.00239	.01840
2,2-DIMETHYLBUTANE	.00288	.00864	.00308	.00290	.00240	.00208	.00025	.00201
CYCLOPENTANE	.00565	.01058	.00672	.00742	.00476	.00353	.00088	.00373
2-METHYLPENTANE	.03370	.05035	.03722	.02659	.03074	.02893	.01018	.02413
3-METHYLPENTANE	.02145	.03036	.02168	.01796	.01978	.01767	.00754	.01582
N-HEXANE	.03191	.04950	.03564	.03669	.03161	.02801	.01681	.02715
METHYLCYCLOPENTANE	.02636	.03327	.02477	.02247	.02475	.02209	.01383	.02039
2,3-DIMETHYLPENTANE	.00225	.00104	.00176	.00103	.00126	.00115	.00044	.00091
CYCLOHEXANE	.04717	.05250	.03953	.03667	.04375	.03910	.02878	.03569
3-METHYLHEXANE	.00671	.00765	.00371	.00555	.00611	.00548	.00526	.00557
ISOHEPTANE	.02337	.02523	.01900	.01778	.02117	.01855	.01733	.01733
2,2,4-TRIMETHYLPENTANE	.02008	.01955	.01488	.01338	.01640	.01443	.01296	.01332
N-HEPTANE	.04536	.05114	.04003	.04222	.04222	.03924	.04117	.03627
METHYLCYCLOHEXANE	.09808	.10077	.07785	.07764	.08896	.07895	.08125	.06950
TOLUENE	.01450	.01810	.01344	.01486	.01618	.01600	.01725	.01433
2,3,4-TRIMETHYLPENTANE	.02817	.03068	.02700	.02745	.02541	.02177	.02595	.02047
OCTANE ISOMERS	.06374	.06459	.05552	.05500	.05401	.04712	.05215	.04399
N-OCTANE	.04482	.05075	.04508	.04583	.04077	.03583	.04391	.03361
ETHYLBENZENE	.01145	.01235	.01039	.01132	.00992	.00834	.00752	.00819
MIXED XYLENES	.03540	.04106	.03740	.03884	.03519	.03112	.02863	.02701
25%-30% FRACTION	.06926	.07342	.06795	.07027	.06331	.05518	.06354	.04953
N-NONANE	.03483	.03683	.03433	.03402	.03057	.02611	.03213	.02364
30%-34% FRACTION	.06842	.07190	.06700	.06535	.06128	.05296	.06268	.04667
N-DECANE	.02651	.02552	.02271	.02101	.02254	.01910	.02294	.01635
34%-38% FRACTION	.03773	.03718	.03604	.03117	.03293	.02857	.03299	.02326
N-UNDECANE	.01625	.01597	.01286	.02274	.01316	.01193	.01439	.00892
38%-42% FRACTION	.01806	.01901	.01725	.01423	.01663	.01385	.01434	.00958
N-DODECANE	.00999	.01162	.00721	.00567	.00717	.00705	.00733	.00376
42%-45% FRACTION	.01584	.02044	.01247	.01106	.01217	.01229	.01173	.00619
N-TRIDECANE	.00689	.01252	.00527	.00452	.00522	.00620	.00529	.00245
45%-48% FRACTION	.00795	.01195	.00537	.00504	.00588	.00624	.00491	.00304
N-TETRADECANE	.00359	.00657	.00271	.00243	.00297	.00342	.00283	.00128
48%-51% FRACTION	.00527	.00853	.00333	.00354	.00400	.00415	.00388	.00212
N-PENTADECANE	.00221	.00440	.00170	.00165	.00181	.00224	.00175	.00080
52%-54% FRACTION	.00386	.00607	.00258	.00298	.00320	.00297	.00284	.00149
N-HEXADECANE	.00170	.00348	.00123	.00146	.00173	.00170	.00143	.00056
54%-57% FRACTION	.00151	.00314	.00111	.00140	.00149	.00149	.00158	.00106
N-HEPTADECANE	.00066	.00122	.00051	.00070	.00054	.00071	.00063	.00026
57%-60% FRACTION	.00102	.00243	.00071	.00104	.00098	.00113	.00103	.00029
N-OCTADECANE	.00041	.00070	.00032	.00054	.00042	.00040	.00035	.00019
60%-62% FRACTION	.00040	.00119	.00086	.00087	.00131	.00067	.00050	.00044
N-NONADECANE	.00042	.00052	.00009	.00028	.00025	.00027	.00024	.00025
62%-65% FRACTION	.00046	.00087	.00006	.00058	.00106	.00035	.00048	.00020
N-EICOSANE	.00011	.00029	.00016	.00021	.00040	.00027	.00011	.00011
65%+ FRACTION	.00003	.00177	.00071	.00078	.00154	.00048	.00086	.00020

TABLE I-II (CONTINUED)  
LIQUID PHASE MOLE FRACTION DATA

RUN NO.	111	112	113	118	124	125	126	127
TEMPERATURE, F.	150.07	150.04	150.05	249.98	250.00	250.00	250.00	250.00
PRESSURE, PSIA	3010.11	5009.34	7006.94	113.86	218.56	314.74	513.40	713.46
METHANE	.45590	.67248	.74323	.02326	.04834	.07029	.11228	.14068
PROPANE	.00183	.00123	.00093	.00411	.00380	.00377	.00346	.00297
ISOBUTANE	.00087	.00087	.00065	.00262	.00296	.00287	.00236	.00219
N-BUTANE	.00347	.00411	.00335	.01362	.01456	.01368	.01153	.01172
2,2-DIMETHYLPROPANE	.00009	.00024	.00020	.00067	.00087	.00040	.00047	.00030
ISOPENTANE	.00184	.00793	.00654	.02384	.02487	.01515	.02199	.01727
N-PENTANE	.00172	.00775	.00701	.02700	.02788	.02594	.02543	.02171
2,2-DIMETHYLBUTANE	.00018	.00097	.00081	.00299	.00263	.00228	.00234	.00236
CYCLOPENTANE	.00071	.00188	.00162	.00520	.00615	.00524	.00534	.00451
2-METHYLPENTANE	.00755	.01166	.00964	.03387	.03498	.03264	.02902	.03018
3-METHYLPENTANE	.00543	.00755	.00608	.02088	.02150	.02044	.01849	.01864
N-HEXANE	.01262	.01157	.01031	.03694	.03733	.03576	.03551	.03333
METHYLCYCLOPENTANE	.01049	.00936	.00782	.02719	.02721	.02569	.02494	.02505
2,3-DIMETHYLPENTANE	.00083	.00049	.00034	.00128	.00132	.00164	.00191	.00108
CYCLOHEXANE	.02175	.01669	.01364	.04733	.04831	.04621	.04441	.04312
3-METHYLHEXANE	.00392	.00241	.00191	.00671	.00648	.00634	.00654	.00591
ISOHEPTANE	.01329	.00823	.00670	.02220	.02296	.02161	.02142	.02007
2,2,4-TRIMETHYLPENTANE	.00983	.00629	.00499	.01688	.01726	.01632	.01590	.01519
N-HEPTANE	.03165	.01640	.01363	.04956	.04980	.04714	.04686	.04519
METHYLCYCLOHEXANE	.06296	.03434	.02813	.10001	.10214	.09762	.08951	.08854
TOLUENE	.01412	.00537	.00465	.02084	.02151	.02314	.02161	.02195
2,3,4-TRIMETHYLPENTANE	.01854	.01000	.00804	.02896	.02928	.02639	.02565	.02520
OCTANE ISOMERS	.03881	.02102	.01641	.05928	.05932	.05632	.05593	.05308
N-OCTANE	.03282	.01607	.01298	.04743	.04822	.04600	.04479	.04383
ETHYLBENZENE	.00712	.00393	.00300	.01179	.01158	.01091	.01034	.01017
MIXED XYLENES	.02825	.01287	.01033	.04080	.04173	.04113	.03734	.03827
258-303F FRACTION	.04733	.02400	.01888	.07090	.07188	.06867	.06529	.06525
N-NONANE	.02352	.01195	.00931	.03572	.03520	.03363	.03182	.03134
304-345F FRACTION	.04515	.02309	.01758	.06907	.06773	.06608	.06141	.06190
N-DECANE	.01621	.00848	.00626	.02599	.02377	.02370	.02171	.02235
346-384F FRACTION	.02279	.01185	.00831	.03772	.03212	.03402	.03032	.03242
N-UNDECANE	.00882	.00487	.00336	.01644	.01238	.01361	.01150	.01328
385-421F FRACTION	.01075	.00470	.00330	.01805	.01314	.01574	.01432	.01519
N-DODECANE	.00519	.00250	.00169	.00832	.00535	.00771	.00667	.00708
422-455F FRACTION	.00918	.00422	.00281	.01450	.00967	.01257	.01140	.01177
N-TRIDECANE	.00410	.00203	.00110	.00570	.00330	.00543	.00490	.00471
456-488F FRACTION	.00504	.00233	.00126	.00683	.00416	.00642	.00634	.00585
N-TETRADECANE	.00242	.00121	.00054	.00294	.00143	.00287	.00266	.00229
489-519F FRACTION	.00337	.00161	.00078	.00425	.00223	.00432	.00435	.00404
N-PENTADECANE	.00151	.00078	.00030	.00152	.00075	.00177	.00179	.00150
520-548F FRACTION	.00279	.00132	.00055	.00276	.00135	.00323	.00282	.00274
N-HEXADECANE	.00115	.00073	.00025	.00112	.00079	.00128	.00154	.00127
549-575F FRACTION	.00129	.00070	.00028	.00103	.00066	.00157	.00139	.00135
N-HEPTADECANE	.00056	.00027	.00010	.00036	.00024	.00082	.00061	.00049
576-602F FRACTION	.00091	.00054	.00008	.00055	.00030	.00044	.00168	.00110
N-OCTADECANE	.00031	.00017	.00004	.00015	.00010	.00035	.00043	.00035
603-627F FRACTION	.00032	.00035	.00001	.00025	.00011	.00021	.00042	.00056
N-NONADECANE	.00019	.00010	.00001	.00012	.00006	.00018	.00039	.00025
628-650F FRACTION	.00012	.00005	.00000	.00017	.00001	.00009	.00037	.00028
N-EICOSANE	.00008	.00007	.00000	.00004	.00001	.00009	.00015	.00015
651F+ FRACTION	.00009	.00013	.00000	.00002	.00000	.00004	.00012	.00012

TABLE I-II (CONTINUED)  
LIQUID PHASE MOLE FRACTION DATA

RUN NO.	128	130	132	133	134	135	136
TEMPERATURE, F.	250.00	250.00	250.00	250.00	250.00	250.00	250.00
PRESSURE, PSIA	712.98	1013.31	1512.99	2012.38	2010.93	3011.41	5004.27
METHANE	.14068	.22225	.29459	.38163	.38163	.53248	.66690
PROPANE	.00297	.00245	.00155	.00124	.00124	.00127	.00104
ISOBUTANE	.00219	.00212	.00148	.00113	.00113	.00106	.00078
N-BUTANE	.01172	.01210	.00904	.00702	.00702	.00631	.00442
2,2-DIMETHYLPROPANE	.00030	.00071	.00047	.00038	.00038	.00028	.00030
ISOPENTANE	.01727	.02263	.01761	.01534	.01534	.01221	.00853
N-PENTANE	.02171	.02572	.02145	.01796	.01796	.01469	.01039
2,2-DIMETHYLBUTANE	.00236	.00229	.00239	.00174	.00174	.00154	.00108
CYCLOPENTANE	.00451	.00485	.00395	.00345	.00345	.00291	.00211
2-METHYLPENTANE	.03018	.03179	.02845	.02334	.02334	.01884	.01360
3-METHYLPENTANE	.01864	.02022	.01745	.01487	.01487	.01167	.00851
N-HEXANE	.03333	.03581	.03181	.02589	.02589	.02109	.01526
METHYLCYCLOPENTANE	.02505	.02493	.02230	.01844	.01844	.01493	.01074
2,3-DIMETHYLPENTANE	.00108	.00149	.00128	.00110	.00110	.00096	.00071
CYCLOHEXANE	.04312	.04477	.04034	.03269	.03269	.02673	.01931
3-METHYLHEXANE	.00591	.00587	.00535	.00430	.00430	.00352	.00252
ISOHEPTANE	.02007	.01999	.01804	.01498	.01498	.01211	.00900
2,2,4-TRIMETHYLPENTANE	.01519	.01260	.01382	.01127	.01127	.00904	.00647
N-HEPTANE	.04519	.04407	.04068	.03310	.03310	.02693	.01960
METHYLCYCLOHEXANE	.08854	.08851	.08157	.06518	.06518	.05325	.03864
TOLUENE	.02195	.02100	.01958	.01538	.01538	.01235	.00857
2,3,4-TRIMETHYLPENTANE	.02520	.02350	.02135	.01751	.01751	.01415	.01018
OCTANE ISOMERS	.05308	.04815	.04521	.03621	.03621	.02954	.02087
N-OCTANE	.04383	.03915	.03616	.02865	.02865	.02341	.01617
ETHYLBENZENE	.01017	.00871	.00784	.00692	.00692	.00524	.00351
MIXED XYLENES	.03827	.03316	.03137	.02416	.02416	.01926	.01256
258-303F FRACTION	.06525	.05517	.05195	.04250	.04250	.03318	.02211
N-NONANE	.03134	.02525	.02364	.02002	.02002	.01486	.00955
304-345F FRACTION	.06190	.04742	.04333	.03911	.03911	.02752	.01757
N-DECANE	.02235	.01526	.01387	.01451	.01451	.00875	.00613
346-384F FRACTION	.03242	.01145	.01764	.02070	.02070	.01192	.00842
N-UNDECANE	.01328	.00826	.00616	.00939	.00939	.00488	.00379
385-421F FRACTION	.01519	.00954	.00730	.01057	.01057	.00563	.00461
N-DODECANE	.00708	.00457	.00316	.00552	.00552	.00278	.00267
422-455F FRACTION	.01177	.00788	.00566	.00986	.00986	.00486	.00453
N-TRIDECANE	.00471	.00343	.00219	.00448	.00448	.00200	.00215
456-488F FRACTION	.00585	.00406	.00304	.00533	.00533	.00239	.00224
N-TETRADECANE	.00229	.00176	.00119	.00228	.00228	.00096	.00090
489-519F FRACTION	.00404	.00245	.00178	.00349	.00349	.00150	.00125
N-PENTADECANE	.00150	.00094	.00074	.00137	.00137	.00048	.00044
520-548F FRACTION	.00274	.00149	.00079	.00251	.00251	.00109	.00067
N-HEXADECANE	.00127	.00068	.00054	.00118	.00118	.00035	.00027
549-575F FRACTION	.00135	.00045	.00069	.00107	.00107	.00026	.00041
N-HEPTADECANE	.00049	.00020	.00015	.00040	.00040	.00009	.00009
576-602F FRACTION	.00110	.00053	.00024	.00098	.00098	.00016	.00009
N-OCTADECANE	.00035	.00008	.00016	.00022	.00022	.00008	.00004
603-627F FRACTION	.00056	.00003	.00013	.00018	.00018	.00014	.00002
N-NONADECANE	.00025	.00001	.00024	.00009	.00009	.00005	.00001
628-650F FRACTION	.00028	.00001	.00000	.00008	.00008	.00002	.00000
N-EICOSANE	.00015	.00000	.00000	.00001	.00001	.00001	.00000
651F+ FRACTION	.00012	.00000	.00002	.00001	.00001	.00000	.00001

TABLE I-III  
EXPERIMENTAL K-VALUES

RUN NO.	101	102	103	104	106	107	109	110
TEMPERATURE, F.	150.05	150.05	150.06	150.07	150.06	150.04	150.04	150.06
PRESSURE, PSIA	114.56	152.56	214.46	313.77	711.00	1034.45	1510.73	2012.44
METHANE	31.88013	23.76561	18.86067	12.80769	5.70000	4.37788	3.48411	2.95380
PROPANE	2.21065	2.09191	1.12444	.75605	.55239	.49354	.52226	.45549
ISOBUTANE	1.39823	.71821	.53269	.37346	.31301	.29361	.43884	.29447
N-BUTANE	1.39671	.46308	.39278	.27952	.23105	.26845	.46822	.34387
2,2-DIMETHYLPROPANE	1.00000	.55555	.40625	.14655	.26101	.22222	.42105	.15909
ISOPENTANE	.68145	.20279	.19080	.16097	.17586	.14308	.83278	.15504
N-PENTANE	.70509	.16230	.16267	.12005	.15993	.13530	1.03347	.14184
2,2-DIMETHYLBUTANE	.26041	.06481	.11688	.09655	.06666	.07211	.52000	.07462
CYCLOPENTANE	.31681	.11153	.15625	.08625	.06722	.07082	.32954	.08579
2-METHYLPENTANE	.21216	.09533	.16899	.10680	.05855	.04631	.15225	.07791
3-METHYLPENTANE	.18881	.08926	.17020	.08908	.04903	.04301	.11140	.06573
N-HEXANE	.19460	.07878	.08501	.06650	.04587	.04034	.07852	.06040
METHYLCYCLOPENTANE	.13391	.06432	.06822	.06586	.03434	.02670	.05495	.04904
2,3-DIMETHYLPENTANE	.04888	.02884	.01136	.03883	.04761	.02608	.11363	.07692
CYCLOHEXANE	.09094	.04914	.05742	.04690	.02445	.01815	.03474	.03530
3-METHYLHEXANE	.06408	.03267	.06199	.03063	.04582	.01459	.02281	.02692
ISOHEPTANE	.06931	.03646	.03684	.03768	.02172	.01994	.02481	.02942
2,2,4-TRIMETHYLPENTANE	.05029	.02710	.03091	.02914	.01768	.01316	.02083	.02477
N-HEPTANE	.04563	.02326	.02648	.02179	.01397	.01019	.01675	.02371
METHYLCYCLOHEXANE	.03588	.01885	.02286	.01983	.01079	.00747	.01304	.01899
TOLUENE	.02689	.02817	.00074	.00134	.00123	-----	.00115	.00139
2,2,4-TRIMETHYLPENTANE	.01171	.00065	.01444	.01129	.00275	.00367	.01078	.01660
OCTANE ISOMERS	.01827	.00789	.00738	.00927	.00888	.00551	.00824	.01091
N-OCTANE	.00937	.00334	.00399	.00436	.00269	.00167	.00432	.00654
ETHYLBENZENE	.00174	-----	-----	.00088	-----	-----	.00132	.00122
MIXED XYLENES	.00084	-----	.00053	.00051	.00028	-----	.00104	.00074
258-303F FRACTION	.00505	.00068	.00147	.00213	.00157	.00054	.00314	.00343
N-NONANE	.00143	.00027	.00029	.00029	.00065	-----	.00062	.00042
304-345F FRACTION	.00190	-----	-----	-----	.00048	-----	.00031	-----
N-DECANE	.00188	-----	-----	-----	-----	-----	-----	-----
346-384F FRACTION	-----	-----	-----	-----	-----	-----	-----	-----
N-UNDECANE	-----	-----	-----	-----	-----	-----	-----	-----
385-421F FRACTION	-----	-----	-----	-----	-----	-----	-----	-----
N-DODECANE	-----	-----	-----	-----	-----	-----	-----	-----
422-455F FRACTION	-----	-----	-----	-----	-----	-----	-----	-----
N-TRIDECANE	-----	-----	-----	-----	-----	-----	-----	-----
456-488F FRACTION	-----	-----	-----	-----	-----	-----	-----	-----
N-TETRADECANE	-----	-----	-----	-----	-----	-----	-----	-----
489-519F FRACTION	-----	-----	-----	-----	-----	-----	-----	-----
N-PENTADECANE	-----	-----	-----	-----	-----	-----	-----	-----
520-548F FRACTION	-----	-----	-----	-----	-----	-----	-----	-----
N-HEXADECANE	-----	-----	-----	-----	-----	-----	-----	-----
549-575F FRACTION	-----	-----	-----	-----	-----	-----	-----	-----
N-HEPTADECANE	-----	-----	-----	-----	-----	-----	-----	-----
576-602F FRACTION	-----	-----	-----	-----	-----	-----	-----	-----
N-OCTADECANE	-----	-----	-----	-----	-----	-----	-----	-----
603-627F FRACTION	-----	-----	-----	-----	-----	-----	-----	-----
N-NONADECANE	-----	-----	-----	-----	-----	-----	-----	-----
628-650F FRACTION	-----	-----	-----	-----	-----	-----	-----	-----
N-EICOSANE	-----	-----	-----	-----	-----	-----	-----	-----
651F+ FRACTION	-----	-----	-----	-----	-----	-----	-----	-----

TABLE I-III (CONTINUED)

## EXPERIMENTAL K-VALUES

RUN NO.	111	112	118	124	126	127
TEMPERATURE, F.	150.07	150.04	249.98	250.00	250.00	250.00
PRESSURE, PSIA	3010.11	5009.34	113.86	218.56	513.40	713.46
METHANE	2.11932	1.45281	31.47635	17.36512	8.17839	6.77509
PROPANE	.60109	1.02439	4.40875	3.02631	1.49132	1.37400
ISOBUTANE	.77011	.75862	3.30534	1.91554	1.13983	1.01500
N-BUTANE	.97694	.76642	2.89941	1.74862	1.08065	.86103
2,2-DIMETHYLPROPANE	1.00000	.37500	1.73134	.43678	.48936	.60000
ISOPENTANE	2.03260	.35939	1.39471	.83514	.46748	.36653
N-PENTANE	2.23837	.35870	1.23111	.75071	.41722	.29341
2,2-DIMETHYLBUTANE	1.38888	.15463	.62876	.41064	.23931	.13983
CYCLOPENTANE	.73239	.18085	.89423	.39674	.21348	.15521
2-METHYLPENTANE	.40264	.15265	.62444	.34362	.20744	.13618
3-METHYLPENTANE	.31123	.12980	.57902	.32325	.17847	.12070
N-HEXANE	.22107	.13656	.51570	.29681	.14052	.10831
METHYLCYCLOPENTANE	.15252	.09401	.39168	.23263	.13592	.07904
2,3-DIMETHYLPENTANE	.06024	.10204	.86718	.10606	.06282	.12037
CYCLOHEXANE	.09931	.07369	.31354	.18070	.10493	.06145
3-METHYLHEXANE	.06887	.05809	.24292	.14351	.08256	.05245
ISOHEPTANE	.07148	.06439	.28333	.13153	.08963	.05879
2,2,4-TRIMETHYLPENTANE	.06002	.05564	.22097	.11645	.07358	.04805
N-HEPTANE	.05150	.05548	.19067	.10120	.06444	.03961
METHYLCYCLOHEXANE	.03907	.04542	.14478	.07812	.05362	.03004
TOLUENE	.01133	.00372	.04174	.04881	.00138	.00091
2,3,4-TRIMETHYLPENTANE	.03451	.02700	.10186	.05464	.05068	.01706
OCTANE ISOMERS	.02344	.03092	.08130	.04501	.02860	.01827
N-OCTANE	.00700	.01804	.04343	.02260	.01830	.00593
ETHYLBENZENE	.00702	.00508	.00678	.00431	.00290	-----
MIXED XYLENES	.00318	.00310	.00563	.00407	.00294	-----
258-303F FRACTION	.01352	.01083	.02214	.01446	.00903	.00275
N-NONANE	.00255	.00251	.00419	.00227	.00188	-----
304-345F FRACTION	.00066	.00086	.00115	.00162	.00032	-----
N-DECANE	-----	-----	.00038	.00420	-----	-----
346-384F FRACTION	-----	-----	-----	-----	-----	-----
N-UNDECANE	-----	-----	-----	-----	-----	-----
385-421F FRACTION	-----	-----	-----	-----	-----	-----
N-DODECANE	-----	-----	-----	-----	-----	-----
427-455F FRACTION	-----	-----	-----	-----	-----	-----
N-TRIDECAE	-----	-----	-----	-----	-----	-----
456-488F FRACTION	-----	-----	-----	-----	-----	-----
N-TETRADECAE	-----	-----	-----	-----	-----	-----
489-519F FRACTION	-----	-----	-----	-----	-----	-----
N-PENTADECANE	-----	-----	-----	-----	-----	-----
520-548F FRACTION	-----	-----	-----	-----	-----	-----
N-HEXADECANE	-----	-----	-----	-----	-----	-----
549-575F FRACTION	-----	-----	-----	-----	-----	-----
N-HEPTADECANE	-----	-----	-----	-----	-----	-----
576-602F FRACTION	-----	-----	-----	-----	-----	-----
N-OCTADECANE	-----	-----	-----	-----	-----	-----
603-627F FRACTION	-----	-----	-----	-----	-----	-----
N-NONADECANE	-----	-----	-----	-----	-----	-----
628-650F FRACTION	-----	-----	-----	-----	-----	-----
N-EICOSANE	-----	-----	-----	-----	-----	-----
651F+ FRACTION	-----	-----	-----	-----	-----	-----





TABLE I-IV

## EXPERIMENTAL LIQUID PHASE DENSITY DATA

<u>Run</u>	<u>Temperature, °F.</u>	<u>Pressure, psia</u>	<u>Density</u>	
			<u>gm/cc</u>	<u>cc/g mole</u>
101	150.05	114.56	0.69478	0.00620
102	150.05	152.57	0.69315	0.00613
103	150.06	214.47	0.59714	0.00561
104	150.07	313.77	0.59266	0.00565
105	150.05	513.50	0.67724	0.00646
106	150.06	711.01	0.65963	0.00651
107	150.04	1034.45	0.66863	0.00721
109	150.04	1510.74	0.64733	0.00708
110	150.06	2012.47	0.60559	0.00756
111	150.07	3010.10	0.60185	0.00866
112	150.04	5009.31	0.51236	0.01061
113	150.05	7006.96	0.47844	0.01181
118	249.98	113.86	0.60762	0.00545
120	249.99	113.81	0.60742	0.00554
122	250.00	115.37	0.60762	0.00545
123	250.00	213.40	0.61259	0.00556
124	250.00	218.61	0.57080	0.00537
125	250.00	314.75	0.61243	0.00572
126	250.00	513.39	0.59754	0.00582
127	250.00	713.46	0.59137	0.00589
128	250.00	712.97	0.59121	0.00585
129	250.00	713.66	0.61465	0.00609
130	250.00	1013.30	0.59614	0.00757
132	250.00	1512.99	0.58311	0.00813
133	250.00	2012.45	0.57057	0.00746
134	250.00	2010.95	0.57057	0.00746
135	250.00	3011.43	0.55350	0.00928
136	250.00	5004.31	0.43811	0.01233

TABLE I-V

## EXPERIMENTAL VAPOR PHASE DENSITY DATA

Run	Temperature, °F.	Pressure, psia	Density	
			gm/cc	cc/g mole
101	150.05	114.56	0.00642	0.00028
102	150.05	152.56	0.00925	0.00045 *
103	150.06	214.47	0.01142	0.00058
104	150.07	131.76	0.01574	0.00085
105	150.05	513.51	0.02491	0.00143
106	150.06	711.00	0.03318	0.00190
107	150.04	1034.45	0.04842	0.00283
109	150.04	1510.73	0.07176	0.00415
110	150.06	2012.44	0.09849	0.00565
111	150.07	3010.10	0.15488	0.00846
112	150.04	5009.35	0.10112	0.00577
113	150.05	7006.95	0.46994	0.01057
118	249.98	113.86	0.00825	0.00025
120	249.99	113.81	0.00844	0.00041
122	250.00	115.37	0.00632	0.00020
123	250.00	213.41	0.01289	0.00049
124	250.00	218.56	0.01289	0.00049
125	250.00	314.74	0.01684	0.00074
126	250.00	513.40	0.02477	0.00117
127	250.00	713.44	0.03058	0.00161
128	250.00	712.98	0.02296	0.00109
129	250.00	713.67	0.03234	0.00162
130	250.00	1013.31	0.04402	0.00229
132	250.00	1512.99	0.06703	0.00347
133	250.00	2012.38	0.09568	0.00491
134	250.00	2010.93	0.09527	0.00476
135	250.00	3011.41	0.14385	0.00700
136	250.00	5004.27	0.42283	0.00922

## APPENDIX J

### NOMENCLATURE

A	-	parameter in the Redlich-Kwong equation of state
	-	area
a	-	parameter in the Redlich-Kwong equation of state
B	-	second virial coefficient, volume/mole
	-	parameter in the Redlich-Kwong equation of state
	-	coefficient in statistical model
b	-	generalized second virial coefficient
	-	parameter in the Redlich-Kwong equation of state
C	-	third virial coefficient
	-	Centigrade
F	-	Fahrenheit
f	-	fugacity, force/area
G	-	$H - TS$ , Gibbs free energy, energy
g	-	acceleration due to gravity
K	-	vapor-liquid equilibrium phase distribution ratio, $y/x$
	-	Kelvin
M	-	molecular weight
	-	mass
N	-	number of components in a mixture
P	-	pressure
$p^\circ$	-	vapor pressure
R	-	Rankine

$S$	-	entropy
$T$	-	temperature
$U$	-	internal energy
$V$	-	volume
$x$	-	liquid mole fraction
$y$	-	vapor mole fraction
$Z$	-	compressibility factor, $PV/RT$

#### Greek Symbols

$\gamma$	-	activity coefficient, $\bar{f}/xf$
$\xi$	-	parameter in Adler consistency test
	-	fractional change in system mass
$\Delta$	-	change in a property
$\delta$	-	$(\Delta U/V)^{0.5}$ , solubility parameter, (energy/mole-volume) $^{0.5}$
$\epsilon$	-	deviation from statistical model
$\omega$	-	acentric factor
$\pi$	-	system pressure
$\nu$	-	$f/P$ , pure component fugacity coefficient
$\rho$	-	density
$\phi$	-	$\bar{f}/P_y$ , fugacity coefficient
$\theta$	-	imperfection pressure correction
$\Sigma$	-	summation over all $N$ components in a mixture

#### Subscripts

1	-	component 1 in a mixture (lighter component)
2	-	component 2 in a mixture (heavier component)
c	-	critical property

- H - heavy component
- HV - heavy component in the vapor phase
- i,j - component i or j, respectively
- k - convergence property
- L - light component
- LV - light component in the vapor phase
- m - mixture property
- r - reduced property
- property at infinite dilution
- T - property evaluated at system temperature

#### Superscripts

- ° - reference state
- simple fluid property,  $\omega = 0$
- - superbar, partial molar quantity
- volume average property for mixture
- E - excess quantity
- L - liquid phase
- V - vapor phase
- ' - correction to simple fluid property
- Berlin form of virial equation

#### Abbreviations

- exp - exponential, i.e., e to the power
- log - logarithm to the base 10
- ln - logarithm to the base e
- R-K - Redlich-Kwong

APPENDIX K

PHYSICAL CONSTANTS

TABLE K-1

## CALCULATION CONSTANTS FOR PURE COMPONENTS

COMPONENT	CRITICAL TEMPERATURE-R	CRITICAL PRESSURE-ATM	ACENTRIC FACTOR	SOLUBILITY PARAMETER	MOLECULAR WEIGHT
METHANE	343.91	45.80	.013	5.45	16.043
ETHANE	550.01	48.30	.105	5.28	30.070
PROPANE	665.95	42.01	.152	6.00	44.097
ISOBUTANE	734.65	36.00	.1918	6.25	58.124
N-BUTANE	765.31	37.47	.2010	6.70	58.124
2,2-DIMETHYLPROPANE	780.77	31.57	.2020	6.65	72.151
ISOPENTANE	829.80	32.90	.2060	6.75	72.151
N-PENTANE	845.60	33.31	.2520	7.05	72.151
2,2-DIMETHYLBUTANE	880.90	30.67	.2041	7.00	86.178
CYCLOPENTANE	921.20	44.55	.2050	8.10	70.134
2-METHYLPENTANE	896.50	29.95	.2816	7.21	86.178
3-METHYLPENTANE	907.90	30.83	.3678	6.35	86.178
N-HEXANE	914.20	29.94	.2900	7.30	86.178
METHYLCYCLOPENTANE	959.00	37.36	.2350	7.85	84.163
2,3-DIMETHYLPENTANE	968.00	29.20	.3037	7.51	100.206
CYCLOHEXANE	997.70	35.17	.2030	8.19	84.163
3-METHYLHEXANE	964.00	28.10	.3288	7.46	100.206
ISOHEPTANE	982.10	27.36	.3248	7.48	100.206
2,2,4-TRIMETHYLPENTANE	979.76	25.50	.3058	7.49	114.223
N-HEPTANE	972.31	27.00	.3520	7.45	100.206
METHYLCYCLOHEXANE	1030.20	34.32	.2420	7.83	98.190
TOLUENE	1069.20	40.15	.2520	8.90	92.142
2,3,4-TRIMETHYLPENTANE	1022.00	27.60	.3180	7.66	114.223
OCTANE ISOMERS	1033.40	25.00	.3760	7.61	114.223
N-OCTANE	1024.31	24.64	.3992	7.55	114.223
ETHYLBENZENE	1115.80	36.74	.3170	8.79	106.169
MIXED XYLENES	1114.00	34.37	.3110	8.79	106.169
258-303F FRACTION	1079.20	22.96	.4240	7.69	128.260
N-NONANE	1073.00	22.60	.4439	7.65	128.260
304-345F FRACTION	1122.50	21.35	.4674	7.78	142.287
N-DECANE	1114.70	20.70	.4869	7.75	142.287
346-384F FRACTION	1157.20	19.69	.5118	7.82	156.314
N-UNDECANE	1153.70	19.20	.5009	7.79	156.314
385-421F FRACTION	1190.10	18.33	.5519	7.85	170.341
N-DODECANE	1187.70	17.80	.5394	7.84	170.341
422-455F FRACTION	1222.40	17.19	.5878	7.90	184.368
N-TRIDECANE	1220.70	17.00	.5818	7.89	184.368
456-488F FRACTION	1252.20	16.12	.6202	7.93	198.395
N-TETRADECANE	1250.70	16.00	.6165	7.92	198.395
489-519F FRACTION	1280.00	15.10	.6487	7.70	212.422
N-PENTADECANE	1277.00	14.97	.6494	7.96	212.422
520-548F FRACTION	1305.50	14.07	.6726	8.00	226.449
N-HEXADECANE	1303.00	14.02	.6748	7.99	226.449
549-575F FRACTION	1329.10	13.07	.6928	8.03	240.476
N-HEPTADECANE	1328.00	13.00	.6866	8.03	240.476
576-602F FRACTION	1351.00	12.15	.7132	8.05	254.504
N-OCTADECANE	1349.70	11.98	.6959	8.04	254.504
603-627F FRACTION	1370.80	11.35	.7382	8.08	268.531
N-NONADECAN	1369.80	11.27	.7318	8.07	268.531
628-650F FRACTION	1388.10	10.77	.7778	8.10	282.558
N-EICOSANE	1387.40	10.69	.7703	8.09	282.558
651F+ FRACTION	142.60	10.49	.8423	8.11	

## VITA

Alto Nelson Stuckey, Jr.

Candidate for the Degree of

Doctor of Philosophy

Thesis: THE PHASE BEHAVIOR OF METHANE IN A NATURAL GAS CONDENSATE

Major Field: Chemical Engineering

Biographical:

Personal Data: Born at Birmingham, Alabama, July 7, 1935, the son of Alto N. and Eugenia B. Stuckey. Married to Wysie Jackson, Columbia, Mississippi, in May, 1960.

Education: Attended elementary school in Birmingham, Alabama; graduated from Ensley High School, Birmingham, Alabama in 1952; received the Bachelor of Science degree in Chemical Engineering from the University of Alabama in May, 1956; received the Master of Science degree, with a major in Chemical Engineering from Oklahoma State University in May, 1963; completed requirements for the Doctor of Philosophy degree in May, 1966.

Organizations: Tau Beta Pi, Sigma Xi, Omega Chi Epsilon, American Institute of Chemical Engineers, American Chemical Society.

Professional Experience: Employed as Junior Engineer with the Linde Air Products Company in the summer of 1955, Employed as an instructor in general chemistry with the University of Alabama for the spring semester of 1956. Employed by Esso Research Laboratories, Baton Rouge, Louisiana in June, 1956 as a Process Development Engineer. Loaned to Lago Oil and Transport Co., Aruba, Netherlands Antilles from February to October, 1957. Employed by Esso Research Laboratories from October, 1957, to present as Process Design and Development Engineer. Registered professional engineer, Louisiana.